INTERNATIONAL DOCTORAL
SCHOOL OF THE USC

Carlos
Casas Arozamena

PhD Thesis

Personalised Medicine in Endometrial Cancer Through the Use of Liquid Biopsy

Santiago de Compostela, 2024

Doctoral Programme in Molecular Medicine

ESCOLA DE DOUTORAMENTO
INTERNACIONAL DA USC

DOCTORAL THESIS

PERSONALISED MEDICINE IN ENDOMETRIAL CANCER THROUGH THE USE OF LIQUID BIOPSY

Author

Carlos Casas Arozamena

Supervisor/s: Dra. Laura Muinelo Romay & Dr. Miguel Abal

Tutor: Dr Rafael López López

PHD PROGRAMME IN MOLECULAR MEDICINE

SANTIAGO DE COMPOSTELA

I, Carlos Casas Arozamena, author of this thesis, have no conflicts of interest to declare.

I, Carlos Casas Arozamena, author of this thesis, declare that, unless clarified, all the images presented in this thesis have been produced by the author. In the case of images reused or adapted from other manuscripts, permission has been granted by the publishers, and the mode of legal use has been clarified at the bottom of the corresponding figures.
Further information can be found in the appendix 3.

USC
UNIVERSIDADE DE SANTIAGO DE COMPOSTELA

The studies described in this thesis were performed within the framework of the Liquid Biopsy Analyses Unit and the Translational Medical Oncology (Oncomet) at the Health Research Institute of Santiago (IDIS) - University Hospital Complex of Santiago de Compostela, Spain.

The work presented in this thesis was supported by grants and support from the Instituto de Salud Carlos III (ISCIII) and FEDER (CP20/00119, PI20/00969, PI20/01566, PI21/00990), CIBERONC (CB16/12/00295, CB16/12/00328), the AECC (Grupos Estables de Investigación 2018-AECC), and GAIN Proyectos de Excelencia (IN607D2021/05) and by the Translational Medical Oncology (ONCOMET) group

USC UNIVERSIDADE DE SANTIAGO DE COMPOSTELA

“Ignorance more frequently begets confidence than does knowledge: it is those who know little, and not those who know much, who so positively assert that this or that problem will never be solved by science”.

Charles Darwin

“Curiosity is the key to problem solving”

Galileo Galilei

USC
UNIVERSIDADE DE SANTIAGO DE COMPOSTELA

TABLE OF CONTENTS

USC
UNIVERSIDADE
DE SANTIAGO
DE COMPOSTELA

TABLE OF CONTENTS

ACKNOWLEDGEMENTS **8**

ABBREVIATIONS AND ACRONYMS **13**

RESUMO IN EXTENSO **19**

SUMMARY **32**

1|INTRODUCTION **36**

1.1|Endometrial Cancer 37

1.2|Liquid Biopsy 59

1.3| Preclinical Models in Endometrial Cancer 73

2|OBJECTIVES **78**

3|MATERIAL & METHODS **81**

3.1|Patients inclusion 82

3.2|Uterine aspirate processing 83

3.3|Blood samples processing 83

3.4|Nucleic Acid Isolation 83

3.5|Sequencing 84

3.6|Cell lines culture 85

3.7|ddPCR Analysis 86

3.8|Statistical Analyses 88

4|RESULTS **90**

4.1|CHAPTER I Precision Oncology in Endometrial Cancer: NGS Perspectives on Minimally Invasive Samples **91**

4.2|CHAPTER II Epigenetic regulation in Endometrial Carcinoma: Insights from Methylome Profiling **118**

USC UNIVERSIDADE DE SANTIAGO DE COMPOSTELA

4.3|CHAPTER III Non-invasive detection of microsatellite instability in patients with endometrial cancer 133

4.4|CHAPTER IV Unveiling Endometrial Cancer Prognosis: Integrating cfDNA and ctDNA for Predictive and follow up Analysis 162

4.5|CHAPTER V CTCs as Prognostic Biomarkers in Endometrial Cancer: Findings from a Multicentred Study.....194

4.6|CHAPTER VI Preclinical models in endometrial cancer 209

5|OVERALL DISCUSSION.....239

6|CONCLUSIONS 252

7|BIBLIOGRAPHY 255

APPENDICES 289

Appendix 1: Index of figures and Tables..... 290

Appendix 2: List of Publications 296

Appendix 3: Ethical considerations and attached permissions..... 298

Appendix 4: NGS sequencing of the UA samples from Chapter III. 319

Appendix 5: Quality statistics for the NGS sequencing of the cfDNA samples. 330

Appendix 6: Alterations found on the NGS sequencing of the cfDNA samples. 333

USC UNIVERSIDADE DE SANTIAGO DE COMPOSTELA

ACKNOWLEDGEMENTS

USC
UNIVERSIDADE
DE SANTIAGO
DE COMPOSTELA

ACKNOLEDGEMENTS

Después de siete años, que se dice pronto, ha llegado el día. El fin de una etapa llena de momentos maravillosos, otros no tanto… Pero que sin duda alguna no hubiera sido ni la cuarta parte de maravillosa sin todos los que habéis formado parte de ella.

En primer lugar, quiero agradecer a todos los pacientes y sus familias por haberse prestado a formar parte del mundo de la investigación pese a todo lo que están pasando. Gracias de corazón, sois el motivo que nos impulsa a seguir adelante.

Gracias a mi tutor y a mis directores de tesis. Gracias Rafa por permitirme formar parte de este grupo, no, de esta gran familia que es ONCOMET. Gracias a Miguel y a Laura, por acoger a un iluso estudiante de biología con poca idea pero muchas ganas de investigar y haberme apoyado y acompañado en toda esta etapa. En especial gracias a Laura, gracias por enseñarme, por preocuparte y siempre tener un segundo (aun cuando no siempre fuera un segundo).

Gracias a todo el equipo de ONCOMET, a los oncólog@s, enfermer@s y todo el equipo. En especial gracias a Juan Cueva por tu dedicación, ilusión y entusiasmo en la investigación. Gracias al equipo de ginecología del CHUS, Ana, Efigenia y Victoria. Vuestro apoyo, cooperatividad y entusiasmo sin duda han sido parte del éxito de todo este trabajo!!

Special thanks to everyone from Oslo, you all made me feel right at home. Thank you Kristina for inviting me into the adventure that was going to Oslo. Thank you to everyone from the ICR, specially to Therese and Karin, thank you for all your help, your support and specially, thank you for welcoming me as another one of the team. *Takk for alt*. Thanks to everyone at the OCCI,

USC UNIVERSIDADE DE SANTIAGO DE COMPOSTELA

Sebastien, Else Marit, Nadia, Stephano, Alicia and everyone else. But specially thanks to Sandy, Christopher and Klara, the B squad. Thank you for all the plans, the laughs and everything you did to make me feel welcome. I love you guys, can't wait to see you again!

Gracias a todos los colaboradores externos, al equipo de Madrid: Gema y Eva Diaz; al equipo de Barcelona Eva Colás y Antonio. En especial gracias a Bea, la futura doctora, sin duda los congresos sin ti no hubieran sido lo mismo, gracias por todo!

Y por supuesto, gracias a la gente del laboratorio 17-18. Esto no hubiera sido igual sin vosotros, compartir esta etapa con vosotros ha sido sin lugar a duda lo mejor. Gracias a Ramón y a Alicia, los mandamases del labo. Ramón, gracias por tu paciencia enseñándome, por tu ayuda, tu paciencia pero sobre todo tu cariño y bondad, por tu preocupación por todos los del labo, eres el mejor. Ali, la primera oficial, mirada de medusa pero corazón gigante, gracias por no desesperarte demasiado con mis preguntas, por tu ayuda y gestión de las pacientes, nadie más podría hacerlo igual.

Al equipo de nasas, Manu, Raquel, Alba, Lore y Jorge. Lore, fuiste la primera persona que conocí en el laboratorio y no pudo ser mejor opción, gracias por enseñarme y por tu ayuda constante. Alba gracias por tu paciencia infinita conmigo y los ratones… Se que no ha sido fácil pero me dan mucho asco… Las visitas al animalario no serán lo mismo sin los cotilleos. Jorge gracias por tu especial dedicación y preocupación con todos los predocs, por siempre estar dispuesto a echarnos un cable por mucho trabajo que tengas y ayudarnos con lo que haga falta.

A las nuevas incorporaciones, Rachel, Aroa, Rocio, Andrea, Sonia, Mimi, Yoel, Ana, Nico gracias por ser vosotros, por vuestra actitud y todo la energía que irradiáis! Mimi, Nico y Yoel, gracias por vuestra constante ayuda con la

USC UNIVERSIDADE DE SANTIAGO DE COMPOSTELA

bioinformática. Rachel y Sonia, gracias por toda vuestra ayuda en el laboratorio, sobre todo estos últimos meses, sin duda marcasteis la diferencia en mi salud capilar.

Gracias a todo el grupo de Oncoline. Pachu, Oscar, Carol, Aitor, Aida, San mis compañeros de tesis desde el inicio. Decir que os quiero es quedarse corto. No tengo duda de que si he llegado hasta aquí ha sido por vosotros. Pachu, mi +1 en todo, gracias por tu ayuda, apoyo, por todos los planes (habidos y por haber), por todas esas tardes hasta las tantas adictos a R intentando cambiar el color de una figura. Oscar, gracias por todos los cafés a primera hora de la mañana, por ser siempre fuente de desahogo y tu apoyo incondicional todos estos años. Carol mi dramas favorita, desde el día uno en el laboratorio 5 me has enseñado, ayudado y apoyado, gracias por todos estos años, por el bodorrio del siglo (jamás superable) y todos los planes. Aitor, gracias por tu optimismo, siempre estar dispuesto a ayudar pero, sobre todo, dispuesto a esas cañas obligatorias post labo! Y por supuesto, a Manu, un epi más. Aida, gracias por los desahogos, marujeos varios, planes de playa, no dejar que me fuese por el *lado oscuro* y siempre estar ahí para lo que hiciera falta. San, mi asturiana por excelencia, gracias por ser siempre un SI a cualquier plan que se proponga, por preocuparte tanto por mí, por siempre estar dispuesta a un bombardeo. No me hubiera podido imaginar esta etapa sin ninguno de vosotros, habéis sido y sois, paz y tranquilidad. Más que compañeros de tesis, habéis sido amigos, 'casa'. Gracias por tanto, os quiero.

Y no me puedo olvidar tampoco de la gente de la UM, en especial a Pablo, Nuria e Inés esta etapa no hubiera sido lo mismo sin vosotros! Pablo, el hombre cojín, gracias por ser tú, no cambies. Nuria e Inés gracias por tantos planes durante la tesis, por esos cafés, vermuts y planes improvisados.

USC UNIVERSIDADE DE SANTIAGO DE COMPOSTELA

Gracias a todo nano, el día que hagáis inventario y os falte algo, prometo que yo no he sido jeje. En especial a Sandra Alijas, Maria C y a Sai. Gracias por vuestra paciencia con mis cálculos de molaridad, por todas las cervezas de desconexión y planes! Gracias también a las nano bebés, Soraya, Laura, Jen (aunque no tan baby) por siempre tener un momento para una conversación en los pasillos y levantar los ánimos!

Por supuesto, gracias también a la gente de fuera del labo. En especial, a Alex, Javi y Martín, gracias por los planes, viajes, risas, las cervezas de desconexión cuando eran necesarios... Gracias por siempre estar ahí y poder contar con vosotros. Os quiero.

Gracias a Adri, sin duda la persona con paciencia infinita, me has acompañado casi desde el primer día en esta etapa y no podría haber escogido mejor. Gracias por escuchar, calmarme y siempre estar ahí.

Y por último a mi familia, gracias por todo lo que me habéis ayudado en esta etapa. Sin vuestro apoyo no hubiera sido lo mismo.

Gracias a todos los que habéis formado parte de esta etapa!

#XuntosAvanzamos

USC UNIVERSIDADE DE SANTIAGO DE COMPOSTELA

ABBREVIATIONS AND ACRONYMS

USC
UNIVERSIDADE DE SANTIAGO DE COMPOSTELA

ABBREVIATIONS AND ACRONYMS

A

AB: Alamar Blue

AKT1: RAC-Alpha Serine/Threonine-Protein Kinase 1

AKT2: RAC-Beta Serine/Threonine-Protein Kinase

AR: Androgen receptors

ARID1A: AT-Rich Interaction Domain 1A

ATM: ATM Serine/Threonine Kinase

AUC: Area under the curve

AXL: Tyrosine-Protein Kinase Receptor UFO

B

BAP1: BRCA1 Associated Protein 1

BME: Basic Membrane Extract

C

CCC: Clear Cell Carcinoma

CCND3: Cyclin D3

CCNE1: Cyclin E1

CDK2: Cyclin Dependent Kinase 2

cfDNA: circulating free DNA

cfTNA: circulating free total nucleic acids

CKS: cytokeratins

CNAs: copy number alterations

CS: carcinosarcomas

CTC: circulating tumour cells

ctDNA: circulating tumour DNA

CTNNB1: catenin Beta 1

CTP: Carboplatin

CT-SCAN: computed tomography scan

CTX: carbotaxol

USC UNIVERSIDADE DE SANTIAGO DE COMPOSTELA

D

DAPI: 4',6-diamidino-2-phenylindole

ddPCR: digital droplet PCR

DFS: disease free survival

DIDO1: Death Inducer-Obliterator 1

DMCpGs: differentially methylated CpGs

dMMR: deficient Mismatch Repair

DSBs: double stranded breaks

DSS: disease specific survival

E

EC: endometrial cancer

ECM: extracellular matrix

EEC: endometrioid endometrial carcinoma

EMT: epithelial-mesenchymal trnasition

ENITEC: European Network for Individualized Treatment in EC

EPCAM: Epithelial Cell Adhesion Molecule

ER: oestrogen receptor

ERBB2:Erb-B2 Receptor Tyrosine Kinase 2

F

FBXW7: F-Box and WD Repeat Domain Containing 7

FDR: false discovery rate

FFPE: formalin fixed paraffin embedded

FGFR2: Fibroblast Growth Factor Receptor 2

FIGO: International Federation of Gynaecology and Obstetrics

G

GABA: Gamma-aminobutyric acid

GABRA5: Gamma-Aminobutyric Acid Type A Receptor Subunit Alpha5

GAD2: Glutamate Decarboxylase 2

GNAS: Guanine Nucleotide Binding Protein (G Protein)

USC UNIVERSIDADE DE SANTIAGO DE COMPOSTELA

GO: Gene ontology

GSEA: Gene Set enrichment analyses

H

h: hour

HCN: high copy number

HR: hazard ratio

HRD: homologous recombination deficiency

HRR: homologous recombination repair

HRT: hormone replacement therapy

I

ICB: immune check point blockade

IF: immunofluorescence

IGV: Integrative Genomics Viewer

IHC: immunohistochemistry

IQR: interquartile range

ISPs: Ion Sphere Particles

ITH: intratumor heterogeneity

ITP: immunotherapy

ITS: insulin-transferrin selenium

K

KEG: Kyoto Encyclopedia of Genes and Genomes

KRAS: KRAS Proto-Oncogene, GTPase

L

LOB: limit of blank

LoD: limit of detection

LVSI: Lymphovascular invasion space infiltration

M

M&M: Material & methods

MC: mixed carcinoma

MDM2: MDM2 Proto-Oncogene

Min: minutes

MLH1: MutL Homolog 1

MMR: mismatch repair

USC UNIVERSIDADE DE SANTIAGO DE COMPOSTELA

MRD: minimal residual disease

MRI: Magnetic resonance imaging

MSH2: MutL Homolog 2

MSH6: MutL Homolog 6

MSI: microsatellite instability

MSI-H: microsatellite instability high

MSI-L: microsatellite instability low

MSS: microsatellite stability

MYC: MYC Proto-Oncogene, BHLH Transcription Factor

N

NAC: N-acetyl L-cysteine

NEEC: Non-Endoemtrioid endometrial carcinomas

NGS: Next-Generation Sequencing

NICO: Nicotinamide

NOG: Noggin

NPBWR2: Neuropeptides B And W Receptor 2

NSG: female NOD.Cg-PrkdcSCID Il2rgtm1Wjl/SzJ

NSMP: Non Specific Molecular profile

P

PARPi: Poly(ADP-Ribose) Polymerase inhibitors

PARP: Poly(ADP-Ribose) Polymerase

PCOS: polycystic ovary syndrome

PD: Relapse

PDL1: Programmed Cell Death 1 ligand

PD1: Programmed Cell Death 1

PDOs: Patient derived organoids

PDSs: patient derived spheroids

PDXs: patient derived xenografts

PIK3CA: Phosphatidylinositol-4,5-Bisphosphate 3-Kinase Catalytic Subunit Alpha

PIK3R1: Phosphoinositide-3-Kinase Regulatory Subunit 1

pMMR: proficient mismatch repair

PMS2: PMS1 Homolog 2, Mismatch Repair System Component

POLE: DNA Polymerase Epsilon, Catalytic Subunit

USC UNIVERSIDADE DE SANTIAGO DE COMPOSTELA

PRA: Progesteron receptors

PTX: Paclitaxel

PTEN: Phosphatase And Tensin Homolog

R

RB1: RB Transcriptional Corepressor 1

RSPO1: R-Spondin 1

RET: Ret Proto-Oncogene

S

SC: Serous carcinomas

SoC: Standard of Care

SNPs: single nucleotide polymorphism

T

TCGA: the cancer genome atlas

TP53: Tumour Protein P53

TME: tumour microenvironment

U

UA: Uterine aspirate

ULA: Ultra-Low Attachment

UC: Undifferentiated carcinomas

V

VAF: Variant Allelic Frequency

USC UNIVERSIDADE DE SANTIAGO DE COMPOSTELA

RESUMO IN EXTENSO

USC
UNIVERSIDADE
DE SANTIAGO
DE COMPOSTELA

RESUMO IN EXTENSO

O cancro de endometrio é a neoplasia xinecolóxica máis común nos países desenvolvidos. Ademais, a incidencia e mortalidade deste cancro foi en aumento nos últimos anos. O prognóstico clínico para o cancro de endometrio é relativamente favorable en comparación con algúns outros cancros xinecolóxicos, especialmente cando se detecta nunha etapa temperá. Con todo, un 10-20% dos pacientes experimentan unha recaída dentro dos primeiros dous anos despois da resección cirúrxica. Estes pacientes teñen un resultado clínico extremadamente pobre cunha resposta mala ao tratamento.

Tradicionalmente as variables clínicas, como histoloxía, grao, infiltración miometrial, entre outras; utilizáronse para a estratificación dos pacientes. Con todo, nos últimos anos incluíuse a clasificación molecular na avaliación do risco da enfermidade con resultados prometedores na avaliación do risco. Con todo, ao redor do 20% dos pacientes clasificados despois da cirurxía como de baixo risco acaban en recorrencias. Identificar a eses pacientes con cancro de endometrio co maior risco post-cirúrxico de recorrencia é esencial para garantir que reciban a atención adecuada, minimizando os efectos adversos e custos de tratamentos innecesarios.

Aínda que incluída no sistema de clasificación de riscos, o manexo molecularmente guiado do cancro de endometrio é limitado con respecto a outros cancros. O tratamento de primeira liña no cancro de endometrio recorrente ou metastásico é principalmente a quimioterapia, independentemente do subtipo molecular. Ademais, o tratamento hormonal e a inmunoterapia son case as únicas terapias dirixidas dispoñibles actualmente para o tratamento dos estadios avanzados. Con todo, para desenvolver enfoques terapéuticos máis personalizados, existe unha clara necesidade de marcadores preditivos precisos para estratificar aos doentes

USC UNIVERSIDADE DE SANTIAGO DE COMPOSTELA

potencialmente sensibles, monitorear a resposta ao tratamento e identificar os mecanismos de resistencia. A priorización de tratamentos require probas funcionais, especialmente en casos nos que a asociación fármaco-biomarcador-actividade non foi claramente validada. Históricamente, as liñas celulares *in vitro* tiveron un papel prominente no desenvolvemento de fármacos contra o cancro, aínda que tales modelos poden carecer de relevancia clínica debido aos procesos de inmortalización e adaptación inducidos polo crecemento continuo en plástico. Por este motivo, existe unha clara necesidade de desenvolver novos modelos *ex vivo* que mellor imiten a fisioloxía orixinal do cancro de endometrio.

A menciña de precisión ten o potencial de revolucionar a atención médica ao ofrecer tratamentos máis efectivos e personalizados, mellorar os resultados para os doentes e reducir os custos de atención médica. Neste sentido, as estratexias baseadas en biopsias líquidas permiten unha caracterización minimamente invasiva da enfermidade, así como a identificación de biomarcadores circulantes que poderían mellorar aínda máis a estratificación dos pacientes. Ademais, estes biomarcadores circulantes poderían empregarse para análises lonxitudinais para avaliar a evolución da enfermidade. No contexto dos doentes con cancro de endometrio, existe unha falta de métodos de diagnóstico non invasivos e precisos.

Dentro desta tese doutoral, abordamos os catro retos clínicos principais, anteriormente descritos; 1) falla de métodos de diagnóstico non invasivos e precisos (Capítulos I-III), 2) falla de métodos de estratificación de risco eficiente (Capítulos IV-V), 3) mellora na selección de tratamento personalizado (Capítulos I e III), e 4) falla de modelos preclínicos para probar terapias personalizadas (Capítulo VI).

USC UNIVERSIDADE DE SANTIAGO DE COMPOSTELA

No Capítulo I avaliamos a eficacia de dous enfoques baseados en NGS (das siglas en inglés, next-generation sequencing) dirixidos a mostras mínimamente invasivas de doentes con cancro de endometrio: o aspirado uterino e o cfDNA (das siglas en inglés, circulating free DNA). Nunha cohorte total de 202 pacientes utilizamos un panel NGS dirixido para avaliar 1) como o aspirado uterino reflicte o panorama xenómico dos doentes, 2) a correlación das alteracións específicas atopadas no aspirado uterino co resultado clínico e 3) o papel de diferentes alteracións como posibles dianas terapéuticas. A análise do aspirado uterino mostrou mutacións prevalentes en xenes clave como PTEN, PIK3CA e TP53. Como esperábamos, as mutacións de POLE foron indicativas dun prognóstico favorable, mentres que as mutacións de TP53 asociáronse cun fenotipo de enfermidade máis agresivo. A integración de datos xenéticos con resultados clínicos mostrou que as alteracións de TP53 son un predictor robusto de mal prognóstico. Ademais, analizando específicamente o perfil mutacional das doentes que acaban progresando, identificáronse as mutacións en RB1, MDM2 e ARID1A como asociadas coa progresión da enfermidade, suxerindo posibles dianas terapéuticas. É importante destacar que, dentro deste capítulo, mostramos que as análises do aspirado uterino permitiron a identificación de doentes con heteroxeneidade intratumoral. Más do 30% dos pacientes presentaron xenes con múltiples alteracións. A heteroxeneidade intratumoral é de gran importancia dentro do contexto clínico, xa que pode levar a variacións nas respostas ao tratamento, o que dificulta o desenvolvemento de terapias dirixidas que erradiquen eficazmente todas as células cancerosas. Ademais, os clons resistentes aos medicamentos dentro dun tumor poden limitar o éxito a longo prazo das estratexias de tratamento. Por tanto, poder identificar a eses pacientes con heteroxeneidade intratumoral mediante a secuenciación do aspirado uterino resalta aínda máis o valor deste tipo de mostra.

USC UNIVERSIDADE DE SANTIAGO DE COMPOSTELA

Con respecto á análise de cfDNA, avaliamos o rendemento dun panel baseado en NGS nunha cohorte de 18 doentes (32 mostras). En xeral, o 71.88% das mostras mostraron polo menos unha mutación patoxénica, predominantemente en TP53, PIK3CA e/ou GNAS. Ademais, dado que tiñamos mostras lonxitudinais, a dinámica do ctDNA (das siglas en inglés, circulating tumour DNA) correlacionou coa recaída. A análise lonxitudinal de cfDNA revelou perfís mutacionais dinámicos, aparecendo novas mutacións que poderían derivar da presión selectiva do tratamento. En xeral, este estudo destaca a utilidade das estratexias baseadas en NGS en mostras mínimamente invasivas para comprender o perfil xenómico no cancro de endometrio, ofrecendo maior evidencia clínica sobre os distintos subtipos moleculares, marcadores prognósticos e preditivos, e novas dianas terapéuticos. Estes achados abren novas estratexias de menciña de precisión destinadas a optimizar o manexo do cancro de endometrio e mellorar os resultados para as doentes.

Dentro do Capítulo II caracterizamos aínda máis o perfil xenético da enfermidade mediante a análise do metiloma de pacientes con cancro de endometrio en mostras mínimamente invasivas. Para iso, aplicamos un array de metilación (MethylationEPIC v1.0) no aspirado uterino, para analizar o perfil epixenético de 57 doentes con cancro de endometrio. O obxectivo principal deste capítulo é identificar un perfil epixenético diferencial entre os subtipos histolóxicos endometrioide e seroso, que permita comprender os mecanismos asociados coa agresividade tumoral e identificar novas dianas terapéuticas. Observamos un perfil de hipometilación asociado coa histoloxía serosa, compatible coa natureza agresiva deste subtipo. Específicamente, a nosa análise revelou a desregulación de vías clave, entre elas as vías de sinalización GABAérgica e a vía de sinalización do calcio, implicando os seus posibles roles na progresión do cancro de endometrio. Estas vías foron

USC UNIVERSIDADE DE SANTIAGO DE COMPOSTELA

descritas previamente noutros tipos de tumores pola súa implicación na progresión do cancro como promotoras da proliferación celular, invasión, diseminación e evasión do sistema inmunolóxico, e aínda que ata o momento non hai medicamentos que ataquen especificamente estas vías, teñen un gran potencial coma novas dianas terapéuticas para o tratamento do cancro de endometrio. A validación mediante pirosecuenciación e análise in silico confirmaron aínda máis os nosos achados, destacando a robustez e relevancia clínica da análise do metiloma en mostras do aspirado uterino. En xeral, o noso estudo proporciona información valiosa sobre o metiloma do cancro de endometrio, ofrecendo posibles novas dianas para a menciña personalizada e destacando a utilidade do aspirado uterino como mostra mínimamente invasiva para a caracterización do perfil molecular deste tumor.

Dentro do seguinte capítulo, Capítulo III, avaliamos o rendemento dun ensaio de ddPCR (das siglas en inglés, droplet digital PCR) altamente sensible para determinar o estado de cinco microsatélites no aspirado uterino e mostras de cfDNA de 90 doentes con cancro de endometrio. O ensaio determina o estado de cinco microsatélites diferentes (BAT25, BAT26, NR24, NR21 e MONO27), previamente descritos como relevantes no cancro de endometrio para a avaliación da inestabilidade de microsatélites. Actualmente na clínica, a análise de proteínas reparadoras determínase en mostras de tecido mediante inmunohistoquímica, o que se considera o estándar de ouro. Para avaliar o rendemento do ensaio, analizamos o estado destes microsatélites no aspirado uterino e comparámolo co estándar na clínica, a expresión das proteínas reparadoras. Observamos unha alta concordancia (96.67%) con só tres casos discordantes. Como validación adicional, en 60 doentes, comparamos o estado dos cinco microsatélites utilizando o mesmo método. Observouse unha concordancia do 100% entre o aspirado uterino e as mostras embebidas en parafina. Por tanto, confirmando

USC UNIVERSIDADE DE SANTIAGO DE COMPOSTELA

os casos discordantes como inestables, o que resalta aínda máis o valor e a utilidade clínica de analizar o aspirado uterino en contraposición a técnicas baseadas en biopsias de tecido.

Respecto á análise das mostras de cfDNA, avaliamos o estado dos microsatélites en 59 mostras e comparámolos co seu aspirado uterino correspondente. A concordancia global foi moderada, con só o 50.85% dos pacientes sendo concordantes entre o cfDNA e o aspirado uterino. Con todo, se nos enfocamos nos pacientes con características clinico-histopatolóxicas de alto risco, atopamos unha boa concordancia global do 70.27%. É salientable que os nosos resultados tamén evidenciaron o valor da análise da inestabilidade de microsatélites en cfDNA para monitorear a evolución da enfermidade. Globalmente os nosos resultados demostraron que a avaliación da inestabilidade de microsatélites en mostras minimamente invasivas en cancro de endometrio é robusta e proporciona unha ferramenta valiosa para a caracterización molecular e o seguimento dos tumores endometriales, abrindo novas oportunidades para o manexo personalizado deste tumor.

No Capítulo IV, analizamos mostras de plasma de 198 pacientes con cancro de endometrio localizado recompiladas de diferentes hospitais españois no momento da cirurxía e tamén durante o curso da enfermidade (n = 130). Primeiro, estudamos o valor prognóstico da análise de cfDNA e ctDNA para predicir a recaída e a supervivencia específica da enfermidade. Baseándonos nas mutacións atopadas na caracterización do aspirado uterino (Capítulo I) puidemos deseñar ensaios ddPCR específicos para o 89.4% das doentes e monitorear a evolución da enfermidade. Baseándonos na cuantificación dos niveis pre-cirúrxicos de cfDNA, dividimos as doentes en grupos de baixo ou alto cfDNA. Os resultados deste capítulo mostraron que os altos niveis pre-cirúrxicos de cfDNA correlacionaron cunha supervivencia

USC UNIVERSIDADE DE SANTIAGO DE COMPOSTELA

libre de enfermidade e global máis curta. En canto ao ctDNA no momento da ciruxía, as doentes clasificáronse como positivas ou negativas segundo a presenza de alteracións identificadas no aspirado uterino, incluindo os marcadores de inestabilidade validados no Capítulo III. As doentes con niveis detectables de ctDNA na ciruxía mostraron unha evolución significativamente peor. Ambos biomarcadores correlacionáronse coa variables clínico-patolóxicas e atopamos que tanto os niveis pre-cirúrxicos de cfDNA como a presenza de ctDNA tiñan valor prognóstico independente. Por tanto, baseándonos nestes resultados, creamos un modelo que combinaba ambos os biomarcadores. Empregando este modelo determinamos que as doentes con altos niveis pre-cirúrxicos de cfDNA e niveis detectables de ctDNA ao inicio correlacionaron cun moi mal prognóstico clinico. É importante destacar que este enfoque é clinicamente significativo ao estratificar aos pacientes segundo a histoloxía, o grao ou a clasificación de risco global, destacando o seu valor adicional para identificar os pacientes cunha mala evolución nos distintos grupos de risco actuais. De feito, os niveis de cfDNA/ctDNA serviron para identificar a doentes que mostraron unha recaída temperá da enfermidade entre os tumores clasificados como de risco intermedio-alto/alto de recorrencia e os de risco baixo-intermedio-baixo. Más do 70% dos doentes con niveis pre-cirúrxicos de cfDNA altos e niveis detectables de ctDNA experimentaron unha recaída dentro do primeiro ano despois da resección cirúrxica. Mentres que só o 30% dos pacientes clasificados como de alto risco, segundo as últimas pautas de ESGO, experimentaron unha recaída tumoral dentro do primeiro ano.

Ademais, dentro deste capítulo, avaliamos o papel do seguimento lonxitudinal de cfDNA e ctDNA en 130 doesntes. Esta análise demostrou ser un poderoso aliado para identificar as doentes que experimentan recaídas, xa que a presenza de ctDNA púidose chegar a detectar meses antes da aparición

USC UNIVERSIDADE DE SANTIAGO DE COMPOSTELA

de calquera evidencia clínica. Ademais, naqueles pacientes que experimentaron unha recaída, a cinética de cfDNA/ctDNA reflectiu a evolución do tumor, resaltando aínda máis o valor de cfDNA/ctDNA para o seguimento da enfermidade. Este estudo representa o traballo máis completo e ambicioso sobre a caracterización de cfDNA/ctDNA en cancro de endometrio e demostra o alto valor desta caracterización para mellorar a estratificación de riscos e anticipar a recaída da enfermidade en pacientes con enfermidade localizada. Ademais, a avaliación dinámica de ctDNA mostrou utilidade para complementar as estratexias de atención estándar para monitorear a evolución da enfermidade e a aparición de resistencias ao tratamento. A implementación da vixilancia de cfDNA/ctDNA na rutina clínica poderá proporcionar unha oportunidade única para mellorar o manexo do cancro de endometrio.

Seguindo coa avaliación de biomarcadores mínimamente invasivos con fins prognósticos, avaliamos o papel das células tumorais circulantes no Capítulo V. Nunha cohorte de 83 pacientes con enfermidade localizada, avaliamos a presenza de células tumorais circulantes utilizando o sistema CellSearch. Este sistema cuantifica os niveis de células tumorais circulantes epiteliales que se aillan en base a expresión de EpCAM e expresan marcadores epiteliais. A nosa análise revelou unha taxa de positividade de células tumorais circulantes do 21.69% entre as doentes incluidas no estudo, con recontos que oscilaron entre 1 a 80 por 7.5mL de sangue. Notablemente, niveis máis altos de desta poboación circulante asociáronse con fenotipos tumorais máis agresivos (pacientes de alto grao, estadios da FIGO avanzados, cun nivel de invasión do miometrio de máis do 50% e LVSI). É importante destacar que as doentes con ppresenza de estas células no momento da ciruxía mostraron tempos de supervivencia libre de enfermidade e supervivencia específica da enfermidade significativamente menores. Cando

USC UNIVERSIDADE DE SANTIAGO DE COMPOSTELA

realizamos este mesmo estudo separando as doentes con <2 ou ≥2 células tumorales circulantes/7,5 ml de sangre confirmáronse peores tempos de supervivencia libre de enfermidade e de supervivencia específica da enfermidade. Con todo, a pesar destas asociacións, as células tumorais circulantes non mantiveron significación pronóstica independente nas análises multivariadas de Cox. Aínda que o noso estudo mostra as implicacións pronósticas adversas da presenza de células tumorales circulantes no cancro de endometrio, é importante destacar que a cuantificación de células tumorais circulantes utilizando o sistema CellSearch só permite o enriquecemento de células epiteliales con expresión relativamente alta da molécula EpCAM na membrana celular, e as células tumorales circulantes están nun estado dinámico, transitando entre fenotipos epiteliais e mesenquimales. Estudos máis completos que apliquen outras tecnoloxías, como as non dependentes de epítopos, poderían ser de interese para avaliar a presenza de células tumorais circulantes mesenquimais no torrente sanguíneo de doentes con cancro de endometrio.

Por último, pero non menos importante, no capítulo VI exploramos a utilidade clínica de modelos preclínicos xerados a partir de mostras mínimamente invasivas. Avaliamos a robustez de dous modelos preclínicos diferentes, esferoides e organoides derivados de pacientes. En liña con traballos previamente publicados, os resultados deste capítulo mostraron que ambos os enfoques poderían usarse para xerar modelos robustos que recapitulan o tecido de orixe. Primeiro, exploramos os esferoides como unha alternativa máis económica para realizar ensaios de resposta a fármacos. Aínda que tivemos unha baixa taxa de éxito na xeración de esferoides, o modelo xerado probou a robustez do modelo e a utilidade clínica. Demostramos que o esferoide ten o mesmo perfil inmunohistoquímico e xenético do tumor primario. Ademais para completar o estudo, os esferoides

USC UNIVERSIDADE DE SANTIAGO DE COMPOSTELA

foron expostos a diferentes fármacos en base ao perfil mutacional da doente. Resultados tanto *in vitro* como *in vivo* reflicten a versatilidade e aplicabilidade clínica do noso enfoque, xa que estes estudos permitiron a identificación de tratamentos personalizados tanto en base á presenza de alteracións especificas como da inmunoterapia como opcións terapéuticas para a paciente.

Ademais, dentro do mesmo capítulo, establecemos un protocolo de xeración de organoides a partir de aspirados uterinos como unha ferramenta máis novidosa para a realización estudos farmacolóxicos. A eficiencia de establecemento destes organoides foi alta, aínda que parte dos cultivos establecidos presentaron baixas taxas de proliferación. Nos organoides xerados avaliamos a capacidade para recapitular o tecido primario e a súa resposta á quimioterapia. En xeral, os nosos resultados mostran a robustez dos esferoides e os organoides como modelos preclínicos para o cancro de endometrio, proporcionando novas oportunidades para probas de drogas e medicina personalizada.

Volvendo aos catro problemas no manexo da enfermidade. Dentro desta tese doutoral habemos explorado a utilidade clínica de diferentes técnicas de biopsia líquida no contexto da enfermidade localizada e avanzada do cancro de endometrio co obxectivo de mellorar o manexo do paciente e abordar estes problemas. Respecto a falta de métodos diagnósticos non invasivos e precisos, dentro dos tres primeiros capítulos (Capítulo I-III) describimos e optimizamos tres enfoques diferentes que baseándose no aspirado uterino, unha mostra minimamente invasiva, permitiron a caracterización da enfermidade a nivel xenético, epixenético e inestabilidade de microsatélites. Ao empregar tecnoloxías baseadas en NGS e/o ddPCR demostramos a fiabilidade e robustez do aspirado uterino para recapitular o tecido de orixe,

USC UNIVERSIDADE DE SANTIAGO DE COMPOSTELA

capturar a heteroxeneidade molecular, e determinar de forma eficiente a presenza de inestabilidade de microsatélites. Ademais, o noso enfoque identificou novas vías con interese terapéutico, abrindo novas vías de traballo para aportar novas dianas de tratamento, resaltando o valor do aspirado uterino como mostra minimamente invasiva para a caracterización molecular do cancro de endometrio.

Dentro dos capítulos IV e V exploramos a utilidade clínica de tres biomarcadores circulantes: cfDNA, ctDNA e células tumorales circulantes, que melloran e proporcionan unha estratificación de riscos máis precisa. Sendo a combinación de cfDNA e ctDNA a ferramenta máis prometedora. A combinación destes biomarcadores ten un valor prognóstico independente sobre as variables clínicas tradicionalmente empregadas. Ademais, demostramos que a cinética de cfDNA e ctDNA permite a identificación de enfermidade mínima residual, identificación de recaídas de forma precoz e resposta á terapia utilizando un enfoque baseado en NGS (Capítulo I) ou un enfoque baseado en ddPCR (Capítulo III-IV).

Tamén describimos métodos alternativos para unha selección de tratamento máis personalizada. Dentro do Capítulo I e III, mostramos que a aplicación de estratexias baseadas en NGS ou ddPCR para caracterizar o aspirado uterino permitirían a identificación de terapias dirixidas, como por exemplo, inhibidores de PIK/AKT/. Ou para a identificación de pacientes con inestabilidade de microsatélites que permitiría administración de inmunoterapia nestas doentes .

Por último, desenvolvemos modelos preclínicos para probar terapias personalizadas (Capítulo VI). Os modelos xerados, xa sexa como esferoides ou organoides, recapitulan o tecido de orixe e baixo tratamento, reflicten a resposta atopada en pacientes. Estes modelos representan unha valiosa

USC UNIVERSIDADE DE SANTIAGO DE COMPOSTELA

ferramenta para comprender mellor os mecanismos de resistencia as terapias convencionais e os tratamentos dirixidos así como a identificación de novas dianas para reverter as resistencias.

Globalmente, o fluxo de traballo baseado en técnicas de biopsia líquida que describimos dentro da tese demostra unha gran utilidade clínica e podería mellorar a atención ao paciente para as doentes con cancro de endometrio. Isto evidenciouse polos resultados obtidos no hospital clínico de Santiago de Compostela, onde, desde a implementación deste fluxo de traballo, varias doentes beneficiáronse deste enfoque. Fomos quen de identificar recaídas da enfermidade antes de calquera evidencia clínica, e testamos a actividade de terapias alternativas en modelos de organoides xerados de mostras de estas doentes identificando potenciais tratamentos alternativos.

USC UNIVERSIDADE DE SANTIAGO DE COMPOSTELA

SUMMARY

USC
UNIVERSIDADE
DE SANTIAGO
DE COMPOSTELA

SUMMARY

Endometrial cancer, the most common gynaecological malignancy in developed countries, has seen rising incidence and mortality rates. Despite generally favourable outcomes when detected early, 10-20% of patients experience tumour relapse post-surgery, leading to poor clinical outcomes. Molecular classification, though promising, has yet to fully inform treatment decisions, with chemotherapy remaining the mainstay for recurrent or metastatic cases although immunotherapy is gaining relevance as a second or a first line of treatment.

Precision medicine holds promise in tailoring treatments, but lacks accurate predictive markers and relevant preclinical models to further test new alternatives. Liquid biopsy-based approaches offer minimally invasive disease characterization and circulating biomarkers that could improve patient stratification and longitudinal monitoring. The current doctoral thesis addresses these challenges, focusing on non-invasive diagnostics, accurate risk assessment, personalized treatment selection, and the development of relevant preclinical models.

In Chapter I, the efficacy of two targeted-NGS approaches in minimally invasive samples from endometrial cancer patients was assessed. The uterine aspirate showed prevalent mutations in key genes like *PTEN*, *PIK3CA*, and *TP53*, with *TP53* alterations indicating poor prognosis. Moreover, mutations in *RB1, MDM2*, and *ARID1A* were linked to disease progression, suggesting potential therapeutic targets. The analysis also identified patients with intratumoral heterogeneity, crucial for treatment response variations. The cfDNA analysis in a smaller cohort revealed pathogenic mutations, predominantly in *TP53*, *PIK3CA*, and/or *GNAS*, with ctDNA dynamics correlating with relapse, indicating evolving mutational landscapes.

USC UNIVERSIDADE DE SANTIAGO DE COMPOSTELA

In Chapter II, the methylome od UAs from endometrial cancer patients was analysed, revealing a hypomethylation profile associated with the aggressive serous histology. Key pathways like GABAergic and calcium signalling were implicated, suggesting potential therapeutic targets. The study supported the clinical relevance of uterine aspirate-based methylome analysis to better understand the biology of the most aggressive endometrial tumours.

Chapter III evaluated the performance of a highly sensitive ddPCR assay to characterize microsatellite instability. The analysis of UAs from endometrial cancer patients showed high concordance with the standard method, highlighting its clinical utility. Besides, the assay showed value to detect the presence of ctDNA in cfDNA from high-risk tumours and monitor the disease evolution.

In Chapter IV we analysed pre-surgery and longitudinal plasma cfDNA and ctDNA from endometrial cancer patients, correlating high pre-surgical levels of both markers with poor prognosis. A combined analysis of both markers improved risk stratification, identifying patients with a fast and poor disease evolution. Longitudinal cfDNA/ctDNA analysis proved effective in predicting relapse and monitoring the therapy response, enhancing endometrial cancer management.

In Chapter V, circulating tumour cells were evaluated in localized endometrial cancer patients, with higher levels associated with aggressive phenotypes and shorter survival times. CTC presence correlated with poor prognosis but lacked independent prognostic significance.

Chapter VI explored the clinical utility of preclinical models generated from minimally invasive samples. Patient-derived spheroids and organoids proved reliable in recapitulating the tissue of origin and identifying effective

USC UNIVERSIDADE DE SANTIAGO DE COMPOSTELA

treatments, showcasing their potential for personalized medicine in endometrial cancer management.

The liquid biopsy-based pipeline described in the thesis demonstrates significant clinical utility, as evidenced by its implementation at the clinical hospital of Santiago de Compostela, resulting in early relapse detection, treatment initiation, and the generation of reliable preclinical models. Overall, the thesis aimed to improve patient management in both localized and advanced endometrial cancer through the clinical application of liquid biopsy techniques.

USC UNIVERSIDADE DE SANTIAGO DE COMPOSTELA

1 | INTRODUCTION

USC
UNIVERSIDADE
DE SANTIAGO
DE COMPOSTELA

INTRODUCTION

1.1 | Endometrial Cancer

1.1.1 | Epidemiology and aetiology

Endometrial cancer (EC) is the most common gynaecologic cancer in developed countries. This tumour incidence varies globally, with higher rates reported in North America and Europe compared to Asia and Africa. In Europe, EC is the fourth most common cancer in women, with an estimated death toll of 27217 in 2024 (1).

EC originates in the endometrium, the inner lining of the uterus. The endometrium is a highly proliferative tissue that undergoes cyclic changes in response to hormonal fluctuations during the menstrual cycle (2,3).

EC is primarily a disease of postmenopausal women, and the incidence increases with age. With the majority of cases being diagnosed in women aged 55 and older. There are also notable racial and ethnic disparities in the incidence and mortality rates of this tumour (2). In general, non-Hispanic white women have higher incidence rates compared to African American, Hispanic, and Asian/Pacific Islander women. Nonetheless, African American women have higher mortality rates (4).

The aetiology contributing to the development of EC, is multifactorial and involves a combination of genetic, hormonal, and environmental factors (2,3,5). For instance:

i) Prolonged exposure to oestrogen without sufficient progesterone. Oestrogen promotes the growth and proliferation of endometrial cells. In a normal menstrual cycle, progesterone acts as a check on oestrogen's stimulatory effects. Prolonged exposure to oestrogen without adequate

USC UNIVERSIDADE DE SANTIAGO DE COMPOSTELA

progesterone, such as in anovulatory cycles or conditions like polycystic ovary syndrome (PCOS), can lead to unopposed oestrogen stimulation, resulting in abnormal growth of the endometrium and an increased risk of cancer.

ii) Conditions like early menarche, late menopause, and hormone replacement therapy without progestin are associated with an increased risk. Early onset of menstruation (menarche) and late menopause expose women to a longer duration of menstrual cycles. This translates to a more extended period of exposure to oestrogen. Hormone replacement therapy (HRT), especially when it includes oestrogen without progestin, can mimic this prolonged exposure, increasing the risk. Progestin is crucial in HRT to balance the effects of oestrogen and reduce the risk of endometrial hyperplasia and cancer.

iii) Obesity is a significant risk factor for endometrial cancer, since adipose tissue produces oestrogen, and excess adiposity can lead to hormonal imbalances. Adipose tissue, particularly visceral fat, is metabolically active and can produce oestrogen through a process called aromatization. Postmenopausal women, who no longer produce oestrogen in their ovaries, rely on peripheral tissues like adipose tissue for oestrogen. Obesity, therefore, leads to increased oestrogen levels, which can promote the development of EC.

iv) Type 2 diabetes and insulin resistance. Insulin resistance, common in type 2 diabetes, results in elevated levels of insulin in the bloodstream. Insulin, apart from its role in glucose metabolism, has mitogenic effects. High insulin levels may stimulate the growth of endometrial cells, potentially increasing the risk of cancer (6).

v) Inherited genetic syndromes and hereditary breast and ovarian cancer syndrome, are associated with an elevated risk of EC. Lynch syndrome is

USC UNIVERSIDADE DE SANTIAGO DE COMPOSTELA

characterized by defects in DNA mismatch repair genes (*MLH1, MSH2, MSH6, PMS2*), leading to microsatellite instability (MSI) and an increased risk of various cancers, including EC. Mutations in *BRCA1* and *BRCA2* genes, known for their role in DNA repair, can also elevate the risk of EC.

iv) Environmental factors. Although more limited in clarity towards the impact on EC, environmental factors such as exposure to endocrine-disrupting chemicals, certain dietary habits, and lifestyle factors might influence EC risk. However, further research is needed to identify and understand the specific environmental elements contributing to this risk.

The overall survival rates for EC are relatively favourable compared to some other gynaecological cancers, especially when detected at an early stage. Five-year survival rates are higher for localized (confined to the uterus) cases compared to regional or distant metastatic cases; where the survival rates decrease down to 10% (3). The good overall survival rates are directly associated with early diagnosis of the disease, thanks to some easily recognizable symptoms: i) abnormal uterine bleeding; ii) pelvic pain; iii) dyspareunia; iv) irregular menstrual cycles, or v) swelling in the abdomen, among others (3).

1.1.2 | Endometrial carcinoma classification

1.1.2.1 | Histology

The histological subtypes of EC, primarily classified as endometrioid (EEC) and non-endometrioid (NEEC), provide insights into the cellular architecture and behaviour of the tumour. The 5th edition of the WHO Classification of Female Genital Tumours recognises the following (7):

1) Endometrioid Carcinomas (EEC) are characterised by glandular structures resembling the normal endometrium. EEC represents the majority

USC UNIVERSIDADE DE SANTIAGO DE COMPOSTELA

of cases and are associated with favourable prognoses, especially when diagnosed at an early stage. Its distinct histopathological features, including well-differentiated cells and a typically indolent behaviour, contribute to a more favourable prognosis (Figure 1A-B) (8).

2) Serous Carcinomas (SC) are considered high grade tumours with an extremely aggressive phenotype. They frequently invade the surrounding tissue and metastasize to distant organs. High grade nuclei, prominent nucleoli are common characteristics, also commonly associated with high aberrant mitotic activity. They represent around 10% of total EC cases but account for up to 40% of EC-related deaths. SC are most commonly found on older patients of African ethnicities. It is usually associated with *TP53* mutations and gene amplifications (Figure 1C) (8–10).

3) Clear Cell Carcinomas (CCC) are characterised by clear cytoplasm within the tumour cells. Although considered a high-grade tumour, it can form glandular structures. It represents less than 10% of total EC cases, more commonly found on women of Asian descent and is associated with poor prognosis.

4) Mixed Carcinomas (MC) present multiple histological subtypes within the same tumour. This heterogeneity translates into a difficult clinical management. The prognosis depends on the histological types and is influenced by the behaviour of the most aggressive histological component. Mixed EEC and SC account for about 10% of EC.

5) Undifferentiated Carcinomas (UC) represent around 2% of tumours characterised by a lack of differentiation. Tumour cells do not exhibit the typical features of glandular or squamous differentiation. They are generally associated with high aggressiveness and poor prognosis.

USC UNIVERSIDADE DE SANTIAGO DE COMPOSTELA

6) Carcinosarcomas (CS) are characterised by the presence of both epithelial and mesenchymal components in the same tumour. They are high grade tumours with an aggressive behaviour and poor prognosis; around 45% of cases are diagnosed at stage III or IV. They account for about 5% of all uterine malignancies.

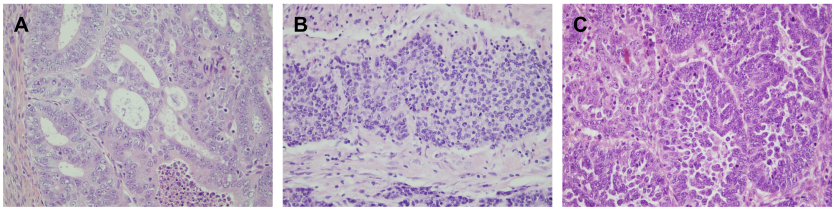


Figure 1: Representative immunohistochemistry haematoxylin and eosin slides of endometrial tumours**. A.** EEC of low grade **B.** EEC of high grade **C.** serous carcinoma. (Images at 40x).

1.1.2.2|Grade

EC grading plays a key role in stratifying the disease based on its cellular characteristics and aggressiveness. Typically classified into three grades (G1, G2, and G3), the grading system reflects the degree of differentiation of cancer cells (3,7).

- **Grade 1 (G1)** tumours exhibit well-differentiated cells, closely resembling normal endometrial tissue, and are associated with a more favourable prognosis. Up to 5% of solid non-glandular growth (Figure 1A).
- **Grade 2 (G2)** tumours display moderate differentiation. Between 6-50% of solid non-glandular growth
- **Grade 3 (G3)** tumours are characterized by poorly differentiated cells, indicating a higher degree of aggressiveness. Over 50% is considered solid non-glandular growth (Figure 1B-C).

USC UNIVERSIDADE DE SANTIAGO DE COMPOSTELA

The presence of severe cytological atypia in most of the cells (>50%) increases the grade by one level. The grading system serves as a critical tool for clinicians to assess the potential for tumour progression and metastasis, guiding treatment decisions and influencing prognostic evaluations (7,11).

1.1.2.3 | Myometrial Infiltration

The degree of myometrial infiltration is a pivotal prognostic risk factor. The degree of myometrial invasion, according to the most recent guidelines, asses the percentage of infiltration relative to the overall thickness of the myometrium. Hence, the following three levels are considered: none, <50% or ≥50% (7). Multiple studies have shown the independent value of myometrial infiltration in clinical outcome (11).

1.1.2.4 | Lymphovascular Space Infiltration

Lymphovascular space invasion (LVSI) refers to the presence of cancer cells within lymphatic channels or blood vessels. In EC, 5-15% of cases present LVSI. It holds particular significance in determining the aggressiveness of the disease and it can influence treatment decisions. Current clinical guidelines highlight the importance of distinguishing between “substantial” or “extensive” LVSI from “focal” or “no” LVSI (7,8,12,13).

1.1.2.5 | Molecular classification

One of the most important advancements on EC research and clinical management has been, with no doubt, the implementation of the molecular classification. The ability to molecularly segregate EC and estimate the risk of recurrence and survival has been a breakthrough for EC. Multiple studies have ventured into the study of genomic alterations in EC, but the two most important have been the TCGA and PROMISE studies (10,14,15). Based on the results from both studies, four molecular groups can be stablished: 1)

USC UNIVERSIDADE DE SANTIAGO DE COMPOSTELA

POLE – ultra mutated, 2) MSI-H/dMMR, 3) $TP53_{abn}$ and/or high-copy number, 4) Non-specific molecular profile.

|POLE ultra muted

The *POLE* ultra mutated group (~12%) is characterized by somatic hotspot mutations in the exonuclease domain of the *POLE* gene (DNA polymerase epsilon), which plays a crucial role in DNA replication and repair (16). The term "ultra mutated" refers to an exceptionally high mutation rate seen in tumours belonging to this subtype. The mutations in the POLE gene result in a hyperactive DNA polymerase, leading to an increased number of genetic mutations within the cancer cells.

Despite the high mutation load, the *POLE* ultra mutated subtype is associated with an excellent prognosis compared to other EC subtypes. Patients within this group often have a better response to treatment and improved overall survival.

Moreover, they frequently show an increased presence of tumour-infiltrating lymphocytes, suggesting an enhanced immune response against the cancer cells. This immunogenicity may contribute to the favourable clinical outcomes observed in this subtype. Moreover, the presence of tumour-infiltrating lymphocytes and the immunogenic nature of *POLE* ultra mutated tumours have sparked interest in exploring immunotherapy as a potential treatment strategy for patients within this molecular subtype.

|Microsatellite Instability (MSI)

Microsatellite instability-high/hypermutated tumours (~30-40%) are characterized by EECs or undifferentiated carcinomas with defects in the DNA mismatch repair (dMMR)/MSI. These tumours are characterized by alterations in the length of repetitive DNA sequences known as

USC UNIVERSIDADE DE SANTIAGO DE COMPOSTELA

microsatellites, which result from defects in the MMR system. MSI in EC is often associated with Lynch syndrome, an inherited genetic condition characterized by germline mutations in MMR genes (*MLH1*, *MSH2*, *MSH6*, *PMS2*). Lynch syndrome increases the risk of various cancers, including EC.

MSI tumours exhibit a higher mutation rate. Therefore, tend to have a higher level of immune system activation, with increased infiltration of immune cells into the tumour microenvironment. This heightened immunogenicity is associated with a more favourable response to immunotherapy. Particularly, immune checkpoint inhibitors represent a good treatment option to treat this tumour type. Of note, MSI tumours have an intermediate prognosis.

| $TP53_{abn}$ / High-copy number

This group of patients (~18%) are characterised by having a high number of somatic copy-number alterations with a low mutation rate. Mutations are mostly (95%) *TP53* mutations. Most of these tumours are SC, but up to 25% are EEC (mostly high-grade) and carcinosarcomas.

Mutations in the *TP53* gene, can result in loss of its tumour-suppressive function. Moreover, they present high genomic instability. This instability can lead to the gain or loss of entire sections of chromosomes, contributing to the development and progression of cancer. This subset of patients often have a more aggressive clinical course. And are associated with a higher likelihood of metastasis, poorer response to treatment, and a less favourable prognosis.

| Non Specific Molecular Profile (NSMP)

This group of patients (~30%) have considerable morphologic and clinical diversity. Which mostly includes EECs and CCCs with low copy-number alterations and low mutational burden. Although considered to be an

USC UNIVERSIDADE DE SANTIAGO DE COMPOSTELA

intermediate group, considerable heterogeneity within the NSMP category exists in terms of clinical outcomes as some patients have an excellent prognosis, whereas others have a more aggressive disease course with associated morbidity and mortality.

| Multiple Classifiers

A small subset of tumours present multiple classifiers (i.e $POLE_{mut}$ and $TP53_{abn}$) they are referred to as "multiple classifiers." In the case of multiple classifiers with $POLE_{mut}$ or dMMR and secondary *TP53* abnormality, the current scientific evidence suggests that they should be classified as $POLE_{mut}$ or dMMR tumours since they retain the favourable prognosis. For tumours both $POLE_{mut}$ and dMMR, data are limited (8).

TCGA molecular-based classification is currently being applied in the clinical practice (11). A simplified surrogate that includes three immunohistochemical markers (*TP53, MSH6*, and *PMS2*) and one molecular test (pathogenic *POLE* mutations) is used to classify tumours into one of the 4 groups (Figure 2).

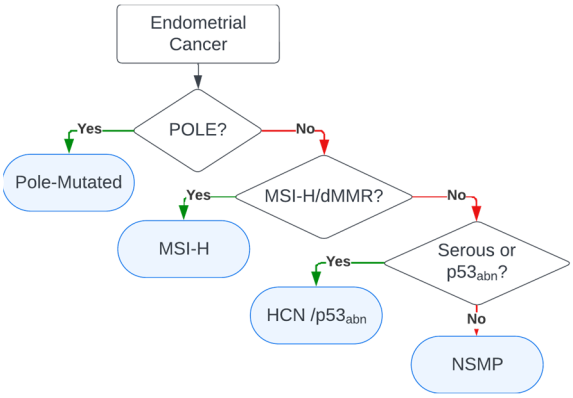


Figure 2: Diagram of the molecular classification and recommendations for molecular profiling in EC.

USC UNIVERSIDADE DE SANTIAGO DE COMPOSTELA

1.1.2.6|FIGO

The FIGO (International Federation of Gynaecology and Obstetrics) staging, ranges from Stage I to IV, considers various factors such as tumour size, invasion, involvement of adjacent structures and the molecular characteristics. The current 2023 FIGO staging classification is summarised on Table 1 (8).

USC UNIVERSIDADE DE SANTIAGO DE COMPOSTELA

Table 1: 2023 FIGO staging of cancer of the endometrium (Adapted from Berek et al, 2023 (8)).

Stage I	Confined to the uterine corpus and ovary
IA	Disease limited to the endometrium OR non-aggressive histological type, i.e., low-grade endometroid, with invasion of less than half of myometrium with no or focal LVSI OR good prognosis disease **IA1** Non-aggressive histological type limited to an endometrial polyp OR confined to the endometrium **IA2** Non-aggressive histological types involving less than half of the myometrium with no or focal LVSI **IA3** Low-grade EEC limited to the uterus and ovary
	IAm$_{POLEmut}$ POLE$_{mut}$ EC, confined to the uterine corpus or with cervical extension, regardless of the degree of LVSI or histological type
IB	Non-aggressive histological types with invasion of half or more of the myometrium, and with no or focal LVSI
IC	Aggressive histological types‖ limited to a polyp or confined to the endometrium
Stage II	Invasion of cervical stroma without extrauterine extension OR with substantial LVSI OR aggressive histological types with myometrial invasion
IIA	Invasion of the cervical stroma of non-aggressive histological types
IIB	Substantial LVSI of non-aggressive histological types
IIC	Aggressive histological types with any myometrial involvement
	IICm$_{p53abn}$ p53$_{abn}$ EC confined to the uterine corpus with any myometrial invasion, with or without cervical invasion, and regardless of the degree of LVSI or histological type
Stage III	Local and/or regional spread of the tumour of any histological subtype
IIIA	Invasion of uterine serosa, adnexa, or both by direct extension or metastasis
	IIIA1 Spread to ovary or fallopian tube (except when meeting stage IA3 criteria)
	IIIA2 Involvement of uterine subserosa or spread through the uterine serosa
IIIB	Metastasis or direct spread to the vagina and/or to the parametria or pelvic peritoneum **IIIB1** Metastasis or direct spread to the vagina and/or the parametria
	IIIB2 Metastasis to the pelvic peritoneum
IIIC	Metastasis to the pelvic or para-aortic lymph nodes or both
	IIIC1 Metastasis to the pelvic lymph nodes
	IIIC2 Metastasis to para-aortic lymph nodes up to the renal vessels, with or without metastasis to the pelvic lymph nodes
Stage IV	Spread to the bladder mucosa and/or intestinal mucosa and/or distance metastasis
IVA	Invasion of the bladder mucosa and/or the intestinal/bowel mucosa
IVB	Abdominal peritoneal metastasis beyond the pelvis
IVC	Distant metastasis, including metastasis to any extra-or intra-abdominal lymph nodes above the renal vessels, lungs, liver, brain, or bone

USC UNIVERSIDADE DE SANTIAGO DE COMPOSTELA

1.1.2.7 | Risk Stratification

Traditional pathologic features, such as histopathologic type, grade, myometrial invasion, and LVSI, have been traditionally used in assessing risk of recurrence after surgery. However, recent guidelines have included the molecular classification since it adds further information to the conventional morphologic features and increases the accuracy of the classification of the patients (12) (Table 2).

USC UNIVERSIDADE DE SANTIAGO DE COMPOSTELA

Table 2: Definition of prognostic (Adapted from Oaknin et al 2022 (12)).

Risk Group	Molecular Classification unknown	Molecular Classification known
Low	Stage IA + low grade + LVSI negative or focal	Stage I-II **POLEmut** with no residual disease
		Stage IA **dMMR/NSMP** EEC + low grade + LVSI negative or focal
Intermediate	Stage IB EEC + low grade + LVSI negative or focal	Stage IB **dMMR/NSMP** EEC + low grade + LVSI negative or focal
	Stage IA EEC + high grade + LVSI negative or focal	Stage IA **dMMR/NSMP** EEC high grade + LVSI negative or focal
	Stage IA NEEC without myometrial infiltration	Stage IA **$TP53_{abn}$** and/or NEEC without myometrial infiltration
High-Intermediate	Stage I EEC + substantial LVSI regardless or grade and depth of invasion	Stage I **dMMR/NSMP** EEC + substantial LVSI regardless of grade and depth of invasion
	Stage IB EEC high-grade regardless of LVSI status	Stage IB **dMMR/NSMP** EEC high grade regardless of LVSI status
	Stage II	Stage II **dMMR/NSMP** EEC
High	Stage III-IVA with no residual disease	Stage III-IVA **dMMR/NSMP** EEC with no residual disease
	Stage I-IVA NEEC with myometrial infiltration and with no residual disease	Stage I-IVA **$TP53_{abn}$** EEC with myometrial infiltration and no residual disease
		Stage I-IVA **dMMR/NSMP** NEEC with myometrial infiltration and no residual disease
Advanced metastatic	Stage III-IVA with residual disease	Stage III-IVA with residual disease of any molecular subtype
	Stage IVB	Stage IVB of any molecular subtype

USC UNIVERSIDADE DE SANTIAGO DE COMPOSTELA

1.1.3 | Therapeutic approaches

Treatment tailored to the tumour biology should be the optimal strategy to balance out the efficacy against toxicity. Treatment strategies for EC are evolving with the development of molecular analysis and precision-based approaches. Nonetheless, the treatment paradigm has not strongly changed in the past 10 years for patients with EC, especially for those with localized disease. Surgical resection, cytotoxic chemotherapy, endocrine or hormonal treatment, and radiation have been the mainstays of treatment for many years (17,18). These strategies are described in more detail below.

1.1.3.1 | Surgical Resection

Standard treatment consists of surgical resection of the affected areas by hysterectomy and bilateral salpingo-oophorectomy. During the surgery, the uterus, cervix, ovaries and fallopian tubes are removed. In patients with high risk of recurrence it is usually accompanied by lymphadenectomy which removes nearby lymph nodes and, potentially, enables the identification of lymph node-positive patients. These patients usually receive adjuvant treatment, including radiotherapy and chemotherapy (3,12).

1.1.3.2 | Hormone Treatment

Progesterone has been the key target of hormonal treatment in EC due to its direct link to cancer tumorigenesis. It has a protective effect against ER-positive EC. Hormonal replacement by the administration of progesterone or analogous components (megestrol acetate or medroxyprogesterone) are given to patients, mainly with unresectable tumours or that want to maintain fertility (12). In terms of effectivity, some discrepancies are found ranging from minimal activity of the drug to 11-50% response rates (19,20). The main

USC UNIVERSIDADE DE SANTIAGO DE COMPOSTELA

drawback of this therapeutic approach is related to the acquisition of resistances due to prolonged exposure (21).

As previously mentioned, another risk factor that promotes EC tumorigenesis is an excessive exposure to oestrogen in absence of progesterone. Therefore, inhibition of oestrogen induced proliferation by anti-oestrogen agents seems like a reasonable path to follow. For instance, Fulvestrant has been evaluated in a phase II clinical trial (NCT00334295) in patients with ER and/or PR positive advanced or recurrent EC with good tolerate and toxicity rates. In terms of effectivity, some discrepancies are found ranging from minimal activity of the drug to improved survival rates (22).

1.1.3.3 | Radiotherapy

Radiation is commonly used after surgery. It kills any hazardous cells that may still be in the treated area. Most commonly used to treat patients with low or intermediate risk. Radiotherapy treatment is based on the usage of high doses of high-energy radiation to kill cancer cells. In EC there are two main forms. It can be either applied locally at the vaginal area (vaginal brachytherapy) or more generalized to an area that includes the pelvis and para-aortic region (external radiotherapy) (3).

Patients above 60 years old with EEC and or LVSI have more favourable responses to adjuvant radiotherapy with a significant decrease on the risk of tumour recurrence (23–25). Although in patients with more aggressive phenotypes (grade 3 or with minimal residual disease) the evidence of decrease risk of recurrence is not significant (23,26). As shown by the randomized clinical trials NSGO-EC-9501/EORTC-55991 and MaNGO ILIADE-III, patients with more aggressive phenotypes benefit from radiotherapy in combination with chemotherapy regiments (27).

USC UNIVERSIDADE DE SANTIAGO DE COMPOSTELA

1.1.3.4 | Chemotherapy

Chemotherapy is mainly used on patients with advance stages of the disease. Previous studies have shown that Stage I does not benefit from chemotherapy (26). Few options are available for patients with high stages or advanced disease, treatments are mainly based on:

- Alkylating agents which induce cytotoxic DNA damage with the addition of mutagenic damage. Some of the most commonly used drugs against EC fall within this category, such as, Carboplatin or Cisplatin.
- Taxanes that block cell cycle progression through centrosome impairment, induction of abnormal spindles and suppression of spindle microtubule dynamics. They tend to trigger apoptosis due to aberrant mitosis (28). One of the most commonly drugs used in EC falls into this category, Paclitaxel.
- Anthracyclines disrupt DNA by affecting the topoisomerase, an enzyme that is involved on the DNA for replication and synthesis, thereby causing growth arrest and programmed cell death (29). Doxorubicin is an anthracycline that has shown effectiveness on EC treatment (30).
- Vinca alkaloids arrest dividing cells in metaphase by binding tubulin and preventing its polymerization into microtubules (31). Vinorelbine is sporadically used on patients with advanced disease, typically in combination with Gemcitabine (32).
- Antimetabolites can either mimic purines and pyrimidines that are required for DNA synthesis or by interfere with the synthesis. Typically they affect the cells in the S phase of the cell cycle (cell-cycle specific) when DNA replication is occurring (33). Gemcitabine is a good example of an antimetabolite agent that has shown good results on EC (34).

USC UNIVERSIDADE DE SANTIAGO DE COMPOSTELA

1.1.3.5 | Targeted Therapy

The knowledge of the intrinsic mechanisms on EC biology has led to the focus on targeted therapies. The most commonly explored therapeutic targets in EC resolve around the immune evasion, apoptosis, angiogenesis and proliferation (17,18). A graphical summary of the most relevant molecular pathways with interest as therapeutic targets can be found on Figure 3.

One of the main hallmarks of cancer is immune evasion, or in other words how cancer cells adapt to evade the detection and destruction by the immune system. Immune checkpoint blockade (ICB) therapies have redesigned the clinical management of many cancers. Of special interest for EC, are anti-PD1 therapies that involve blocking the programmed cell death protein 1 (PD-1) receptor on immune cells, preventing its interaction with PD-L1 on cancer cells, thereby enhancing the immune response against cancer by removing an inhibitory signal. Since 2017, two anti-PD1 treatments (Dostarlimab and Pembrolizumab) have been approved by the FDA, for the treatment of advanced or unresectable EC with either MSI or dMMR proteins (35,36).

Although immunotherapy is still not approved for the treatment of EC at first line, studies like DOMENICA (GINECO-EN105b/ENGOT-en13) are trying to show the efficacy of Dostarlimab in first line *versus* the traditional chemotherapy regimen. The study is designed to expect a 17.8-months PFS in Dostarlimab arm and a 10-months PFS in the CT arm, translating to a hazard ratio of 0.58 (37).

USC UNIVERSIDADE DE SANTIAGO DE COMPOSTELA

Table 3: Summary of the ESGO recommended treatments to treat EC (38).

Risk of Recurrence	Clinical features	ESGO Recommendations
Low Risk	Regardless of clinicopathological features	No adjuvant treatment is recommended
Intermediate Risk	EEC Stage IA G3 (dMMR or NSMP) and no or focal LVSI	Adjuvant vaginal brachytherapy
	EEC Stage IB G1-G2 (dMMR or NSMP) and no or focal LVSI	
	EEC Stage II G1 (dMMR or NSMP) and no or focal LVSI	
	P53abn tumours Stage IA	No adjuvant treatment is recommended
High-Intermediate Risk	Stage IA and IB with substantial LVSI	External beam radiotherapy
	Stage IB G3	
	Stage II G1 with substantial LVSI	External beam radiotherapy + concomitant chemotherapy
	Stage II G2-G3 (dMMR or NSMP)	
High Risk	All stages and all histologies with p53abn and myometrial infiltration	Adjuvant external beam radiotherapy and concurrent chemotherapy Sequential chemotherapy and radiotherapy Chemotherapy alone
	All stages with SC or UC including CS with myometrial infiltration	
	All stages III and IVA with no residual tumour, regardless of histology and molecular subtype	
Advanced Disease (1st Line)	Low-grade carcinomas with EEC low-volume/indolent disease	Hormonal therapy (Progestings, Ais, Tamoxifen, Fulvestrant)
	Others	Chemotherapy (Carboplatin AUC 5-6)+ Paclitaxel (175mg/m^2)
Advanced Disease (rechallenge)	MSI-H/dMMR	Rechallenge with platinum-based therapy
		Other chemotherapies (Doxorubicin or Paclitaxel)
		Dostarlimab or Pembrolizumab-Lenvatinib
	MSS/pMMR	Rechallenge with platinum-based therapy
		Other chemotherapies (Soxorubicin or Paclitaxel)
		Pembrolizumab-Lenvatinib

USC UNIVERSIDADE DE SANTIAGO DE COMPOSTELA

Antiangiogenics therapies are usually used in combination with immunotherapy treatments. Antiangiogenics are a class of kinase inhibitors that bind either the angiogenic factors or their receptors. This treatment usually reshapes the irregular vessels back to a normal intra-tumoral vascular network. This remodelling translates into a better delivery of other anti-tumoral drugs. Moreover, antiangiogenics have a clear effect on the immune system. They reduce the hypoxia conditions which favours an immune-suppressive phenotype since it increases the expression of PD-L1 in cytotoxic lymphocytes (39). The current approved antiangiogenics treatment for EC are anti-VEGF (Lenvatinib, Bevacizumab) monoclonal antibodies that binds to VEGF, a protein that promotes the growth of new blood vessels (17).

On the other hand, the PI3K/AKT/mTOR signalling pathway is one of the most commonly affected pathways in EC. It has a crucial role in cell growth, survival, proliferation, metabolism, apoptosis and angiogenesis (17). This pathway has also crosstalk with the RAS pathway or the oestrogen receptors. Deregulation of this signalling pathway leads to overactivation in gynaecological tumours. Based on the high incidence of alterations, inhibitors of different components within the pathway have been explored in EC (17,40,41). Although PI3K inhibitors (Alpelisib, Everolimus) have been approved by the FDA for the treatment of other tumours such as breast cancer, there are no FDA-approved drugs indicated for the treatment of advanced EC. Nonetheless, despite the contradictory results on the efficacy of PI3K/AKT/mTOR inhibitors, there are several of preclinical studies still researching the potential applicability on advanced EC.

Another focus of interest for targeted therapies in EC resolves around PARP inhibitors (PARPi). This treatment works under the premise of generating DNA double stranded breaks (DSBs), the most aggressive type of

USC UNIVERSIDADE DE SANTIAGO DE COMPOSTELA

DNA damage. Cells with a functional homologous-recombination repair (HRR) system would be able to efficiently get rid of the DSBs (42). Gynaecological tumours have moderate rates (~10-15%) of alterations in genes related to the HRR system, such as *BRCA1/2, ARID1A, ATM, PALB2* or *RAD50*, among others (10). Therefore, PARPi, such as Olaparib or Niraparib, could be promising treatment options for patients with alterations in the HRR system. On going clinical trials (NCT05320757, NCT04716686) are evaluating the efficacy of PARPi on advanced EC patients and the impact on the tumour microenvironment. Nevertheless, currently the usage of PARPi on advanced patients is not FDA-approved.

It is important to mention that, traditionally, the molecular characterization of EC has been addressed by the analysis of solid biopsies but personalized targeted treatments need for a dynamic way to characterize the molecular evolution and heterogeneity of EC. Therefore, the use of minimally invasive biopsies to characterize EC represents a key pillar for the application of targeted therapies in EC patients.

USC UNIVERSIDADE DE SANTIAGO DE COMPOSTELA

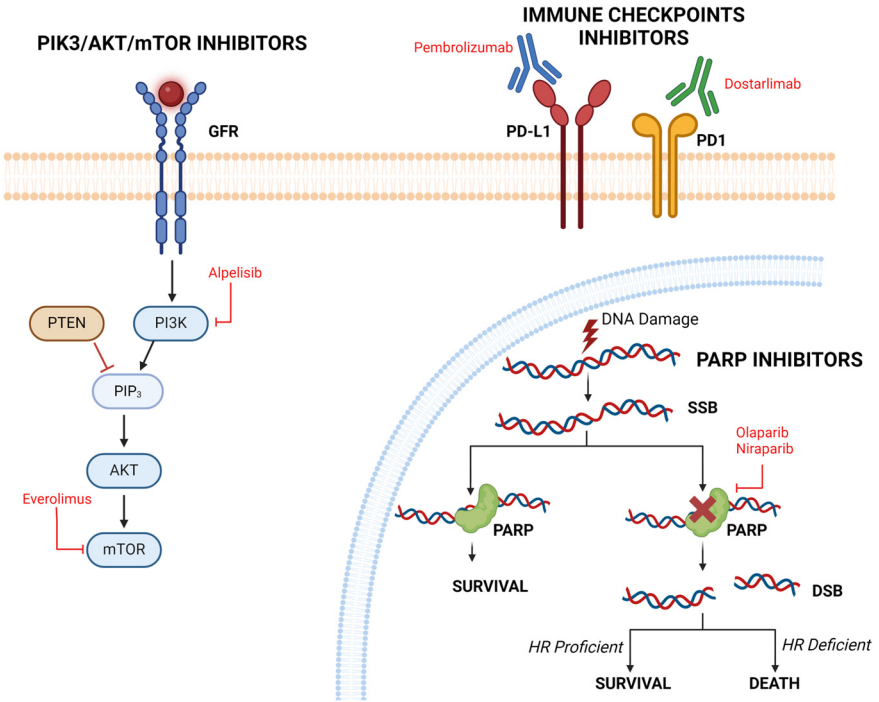


Figure 3: Graphical representation of the most relevant pathways in EC carcinogenesis and the targetable elements. *Created with BioRender.com.*

1.1.4 | Main Clinical Challenges For Personalized Management Of EC

Lack of non-invasive and accurate diagnostic methods. Early and precise diagnosis of EC is difficult using the currently available techniques. There are no screening programmes and very often the diagnostic process starts when symptoms, such as abnormal uterine bleeding, occur (43). Symptomatic women often undergo invasive procedures like outpatient biopsies including hysteroscopy. Whilst causing (sometimes significant) physical discomfort and psychological stress, only 5%–10% of the women subjected to these procedures will be diagnosed with EC or an EC precursor (44). Therefore, non-invasive and accurate methods for EC detection, especially in high-risk population, are a major need in EC.

USC UNIVERSIDADE DE SANTIAGO DE COMPOSTELA

Accurate risk stratification. Identifying those EC patients at the highest postsurgical risk of recurrence is essential to ensure that patients receive appropriate care whilst avoiding the harms and costs of unnecessary treatments. However, optimal risk stratification remains an unsolved question in EC, since about 20% of patients classified post-surgery as low risk face recurrence disease. Although included in the risk classification system, molecularly guided management of EC lags behind most other cancers. Besides, the development of new clinical tools that combine clinical-pathologic, radiologic, and molecular characteristics to accurately predict the risk of recurrence is essential to better treat and thus improve the survival of these patients.

Personalised treatment selection. As previously commented, first-line treatment in recurrent or metastatic ECs is mainly chemotherapy independently of the molecular subtype. Besides, hormonal treatment and immunotherapy are almost the unique targeted therapies that are nowadays available for the treatment of advanced EC (45). Immunotherapy with single agent immune checkpoint inhibitors has shown activity in recurrent microsatellite unstable (MSI-high/dMMR) EC, but microsatellite stable ones can respond using a combination of approaches (46,47). Endocrine therapy is considered in recurrent/metastatic low-grade endometrioid tumours. Retained ER/PR expression is often used to consider this endocrine therapy, however, tumours with negative ER/PR expression may also respond to this therapeutic strategy (45,48–50). Notably, as described in previous section, other agents targeting specific mutations or pathways altered in EC are under evaluation in different clinical trials, including *PIK3CA* pathway, *PTEN*, *HRD*, *ARID1* and *FGFR2* mutations. However, to develop more tailored therapeutic approaches there is a clear need for accurate predictive markers to stratify

USC UNIVERSIDADE DE SANTIAGO DE COMPOSTELA

potentially responsive patients, monitor therapy response and identify resistance mechanisms (51).

Preclinical models to test personalized therapies. The increasing availability of targeted molecular therapies to treat EC opens new opportunities to develop a more personalized treatment and improve survival outcomes for women with advanced disease. However, prioritization of treatments requires functional testing, especially in cases in which the drug-biomarker-activity association has not been clearly validated. Historically, *in vitro* cell lines have had a prominent role in anticancer drug development, although such models may lack clinical relevance due to the immortalization and adaptation processes induced by the continuous growth on plastic. For this reason, there is a clear need for the development of new *ex vivo* models that would better mimic the original EC physiology.

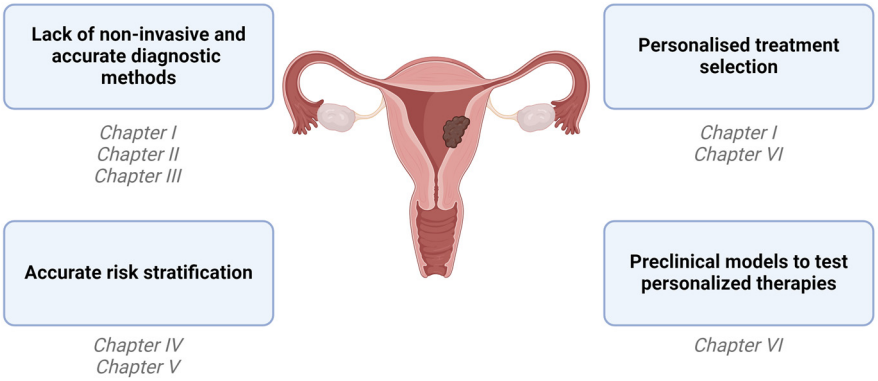


Figure 4: Summary of the main clinical challenges and the chapters where said challenges are tackled. *Created with BioRender.com.*

1.2 | Liquid Biopsy

The term liquid biopsy was first stablished in the early 21st century and has been gaining popularity ever since. It was born with the aim to improve

USC UNIVERSIDADE DE SANTIAGO DE COMPOSTELA

the management of different diseases, such as cancer, prenatal studies or infectious disease, among others (52). The objective was to study biomarkers in minimally invasive samples, that could provide information of the condition in real time. This field is being explored not just for its value as a potential tool to monitor the disease, but also as a tool to assess prognostic, patient stratification and early detection (52–54).

Since the beginning, liquid biopsy has revolutionised the clinical paradigm, especially in the oncological field, complementing the tissue biopsy to obtain diagnostic information. Although, both solid and fluid biopsies have its own limitations and advantages, both approaches are complementary in their own way.

Tissue biopsy has traditionally been the gold standard for diagnosis within the clinical context. It involves invasive procedures that may require anaesthesia. It provides highly accurate information of the tumour, but it only reflects a snapshot of the tumour with the risk of losing relevant information to select the proper therapy (55)

On the other hand, liquid biopsy analyses allow for the dynamic characterization of the disease in a minimally invasive way through the analyses of circulating biomarkers, such as circulating tumour DNA (ctDNA), circulating tumour cells (CTCs), extracellular vesicles, or other circulating elements. Moreover, liquid biopsy is not limited by tissue availability and provides a general overview of the tumour heterogeneity, not just a snapshot. Therefore, it represents a unique diagnostic opportunity for patients with non-accessible or widely spread tumours. Nonetheless, liquid biopsy has limitations in sensitivity and specificity since most of the circulating biomarkers analysed are found in a very low concentration (55) (Figure 5).

USC UNIVERSIDADE DE SANTIAGO DE COMPOSTELA

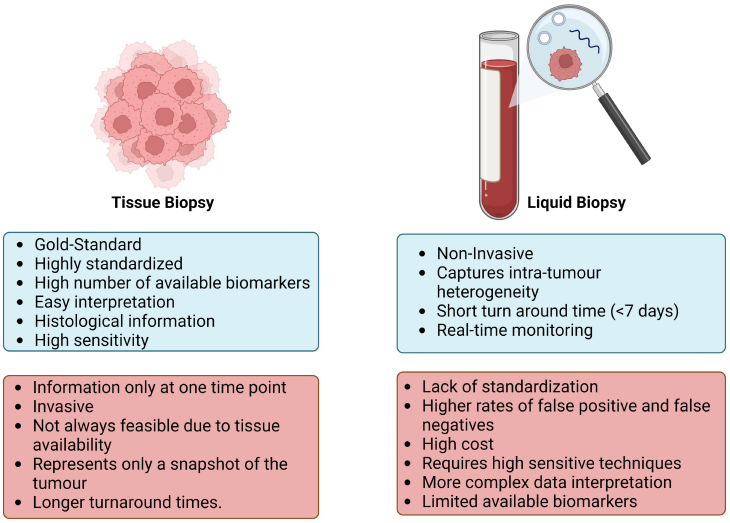


Figure 5: Limitations and advantages of liquid and solid biopsies. *Created with BioRender.com.*

The most frequently analysed circulating biomarkers are the CTCs and cfDNA/ctDNA. CTCs are tumour cells released into the bloodstream during the metastatic cascade (56). cfDNA is the total amount of circulating DNA within the bloodstream and the cfDNA of tumour origin is referred as ctDNA (52,57,58). Due to the numerous advantages of liquid biopsy, numerous clinical trials are being conducted around these biomarkers. In the database clinicaltrials.gov (Accessed December 2023) there are nearly 700 active clinical trials focused on the study of cfDNA/ctDNA and around 900 focused on CTCs in different tumour types.

USC UNIVERSIDADE DE SANTIAGO DE COMPOSTELA

1.2.1 | Circulating Blood based biomarkers

1.2.1.1 | Circulating free DNA

One of the most studied and widely used biomarkers in liquid biopsy research is the cfDNA. The term refers to the complex and heterogenous fraction of nucleic acids within bodily fluids (59). Although found in all individuals, higher levels of cfDNA have been found on patients with cancer, leading to the new term of circulating tumour DNA (ctDNA) to refer to the specific DNA of tumour origin. The concentration of cfDNA in healthy individuals its usually low, with concentrations around 10ng/mL (60,61). On patients with cancer, this concentration is much higher; nonetheless, it depends on the stage of the disease with proportions ranging from <0.1 to 90% of the total cfDNA being of tumour origin (52). Clearence is mediated primarily by the liver and it´s half-life is relative short. For instance in foetal DNA in maternal plasma has shown a two phase clearance ranging from 1h to 13h (62). In cancer patients the ctDNA half-life is around 2h (63).

The cfDNA is usually found as double stranded fragments of around 150-200bp, the size of the nucleosome, whereas ctDNA is usually found <145bp (64,65). This difference on size is most likely linked to the release mechanism and origin of the material (59). There are two main mechanisms as to how cfDNA is released into bodily fluids: secretion and cell death (Figure 6) (52,64,66).

(i) Active secretion, via exosomes or other type of extracellular vesicles has been described as the main release mechanism, accounting for over 90% of the total cfDNA. The cfDNA within the vesicles is protected from exonucleases (66).

USC UNIVERSIDADE DE SANTIAGO DE COMPOSTELA

(ii) Apoptosis, or programmed cell death is a process where through the binding of extracellular signals the caspase signalling pathway is activated. The caspase activation induces morphological and physiological changes within the cells that end up in nuclear retraction, lipid redistribution and DNA fragmentation. The caspase-activated DNase generate highly fragmented double stranded DNA (150-200bp) which is later released into the bodily fluids (66).

(iii) Necrosis, in contrast with apoptosis, is an unprogrammed cell death mechanism that occurs much more abrupt as a result of irreparable cell damage. The integrity of the membrane is compromised and the contents are released without specific DNase activity. Therefore, the resulting cfDNA fragments are much larger (>1000bp) (66).

(iv) NETosis, is a form or programmed cell death in neutrophils characterised by the release of granule components and decondensed chromatin into the extracellular space. The released cfDNA is around 1000bp in length (66,67).

(v) Pyroptosis, is an inflammatory form of cell death triggered mainly by microbial infections This process is mediated by cytokines and interleukins which induce a rapid cell death. The resulting cfDNA fragments are in line with the outcome of necrosis (66).

USC UNIVERSIDADE DE SANTIAGO DE COMPOSTELA

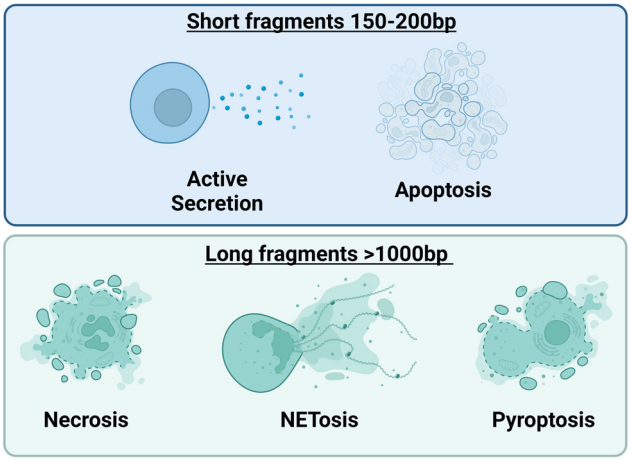


Figure 6: Release mechanism of cfDNA**.** Processes where the DNA is degraded such as through active secretion of apoptosis generates short fragments, whereas abrupt cell death, such as necrosis of pyroptosis, or NETosis produce long fragments. *Created with BioRender.com.*

1.2.1.1.1|Techniques to analyse cfDNA and ctDNA

During the past years, different technologies have been developed to study the cfDNA and the ctDNA. Starting with the cfDNA, numerous commercial kits have been developed to efficiently isolate cfDNA from bodily fluids, being the most commonly and efficient used isolation kit being QIAamp Circulating Nucleic Acid Kit (Qiagen) (68,69). For the quantification and size distribution studies of cfDNA, four main technologies are being used: spectrometry, electrophoresis, fluorometry and qPCR. The latter is the most specific strategy to analyse the cfDNA. More specific studies of the cfDNA are feasible and could be used to asses therapy efficacy or guide treatment selection (52,65). The study of specific alterations like epigenetic changes, genetic rearrangements, MSI, copy number alterations (CNA) or point mutations can be achieved through highly sensitive techniques, such as Next-Generation sequencing (NGS) or droplet-digital PCR, among others.

USC UNIVERSIDADE DE SANTIAGO DE COMPOSTELA

Nonetheless, the low concentration and sample availability poses a challenge for the study of these alterations (70). To circumvent said limitations, the consensus is to apply one of the following approaches: (a) the study of a single alteration or a small panel of alterations via PCR approaches; or (b) genome-wide studies using an NGS approach (71,72).

PCR-based approaches are a cost-efficient alternative that work under the premise of previous knowledge of the genetic background of the patients to focus on specific alterations. In the last years, new versions of the PCR were developed to improve the sensitivity via generation of emulsions and/or including magnetics beads (ddPCR, BEAMing). The sensitivity of PCR-based approaches ranges from 0.01%-1% usually dependant on the assay and input material. There are 3 FDA approved kits based on PCR technologies: (a) Cobas® EGFR Mutation Test v2, (b) Therascreen *PIK3CA* RGQ PCR Kit, and (c) mSEPT9 Blood Test (Epi proColon) (73).

NGS-based approaches perform genome-wide analyses. They could be divided into two options, (i) Panel-based approaches and, (ii) genome wide sequencing. NGS-based approaches have the advantage of providing patient-specific information and are more proficient at capturing intra-tumour heterogeneity and to assess clonal evolution through time. For panel-based approaches the sensitivity depends on the assay used but analytical limit of detections (LoD) of 0.01%-0.1% can be reached, although they have the limitation of analysing only a specific set of genes/alterations. There are two FDA approved targeted panels that can be applied on cfDNA samples (a) FoundationOne Liquid CDx, and (b) Guardant360 CDx (73). As for genome-wide sequencing approaches, whole-genome sequencing and whole-exome sequencing has been performed on cfDNA. The requirement of high cfDNA

USC UNIVERSIDADE DE SANTIAGO DE COMPOSTELA

input combined with more complex bioinformatic analyses make the clinical applicability of WGS or WES limited on cfDNA studies.

1.2.1.1.2 | Clinical applicability of cfDNA and ctDNA

Due to the numerous advances within the field and the rise of different technological approaches for the detection of cfDNA and ctDNA. Nowadays, the cfDNA/ctDNA analyses is implemented into the clinic (72). As previously mentioned, there are 3 FDA approved kits based on PCR technologies: (a) Cobas® EGFR Mutation Test v2, (b) Therascreen *PIK3CA* RGQ PCR Kit, and (c) mSEPT9 Blood Test (Epi proColon). The Cobas® *EGFR* Mutation Test v2 (Roche) allows for the screening of 42 EGFR mutations in patients with lung cancer and is approved to guide therapeutic decisions in anti-EGFR therapy (74). The Therascreen *PIK3CA* RGQ PCR Kit (Qiagen) is a qPCR that asses the mutation status of *PI3KCA* (11 alterations) in patients with breast cancer with the intend to identify eligible patients for *PIK3* inhibitors such as Alpelisib (75). And last, the Epi proColon (epigenomics) is the first FDA approved colorectal screening tool. It is based on the methylation pattern of the promoter SEPT9 that has been associated with the occurrence of colorectal cancer (76).

On the other hand, there are two FDA approved NGS-based technologies. One is the FoundationOne Liquid CDx (Foundation Medicine), approved for different solid tumours (77,78) and that analyses over 300 genes and interrogate TMB and MSI status. The other is the Guardant360 CDx (Guardant Health) mainly used for patients with lung and/or breast cancer to screen for actionable genes (79).

USC UNIVERSIDADE DE SANTIAGO DE COMPOSTELA

1.2.1.2 | Circulating tumour cells

Another classic liquid biopsy biomarker are the CTCs. These cells intravasate into the bloodstream from either primary or metastatic locations. In fact, CTCs are key for cancer dissemination during the metastatic cascade (80–82).

The metastatic cascade is a multi-stage process where cells from the primary tumour spread to other anatomical sites (83). The intravasation of the cells could happen in a passive manner, through the exponential growth of the tumour that it burst into blood vessels, finding more of an epithelial CTCs profile. Or through an active intravasation via the epithelial-mesenchymal transition (EMT), this phenotype allows them to intravasate through the endothelial walls of blood vessels to reach the blood stream (84,85). These cells are characterised by a mixed phenotype which may be an advantageous phenotype that promotes survival (83,84). While on circulation CTCs need to survive the shear stress and evade the immune system, which translates into a very short half-life (1-2.4h) (86). Nonetheless, a small percentage is able to extravasate to distant locations where they can remain dormant for years or form new tumour foci (Figure 7).

Due to the biological importance of CTCs, multiple studies have focused on the clinical significance of these cells and showed value to predict prognosis and response to treatment. The relevance of CTCs has been well documented on multiple cancer types, such as breast, lung, prostate or colorectal (86–88). Nonetheless, there is limited literature of the current value of CTCs for EC. Few studies have shown higher number of CTCs in patients with more aggressive phenotypes (89–91).

USC UNIVERSIDADE DE SANTIAGO DE COMPOSTELA

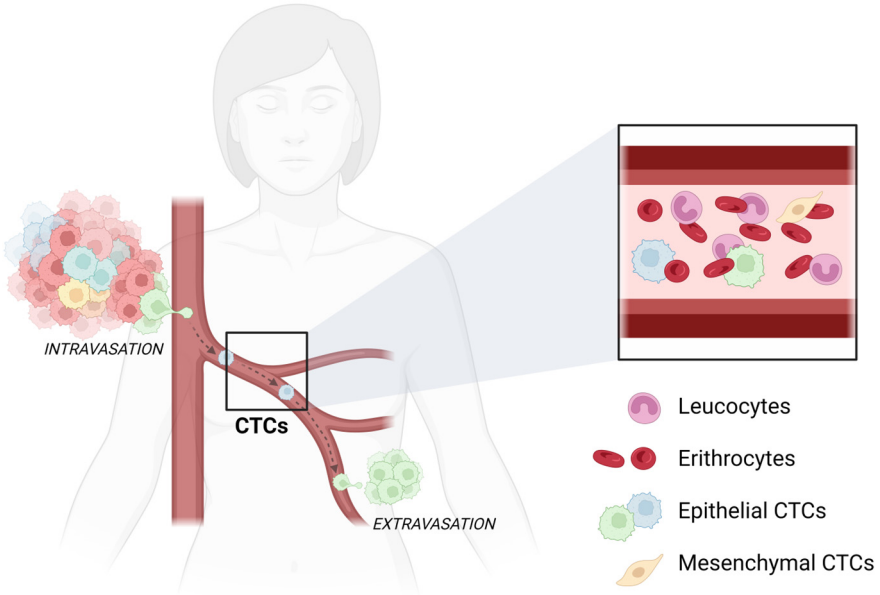


Figure 7: The metastatic cascade. Through the process of intravasation CTCs are release into the bloodstream until they find a new niche where they can extravasate and generate distant metastases. *Created with BioRender.com.*

1.2.1.2.1|Isolation technologies

The sparse number of CTCs in the bloodstream combined with the high heterogeneity are the main challenges that need to be tackle for the study of this biomarker. Currently, there are several isolation techniques to obtain an enriched fraction of CTCs. They are based on different physiological and physical properties, such as size, deformability and expression of different biomarkers (92). Following this premise, two main methods are being used (a) antigen dependant and (b) antigen independent.

USC UNIVERSIDADE DE SANTIAGO DE COMPOSTELA

|Antigen-dependant

Isolation in an antigen dependent manner is based on the presence of differential protein markers in the surface of CTCs that cannot be present on the surface of blood cells (positive enrichment) or vice versa (negative enrichment).

- Positive enrichment is based on the presence of surface biomarkers associated with the CTCs, being the most commonly marker used the epithelial cell adhesion molecule (EpCAM). The CellSearch® system (Menarini Silicon Biosystems) allows for the isolation of CTCs of epithelial origin (CD45-, EpCAM+, and cytokeratins 8, 18+, and/or 19+) in whole blood. First, a ferrofluid coated with anti-EpCAM captures the EpCAM+ population. Next, the captured population is screened with the nuclear marker DAPI, cytokeratins to identify the epithelial population and CD45 to discern from the blood cells. It is currently considered the 'gold standard' within the clinic and unique FDA-approved CTC isolation technologies together with the Parsortix™ system (Angle) (93,94). However, CellSearch system has limitations since it only allows the capture of epithelial CTCs, missing those cells with more mesenchymal profiles (94).

Nonetheless, new technologies are being developed based on other antigen-dependant strategies. For example, dual-antibody-modified fluorescent-magnetic nanoparticles have been developed to capture both epithelial and mesenchymal CTCs based on the expression of targeting EpCAM and N-cadherin (95). Other technologies are attempting to combine microfluidic devices with a combination of antibodies to immobilize the CTCs within the system for further studies (96).

USC UNIVERSIDADE DE SANTIAGO DE COMPOSTELA

- Negative enrichment focuses on removing the red and white blood cells from the samples to leave an enriched sample in CTCs. The RosetteSep™ technology (STEMCELL Technologies, Vancouver, BC, Canada) is one of the most used negative enrichments. It is based on bispecific antibodies that can crosslink red and white blood cells to form clusters, that can be removed through density gradient centrifugation (97,98).

|Antigen-independent

Isolation of CTCs can also be accomplished taking into consideration the different physical properties of the CTCs, such as size, deformability, density or electrical charges. Since CTCs are significantly larger when compared to other cells within the bloodstream, microfiltration devices have been developed to isolate them that combine both size and the deformability properties of the CTCs, an example is the Parsortix™ PC1 system (98,99). In May 2022, the FDA approved the usage of the Parsortix™ PC1 system for the isolation of CTCs from metastatic breast cancer patients. Other antigen-independent approaches take advantage of the differential density of the CTCs. The mononuclear cells and CTCs have a density <1.077 g/mL, while the other cells and granulocytes have a density >1.077 g/mL (100). Further label-free separation methods are based on hydrodynamic forces (96) or electrophysical properties of CTCs (101). Single cell CTC DNA/RNA analyses could provide new insights into novel therapeutic approaches that target the metastatic cascade itself (82).

1.2.1.2.2|Clinical applicability of CTCs

As previously mentioned, several clinical trials are being conducted on CTCs. Most of these studies are primarily focused on enumeration and how it can be correlated with the disease prognosis. CTCs have been detected in

USC UNIVERSIDADE DE SANTIAGO DE COMPOSTELA

almost all carcinomas, and prognostic value has been proven in breast, colorectal, pancreatic, prostate and non-small cell lung cancer, among others (102–108). In general lines, in the context of localised disease higher number of CTCs at baseline correlate with shorter DFS and DSS. Moreover, the presence of CTC clusters have been associated with an even worse clinical outcome in breast cancer (109,110). Therefore, the enumeration of CTCs in localised disease has prognostic value and can help clinicians to identify patients with poor clinical outcome.

CTCs not only have been described as having prognostic value at baseline, but also at longitudinal sampling. Several studies have shown that changes on the number of CTCs along treatment can be indicative of tumour response. Patients with a low clearance rate of CTCs have significantly shorter PFS and OS times (111). Once again, the enumeration of clusters improves the prognostic value while undergoing treatment, and patients with CTC clusters have worse prognosis (86). Moreover, the enumeration of CTCs after surgery on longitudinal samples can be useful to asses minimal residual disease (MRD) (112,113) or as a tool for early relapse detection (112,113).

Although most studies focus on the enumeration of CTCs, some studies have interrogated the molecular landscape of the CTCs to better understand the mechanisms of dissemination but also as a tool to guide the selection of targeted therapies.

Beyond the CTCs enumeration, this circulating tumour population represents itself a therapeutic target. Since CTCs are the vehicle to the metastatic disease, preventing or eliminating the presence of CTCs seems like an appealing therapeutic approach. Nonetheless, current strategies follow the same lines as those applied to the primary tumour: to prevent growth and tumorigenesis. Some of the current strategies are (114): (a) the inhibition of

USC UNIVERSIDADE DE SANTIAGO DE COMPOSTELA

intravasation, (b) break up CTC-clusters, (c) immune check-point inhibitors, (d) chronotherapy, and (e) metabolism inhibition. For instance, the HER2 status on CTCs has been used to select metastatic breast cancer patients for Trastuzumab or Trastuzumab + Pertuzumab treatment in the HER2Cell clinical trial (NCT04993014).

Despite the vast evidence of the prognostic value of CTCs in other tumour types (86–88). The value of CTCs in EC still lacks clinical evidence with only a handful of studies focused on it. Nonetheless, the limited research conducted suggests that the presence of CTCs in the bloodstream is linked to more aggressive phenotypes (89–91,115). For instance, Bogani and collaborators showed back in 2015 a 7% prevalence of positive CTCs in grade 3 EC patients, with associations noted between CTC presence and deep myometrial infiltration and positive lymph nodes in patients with EEC (116) . Alonso-Alconada and collaborators showed that the presence of CTC with high-risk EC. Moreover, gene-expression profiling characterized a CTC-plasticity phenotype with stemness and EMT features which demonstrated an advantage in the promotion of metastasis in an *in vivo* mouse model of CTC dissemination and homing (90).

1.2.2 | Other minimally invasive samples: The uterine aspirate

The uterine aspirate (UA) or uterine lavage is a form of liquid biopsy highly relevant in the context of gynaecological malignancies. It is an office procedure that serves as a helpful tool for diagnosis of different malignancies or abnormalities within the uterus. This type of biopsy is obtained through the use of the Pipelle de Cornier that is inserted through the cervix into the uterine cavity (117). Twirling the catheter while moving it in and out of the uterine cavity promotes the uptake of uterine tissue, which is aspirated into the catheter and collected. This minimally-invasive endometrial biopsy is used

USC UNIVERSIDADE DE SANTIAGO DE COMPOSTELA

in the diagnosis of abnormal uterine bleeding, cancer screening, endometrial dating and infertility (118).

This minimally invasive sample is a complex biological fluid which is in direct contact with the endometrial cavity and contains a multitude of proteins, nucleic acids and other analytes secreted from the endometrium (119,120). Therefore, it has been the focus of several studies in different gynaecological malignancies with the aim to identify new clinical biomarkers. Numerous studies have been focused on the proteomic characterization and the study of extracellular vesicles present in the UA, mainly for early detection and diagnosis of different gynaecological malignancies (121–129).

Moreover, the genetic and transcriptomic profile of the UA in different gynaecological malignancies has also been assessed using the UA showing high value to characterize the disease (130–136). One of the most relevant studies is from Mota et al. which demonstrated the value of the UA to reflect the intra-tumour heterogeneity of endometrial tumours. For this purpose, they profiled pair samples from 54 patients with EC using a targeted NGS panel. Interestingly, they found that the UA was able to recapitulate the entire mutational profile found at different tumour regions. This study highlighted the fact that intra-tumour heterogeneity may be represented in the UA, since it contains cells from different parts of the uterus; therefore, providing a more representative picture of the entire tumour (131).

1.3| Preclinical Models in Endometrial Cancer

Preclinical models serve as crucial tools in biomedical research to study diseases, test potential treatments, and understand biological mechanisms before moving into human trials. These models can range from cell cultures and tissue samples to animal models like mice (137). By mimicking aspects of human physiology and pathology, preclinical models help researchers

USC UNIVERSIDADE DE SANTIAGO DE COMPOSTELA

gather valuable insights into disease progression and therapeutic interventions, ultimately paving the way for safer and more effective clinical trials.

1.3.1 | 2D Cell Cultures

Traditional 2D monolayer cell cultures have long been the gold standard for cancer biology research. The reproducibility and user-friendly nature of 2D cell cultures have been key strengths that explain their widespread success. Their standardized protocols and simple experimental setups enable broad accessibility and facilitate consistent, comparable results across studies. However, the immortalization of the cell lines as well as changes related to the culture conditions limit the reliability of the results (138). Moreover, they lack cell-cell and cell-extracellular matrix (ECM) interactions, the tumour microenvironment (TME), and they have unlimited access to nutrients, oxygen, and metabolites (138,139). Moreover, cells cultured in 2D modify their morphology that causes cytoskeletal rearrangements leading to aberrant gene and protein expression (140). The combination of this factors adds up to less translational research.

In EC, multiple cells lines have been stablished for basic cancer research. Most of the cells lines are of EEC origin from primary tumours (141). Therefore, there is an under representation of the most aggressive subtypes of EC such as SC, CCC or MC, which leads to skewed research towards EEC.

1.3.2 | 3D Cell Cultures

To bypass these limitations, research has moved towards the generation of 3D models from patient samples that do a better job at capturing the different subtypes and intricacies of the disease. 3D models can preserve the tumour microenvironment and tumour-stromal interactions, which allows for

USC UNIVERSIDADE DE SANTIAGO DE COMPOSTELA

the study of, for example, the interaction of cells the tumour microenvironment during immunotherapy treatment (140,142,143). The two main categories for 3D cell cultures are: spheroids and organoid models.

|Spheroid cultures

Spheroids are cell clusters that grow in suspension without the presence of ECM (138,144–146). Spheroids can be generated from a broad range of cell types and through different methodologies, such as the hanging-drop technique (147) or culture in ultra-low attachment flasks. They can be either mono cellular (only one cell type) or multicellular spheroids (148).

These models better mimic the tumour biology than 2D cell cultures. They provide a 3D architecture and microenvironment of the tissue of origin, offer enhanced cell-cell interactions, better recapitulation of tissue heterogeneity, and improved predictability of drug responses (148). Spheroid cultures also exhibit long-term stability, making them a valuable tool to understand diseases and developing more effective therapeutic strategies (138,149,150).

Importantly, several studies have shown discrepancies in the sensitivity to different drugs between 2D and 3D cultures, whereas the same cell line in 2D was sensitivity to treatment, in 3D was considered to be resistant (151). This further highlights the importance of more reliable preclinical models for pharmacological studies.

|Organoid Models

In 2009 Sato and collaborators stablished the first organoid cultures from gut cells (152). In contrast to spheroids, organoids are grown within an ECM. Thus, cells can generate polarised structures that mimic the organ of origin and can accomplish the functions of the tissue of origin. They are a much more complex model when compared to 2D cell lines or spheroids (153,154).

USC UNIVERSIDADE DE SANTIAGO DE COMPOSTELA

They are composed of different cell types organised reproducing the histological structure of origin.

In EC, organoid models have been established from healthy tissue and tumoural tissue from EC patients (155–159). EC organoids maintained the architecture of the original tumours and can be expanded for long periods of time with genetic and molecular stability (155,157–159). Furthermore, these PDOs have allowed for the identification of potential therapies and the subsequent cell viability assays (155,157–159).

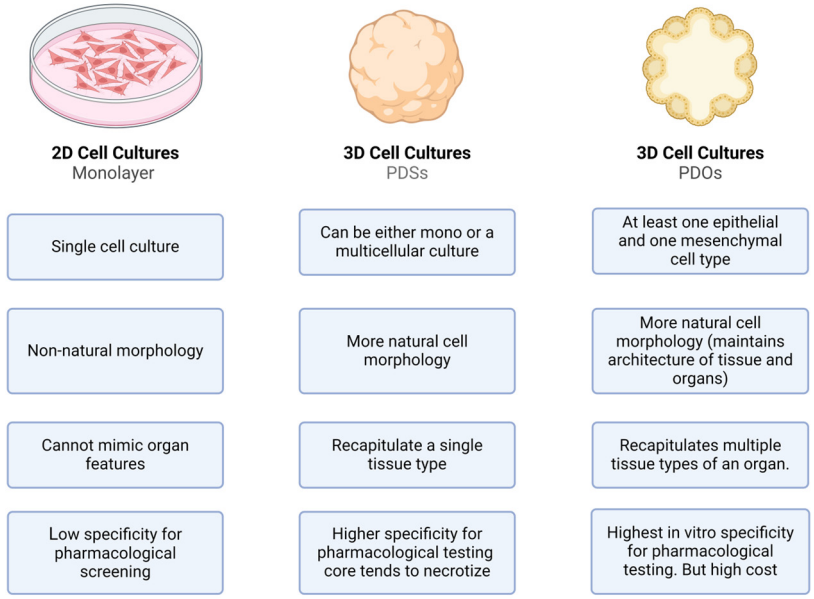


Figure 8: Key differences between the different types of cell cultures. Adapted with permissions from Sakalem et al (146). *Created with BioRender.com.*

1.3.3 | Animal Models

Perhaps one of the most useful preclinical models are the patient-derived xenografts (PDXs), in which cells or fragments from fresh tumour biopsies are transplanted into immunocompromised mice (137,156,160,161). PDXs

USC UNIVERSIDADE DE SANTIAGO DE COMPOSTELA

recapitulate histopathological features of the tumour and maintain the different subclones through the different generations (162). However, some studies have shown that over serial passaging clonal selection may arise (163).

PDX models have been developed from all EC subtypes (91,162,164). In fact, previous work from our group have shown that PDXs could be originated from minimally invasive samples such as the UA, and the model recapitulated not only the histopathological features of the tumour but also the genomic landscape (162,165). Moreover, PDXs generated from EC models recapitulate the response found on patients to, not only chemotherapy regimens, but also targeted therapies such as PARPi or PIK/AKT/mTOR inhibitors (162,165). Importantly, PDXs models from gynaecological origin recapitulate not only the relapse pattern, but also ascites or metastases observed in humans (166).

Nonetheless, PDXs cannot be used for high-throughput screenings due to ethical considerations, high costs and slow tumour growth. Other models, such as zebrafish, PDOs or PDSs should be considered for that purpose. Furthermore, generally speaking, PDXs are generated in immunocompromised mice, which limits the range of therapies that can be employed. For instance, immunotherapy testing in PDXs models requires of specific strands of mice that could be humanised to assess the effectiveness of the treatment (167).

USC UNIVERSIDADE DE SANTIAGO DE COMPOSTELA

2|OBJECTIVES

USC
UNIVERSIDADE
DE SANTIAGO
DE COMPOSTELA

OBJECTIVES

Overall, the objective of the current doctoral dissertation was to determine the applicability of liquid biopsy in EC patients to characterize circulating biomarkers to improve the risk stratification and monitoring, and to generate patient derived organoids with value as preclinical models.

The secondary objective within this doctoral thesis are:

CHAPTER I Precision Oncology in Endometrial Cancer: NGS Perspectives on Minimally Invasive Samples.

1.1. To elucidate the genomic landscape of EC and correlate the presence of specific alterations with the clinical outcome.

1.2. To determine the value of targeted NGS-based approaches to identify novel mutations for therapy selection on cfDNA of progressing EC patients.

CHAPTER II Epigenetic Dysregulation in Endometrial Carcinoma: Insights from Methylome Profiling

2.1. To identify methylation alterations associated with EC aggressiveness that could be used as a potential therapeutic approach.

CHAPTER III Non-invasive detection of microsatellite instability in patients with endometrial cancer

3.1. To evaluate the efficacy, accuracy and clinical potential of a ddPCR based test for the characterization of microsatellite instability in the uterine aspirate and blood samples of EC patients.

USC UNIVERSIDADE DE SANTIAGO DE COMPOSTELA

CHAPTER IV Unveiling Endometrial Cancer Prognosis: Integrating cfDNA and ctDNA for Predictive and follow up Analysis

4.1. To determine the viability of monitoring the ctDNA levels by tumour informed ddPCR assays designed based on the UAs characterization.

4.2. To evaluate the role of cfDNA and ctDNA as minimally invasive biomarkers to predict the patients' outcome, anticipate the disease relapse and the development of resistance to the treatment.

CHAPTER V CTCs as Prognostic Biomarkers in Endometrial Cancer: Findings from a Multicentred Study.

5.1 To determine the prognostic value of pre-surgery CTC levels in patients with localized EC.

CHAPTER VI Preclinical models in EC.

6.1. To evaluate the viability of generating PDOs and PDXs from uterine aspirates that recapitulate the molecular features of the primary tumour.

6.2. To assess the efficacy and applicability of the UAs derived PDOs and PDXs to test conventional and alternative therapies.

USC UNIVERSIDADE DE SANTIAGO DE COMPOSTELA

3 | MATERIAL & METHODS

USC
UNIVERSIDADE DE SANTIAGO DE COMPOSTELA

MATERIAL & METHODS

3.1 | Patients inclusion

All patients included within this doctoral dissertation presented EC and were prospectively recruited between January 2018 and June 2023 at the Gynaecology Department of Vall d'Hebron University Hospital (Barcelona, Spain), the MD Anderson Cancer Center (Madrid, Spain), the University Clinical Hospital of Santiago de Compostela (Santiago de Compostela, Spain), the University Hospital La Fe (Valencia, Spain) and the Bellvitge University Hospital (Barcelona, Spain). Patients were included in the study if the following criteria were met:

(a) Patients were diagnosed with endometrial carcinoma of any histology (excluding sarcomas or carcinosarcomas).

(b) Patients were over 18 years old.

(c) Patients signed informed consent.

(d) There was availability of UA.

(e) Patients were not undergoing anti-tumour treatment at the time of sample collection.

(f) Patients did not have any nonbenign tumour within the last 5 years before the sample collection.

This study was carried out according to the rules of the Declaration of Helsinki of 1975, revised in 2013, and according to the standards for good clinical practice and other local ethical laws and regulations. Informed consent forms, approved by the pertinent ethical committees, were signed by all patients (Autonomic Galician Ethical Committee Code 2017/430, approval

USC UNIVERSIDADE DE SANTIAGO DE COMPOSTELA

number PRAMI276–2018 of the Vall d'Hebron Ethical Committee) (Appendix 3).

Number of patients included as well as any further inclusion criteria has been reflected in the specific material and methods section of each result chapter.

3.2 | Uterine aspirate processing

The UA was collected using a Pipelle de Cormier prior to surgical resection of the tumour. Once collected, the UA was stored on ice and processed within the next 20 min according to the following protocol. First, the UA was homogenised with ice-cold PBS in a 1:1 ratio and mix thoroughly. Next, the sample was centrifuged for 20 min at 2500xg and 4ºC. The supernatant and the pellet were separated and the sample was immediately frozen at -80ºC.

3.3 | Blood samples processing

Peripheral blood samples were collected at surgery and during the patients' follow-up (every 6 months until recurrence/progression of the disease) using CellSave Preservative tubes (Silicon Biosystems Inc, Huntingdon Valley, PA) following the venipuncture procedure. Plasma was isolated by a two-step centrifugation. First, it was centrifuged for 10 min at 1,600xg without brake or acceleration, from there the plasma was carefully collected avoiding touching the cell phase. The collected plasma was centrifuged for another 10 min at 5500-6000xg with brakes to remove any possible cell debris, aliquoted and frozen at -80ºC until use.

3.4 | Nucleic Acid Isolation

DNA and RNA from the UA were obtained using RecoverAll™ Total Nucleic Acid Isolation Kit (Thermo Fisher Scientific, Waltham, MA, USA) following the

USC UNIVERSIDADE DE SANTIAGO DE COMPOSTELA

manufacturer´ conditions. DNA from plasma samples was extracted with the QIAamp DNA Circulating Nucleic Acid Kit (Qiagen, Venlo, Netherlands), according to the manufacturer's instructions. All cfDNA extractions were performed using the same volume of plasma (3-5 mL) and the concentration was normalized based on the extraction volume and the elution volume. Samples were stored for a maximum of 10 months before the cfDNA was isolated. DNA and RNA from FFPE samples was isolated using the AllPrep DNA/RNA FFPE Kit (Qiagen, Venlo, Netherlands) according to the manufacturer's instructions. All DNA samples were quantified using the Qubit Fluorometer (Thermo Fisher Scientific, Waltham, MA, USA) and stored at -20ºC until use.

3.5 | Sequencing

The UAs underwent targeted sequencing using the Oncomine Comprehensive Panel v3 (Thermo Fisher, Pleasanton, CA) following previously published protocols (91,168) at the MD Anderson Madrid. This panel comprises 161 genes categorized by somatic alteration type, including 87 Hotspots genes, 43 focal CNV gains, 48 Full CDS for DEL mutations, and 51 fusion drivers.

In summary, 10 ng of both DNA and cDNA from each UA were utilized for library assembly via multiplex PCR on an AB2720 Thermal Cycle (Life Technologies), adhering to the manufacturer's instructions. PCR amplification involved 18 and 20 cycles. Subsequently, primary primers underwent partial digestion using FuPa reagent (Thermo Fisher Scientific, Waltham, MA, USA). Ion P1 Adapter and Ion Xpress Barcode X were employed for amplicon ligation, followed by library purification and quantification using the Ion Library TaqMan Quantitation Kit and ViiA 7 system. Libraries were diluted to match the concentration range of the *Escherichia coli* DH10B Control Library

USC UNIVERSIDADE DE SANTIAGO DE COMPOSTELA

standards, with relative concentration determined through qPCR analysis. Template preparation and enrichment were conducted using the Ion S5 XL system. Diluted libraries were combined with template-positive Ion Sphere Particles (ISPs) and Ion S5 enzyme mix for emulsion PCR, followed by enrichment on the Ion OneTouch 2. Targeted massive sequencing was performed on the S5 sequencer (Thermo Fisher Scientific, Waltham, MA, USA) with six libraries (RNA and DNA) run in 540 chips. Duplicates were analysed for 10% of the samples and yielded consistent results.

For the bioinformatics analysis, alignment to the Hg19 human reference genome and variant calling were executed using Torrent Suite Software v.15.1 (Life Technologies). Variants with a Phred quality score field value <100 were considered low-quality, while the prediction of genomic variant effects on protein function was conducted using the PROVEAN Genome Variants tool (http://provean.jcvi.org/index.php) and Alamut Visual Plus. Variants predicted as possibly damaging or deleterious by at least one PROVEAN predictor were visually inspected with Integrative Genomics Viewer (IGV) v.2.3.40, Broad Institute. Variants with a global minor allele frequency above 0.05 were categorized as single nucleotide polymorphisms and excluded (data from dbSNP, [http://www.ncbi.nlm.nih.gov/SNP/]).

3.6 | Cell lines culture

The EC cell lines HEC-1-A (RRID:CVCL_0293) and AN3-CA (RRID:CVCL_0028) were maintained in a humidified atmosphere at 37ºC and 5% CO_2. HEC-1-A and AN3-CA were cultured in Dulbecco's Modified Eagle's Medium-Nutrient Mixture F-1 Ham2 (Sigma-Aldrich, St. Louis, MO) supplemented with 1% penicillin-streptomycin (Gibco, Waltham, MA) and 10% foetal bovine serum (Gibco, Waltham, MA), according to the ATCC recommendations.

USC UNIVERSIDADE DE SANTIAGO DE COMPOSTELA

3.7 | ddPCR Analysis

For each patient, specific ddPCR assays were designed and run on a QX-200 dPCR system (Bio-Rad, California, USA) using TaqMan chemistry, based on the specific mutational profile found on the UAs, with primers and probes at final concentrations of 900 nM and 250 nM, respectively. For each patient-specific assay, one non-target control, one wild-type and one positive control were used. Custom TaqMan assays were used (Bio-Rad, CA, USA). Following the current guidelines (71) the analytical sensitivity was estimated using serial dilutions of mutated DNA in a background of 20,000 copies of WT DNA, with variant allelic frequencies (VAFs) ranging from 100% to 0.1%. The Pearson correlation between the estimated and experimental mutant copies detected was calculated to determine the sensitivity for the assays. An analytical LoB was established at 0.03% and a LoD of 0.1% for all assays according to the approved guidelines. All assays were run in triplicates, with 30 ng of DNA, when possible, analysed per sample, and to assure their performance, the Pearson correlation between the estimated and experimental mutant copies detected was calculated (Pearson r = 0.995) (168) (Figure 1).

USC UNIVERSIDADE DE SANTIAGO DE COMPOSTELA

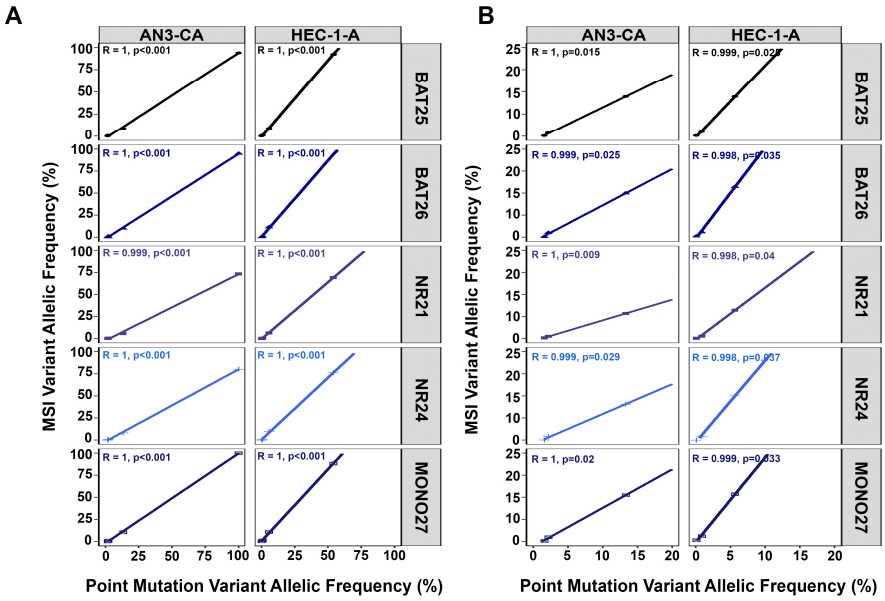


Figure 1: Limit of detection for the ddPCR assays**.** Representative scatter plot of the LoD for the MSI assays. **A.** Correlation, between the VAF of each mononucleotide marker and the VAF of point mutation variants identified by ddPCR in a range of 0-100 and **B** 0-10% in the AN3-CA and HEC-1-A cell lines.

PCR was performed with the ddPCR Supermix for probes (Bio-Rad, Santa Rosa, CA, USA). The sample was partitioned into a median of 50,000 droplets (run in triplicates) in an automated droplet generator (Bio-Rad, CA, USA), according to the manufacturer's instructions. Emulsified PCR reactions were run on 96-well plates on a C1000 Touch™ thermal cycler (Bio-Rad, CA, USA) according to the manufacturer's instructions. Plates were read on a Bio-Rad QX-200 droplet reader with Bio-Rad's QuantaSoft v1.7.4 software to quantify the number of droplets positive for mutant DNA, wild-type DNA, both, and neither. Analysis was performed manually by two independent molecular biologists according to the following guidelines: a minimum of 30,000 positive droplets across wells were required for a valid assay, and a minimum

USC UNIVERSIDADE DE SANTIAGO DE COMPOSTELA

of five, single FAM-positive or HEX-positive droplets with under3 positive events the WT control were required to consider samples as mutated.

3.8|Statistical Analyses

Analyses were conducted using the R Statistical language (version 4.2.3; (169)) on Windows 10 x64 (build 22631)

Table 1: Summary of the packages used for the statistical analysis in R.

Package	Reference	Package	Reference
randomcoloR	version 1.1.0.1;(170)	pROC	version 1.18.5;(171)
magrittr	version 2.0.3; (172)	ggbreak	version 0.1.2; (173)
lubridate	version 1.9.3;(174)	ROCR	version 1.0.11;(175)
ComplexHeatmap	version 2.14.0; (176)	gtsummary	version 1.7.2;(177)
ggpubr	version 0.6.0;(178)	survival	version 3.5.3; (179)
rstatix	version 0.7.2;(180)	corrplot	version 0.92; (181)
survminer	version 0.4.9;(182)	swimplot	version 1.2.0;(183)
factoextra	version 1.0.7; (184)	ggplot2	version 3.4.4; (185)
labelled	version 2.12.0; (186)	forcats	version 1.0.0; (187)
FactoMineR	version 2.9; (188)	stringr	version 1.5.1; (189)
tibble	version 3.2.1; (190)	tidyverse	version 2.0.0; (191)
RColorBrewer	version 1.1.3; (192)	readxl	version 1.4.3; (193)
patchwork	version 1.2.0; (194)	dplyr	version 1.1.4; (195)
purrr	version 1.0.2; (196)	readr	version 2.1.5; (197)
scales	version 1.3.0; (198)	tidyr	version 1.3.0; (199)
survivalAnalysis	version 0.3.0; (200)		

A Cox-proportional hazard model was used to determine the correlation of clinical and experimental variables with clinical outcomes; graphical representation of the impact on DFS and DSS was represented with Kaplan Meiers. DFS is defined as the time until relapse or last update since surgical

USC UNIVERSIDADE DE SANTIAGO DE COMPOSTELA

resection of the tumour specimen, DSS is defined as the time until death or last update since surgical resection of the tumour. Wilcoxon's signed-rank test was used to evaluate statistical differences in non-parametric experimental variables. The Spearman correlation test was performed to determine the relationship between experimental nonparametric variables. Kappa Cohen analysis was used to evaluate the concordance between variables. The Pearson correlation test was performed to determine the relationship between parametric quantitative experimental and clinical variables. Associations between clinicopathologic features and the experimental variables were examined with the chi-square test (Fisher's exact test). For in vitro and in vivo studies raw values were normalised to the starting values and normality was assessed using Shapiro-Wilk test, statistical significances at the different time points were assessed using a two-way ANOVA. A p-value <0.05 was set as the level of statistical significance.

USC UNIVERSIDADE DE SANTIAGO DE COMPOSTELA

4 | RESULTS

USC
UNIVERSIDADE
DE SANTIAGO
DE COMPOSTELA

4.1 | CHAPTER I

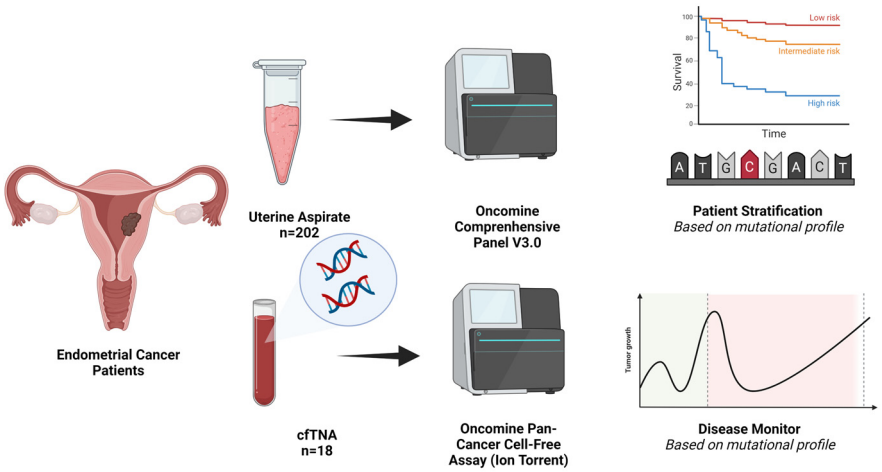
Precision Oncology in Endometrial Cancer: NGS Perspectives on Minimally Invasive Samples

USC
UNIVERSIDADE DE SANTIAGO DE COMPOSTELA

CHAPTER I

Precision Oncology in Endometrial Cancer: NGS Perspectives on Minimally Invasive Samples

GRAPHICAL ABSTRACT



Created with BioRender.com

Keywords: endometrial cancer, liquid biopsy, cfDNA, ctDNA, disease monitoring, targeted sequencing, genomic characterization, targeted sequencing, uterine aspirate, prognostic.

USC UNIVERSIDADE DE SANTIAGO DE COMPOSTELA

CHAPTER I

Precision Oncology in Endometrial Cancer: NGS Perspectives on Minimally Invasive Samples

Abstract:

EC is characterized by a heterogeneous genetic landscape that impacts on the disease relapse and treatment outcomes. Moreover, there is a non-neglectable lack of minimally invasive strategies to monitor the genetic evolution of the tumour under the therapy pressure. Therefore, the aim of this study was to evaluate the utility of targeted-NGS applied on UAs and cfDNA to characterize EC at surgery and during the follow-up.

The analysis of the UA showed prevalent mutations in key genes like *PTEN*, *PIK3CA*, and *TP53*. As expected, *POLE* mutations were indicative of a favourable prognosis, while *TP53* mutations were associated with a more aggressive disease phenotype. Integrating genetic data with clinical outcomes showed *TP53* alterations as a robust predictor of poor prognosis. Moreover, mutations in *RB1*, *MDM2*, and *ARID1A* were associated with disease progression, suggesting potential therapeutic targets. The analysis also allowed for the identification of patients with intratumoral heterogeneity, emphasizing the need for tailored therapeutic approaches.

Regarding the cfDNA, 71.88% of samples showed at least one pathogenic mutation, predominantly in *TP53*, *PIK3CA*, and/or *GNAS*. Besides, ctDNA dynamics correlated with the disease evolution. In fact, longitudinal cfDNA analysis revealed an evolving mutational landscape, including novel mutations potentially arising from treatment pressure.

USC UNIVERSIDADE DE SANTIAGO DE COMPOSTELA

Overall, this study highlights the utility of targeted-NGS based strategies on minimally invasive samples for a comprehensive genomic profiling in EC, offering insights into molecular subtypes, prognostic and predictive markers, and therapeutic approaches. These findings support the high value of applying NGS strategies for a precise and dynamic molecular characterization of EC.

USC UNIVERSIDADE DE SANTIAGO DE COMPOSTELA

4.1.1 | Introduction

EC exhibits a complex genetic landscape that greatly influences its development and clinical outcomes. The interplay of genetic alterations, including mutations in key genes like *TP53*, *POLE*, *PTEN*, and *CTNNB1*, has been a focal point of investigation. Studies such as the ones from the TCGA or PROMISE study have been key milestones into the unravelling of the molecular subtypes and its prognostic implications (10,14,15). The integration of these results in the clinical practice allowed for a comprehensive understanding of the genetic landscape and potential therapeutic avenues in EC (12). Based on the results from both studies (10,14,15), four molecular groups were stablished: 1) *POLE* – ultra mutated, 2) MSI-H/dMMR, 3) $TP53_{abn}$ and/or high-copy number, 4) NSMP.

Among the findings within these studies its especially important the mutations found within *POLE* and *TP53*. Alterations within these two genes are key findings that define the disease. For instance, according to the latest ESMO/ESGO guidelines, in early stages the presence of *POLE* or *TP53* alterations redefine the FIGO stage (8). Mutations involving the *POLE* gene, which encodes a DNA polymerase responsible for DNA replication and repair, result in patients exhibiting a remarkably high mutation burden, particularly in the coding regions of the genome (201). The high mutational load is associated with a favourable prognosis, suggesting that EC patients with *POLE*-mutated tumours experience improved overall survival (10,14,15,202,203).

On the other hand, mutations in *TP53*, a critical tumour suppressor gene involved in cell cycle regulation and DNA damage response, are associated with a more aggressive tumour phenotype and poorer prognosis (204). Tumours harbouring *TP53* mutations often exhibit advanced stages at

USC UNIVERSIDADE DE SANTIAGO DE COMPOSTELA

diagnosis and increased resistance to conventional treatments (201,204). Therefore, the presence of *TP53* mutations is of high importance for prognostic assessments and treatment decisions. Targeted therapies tailored to the *TP53*$_{abn}$ tumours represent a crucial avenue for improving outcomes in these patients.

In this chapter, we perform a comprehensive analysis of the genetic landscape of EC. The UA from 202 patients were subjected to targeted sequencing with the aim to validate this type of biopsy for EC genotyping. By integrating clinical data and genetic information, we aim to generate more evidence about the utility of UAs as a reliable sample for genomic characterization of the disease and to identify a molecular profile associated with poor prognosis and actionable pathways.

Moreover, previous studies have shown that EC genomic landscape is unstable and can undergo changes through the course of the disease (205). In this regard, the analyses of minimally invasive samples, such as the cfDNA, could be a powerful asset for the dynamic characterization of the disease. However, the low concentration of the tumour fraction of the cfDNA present in plasma represents a challenge for biomarker analysis (70). Current guidelines propose two main strategies: first, studying a single alteration using PCR methods; or second, conducting genome-wide analyses with NGS techniques (71,72). In order to track the disease's evolution over time, in the current chapter, we used an NGS-based approach through the application of a targeted panel. This methodology offers several advantages, including the ability to gather patient-specific genetic information, capture ITH, and track clonal evolution over time. By employing this approach, we aimed to gain deeper insights into the dynamic changes in the tumour's mutational landscape throughout the disease course, providing a more comprehensive

USC UNIVERSIDADE DE SANTIAGO DE COMPOSTELA

understanding of disease progression and potential therapeutic vulnerabilities.

4.1.2 | Material & Methods

4.1.2.1 | Patients' inclusion and samples collection

Two cohorts of patients were employed in this chapter. A global cohort of 202 patients with EC where the UA was sequenced using the Oncomine™ Comprehensive Panel v3 (Thermo Fisher, Pleasanton, CA), and a subset of 18 patients from this first cohort, mainly composed of patients with advanced disease, where the cfDNA was sequenced using the Oncomine™ Pan-Cancer cell free assay (Thermo Fisher, Pleasanton, CA).

The UA was collected at surgery from 202 patients with EC. Samples were collected at the University Hospital of Santiago de Compostela (Santiago de Compostela, Spain) (n= 98), Val d'Hebron Hospital (Barcelona, Spain) (n=62), MD Anderson Hospital (Madrid, Spain) (n=54) and La Fe Hospital (Valencia, Spain) (n=7). The clinical characteristics of the included cohort are summarised on the Figure 1.

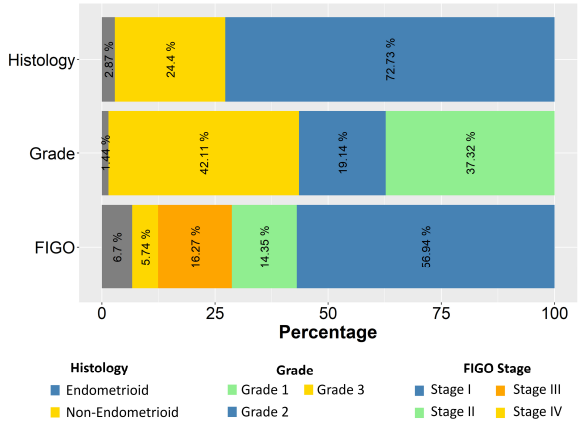


Figure 1: Clinico-pathological features of the studied cohort (n=202).

USC UNIVERSIDADE DE SANTIAGO DE COMPOSTELA

Peripheral blood samples (n=32) from 18 patients with EC disease were collected at surgery (n=12), at relapse (PD) (n=10) after first line systemic treatment and at sequential progressions (n=10). A summary of the clinico-pathological features of this cohort can be seen on Table 1.

Table 1: Summary of the most relevant clinico-pathological features.

ID	Histology	Grade	FIGO	Myometrial Infiltration	LVSI	TCGA	Risk	Relapse
BL005	Endometrioid	G1	II	>50%	No	NSMP	Intermediate	Yes
BL010	Serous	G3	II	<50%	No	HCN	High	Yes
BL024	Serous	G3	I	>50%	No	HCN	High	Yes
BL036	Endometrioid	G2	I	<50%	No	HCN	Low	No
BL041	Endometrioid	G2	II	>50%	No	MSI	Intermediate	Yes
BL063	Endometrioid	G3	I	>50%	Yes	HCN	Intermediate	Yes
BL067	Endometrioid	G3	I	>50%	Yes	MSI	High-Intermediate	Yes
BL088	Endometrioid	G3	I	>50%	No	MSI	High-Intermediate	No
BL079	Endometrioid	G2	I	>50%	No	NSMP	Intermediate	Yes
BL121	Endometrioid	G2	I	<50%	No	MSI	Low	No
BL127	Endometrioid	G3	III	<50%	No	MSI	High	Yes
BL132	Serous	G3	IV	>50%	Yes	HCN	Advanced	Yes
BL134	Serous	G3	I	<50%	No	NSMP	Intermediate	No
BL136	Serous	G3	I	<50%	No	HCN	Intermediate	Yes
BL141	Serous	G3	IV	>50%	No	HCN	Advanced	Yes
BL160	Serous	G3	III	>50%	Yes	MSI	High	Yes
BL199	Endometrioid	G2	I	>50%	No	MSI	Intermediate	Yes
BL219	Endometrioid	G1	I	<50%	No	NSMP	Low	No

4.1.2.2|UA processing and sequencing.

DNA from the UA was isolated as previously described in the material and methods section (Subsection 3.5) and sequenced using the Oncomine Comprehensive Panel v3 (Thermo Fisher, Pleasanton, CA).

USC UNIVERSIDADE DE SANTIAGO DE COMPOSTELA

4.1.2.3 | cfDNA sequencing using the targeted panel

Total cfDNA was isolated from 5mL of plasma using QIAamp DNA Circulating Nucleic Acid Kit, as previously described. Isolated cfDNA was quantified using Qubit and integrity using the TapeStation (Agilent Technologies, CA, US). After quality control the cfDNA was sequenced using the Oncomine™ Pan-Cancer cell free assay (Thermo Fisher, Pleasanton, CA) according to the manufacturer instructions.

Briefly, manually prepared targeted sequencing libraries were generated using the Oncomine™ Pan-Cancer Cell-Free Assay (Thermo Fisher, Pleasanton, CA). The total input of cell-free tumour nucleic acid (cfTNA) ranged from 4.63 to 58.24ng (Median=20.23ng). After library preparation, the quality was screened using the Tape Station D1000 and were quantified using the Ion Library TaqMan quantification kit. Subsequently, 100 mM of the library was loaded onto Ion 540 chips via Ion Chef and sequenced using the Ion GeneStudio™ S5 system (Thermo Fisher, Pleasanton, CA). Data output was processed using Ion Reporter software (Thermo Fisher, Pleasanton, CA) with the "Oncomine TagSeq Pan-Cancer Liquid Biopsy w2.1" workflow. A summary of the coverage can be found on appendix 5.

4.1.3 | Results

4.1.3.1 | The value of targeted NGS to characterize the uterine aspirate

4.1.3.1.1 | Overview of the results

By analysing the UA with the targeted NGS panel, 187 out of the 202 (92.57%) patients had pathogenic alterations (Figure 2). The top 10 most commonly mutated genes for SNPs were *PTEN* (54.46%), *PIK3CA* (48.51%), *TP53* (30.69%), *ARID1A* (28.71%), *KRAS* (20.79%), *CTNNB1* (19.31%), *PIK3R1* (17.82%), *FBXW7* (14.36%), *PPP2R1A* (13.37%) and *FGFR2* (9.41%). When

USC UNIVERSIDADE DE SANTIAGO DE COMPOSTELA

focusing on the CNAs, 19 patients out of 202 (9.41%) had CNAs. The top 10 most altered genes for CNAs are *CCNE1* (4.46%), *ERBB2* (2.48%), *CDK2* (1.98%), *AKT2* (0.99%), *MDM2* (0.99%), *MYC* (0.99%), *PIK3CA* (0.99%), *AR* (0.50%), *AXL* (0.50%) and *CCND3* (0.50%).

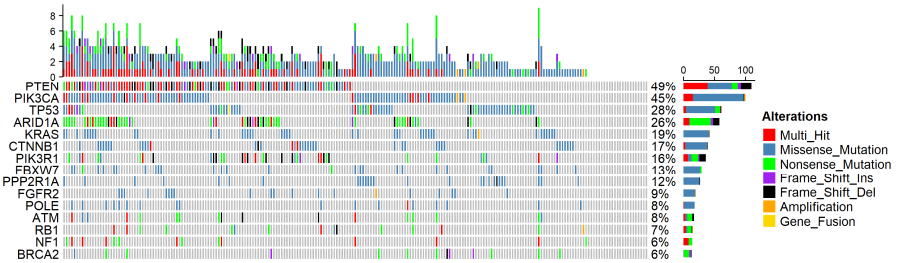


Figure 2: Heatmap representative of the top 15 alterations found through the sequencing of the UA, type of alteration and the distribution across samples.

When comparing our results to those obtained by the TCGA (https://www.cbioportal.org/ data accessed: 2024/01/09) similar results were found. Nonetheless, it is important to highlight that different technologies were employed, and not all genes analysed by the TCGA are covered by the panel. Although the coverage of the panel regarding CNAs is more limited, the high similarity between both results furthers validates the UA as a reliable sample for NGS characterization. The summary of the comparison can be found on Table 2.

USC UNIVERSIDADE DE SANTIAGO DE COMPOSTELA

Table 2: Comparison of the SNPs and CNAs found in the UA using targeted NGS panel with the TCGA available data.

SNPs			**CNAs**		
Gene	**TCGA (%)**	**Targeted Panel (%)**	**Gene**	**TCGA (%)**	**Targeted Panel (%)**
PTEN	64.90%	54.46%	*CCNE1*	9.30%	4.46%
PIK3CA	53.20%	48.51%	*ERBB2*	6.70%	2.48%
ARID1A	33.50%	28.71%	*CDK2*	3.00%	1.98%
PIK3R1	33.10%	17.82%	*AKT2*	3.70%	0.99%
CTNNB1	29.80%	19.31%	*MDM2*	0.6%	0.99%
TP53	27.80%	30.69%	*MYC*	10.40%	0.99%
KRAS	21.00%	20.79%	*PIK3CA*	8.30%	0.99%
FBXW7	15.30%	14.36%	*AR*	0.6%	0.50%
FGFR2	12.50%	9.41%	*AXL*	1.50%	0.50%
ATM	11.70%	8.42%	*CCND3*	9.30%	0.50%

Next up, we compared the mutation distribution across different histological subtypes. Patients with endometrioid histology presented mostly mutations on *PTEN, PIK3CA, ARID1A, CTNNB1, KRAS, PIK3R1, TP53* and *FGFR2,* among others (Figure 3A). On the other hand, patients with non-endometrioid histology (mostly SC but also included within this group are CCC and MC) presented mostly alterations in *TP53, PIK3CA, PTEN, PPP2R1A* and *FBXW7* (Figure 3B). Not surprisingly, NEEC tumours presented mostly SNPs in the *TP53* gene and a high number of CNAs. Interestingly, a high number of SNPs with multi-hit variants were found on *PTEN*, *PIK3CA* and *ARID1A* in the EEC subtype.

USC UNIVERSIDADE DE SANTIAGO DE COMPOSTELA

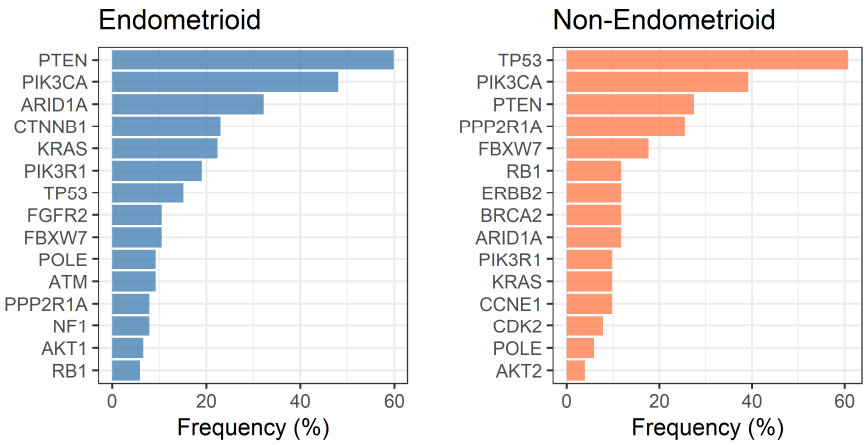


Figure 3: Distribution of the most prevalent mutations detected in the UAs according to histology**: A.** Endometrioid carcinoma (EEC) **B.** Non-Endometrioid Carcinoma (NEEC).

The high number of multi-hit alterations on the EEC tumours led us to assess the intra-tumour heterogeneity (ITH) in the entire cohort. The ITH reflects the presence of diverse genetic and phenotypic profiles within a single tumour (91,131,165). Interestingly, 32.67% of patients (66 out of 202) presented genes with multi hit alterations, potentially indicative of ITH. The most prevalent genes that seemed to be related to ITH were as follows: *PTEN* (59.09%), *PIK3CA* (22.73%), *ARID1A* (13.64%), *NF1* (12.12%), *PIK3R1* (10.61%), *RB1* (6.06%), *TP53* (6.06%), *ATM* (4.55%) and *CTNNB1* (4.55%).

4.1.3.1.2 | Genes distribution across the TCGA/PROMISE classification

The TCGA and PROMISE classification consider the genetic background of the tumours to perform a cluster classification of the patients. Based on the genetic and immunohistochemistry results we classified our cohort of patients following the diagram reflected on the introduction, and survival rates of these groups were assessed in patients with follow-up data. Similar results than previous studies were obtained (10,14,15). Patients of the POLE

USC UNIVERSIDADE DE SANTIAGO DE COMPOSTELA

mutated group had an extremely good prognosis, patients in the NSMP and MSI/dMMR had an intermediate risk and the $p53_{abn}$/CNA-high a really poor prognosis (Figure 4).

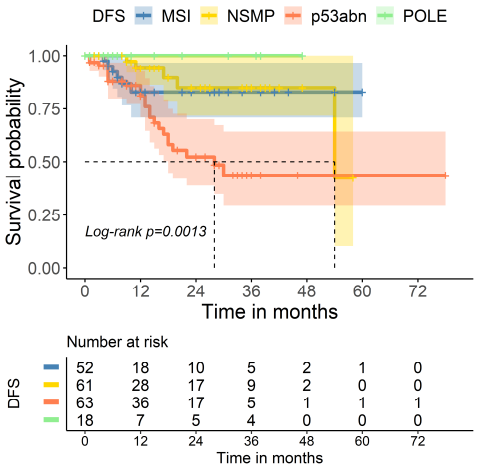


Figure 4: Kaplan Meier according to the four molecular groups of the TCGA.

Next, we wanted to evaluate the potential clinical impact of other genes to improve the accuracy of the genomic profiling of EC patients for clinical outcome. We performed survival analyses with the 10 most commonly mutated genes. Therefore, a survival analyses was performed with the following genes: *PIK3R1, PIK3CA, PPP2R1A, PTEN, TP53, FGFR2, FBXW7, KRAS, ARID1A* and *CTNNB1*. Not surprisingly, patients with *TP53* alterations presented a significantly worse prognosis when compared to the wild type phenotype (Figure 5), even after stage correction (HR:2.3, p-value=0.039). Another gene that showed interesting results where the *PIK3R1* mutated patients seemed to have a better clinical outcome (HR= 0.59, p-value=0.037). Within the remaining genes, although no significance was reached some had either no effect on prognosis: *CTNNB1, PPP2R1A, FGFR2* or *FBXW7* (HR~1, p-

USC UNIVERSIDADE DE SANTIAGO DE COMPOSTELA

value>0.05); or a positive association: *ARID1A, PIK3CA, PTEN* or *KRAS* (HR<0.6, p-value>0.05) (Table 3).

Table 3: Summary of the hazards ratio and p-values obtained with the Cox-proportional regression model.

Gene	HR (95% CI)	p-value	p-value Stage corrected
PIK3R1	0.23 (0.053-0.97)	0.037	0.045
PIK3CA	0.59 (0.27-1.3)	0.160	0.188
PPP2R1A	1.3 (0.45-3.7)	0.675	0.640
PTEN	0.63 (0.3-1.3)	0.178	0.221
FGFR2	0.76 (0.23-2.6)	0.635	0.660
TP53	2.3 (1.0-4.9)	0.027	0.039
FBXW7	1.0 (0.31-3-5)	0.981	0.945
KRAS	0.55 (0.19-1.6)	0.232	0.263
ARID1A	0.35 (0.12-1.0)	0.043	0.053
CTNNB1	0.93 (0.31-2.80)	0.901	0.904

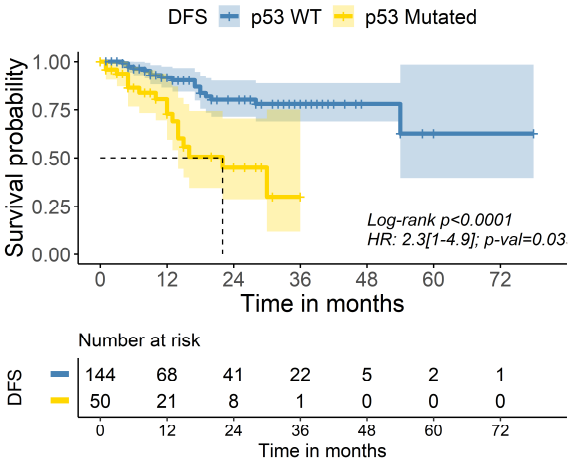


Figure 5: Patients with *TP53* mutated present significantly shorted DFS independently of the FIGO Stage**.** Kaplan Meier curve according to the presence of *TP53* mutations on the UA.

USC UNIVERSIDADE DE SANTIAGO DE COMPOSTELA

The NSMP subtype of patients has an intermediate prognosis and has no mutational profile associated to it. Therefore, we explored the frequency distribution of the most altered genes and correlated them with clinical prognosis. The most altered genes in the NSMP group were: *PTEN, PIK3CA, CTNNB1, ARID1A, KRAS, PIK3R1, FGFR2, AKT1, ESR1, FBXW7* and *BAP1* (Figure 6A). The only gene linked to patient prognosis was *PTEN*, patients with a wild type phenotype of *PTEN* presented significantly shorter DFS. However, wild type expression of *PTEN* seemed to be associated with worse clinical outcome (Figure 6B).

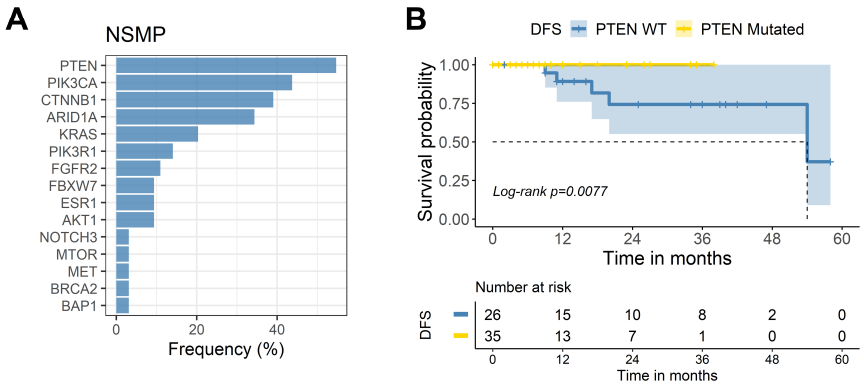


Figure 6: Genomic distribution in the NSMP molecular subtype**. A.** List of the most prevalent mutations, **B.** Patients with a wild-type phenotype of *PTEN* present significantly shorter DFS.

4.1.3.1.3 | Alterations linked to disease progression and death

Although the number of patients that underwent tumour relapse and perished due to the disease in our cohort is limited, we analysed the alterations found within these patients to determine its prognostic value. As expected, the most common altered genes found in the most aggressive tumours were *TP53, PTEN* and *PIK3CA*. Nonetheless, although found in low

USC UNIVERSIDADE DE SANTIAGO DE COMPOSTELA

percentage, alterations in *RB1*, *MDM2* or *ARID1A* are of special interest and could represent potential therapeutic targets (Figure 7). *RB1* is a well-known tumour suppressor gene and key regulator of the G1/S transition of the cell cycle (206). It encodes for a protein that stabilizes heterochromatin, defects on this protein have been linked to multiple types of cancer (207). *MDM2* is a protooncogene linked to the p53 pathway. It encodes a E3 ubiquitin ligase that ubiquitinates p53/TP53, leading to its degradation by the proteasome (208) as well as control the cell cycle, apoptosis, differentiation, and genomic stability in a p53-independent fashion (209,210). And *ARID1A* is involved in transcriptional activation and repression of select genes by chromatin remodelling. It is one of the most altered genes in EC (33.50%) and has great potential for therapeutic targeting.

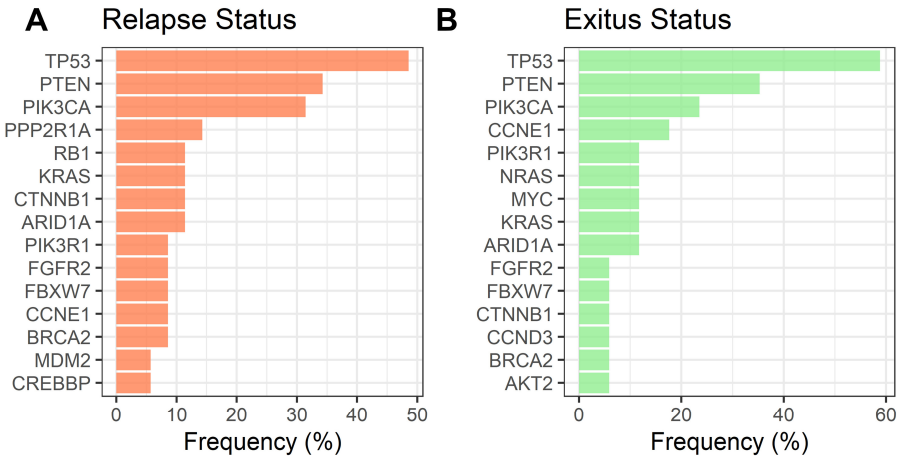


Figure 7: Genomic alterations in advanced disease. List of the most prevalent alterations found on patients that underwent relapse (**A**) or deceased due to the disease (**B**).

USC UNIVERSIDADE DE SANTIAGO DE COMPOSTELA

4.1.3.2 | The value of targeted NGS-based approaches in cfDNA

We explored the accuracy and performance of a pan-cancer NGS panel to characterize genetic alteration on the plasma cfDNA as a comprehensive non-invasive way to monitor the tumour evolution.

4.1.3.2.1 | Cohort characteristics

The study included 18 individuals diagnosed with EC, encompassing various clinical profiles detailed in Table 2. The cohort consisted of patients with both EEC and NEEC, ranging from Grade 1 to Grade 3, and FIGO stages I to IV, classified according to the latest ESMO/ESGO consensus guidelines (8). Notably, as illustrated in Table 2, the cohort primarily consisted of high-risk patients who experienced relapse, constituting 72% (13/18) of the total sample.

4.1.3.2.2 | Sequencing results

The Oncomine™ Pan-Cancer Cell-Free Assay included 52 genes, encompassing SNPs, gene fusions, CNAs, and tumour suppressor genes. A total of 32 samples from 18 unique patients underwent NGS analysis. cfDNA input varied from 4.63 to 58.24ng with a median of 20.23ng, with no statistically significant differences observed between patients with detectable and undetectable ctDNA levels (Figure 8A). Regarding the LoD, it ranged from 0.076% to 0.56% with a median of 0.19%, once again showing no statistically significant variances between patients with detectable and undetectable ctDNA (Figure 8B). Unsurprisingly, a reasonably good correlation between cfDNA input and the LoD was observed (r^2~0.6, p-value<0.001) (Figure 8C), supporting the need to include large amounts of cfDNA to reach a reasonable LoD.

USC UNIVERSIDADE DE SANTIAGO DE COMPOSTELA

In terms of sensitivity, 68.75% (22/32) of the sample showed detectable alterations, with higher rates observed at disease relapse (70%, 14/20) compared to baseline (66.67%, 8/12). A summary of these alterations is provided in Appendix 6. The most frequently mutated genes included *TP53, PIK3CA, GNAS, RET, KRAS, FGFR2, FBXW7* and *CTNNB*1 (Figure 9). We could compare the results obtained in the UAs and cfDNA although we used different NGS panels. Among the 22 samples with detectable ctDNA levels, 50% showed at least one alteration also found in UA, while the remaining 50% had mutations not detected in UA (Figure 9). Although the number of discordant cases is considerable, it's worth noting that most samples were collected during relapse. Consequently, the mutational profile may have changed, and the dominant disease subclones may have shifted, making it more challenging to detect the same mutations found in primary tissue. However, upon examining the concordances and discrepancies at different time points, we observed that at baseline, only 37.50% of samples showed concordance (3/8), whereas during relapse, 64.28% of samples exhibit concordance (9/14). Thus, the correlation between cfDNA and tissue appears to be closely linked to tumour secretion, suggesting that patients with higher tumour burden are more easily identifiable.

USC UNIVERSIDADE DE SANTIAGO DE COMPOSTELA

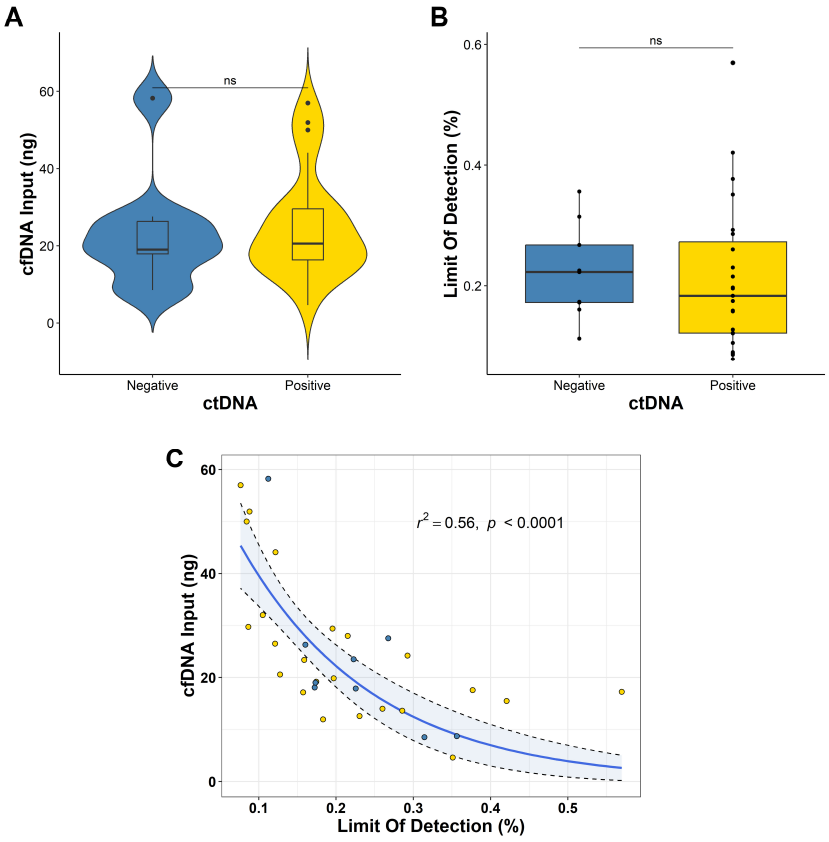


Figure 8: Summary of the quality metrics for the NGS analyses of the cfDNA. **A.** Violin plot of DNA input (ng) between ctDNA positive and negative patients. **B.** Box plot of the different LoD between ctDNA positive and negative patients. **C.** Scatter plot of the correlation between cfDNA input and the LoD.

USC UNIVERSIDADE DE SANTIAGO DE COMPOSTELA

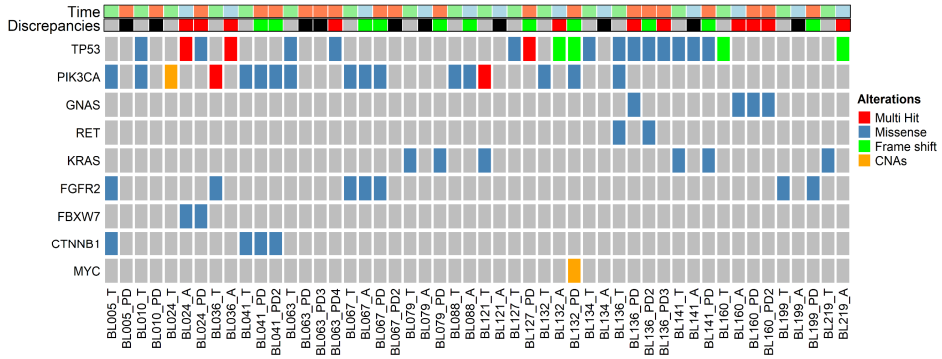


Figure 9: Heatmap with the alterations found in cfDNA and correspondence with the UAs. The type of sample can be tracked by the colour legend on the top annotation (green: primary tumour, blue: baseline cfDNA sample, orange: relapse cfDNA sample) as well as the sample name: _T refers to the UA, _A refers to the cfDNA collected at baseline; _PD refers to the sample collected at the time of relapse. Discrepancies are highlighted on the top annotation with the following colour legend: black, no mutations detected; green, at least one concordant mutation found; red, no common mutations found.

4.1.3.2.3 | Disease monitoring

Once we established the sensitivity of the approach, we assessed its potential applicability in monitoring disease evolution. In four patients, we detected ctDNA at multiple time points throughout the disease, reflecting dynamic changes due to therapy or disease progression.

Patient #024, a 69-year-old woman diagnosed with high-grade SC with FIGO stage IB, exhibiting over 50% myometrial infiltration and without LVSI, was classified as high risk for recurrence. Within a year following surgical resection of the primary tumour, the patient experienced a relapse at the bone marrow. The UA sequencing revealed amplification of the *PI3KCA* gene. Subsequent targeted sequencing of cfDNA collected at baseline and during relapse identified mutations in *FBXW7* and *TP53*, as well as a second *TP53*

USC UNIVERSIDADE DE SANTIAGO DE COMPOSTELA

alteration exclusively observed at baseline. Figure 10A illustrates that the alterations with higher VAF at baseline experience exponential increases during relapse, indicating a higher tumour burden.

Patient #067, a 57 year-old woman diagnosed with high-grade EEC with FIGO stage IB, exhibiting over 50% myometrial infiltration and with LVSI, was classified as high-intermediate risk for recurrence. Within two years post-surgical resection, the patient experienced a relapse at the peritoneum, followed by chemotherapy treatment, and subsequently a second relapse at the brain. UA sequencing revealed alterations in the *PIK3CA* and *FGFR2* genes. Plasma samples were collected at surgery, first relapse, and second relapse. In Figure 10B, it can be observed that alterations in *PIK3CA* and *FGFR2* were present at baseline and increased at the time of tumour relapse. However, after the second line of treatment, no detectable levels were found at the time of the second progression. It's crucial to note that this second progression occurred in the brain, posing a new challenge for the detection of ctDNA.

Patient #132, a 85 year-old woman was diagnosed with high-grade serous EC with FIGO stage IVA, exhibiting >50% myometrial infiltration and LVSI, was classified as a patient with advanced disease. Following a chemotherapy regimen and surgical resection, the patient experienced a relapse at the peritoneum. UA sequencing revealed alterations in *PIK3CA*, *BRCA2*, *CREBBP*, and *PPP2R1A*. Samples were collected at surgery and at the time of relapse. In Figure 10C, it is evident that an alteration in *TP53* was detected in cfDNA but not in the UA. Interestingly, this *TP53* alteration was not present at the time of relapse; instead, a new *TP53* alteration emerged. Additionally, at the time of relapse, two more alterations were found: one in *PIK3CA*, consistent with the UA findings, and a novel amplification in *MYC*.

USC UNIVERSIDADE DE SANTIAGO DE COMPOSTELA

Patient #136, a 83 year-old woman, diagnosed with high-grade SC of FIGO stage IA, without any myometrial infiltration of LVSI, classified as of high-intermediate risk of recurrence. A year post-surgical resection, the patient experienced a relapse with a local recurrence. Within the subsequent year, the patient suffered from two distinct relapses and underwent various treatment regimens. UAs sequencing revealed alterations in *PIK3CA*, *RET*, and *TP53*. Samples were collected at the first, second, and third relapse. Interestingly, although alterations were detected at all three time points, the mutations identified were not consistent. Only at the time of the first relapse were there concordant alterations (Figure 10D).

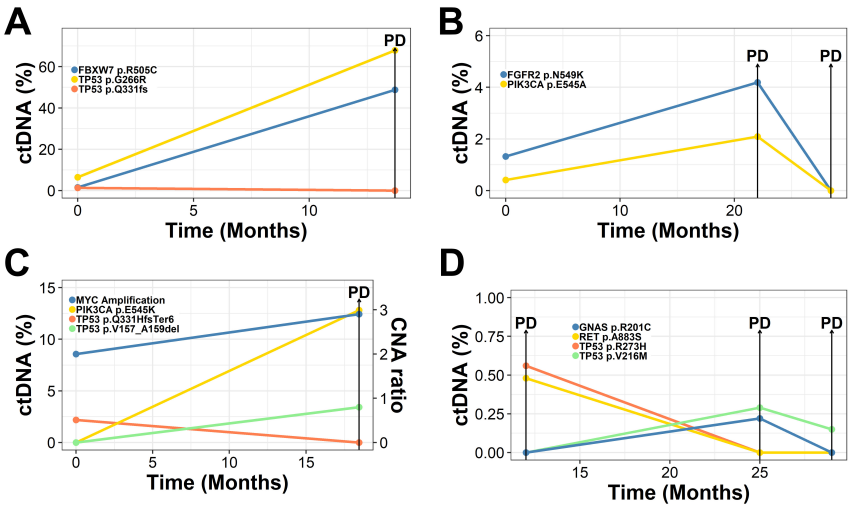


Figure 10: The longitudinal analyses of ctDNA through targeted NGS allows to monitor the disease evolution**. A-D**. Example figures of the ctDNA kinetics in patients with advanced EC.

4.1.4 | Discussion

Within this chapter we have shown that targeted-based NGS approaches to characterize the genomic landscape of EC utilizing minimally-invasive

USC UNIVERSIDADE DE SANTIAGO DE COMPOSTELA

samples is not only feasible, but yields robust and comparable results to those obtained using other technologies.

We sequenced the UA of 202 patients with EC, identifying a genomic landscape comparable to those obtained using WES in larger studied cohorts such as the TCGA and PROMISE studies (10,14,15) and being able to identify alterations in over 90% of the samples. The most common alterations found were *PTEN*, *PIK3CA*, *TP53*, *ARID1A*, *KRAS*, *CTNNB1*, *PIK3R1*, *FBXW7*, *PPP2R1A* and *FGFR2*. Targeted-based NGS panels are a more cost-efficient option and easier to analyse when compared to the vast cost associated with WES or WGS, therefore much more translatable into the clinical context. Nonetheless, it is important to highlight that regarding the CNAs the targeted NGS approach presents further limitations and the results were not as comparable with other studies.

Moreover, we were able to evaluate the presence of ITH. Over 30% of patients (66 out of 202) presented genes with multi hit alterations, potentially indicative of ITH. The genetic heterogeneity is of significant importance within the clinical context, since it is known to lead to variations in treatment responses, making it difficult to develop targeted therapies that effectively eradicate all cancer cells (211). Moreover, drug-resistant clones within a tumour may limit the long-term success of treatment strategies. Therefore, UAs sequencing represents a good alternative to better capture the ITH as previously described Mota and collaborators (165,212). Interestingly, ITH was more present in patients of EEC histology when compared to the NEEC, most likely linked to the higher rate of $POLE_{mut}$ and dMMR/MSI-H EEC tumours.

We also evaluated the potential clinical implication of other genes on the patients' prognosis. As expected, patients harbouring *TP53* alterations

USC UNIVERSIDADE DE SANTIAGO DE COMPOSTELA

presented significantly shorter DFS and DSS when compared to TP53-WT phenotypes (10,14,15,213). In line with other studies, patients with $POLE_{mut}$ presented an excellent prognosis and only a patient underwent relapse within the studied timeframe (10,14,15,213,214). Interestingly, a more indolent disease was observed in tumours with *ARID1A* alterations. This effect is most likely linked to EEC histological subtype which has a more favourable clinical outcome, as *ARID1A* mutations are predominantly on EEC subtypes. Moreover, patients with a wild type phenotype of *PTEN* presented significantly shorter DFS. Conflicting reports have been made regarding the implication of *PTEN* alterations and clinical outcome. Whereas some studies have reported a link to less aggressive phenotypes (215), others have shown that *PTEN* alterations are significantly correlated with significantly poorer prognosis in survival and disease recurrence, they are prone to distant metastasis (216,217).

As research progresses and clinical trials unfold, more light is being shed into the molecular classification and recent studies have shown that the NSMP molecular subgroup could be further stratified based on *CTNNB1* alterations. *CTNNB1* mutations are significantly associated with recurrence in early stage EEC, especially in the NSMP, appearing potentially useful in directing adjuvant treatment (218–221). In contrast with previous studies, in our cohort no correlation was found between *CTNNB1* alterations and poor clinical outcome. Nonetheless, further studies with bigger cohorts are needed to identify key mutational signatures within this molecular subtype.

Genomic insights from these studies not only inform prognostic assessments but also lay the foundation for targeted therapies. For instance, MMR-deficient tumours identified in both studies may respond favourably to immune checkpoint inhibitors, reflecting a paradigm shift in the treatment of

USC UNIVERSIDADE DE SANTIAGO DE COMPOSTELA

EC (222). The identification of genetic alterations allows for the tailoring of therapies based on the tumour's unique genomic profile, improving effectiveness while minimizing adverse effects (11,17). With the aim to identify potential novel therapeutic targets we analysed the mutations on patients who underwent relapse and deceased due to the disease. Three genes were identified as potential candidates: *RB1, MDM2* and *ARID1A.* Although further studies are needed to evaluate the role of *RB1* as a prognostic biomarker in EC (223), therapeutic targeting of *RB1* or related genes within the pathway is feasible and tumours with the *RB1*-defecient status in cancers generates a variety of therapeutic benefits through the upregulation of *RB1* targets (224,225). *MDM2* has been previously reported as altered in 2% of EC patients. Although only a handful of patients present alterations on *MDM2,* targeted therapies are available and could constitute a potential therapeutic approach for EC patients (226). *ARID1A* is one of the genes related to the HRR system, thus, patients harbouring mutations in *ARID1A* could benefit from PARPi treatment. Moreover, Trabectedin a chemotherapy drug used to treat soft tissue sarcomas has shown effectiveness in combination with a small-molecule inhibitor of the PI3K/AKT pathway in a cohort of patients with ovarian clear cell carcinomas harbouring the *ARID1A* mutation (227).

To further complete our capacity to characterize the genetic landscape of EC, we employed another targeted NGS-panel on cfDNA. We used a different panel because due to the high sensitivity required for the ctDNA detection. Through this method, genetic alterations were detected in 68.75% (22/32) of the samples. Notably, our cohort included diverse disease stages but was notably enriched with patients exhibiting a highly aggressive tumour evolution. Therefore, any conclusions drawn from this study should be contextualized within the predominantly advanced-stage disease setting.

USC UNIVERSIDADE DE SANTIAGO DE COMPOSTELA

The utilization of a targeted panel offers several advantages, including the capacity to obtain patient-specific genetic information and monitor clonal evolution over time without sequencing the primary tumour (71,228,229). However, it is not without limitations. For instance, it needs larger quantities of cfDNA compared to ddPCR but offers a more comprehensive view of the mutational landscape. Additionally, the lack of information about the primary tumour presents a challenge due to clonal haematopoiesis (230).

Clonal haematopoiesis, characterized by the expansion of mutated hematopoietic stem or progenitor cells, can introduce mutant DNA sequence into circulating DNA (231,232). While commonly associated with aging, clonal haematopoiesis can also arise from environmental exposures or medical treatments (232). These mutations, although not inherently indicative of haematological malignancies, are increasingly recognized for their potential involvement in various diseases, including cancer.

The presence of mutations originating from clonal haematopoiesis represents a challenge for cfDNA sequencing interpretation. These mutations may be erroneously attributed to the tumour, since they can affect relevant tumour suppressors like *TP53*, leading to false positive results and potentially affecting treatment decisions (233). Strategies such as deep sequencing and variant allele frequency analysis, along with comparisons to mutations present in hematopoietic cells, can help mitigate these challenges and enhance the accuracy of liquid biopsy-based diagnostics and monitoring in cancer patients (233,234). In our cohort, alterations in *TP53* and *GNAS* were among the most commonly mutated genes, often associated with clonal haematopoiesis (234,235).

Despite the previously limitations, the results obtained through the targeted NGS approach are promising. They allowed for the identification of

USC UNIVERSIDADE DE SANTIAGO DE COMPOSTELA

traceable mutations throughout the disease course, as evidenced by follow-up graphs, and enabled the discovery of novel alterations such as *MYC* amplifications, which could potentially serve as new therapeutic avenues for patients with advanced EC.

Whereas the UA is a reliable sample that captures the ITH and can be used to assess the genomic landscape of the primary tumour, prior to surgical resection. It lacks value to perform longitudinal analyses once the patient undergoes surgery. In this regard, the analyses of cfDNA using targeted-NGS approaches allows for the identification of novel alterations that may arise through-out the course of the disease that could be potentially actionable pathways. Therefore, both approaches with their limitations and advantages should be considered as complementary in the assessment of the mutational landscape of EC patients and the potential implementation into the clinic to improve patient management.

4.1.5 | Conclusions

Overall, our study underscores the value of UA-based and cfDNA-based NGS profiling in elucidating the genomic landscape of EC, offering insights into tumour heterogeneity, prognostication, and therapeutic avenues for improved patient care.

USC UNIVERSIDADE DE SANTIAGO DE COMPOSTELA

4.2 | CHAPTER II

Epigenetic regulation in Endometrial Carcinoma: Insights from Methylome Profiling

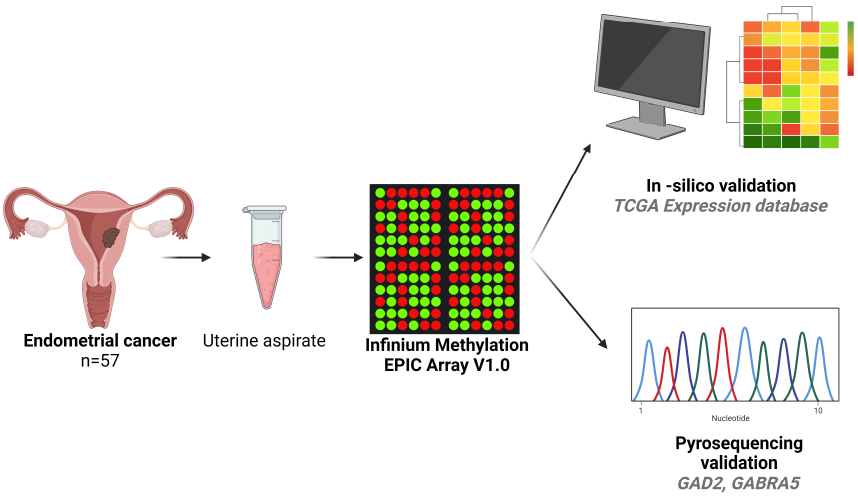
Results from this chapter have been presented at the Liquid Biopsy meeting in Santiago de Compostela, 2023.

USC
UNIVERSIDADE DE SANTIAGO DE COMPOSTELA

CHAPTER II

Epigenetic regulation in Endometrial Carcinoma: Insights from Methylome Profiling

GRAPHICAL ABSTRACT



Created with BioRender.com

Keywords: endometrial cancer, liquid biopsy, methylome characterization, Methylation Epic array, uterine aspirate, prognostic.

USC UNIVERSIDADE DE SANTIAGO DE COMPOSTELA

CHAPTER II

Epigenetic regulation in Endometrial Carcinoma: Insights from Methylome Profiling

ABSTRACT

EC poses a significant health burden globally, with increasing incidence and mortality rates. Despite advancements in understanding its molecular profile, there remains a crucial need for minimally invasive biomarkers to guide patient stratification and treatment decisions. Here, we conducted a comprehensive study using the MethylationEPIC v1.0 array to analyse the methylome of 57 EC patients' UA samples. Our primary objective was to identify differential methylation profiles between EEC and SC histological subtypes, with the aim of understanding the mechanisms associated with the tumour aggressiveness and identify novel therapeutic pathways. We observed a robust hypomethylation profile associated with SC, compatible with the aggressive nature of this subtype. Specifically, our analysis revealed deregulation of key pathways, including the GABAergic and calcium signalling pathways, implicating their potential roles in EC progression. Pyrosequencing validation and *in silico* analyses further confirmed our findings, highlighting the reliability and clinical relevance of UA-based methylome analysis. Overall, our study provides valuable insights into EC's methylome landscape, offering potential new avenues for personalized medicine and highlighting the utility of UA as a minimally invasive sample for molecular profiling in EC patients.

USC UNIVERSIDADE DE SANTIAGO DE COMPOSTELA

4.2.1| Introduction

Although usually associated with good clinical outcome, a non-neglectable 10-30% of patients undergo tumour progression within the first two years of the disease (236,237), being the SC (5-10% of EC) responsible for over 40% of all EC related deaths (3,9). The SC are usually associated with older women and higher stage at diagnosis (3,9). According to the molecular profile, the SC is characterised by a high number of amplifications on the oncogenes *MYC*, *ERBB2* and *CCNE1*, as well as mutations in the *TP53* gene (90%) (10).

Epigenetic regulation has been described as a key player in tumorigenesis in multiple cancer types, including EC (238,239). One of the most important alterations is the DNA hypermethylation, since it may lead to transcriptional regulation of relevant cellular pathways (240,241). In EC, DNA methylation plays a key role in the tumour biology, even at early phases of the disease. For instance, hypermethylation of the *MLH1* promoter is one of the main characteristics of the MSI hypermutated TCGA subgroup (10). Besides, some studies have performed methylation analyses attempting to identify a specific profile that would allow fort the identification of patients with SC as well as new targetable pathways that could improve patients care (242,243). Recent studies have shown the value of methylation analyses in liquid biopsy samples. For instance, Beinse et al have shown that through the analyses of hypermethylation levels in *OXT* and *ZSCAN12* in ctDNA samples they can identify the EC patients with a high sensitivity and specificity, regardless of the molecular subgroup (244).

This chapter focused on study of the methylome of UAs collected at surgery from 57 patients diagnosed with EC utilizing methylation arrays. The primary objective was to compare differential methylation profiles between EEC and SC subtypes. Through this comparative analysis, the study aims to

USC UNIVERSIDADE DE SANTIAGO DE COMPOSTELA

understand the biology of the most aggressive endometrial tumours and identify potential novel therapeutic pathways, that could open new avenues into personalized medicine approaches tailored to individual patient needs.

4.2.2 | Material & Methods

4.2.2.1 | Patients' inclusion and sample collection

This study was performed in samples from 57 patients with EC, including SC and EEC, grade 1-3 and FIGO stage I-IV tumours. Clinical variables of the patients are summarised on Table 1. Patients were recruited between January 2018 and June 2022 at the Gynaecology Department of Vall d'Hebron University Hospital (Barcelona, Spain), the MD Anderson Cancer Center (Madrid, Spain) and the University Clinical Hospital of Santiago de Compostela (Santiago de Compostela, Spain).

Table 1: Clinical characteristics of the studied cohort in Chapter II.

CLINICAL VARIABLES	*N=57*	CLINICAL VARIABLES	*N=57*
Age	55	**Lymphovascular Space Infiltration**	50
Median (IQR)	69 (59,76)	No	34 (68%)
Histology	57	Yes	16 (32%)
NEEC	36 (63%)	**TCGA**	57
EEC	21 (37%)	*POLE*	4 (7%)
Tumour Grade	57	*MSI*	19 (33%)
Grade 1	8 (14%)	*NSMP*	9 (16%)
Grade 2	13 (23%)	*HCN*	25 (44%)
Grade 3	36 (63%)	**Relapse**	57
FIGO Stage	57	No	33 (58%)
I	30 (53%)	Yes	24 (42%)
II	9 (16%)	**Exitus Status**	57
III	12 (21%)	Dead	36 (63%)
IV	6 (11%)	Alive	21 (37%)
Myometrial Infiltration	56		
<50%	23 (41%)		
>50%	33 (59%)		

USC UNIVERSIDADE DE SANTIAGO DE COMPOSTELA

4.2.2.2 | DNA extraction and bisulfite conversion.

DNA isolated form the UA was subjected to bisulfite conversion using the EZ DNA methylation kit (ZYMO Research) according to the manufacturer's instructions.

4.2.2.3 | Methylome analyses

The bisulfited DNA was analysed using Infinium MethylationEPIC v1.0 array (Illumina) according to the manufacturer's instructions. In brief, the bisulfited DNA was fragmented, precipitated and later resuspended to the appropriate concentration to be hybridize to the BeadChips; then the chips were stained and imaged on the iScan System (Illumina).The methylation data was analysed using the RnBeads package (245). In brief, the methylation data was corrected and normalised using two different pipelines, further described on the 4.2.3.1 section. CpGs were annotated using the R package minfi. Statistical significance between groups was evaluated using a threshold of false-discovery rate (FDR) <0.1 and with a Δ-β ≥|0.2|. Differentially methylated CpGs (DMCpGs) were subjected to gene set enrichment analyses (GSEA) using the R packages methylGSEA and missMethyl for the Gene Ontology (GO) analyses. For the pathway analyses the Kyoto Encyclopedia of Genes and Genomes (KEGG), PANTHER and Wikipathways in Genecodis (https://genecodis.genyo.es/) was used as the primary database (246).

4.2.2.4 | Pyrosequencing validation

In order to validate the results of the MethylationEPIC v1.0 array, two different CpGs (*GABRA5, GAD2*) with the highest fold change between the different comparisons were validated through pyrosequencing. Total genomic DNA (500 ng) from the UA's was treated with sodium bisulfite with the EZ

USC UNIVERSIDADE DE SANTIAGO DE COMPOSTELA

DNA Methylation kit (Zymo Research) following the manufacturer's recommendations. For pyrosequencing, primer sequences were designed with PyroMark Assay Design 2.0 (Qiagen). Standard PCRs were carried out with bisulfite-converted genomic DNA. PCR products were analysed on 2% agarose gels before pyrosequencing. A PyroMark Q24 Vacuum Workstation was used for the immobilization and preparation of PCR products. Pyrosequencing reactions were performed using a PyroMark Gold Q24 Reagent Kit (Qiagen) following the manufacturer's instructions. DNA methylation values were obtained using the PyroMark Q24 software 2.0 (Qiagen). Human methylated and non-methylated DNA samples (Zymo Research) were used as positive and negative control, respectively. Water was used as no-template control.

4.2.2.5 | Statistical Analysis

To access the transcriptomic database of The Cancer Genome Atlas (TCGA), we employed TCGAbiolinks package (247). Following data retrieval, we performed preprocessing steps to ensure data quality and compatibility for downstream analysis, including normalization and filtering of low-quality samples or genes. The processed data was then subjected to exploratory data analysis, differential gene expression analysis, and advanced statistical methods to derive biological insights.

4.2.3 | Results

4.2.3.1 | The uterine aspirate as a reliable sample for methylome analyses.

The raw methylation data was analysed using the RnBeads package. Two different normalization methods ('SWAM' and 'BMIQ') were tested to identify the best option for the UA (Figure 1A-B), being the 'BMIQ' method the better option based on the β-values density representation (Figure 1B). From the 57

USC UNIVERSIDADE DE SANTIAGO DE COMPOSTELA

samples included in the array, only 1 sample did not pass the quality control. From the 866895 probes included within the array, a total of 11089 probes (1.27%) were removed based on the Greedycut approach. From the remaining 681821 probes, a total of 1312 probes (0.19%) were removed: 1154 probes (87.95%) were removed based on the context and 158 probes (12.05%) were removed due to high number of missing values. From the remaining 680509 probes only 245 probes could not be annotated (Figure 1C).

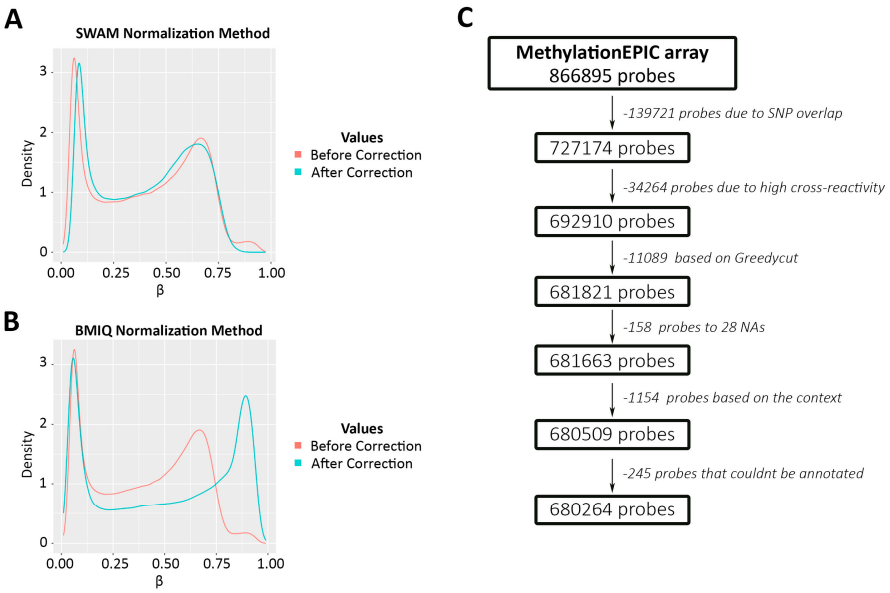


Figure 1: Quality metrics of the methylome studies applied in the UA. **A.** β-value distribution before and after correction and normalization using the SWAM normalization method **B.** β-value distribution before and after correction and normalization using the BMIQ normalization method **C.** Summary of the followed probes trimming.

4.2.3.2 | Differential methylome profiling based on histological subtype.

Differential analyses were performed according to the different histological subtypes: EEC vs SC. A total of 11515 differentially methylated

USC UNIVERSIDADE DE SANTIAGO DE COMPOSTELA

CpGs (DMCpGs) were found with FDR<0.1. Of those, 667 were found in promoter regions within CpG islands. When taking into consideration the Δβ-value >|0.2| we identified 177 DMCpGs, mainly hypomethylated (173 DMCpGs) in USC patients (Figure 2A).

Overall, there was a balanced between hypomethylated and hypermethylated CpGs between both groups (Figure 2B). When focusing on the 177 DMCpGs we identified a specific pattern that allows us to discriminate between the EEC and SC (Figure 2C-D). In fact, 90% (18/20) of the SC patients were correctly identified with this methylation signature. Interestingly, there was a homogeneous distribution of the hypomethylated CpGs and a cluster of hypermethylation on the Chr20 (Figure 2E).

Next, GSEA was performed on the DMCpGs. With this approach we found that most DMCpGs were related to signal transduction, chemical synaptic transmission, and cell proliferation (Figure 2F). If we focused on the 173 hypomethylated DMCpGs (104 genes) we identified pathways related to: neuroactive ligand-receptor interaction, cAMP signalling and calcium signalling as the main enriched pathways in the KEGG database (Figure 2G); when using the PANTHER database, we found that the most affected pathways related to synaptic vesicle trafficking, ionotropic glutamate receptor pathway and β-adrenergic receptor signalling pathway (Figure 2H). As for the 4 hypermethylated DMCpGs, only 2 genes were found to have a differential methylation, *DIDO1* and *NPBWR2*.

USC UNIVERSIDADE DE SANTIAGO DE COMPOSTELA

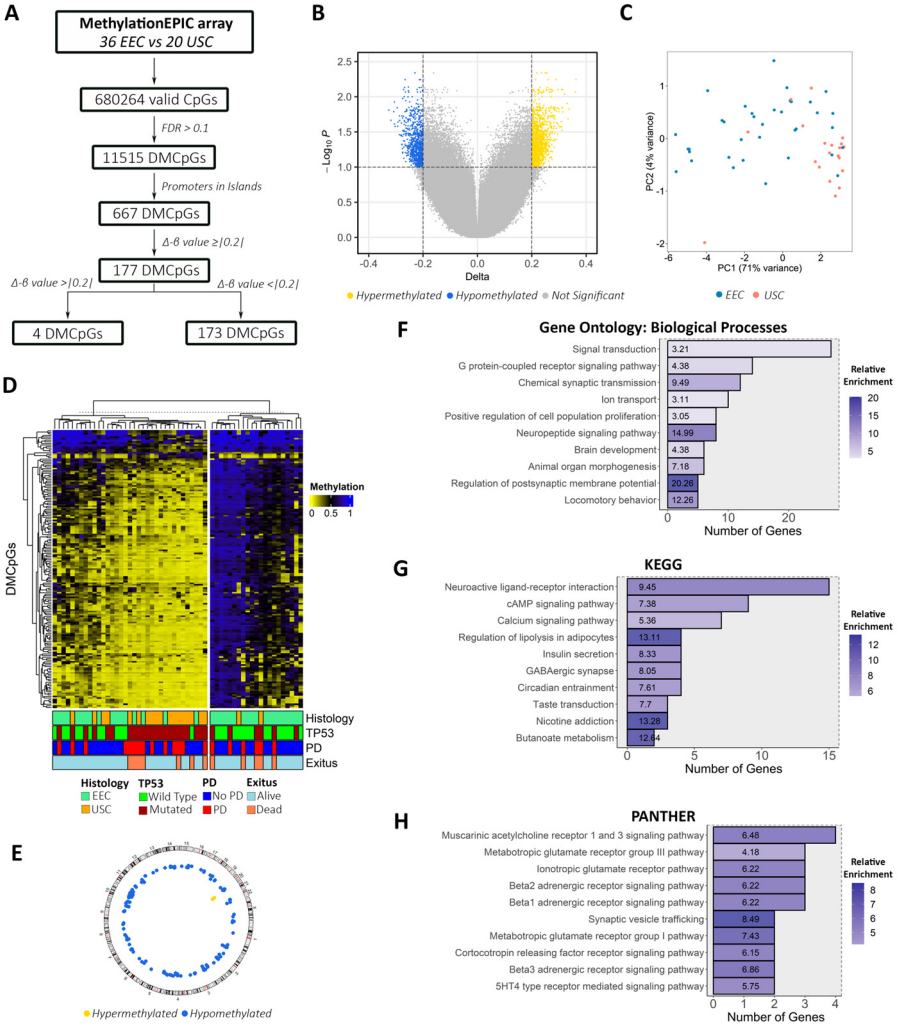


Figure 2: NEEC present a differential methylome profile**. A.** Schematic representation of the followed pipeline and identified CpGs **B.** Volcano plot of the differentially methylated CpGs. **C.** PCA of the 177 DMCpGs identified in the EPIC array. **D.** Heatmap representation of the 177 differentially methylated CpGs **E.** Circle plot showing the distribution of the 177 DMCpGs along the genome **F.** Bar plot representation of the GO: Biological Processes identified with an FDR> 0.1. **G.** Bar plot representation of the KEGG pathways identified with an FDR > 0.1. **H.** Bar plot representation of the PANTHER pathways identified with an FDR > 0.1.

USC UNIVERSIDADE DE SANTIAGO DE COMPOSTELA

4.2.3.3 | Validation of the methylation pattern by Pyrosequencing

In order to technically validate the results of the MethylationEPIC v1.0 array, two CpGs with some of the highest foldchange in the methylation levels (*GABRA5* and *GAD2*) were characterized by pyrosequencing. Out of the 57 patients, 56 passed the quality metrics after pyrosequencing. The results from the pyrosequencing further validate the results obtained with the array for these two genes, since the same tendency was found. *GAD2* and *GABRA5* showed significant hypomethylation in the SC subtype when compared to the EEC (Figure 3A-C). Moreover, the correlation between pyrosequencing and the MethylationEPIC v1.0 array showed high concordance (R=0.4-0.6, p-value<0.001, Figure 3B-D). Although the comparison of different technologies such as the MethylationEPIC array and pyrosequencing render different frequencies, even when analysing the same variant, these results agree with the fact that *GAD2* and *GABRA5* are hypomethylated in the SC subtypes.

USC UNIVERSIDADE DE SANTIAGO DE COMPOSTELA

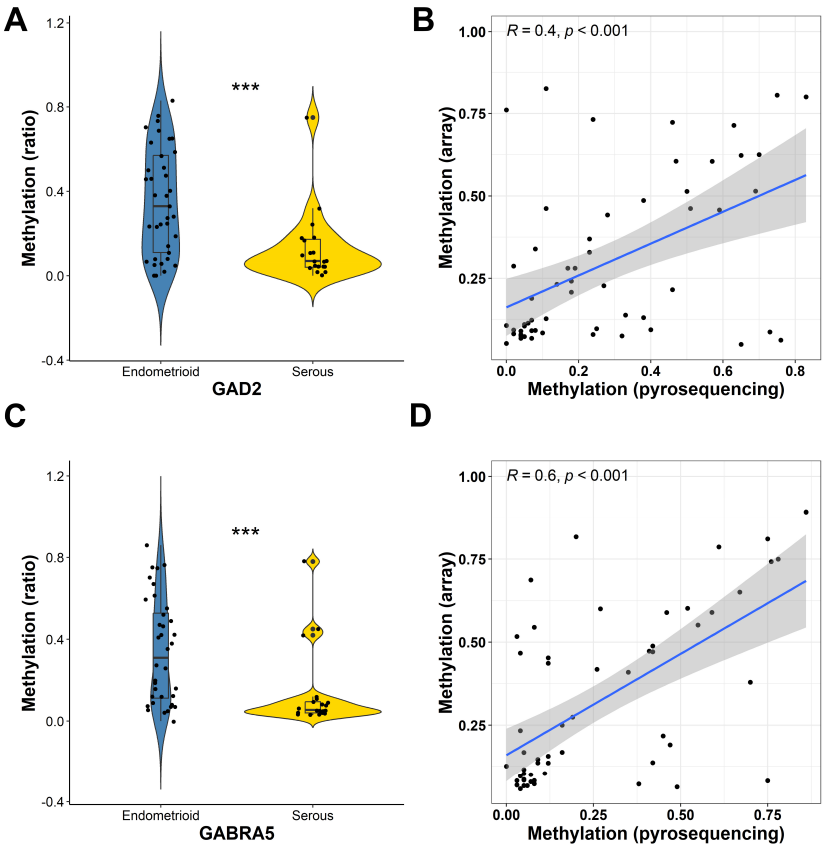


Figure 3: Validation of the results from the methylation epic array by pyrosequencing**. A-B.** Results from the *GAD2* validation, A. violin plot showing significant hypomethylation of the gene in the serous histology. B. Correlation between the array results and the pyrosequencing validation. **C-D.** Results from the *GABRA5* validation, C. violin plot showing significant hypomethylation of the gene in the serous histology. D. Correlation between the array results and the pyrosequencing validation.

4.2.4 | Discussion

Epigenetic deregulation is one of the main drivers of oncogenesis. Being the most studied promoter methylation within CpG islands, since it has been directly linked to altered expression of the affected genes. In EC, epigenetic

USC UNIVERSIDADE DE SANTIAGO DE COMPOSTELA

alterations are closely related to patient prognosis (238). Despite recent advances in the field, EC lacks minimally invasive biomarkers that could be used for early detection and risk stratification. Early detection, specially through minimally invasive samples, is a key factor to improve patient survival. Our study was pioneer on characterising the methylome of EC patients in a minimally invasive manner through the UA. Our results further validate the UA as a powerful tool, not only for the characterization of the mutational landscape through NGS approaches as seen on the previous chapter (91,168), but also for methylome analyses.

Overall, our study showed that patients with poor clinical outcome have a global hypomethylation profile in promoter regions within CpG islands in genes involved in pathways that lead to higher cell proliferation rates, survival, more invasive phenotypes, and migration capabilities. The most affected pathways related to the GABAergic pathway and Calcium signalling pathways.

The GABAergic pathway is not limited to the neuronal tissue, but there is also expression of GABA, and its receptor in other tissues, such as lung, pancreas, kidney, intestine, prostate, liver, skin, immune cells, and more importantly, in tumoral states, sometimes promoting proliferation and migration and immune evasion (248–252). Several studies have shown how through multiple mechanisms GABA can promote and regulate cancer cells, such as enhanced metabolism, receptor signalling or modulating the tumour microenvironment (248,249,251–256). Through the methylation analyses we were able to identify 4 genes with DMCpGs (*GAD2*, *GABRA5*, *SLC6A11*, *ADCY8*). Of those, *GAD2* is involved with GABA metabolism; in line with previous publications, *GAD* enzymes are overexpressed in some tumours, like ovarian, gastric, lung and breast, which enhances proliferation and invasion,

USC UNIVERSIDADE DE SANTIAGO DE COMPOSTELA

and increases the concentration of GABA (249,251,254,257–260). Regarding the GABA-receptors, GABA-AR activation suppresses neural tumours, but promotes cell proliferation and migration in malignancies outside of the nervous system (251,252). The key components to promote proliferation in different cancer types are the GABA-AR subunits: *GABRB1*, *GABRB3*, *GABRA5* and *GABRAG16-19*. *GABRA5* (subunit α 5) is one of the differentially hypomethylated genes found in SC patients. The role of the GABA pathway in EC is still widely unknown but given the wide variety of tumoral types that show a correlation between GABA and cell proliferation and migration, which confers a more aggressive phenotype, it may be linked to more aggressive EC subtypes and could be a novel target for therapeutic approaches.

On the other hand, we found a specific regulation of the calcium signalling pathway in EEC, where we found 7 genes with a differentially methylation expression (*ADCY8, AGTR1, GNAL, GRIN2A, NMDA, NTRK3, RYR2, TACR3*). Overall, the calcium signalling pathway has been described as a promotor of cell proliferation, survival and differentiation, since the flux of Ca^{2+} acts as an activator of the PIK/AKT/mTOR or ERBB pathways (261). Alterations in the PIK/AKT/mTOR or ERBB pathways have been previously described as being deregulated in EC (262,263) and inhibitors against this pathways are already in use within clinical trials as potential new targeted therapies in advanced EC patients (17). Moreover, calcium signalling deregulation has also been shown to promote EMT transition in other cancer types by promoting angiogenesis, extracellular matrix remodelling, tumour invasion, immune invasion or drug resistance, among others (264). Our methylation analyses showed that the GPCR are mainly hypomethylated in the SC patients, which would lead to an increase on its activity and a higher induction rate of EMT through the recruitment of tumour associated macrophages (265). Therefore, generating a favourable environment for invasion and metastases.

USC UNIVERSIDADE DE SANTIAGO DE COMPOSTELA

Interestingly with our approach only 4 genes (*DIDO1, NPBWR2, c11orf36, MRGPRG and LOXHD1*) were found be significantly hypermethylated in the SC patients. Overall these genes are involved in G protein activity which is associated mainly to MAP kinases pathway activation and β-arrestins scaffold enzymes which degrade second messengers generated by G protein activity (266). Importantly, *DIDO1* (Death Inducer-Obliterator 1) is a protein coding gene that acts as a tumour suppressor gene, and when overexpressed is linked to higher levels of apoptosis (267,268). Moreover, products of *DIDO1* transcripts could impair cancer progression as shown by Zhang et al in gastric cancer (267,268). Therefore, *DIDO1* could represent a potential therapeutic target for EC.

4.2.5 | Conclusions

In conclusion, our study demonstrates the utility of UA samples for methylome analyses of EC, offering insights into epigenetic alterations associated with histological subtypes and clinical outcomes. Our findings revealed differential methylation patterns in promoter regions within CpG islands, with SC patients exhibiting predominantly hypomethylated CpGs compared to EEC patients. Moreover, the implicated pathways were related to cell proliferation, migration and invasion, further elucidating the molecular mechanisms underlying disease progression; thus, contributing to tumour progression and metastasis in EC.

Overall, our study provides novel insights into the methylome landscape of EC, emphasizing the importance of epigenetic regulation in disease pathogenesis and progression. By identifying the molecular mechanisms underlying different histological subtypes and clinical outcomes, our findings contribute to the development of minimally invasive biomarkers and targeted therapies for improved management of EC patients.

USC UNIVERSIDADE DE SANTIAGO DE COMPOSTELA

4.3 | CHAPTER III

Non-invasive detection of microsatellite instability in patients with endometrial cancer

Results from this chapter have been published in the International Journal of Cancer (168)

USC
UNIVERSIDADE DE SANTIAGO DE COMPOSTELA

CHAPTER III

Non-invasive detection of microsatellite instability in patients with endometrial cancer

Carlos Casas-Arozamena[1,2], Cristian Pablo Moiola[3], Ana Vilar[4], Marta Bouso[5], Juan Cueva[1,6], Silvia Cabrera[3], Victoria Sampayo[4], Efigenia Arias[4], Alicia Abalo[1], Ángel García[7], Ramón Manuel Lago-Lestón[1], Sara Oltra[8], Eva Díaz[8], Juan Ruiz-Bañobre[1,6,9,10], Rafael López-López[1,6,10], Gema Moreno-Bueno[8,10,11], Antonio Gil-Moreno[3,10,12], Eva Colás[3,10], Miguel Abal[1,10], Laura Muinelo-Romay[1,10]

[1]Translational Medical Oncology Group (Oncomet), Health Research Institute of Santiago de Compostela (IDIS), University Hospital of Santiago de Compostela (SERGAS), Trav. Choupana s/n, 15706 Santiago de Compostela, Spain.

[2]University of Santiago de Compostela (USC), Praza do Obradoiro, 0, 15705 Santiago de Compostela, Spain

[3]Biomedical Research Group in Gynaecology, Vall Hebron Research Institute (VHIR), Universitat Autonoma de Barcelona, 119-129 Pg. Vall d'Hebron, 08035 Barcelona, Spain.

[4]Department of Gynaecology, University Clinical Hospital of Santiago de Compostela (SERGAS), Trav. Choupana s/n, 15706 Santiago de Compostela, Spain.

[5]Department of Pathology, University Clinical Hospital of Santiago de Compostela (SERGAS), Trav. Choupana s/n, 15706 Santiago de Compostela, Spain.

[6]Department of Medical Oncology, University Clinical Hospital of Santiago de Compostela, University of Santiago de Compostela (USC), 15706 Santiago de Compostela, Spain.

[7]Pathology Department, Vall Hebron University Hospital, Barcelona, Spain.

[8]Foundation MD Anderson International, C/Gómez Hemans 2, 28033 Madrid, Spain.

[9]Genomes and Disease, Centre for Research in Molecular Medicine and Chronic Diseases (CiMUS), University of Santiago de Compostela, 15706 Santiago de Compostela, Spain.

[10]Centro de Investigación Biomédica en Red de Cáncer (CIBERONC).

[11]Biochemistry Department, Medicine Faculty, Universidad Autónoma de Madrid (UAM), C/Arturo Dupurier 4, 28029 Madrid-Spain.

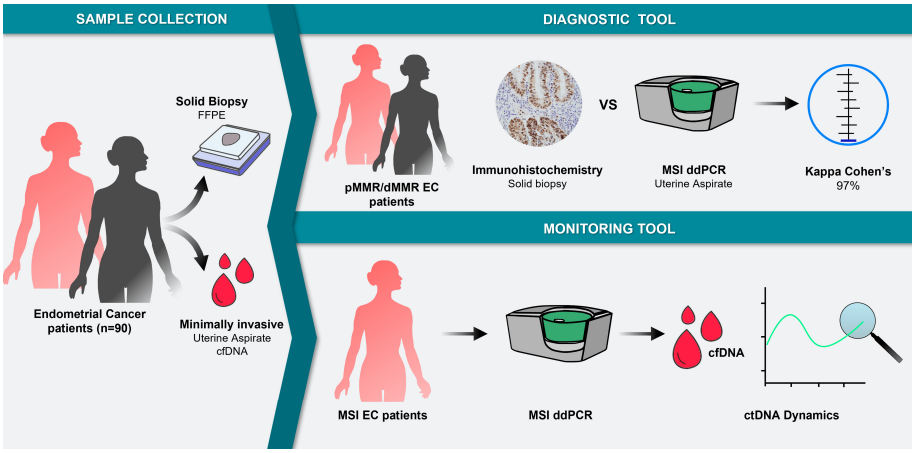
[12]Gynaecology Department, Vall Hebron University Hospital, Barcelona, Spain

USC UNIVERSIDADE DE SANTIAGO DE COMPOSTELA

CHAPTER III

Non-invasive detection of microsatellite instability in patients with endometrial cancer

GRAPHICAL ABSTRACT



Keywords: cfDNA, ctDNA, disease monitoring, endometrial cancer, liquid biopsy, microsatellite instability, uterine aspirate.

USC UNIVERSIDADE DE SANTIAGO DE COMPOSTELA

CHAPTER III

Non-invasive detection of microsatellite instability in patients with endometrial cancer

ABSTRACT

The analysis of MMR proteins in solid tissue is the SoC for the MSI characterization in EC. UAs or cfDNA samples capture the intratumor heterogeneity and provide a more comprehensive and dynamic molecular diagnosis. Thus, MSI analysis by ddPCR in UAs and cfDNA can provide a reliable tool to characterise and follow-up the disease. The UAs, FFPE and longitudinal plasma samples from a cohort of 90 EC patients were analysed using ddPCR panel and compared to the SoC. A high concordance (96.67%) was obtained between the analysis of MSI markers in UAs and the SoC. Three discordant cases were validated as unstable by ddPCR on FFPE samples. Besides, a good overall concordance (70.27%) was obtained when comparing the performance of the ddPCR assay on UAs and cfDNA in high-risk tumours. Importantly, our results also evidenced the value of MSI analysis to monitor the disease evolution. MSI evaluation in minimally invasive samples shows great accuracy and sensitivity and provides a valuable tool for the molecular characterization and follow-up of endometrial tumours, opening new opportunities for personalized management of EC.

USC UNIVERSIDADE DE SANTIAGO DE COMPOSTELA

4.3.1 | Introduction

MSI represents a clinically relevant molecular alteration in EC and other tumours (269). Microsatellites are short-tandem repeats observed in coding and noncoding regions throughout the human genome (270,271). DNA polymerases are prone to introduce errors in these regions, generating mismatched DNA strands. Tumours with a deficiency in any of the main proteins of the DNA MMR pathway are characterized by the presence of MSI (272).

Moreover, the MMR deficiency resulting from germline mutations or epigenetic alterations in any of the MMR genes, as well as deletions in the *EPCAM* gene, are the principle cause of Lynch syndrome and its variants (Muir-Torre or Turcot syndromes) (273). Approximately 20% to 30% of sporadic ECs are characterized by MSI, mainly caused by somatic promoter hypermethylation and silencing of *MLH1* gene (10) while defective pathway due to Lynch syndrome accounts for 2% of ECs (274).

Although the diagnosis of MMR-deficiency/MSI in ECs is recommended as an initial step in Lynch syndrome screening algorithms, today this particular molecular feature has also therapeutic implications as predictive biomarker for various anti-PD1 therapies across different tumour types, particularly in colorectal and ECs (275,276). Moreover, MSI represents a well-established prognostic biomarker associated in ECs with a better prognosis (277).

MMR-deficiency can be detected by MSI analysis and/or IHC characterization of the four MMR proteins. IHC has been used as the standard technique in numerous institutions since the loss of MMR protein expression is normally homogeneous and easy to detect (278). However, despite the concordance between the MMR proteins and the MSI assessment has demonstrated to be robust, some centres combine both tests, since some

USC UNIVERSIDADE DE SANTIAGO DE COMPOSTELA

discordances have been described, mainly due to false positive or negative cases after the IHC analysis (279).

Traditionally, MMR/MSI deficiency is interrogated in solid tissue samples with the limitation of analysing only a snapshot of the tumour diversity, which is relevant especially in the context of advanced EC (205,280). Our group has previously demonstrated the value of the genomic characterization of the UAs to capture the ITH and identify potential targeted therapies to treat EC patients (91). Besides, ctDNA monitoring has shown to be feasible and informative in the context of EC, representing a promising tool to characterize the genetic landscape of endometrial tumours within their temporal evolution (91,212).

With the goal of translating the MSI testing into minimally invasive scenarios and improving the current diagnostic and monitoring tools, in the present chapter we sought to validate the analysis of MSI in UAs and cfDNA obtained from patients with EC through the application of a high-sensitive ddPCR assay.

4.3.2 | Material and methods

4.3.2.1 | Patient inclusion and samples collection

A total of 90 patients with EC were recruited between January 2018 and June 2021 at the Gynaecology Department of Vall d'Hebron University Hospital (Barcelona, Spain), the MD Anderson Cancer Center (Madrid, Spain) and the University Clinical Hospital of Santiago de Compostela (Santiago de Compostela, Spain).

All UAs were collected at surgery using a Cornier canula and processed as previously described in the general M&M section. Peripheral blood samples were collected at surgery and during the patients' follow-up (every 6 months

USC UNIVERSIDADE DE SANTIAGO DE COMPOSTELA

until recurrence/progression of the disease) as previously described in the general M&M section. FFPE tumour tissue resected after hysterectomy was obtained from the Pathology Departments of the participating hospitals. FFPE samples were selected by the pathologist as of being representative of the tumour of origin.

4.3.2.2|Immunohistochemistry characterization

The immunohistochemistry characterization of all samples was performed at the Pathology Services from the hospitals involved in the study. Sections (4µm thick) from FFPE tumour tissue were automatically stained in a Dako Omnis immunostainer (Dako-Agilent, Santa Clara, CA). Briefly, the immuno-histochemical protocol included the following steps: (a) heat-induced epitope retrieval solution at high pH (Dako-Agilent) for 20 min at 97ºC; (b) incubation with ready to use FLEX primary monoclonal anti-bodies (Dako-Agilent) which recognize *MLH1* (mouse antibody, clone ES05), *MSH2* (mouse antibody, clone FE11), *MSH6* (rabbit antibody, clone EP49) and *PMS2* (rabbit antibody, clone EP51) for 20 min; (c) mouse and rabbit linker (Dako-Agilent) for 10 min each;(d) EnVision FLEX/HRP (Dako-Agilent) for 20 min; (e) 3,30-diaminobenzidine tetrahydrochloride chromogen solution (Dako-Agi-lent) for 5 min and (f) EnVision FLEX haematoxylin (Dako-Agilent) for 5 min. Nuclear negativity for *MLH1, MSH2, MSH6* or *PMS2* in tumour cells implies a genetic or genomic alteration of the corresponding DNA mismatch repair genes (Figure 1A). Adjacent normal glands and surrounding lymphocytes were employed as internal positive controls.

4.3.2.3|ddPCR analyses

The MSI status was interrogated in UAs, cfDNA and FFPE samples with the MSI multiplex assay (Bio-Rad, CA) and run on the QX-200 ddPCR system (Bio-Rad, CA) using TaqMan chemistry. The assay consists in two probes

USC UNIVERSIDADE DE SANTIAGO DE COMPOSTELA

competing for the same target sequence. Depending on the alteration one or the other probe is out-competed, indicating MSI. It can be distinguished between mutant (shortened) and wild-type alleles if the length difference is at least two base pairs in the microsatellite repeat region, therefore it does not require the usage of a paired normal sample (Figure 1B-C).

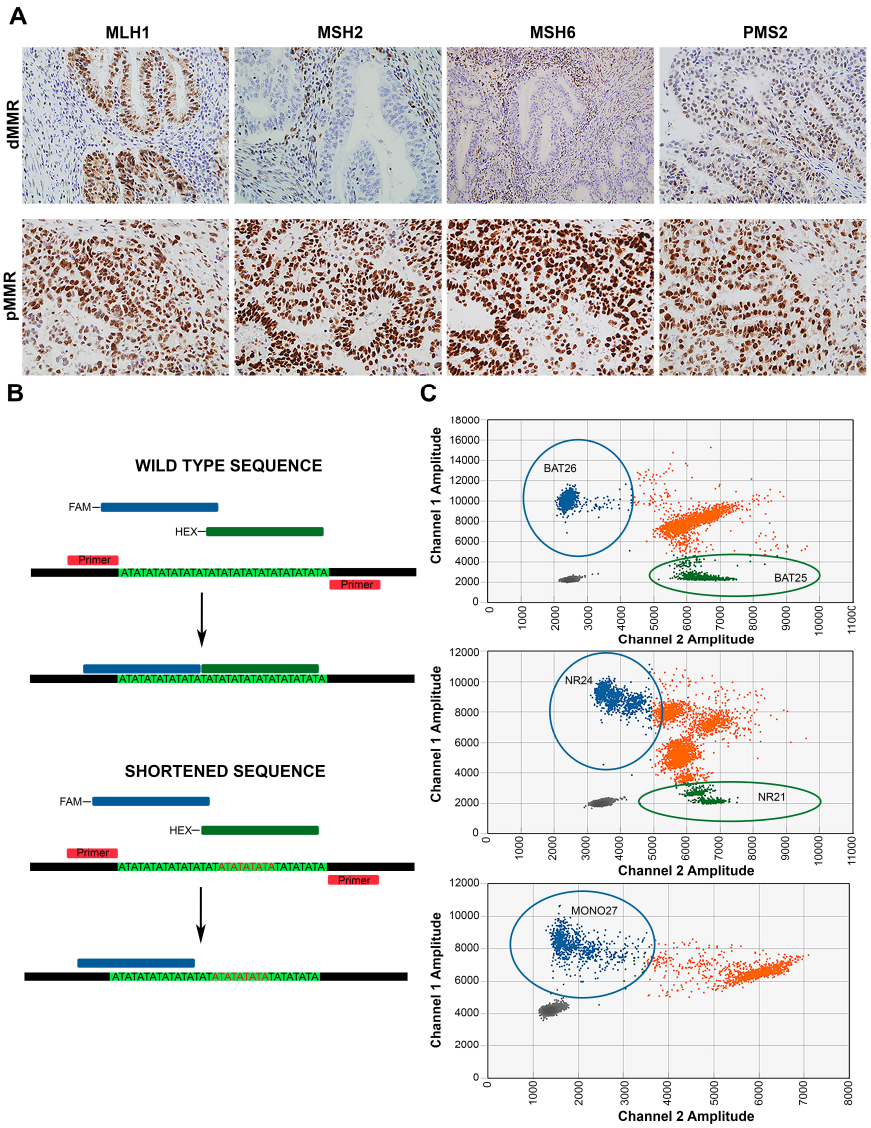


Figure 1 A. Representative images of immunohistochemistry staining for the mismatch repair proteins MLH1, MSH2, MSH6 and PMS2 (60) in one case MMR proficient (pMMR down image) and one case MMR deficient (dMMR, up image). **B.** Schematic representation of BioRad's MSI determination panel, two probes recognize the sequence of interest, one marked with FAM and one with HEX, whenever there is a reduction in the sequence, one of the probes will not be able to attach. Therefore, identifying the altered sequences with only one probe. **C.** Results of the MSI assay (assessment of the mononucleotide repeats BAT26, BAT25, NR24, NR21 and Mono27) by ddPCR on the UA obtained from the patient with the dMMR tumour described in A.

4.3.3|Results

4.3.3.1|ddPCR-based analysis of MSI in uterine aspirates and FFPE tissue improves the instability detection in comparison with IHC study

The MSI status was analysed on the UAs of 90 patients with EC using a multiplex ddPCR assay which interrogates the status of five mononucleotide markers (BAT26, BAT25, NR24, NR21 and Mono27) (Table 1). The cohort included low to high risk of recurrence, Grades 1 to 3, FIGO I to IV patients (Table 1), being most of the cases EEC tumours (76.6%), Grade 3 (47.8%) and high risk of recurrence (63.3%). Patients were classified as either low, intermediate or high risk of recurrence, being the patients with NEEC histology, EEC histology Grade 3 with FIGO stage IB-IV or EEC Grades 1 and 2 with FIGO stages II to IV classified as of high risk; EEC with Grade 3 FIGO stage IA or EEC with Grades 1 and 2 FIGO stage IB, as intermediate and EEC with Grades 1 and 2 and FIGO stage IA as of low risk of recurrence, according to the ESGO/ESTRO/ESP guidelines (11).

Cases with at least three markers altered were classified as MSI-high (MSI-H), those with one or two markers altered as MSI-low (MSI-L) while stable cases (MSS) were those without any marker altered (281–284). Thus, after the analysis, we identified 64.45% (58/90) of the cases as MSI-H,2.22%

USC UNIVERSIDADE DE SANTIAGO DE COMPOSTELA

(2/90) as MSI-L and 33.33% (30/90) as MSS. All the questioned markers showed similar levels of VAFs within samples, except for the mononucleotide repeat NR21 that showed a lower level of alteration in most of the cases (Wilcoxon Signed-Rank test: P-value≤.001; Figure 2A).

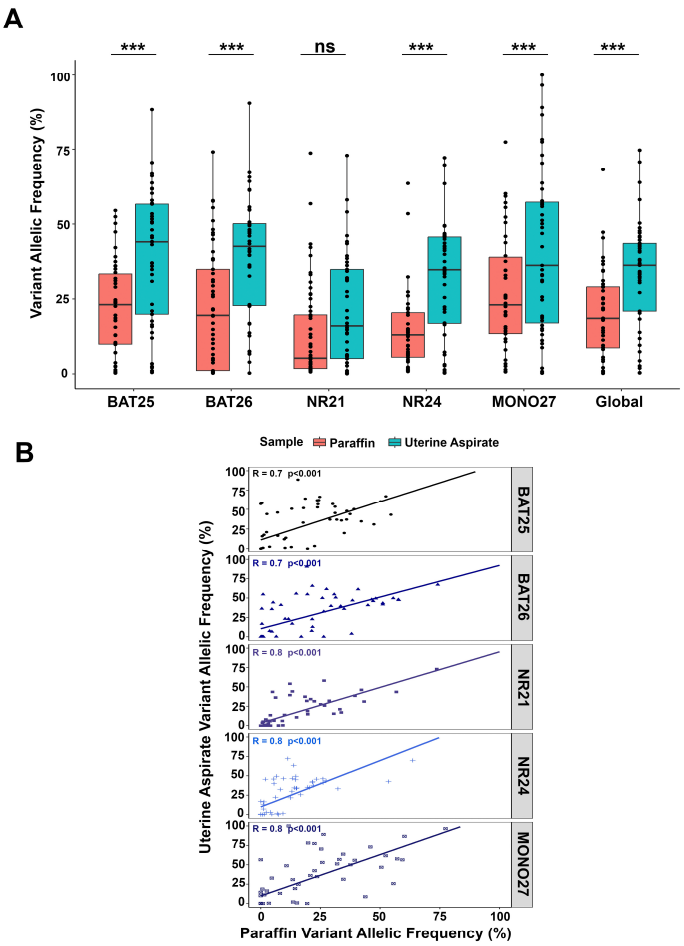


Figure 2: A. Comparison of BAT25, BAT26, NR21, NR24 and Mono27 VAFs between the paired UA (green) and the FFPE tumour tissue (red) from EC patients. **B.** Correlation between each mononucleotide marker in the UA and the corresponding FFPE tissue (n=61). ***p-value<0.001.

USC UNIVERSIDADE DE SANTIAGO DE COMPOSTELA

Importantly, when the results obtained with the MSI test in the UAs were analysed based on the SoC, the MMR proteins status by IHC in solid biopsies, 91.42% (32/35) of pMMR cases showed <3 MSI markers altered (5.71%, 2/35 MSI-L and 85.71%, 30/35 MSS) while three pMMR cases (8.58%, 3/35) were classified as MSI-H. Of note, all patients with dMMR showed three or more MSI markers altered (55/55) (Figure 3A, B). Therefore, a high global agreement of 96.67% (Kappa Cohen=0.93) was obtained between the MSI results in the UAs and the MMR proteins status in tissue (Figure 3D). Indeed, when analysing the cohort based on clinical variables, the agreement was over 91% (Kappa Cohen >0.81) in all the clinico-pathologic groups (Figure 3D).

Additionally, to further validate the assay, DNA from FFPE tumour tissue was also analysed using the ddPCR assay and the results were compared to those obtained on UAs samples with the same assay. A global concordance of 100% was reached (Kappa Cohen=1.00) between both samples, including the three discordant cases (MSI-H in UAs and pMMR with the IHC) found when comparing the MSI panel and the proficiency of the MMR proteins (Figure 3C). Of note, one of the discordant cases had focal expression of PMS2 and MLH1 in the IHC analysis, indicating that molecular heterogeneity could explain this discordant case. In the other two cases an abnormal preserved antigenicity could be behind the false negative for MSI. Therefore, by analysing the MSI status in UAs or FFPE tissues with the ddPCR assay we were able to reclassify three cases determined as stable by the SoC, showing the advantage of the ddPCR strategy in comparison with the IHC. Moreover, the mean VAF of the MSI markers was significantly higher in the UAs (Wilcoxon Signed-Rank test:P-value≤.05), except for the case of NR21, suggesting the presence of a higher tumoral content in the UA compared to the FFPE tumour tissue (Figure 2A). Furthermore, the VAF levels of each

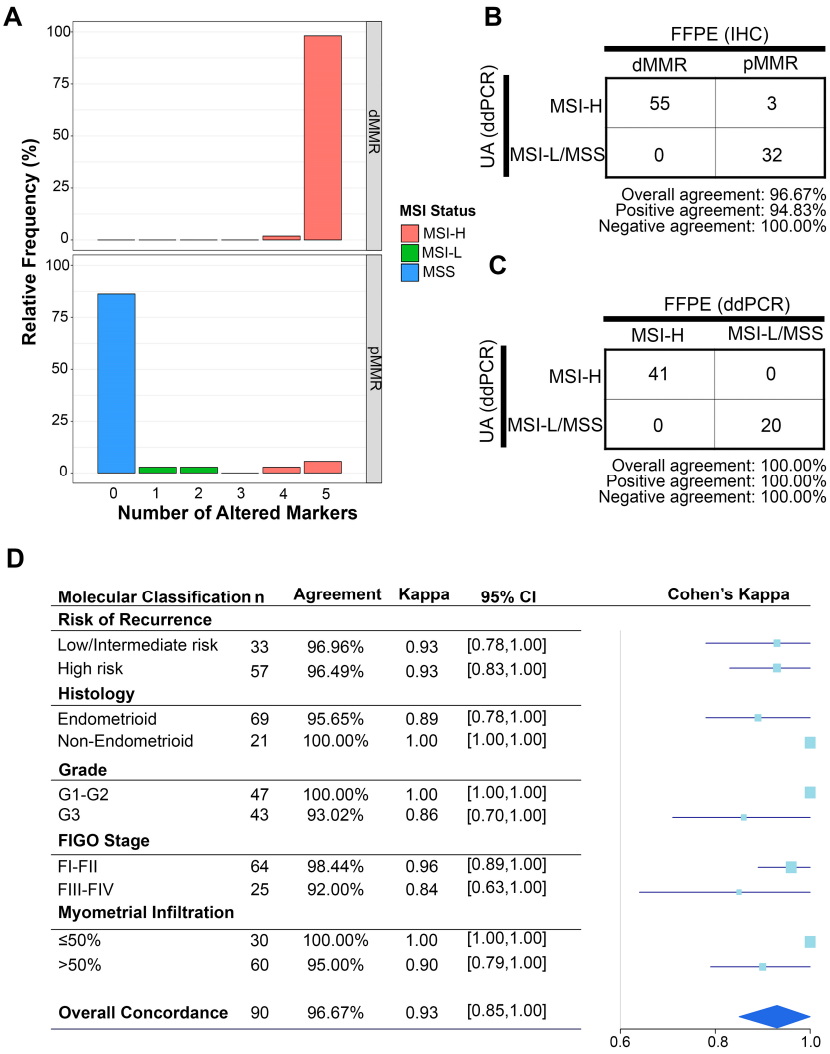
USC UNIVERSIDADE DE SANTIAGO DE COMPOSTELA

mononucleotide marker found in the UA showed a good correlation with its corresponding FFPE sample (Figure 2A, B; Spearman's test: R≥.6,P-value <.001).

Table 1: Clinico-pathological features of the EC cohort of included in the study. pMMR: proficient mismatch repair proteins. dMMR: deficient mismatch repair proteins.

FEATURE	**pMMR** n=35 (38.89%)	**dMMR** n=55 (61.11%)	**Total** n=90 (100%)
TIME OF DIAGNOSIS			
First Diagnosis	33 (94.28%)	54 (98.18%)	87 (96.67%)
Recurrence	2 (5.71%)	1 (1.82%)	3 (3.33%)
HISTOLOGY			
Endometrioid	21 (60.00%)	48 (87.27%)	69 (76.67%)
Non-Endometrioid	14 (40.00%)	7 (12.73%)	21 (23.33%)
GRADE			
G1	7 (20.00%)	11 (20.00%)	18 (20.00%)
G2	9 (25.71%)	20 (36.36%)	29 (32.22%)
G3	19 (54.29%)	24 (43.64%)	43 (47.78%)
FIGO STAGE			
I	17 (48.57%)	31 (56.36%)	48 (53.33%)
II	4 (11.43%)	12 (21.82%)	16 (17.79%)
III	12 (34.29%)	9 (16.36%)	21 (23.33%)
IV	2 (5.71%)	2 (3.64%)	4 (4.44%)
na	0 (0.00%)	1 (1.82%)	1 (1.11%)
MYOMETRIAL INFILTRATION			
<50%	8 (22.86%)	22 (40.00%)	30 (33.33%)
≥50%	27 (77.14%)	33 (60.00%)	60 (66.67%)
RISK OF RECURRENCE			
Low/Intermediate Risk	10 (28.57%)	23 (41.82%)	33 (36.67%)
High Risk	25 (71.43%)	32 (58.18%)	57 (63.33%)

USC UNIVERSIDADE DE SANTIAGO DE COMPOSTELA



D

Molecular Classification	n	Agreement	Kappa	95% CI
Risk of Recurrence				
Low/Intermediate risk	33	96.96%	0.93	[0.78,1.00]
High risk	57	96.49%	0.93	[0.83,1.00]
Histology				
Endometrioid	69	95.65%	0.89	[0.78,1.00]
Non-Endometrioid	21	100.00%	1.00	[1.00,1.00]
Grade				
G1-G2	47	100.00%	1.00	[1.00,1.00]
G3	43	93.02%	0.86	[0.70,1.00]
FIGO Stage				
FI-FII	64	98.44%	0.96	[0.89,1.00]
FIII-FIV	25	92.00%	0.84	[0.63,1.00]
Myometrial Infiltration				
≤50%	30	100.00%	1.00	[1.00,1.00]
>50%	60	95.00%	0.90	[0.79,1.00]
Overall Concordance	90	96.67%	0.93	[0.85,1.00]

Figure 3: A. Distribution of the number of altered mononucleotide repeats identified by ddPCR in the UAs of the cohort of 90 EC patients based on the MMR status, determined by IHC in tissue samples. All dMMR cases were classified as MSI-H using the ddPCR assay while three MSI-H UAs were classified as pMMR by IHC. **B.** Concordance table between the UAs analysed by ddPCR and the FFPE analysed by IHC.

USC UNIVERSIDADE DE SANTIAGO DE COMPOSTELA

C. Concordance table between the UA analysed by ddPCR and the FFPE analysed by ddPCR. **D.** Concordance analysis comparing the results obtained after the MSI-panel assessment on UAs and the FFPE analysed by IHC accordingly to the different clinic-pathologic characteristics. The concordance was analysed with the Kappa-Cohen statistics.

4.3.3.2|VAFs of the five MSI markers correlates with the VAFs of point mutation identified by targeted sequencing in the UAs

In addition to the analysis of the five MSI markers, in 60 patients (26 MSI-L/MSS and 34 MSI-H) of the cohort we had data regarding the genomic landscape of the UAs (Chapter I, Annex 4) obtained after their analysis with targeted sequencing as previously described. Importantly, in 8 of the 34 MSI-H patients a mutation in *MLH1* (3/8), *MSH2* (3/8), *PMS2* (1/8) or *MSH6* (1/8) was found, indicating a genomic origin of the MMR deficiency in these 8 cases and a possible epigenetic regulation in the remaining cases. In fact, the methylated status of *MLH1* was studied and defined as positive in three of the cases without mutation in the MMR genes.

Besides, genes enriched in MSI-H tumours included *PTEN* (21.7%), *PIK3CA* (13.8%), *ARID1A* (9.2.%), *KRAS* (7.2%) and *TP53* (5.9%) as the most frequently altered genes. Those enriched in MSI-L/MSS tumours included *PIK3CA* (15.2%), *PTEN* (12.4%), *TP53* (11.4%), *PIK3R1* (7.6%) and *ARID1A* (6.7%) (Figure 4A, B). Although PI3K-AKT pathway mainly supports the impact of the common alterations between the two groups the alteration of RAS family genes has been previously associated with MSI-H endometrial tumours (285), as also shows our cohort of patients.

Additionally, to determine if the levels of the MSI markers and if the variants identified after sequencing correlate and equally represent the tumour content of the samples, we compared the VAFs value of each

USC UNIVERSIDADE DE SANTIAGO DE COMPOSTELA

nucleotide marker in the UA and the average VAF value of the pathogenic variants using in both cases the same DNA input (Figure 4C). A strong correlation was found between BAT26 and BAT25 and the NGS analysis (Spearman's test: R≥.6, P-value≤.01), a moderate correlation with NR24 (Spearman's test: R=.5, P-value≤.05) and no correlation was found with NR21 and Mono27 (Spearman's test: R≤.4, P-value≤.05). Although the comparison of different technologies such as the ddPCR and NGS render different VAFs, even when analysing the same variant, these results agree with the fact that alterations in MSI markers, normally represent an early event during EC development.

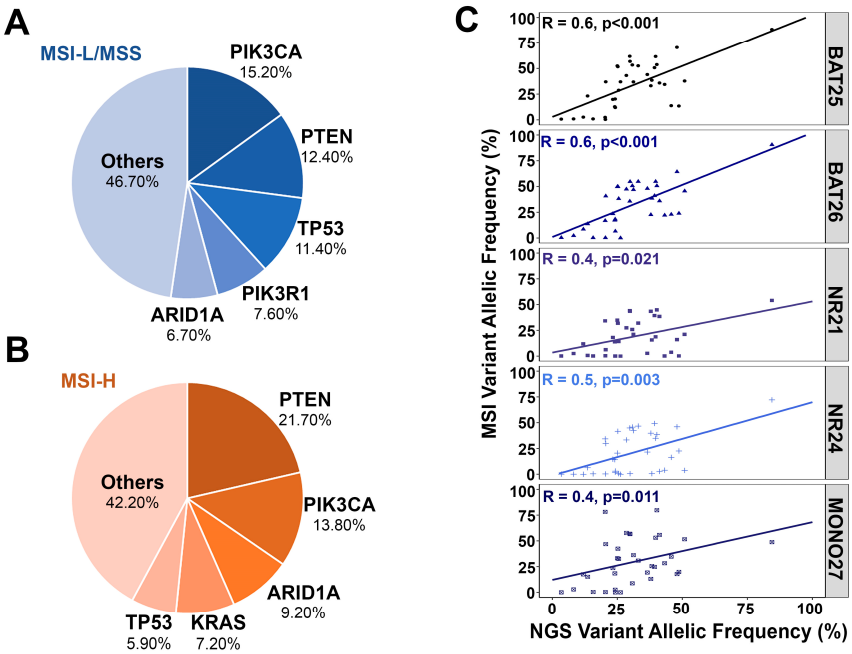


Figure 4: A. Distribution of the most altered genes found in the cohort of MSI-L/MSS (n=26) and **B.** MSI-H tumours (n=34) after analysing the UA by targeted sequencing. **C.** Correlation between each mononucleotide marker in the UA and the VAF value of point mutation variants identified by targeted sequencing.

USC UNIVERSIDADE DE SANTIAGO DE COMPOSTELA

4.3.3.3 | cfDNA represents a valuable sample to evaluate the MSI status and monitor the disease evolution.

The cfDNA was isolated from plasma samples of 59 patients and analysed for its potential usage as a diagnostic and monitoring tool. First, the LoD of the assay was determined using dilutions of DNA from EC cell lines with known pathogenic mutations and MSI. Our study determined a LoD=0.1% VAF and a good correlation between the MSI markers and point mutations, as we also observed when analysing the UAs (Figure 5A, B). Importantly, in 47 of the 59 samples, we had data regarding the presence of detectable ctDNA based on the presence of patient-specific point mutations or CNAs, (Chapter IV).

Of note, most of the plasma samples (57/59) analysed were collected at surgery and the remaining samples were collected at the time of tumour progression (2/59) (Table 2). When considering the threshold of≥3 markers altered to define MSI-H cases, the overall agreement between the results on the UAs and the cfDNA was 50.85% (Kappa Cohen=0.21; Figure 5A).

USC UNIVERSIDADE DE SANTIAGO DE COMPOSTELA

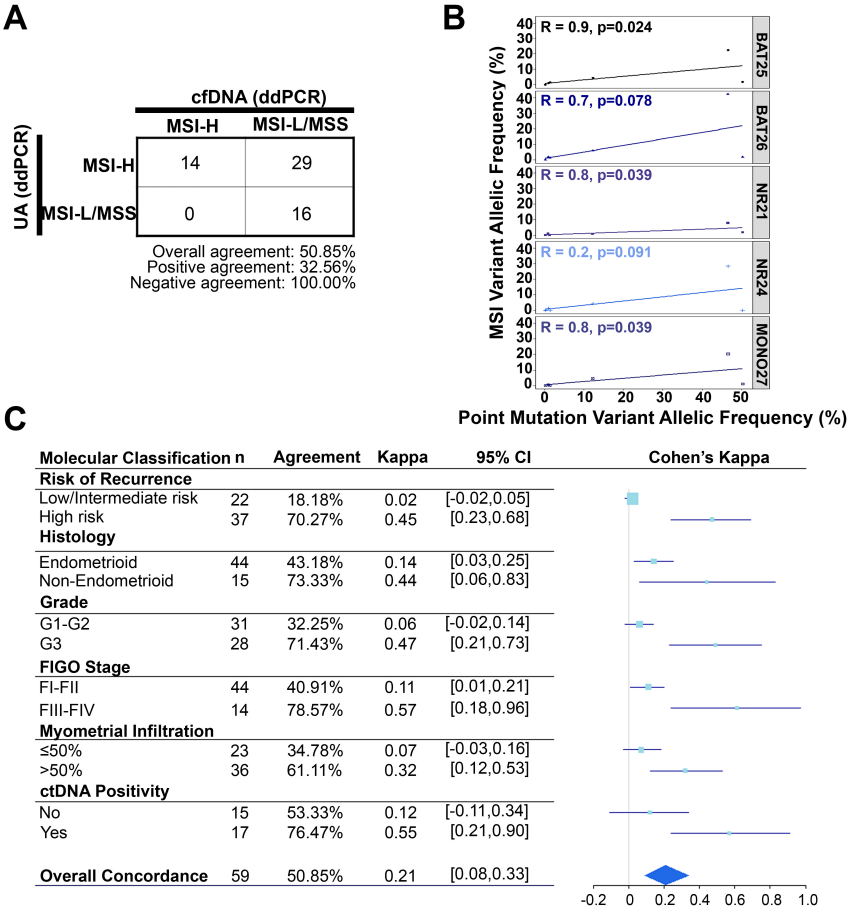


Figure 5: A. Concordance table comparing the results obtained on the UA and the cfDNA analysed by ddPCR using three MSI markers altered as threshold. **B.** Correlation between each mononucleotide marker in the cfDNA and the VAF value of point mutation variants identified by ddPCR in the cfDNA (n=8). **C.** Concordance analysis comparing the results obtained after the MSI-panel assessment on UAs and the cfDNA according to the different clinic-pathologic characteristics using as threshold the presence of 3 mononucleotide markers altered. The concordance was analysed with the Kappa-Cohen statistics.

USC UNIVERSIDADE DE SANTIAGO DE COMPOSTELA

Table 2: Clinico-pathological characteristics of the cfDNA analysed cohort of EC patients. pMMR: proficient mismatch repair proteins. dMMR: deficient mismatch repair proteins.

	pMMR	**dMMR**	**Total**
FEATURE	19 (32.20%)	40 (67.80%)	59 (100%)
TIME OF DIAGNOSIS			
First Diagnosis	17 (89.47%)	40 (100.00%)	57 (96.61%)
Recurrence	2 (10.53%)	0 (0.00%)	2 (3.39%)
HISTOLOGY			
EEC	11 (57.89%)	33 (82.50%)	44 (74.57%)
NEEC	8 (42.11%)	7 (7.50%)	15 (16.95%)
GRADE			
G1	2 (10.53%)	10 (25.00%)	12 (20.34%)
G2	5 (26.31%)	14 (35.00%)	19 (32.20%)
G3	12 (63.16%)	16 (40.00%)	28 (47.46%)
FIGO STAGE			
I	9 (47.37%)	22 (55.00%)	31 (52.55%)
II	4 (21.05%)	9 (22.50%)	13 (22.03%)
III	5 (26.32%)	6 (15.00%)	11 (18.64%)
IV	1 (5.26%)	2 (5.00%)	3 (5.08%)
Unknown	0 (0.00%)	1 (2.50%)	1 (1.70%)
MYOMETRIAL INFILTRATION			
<50%	6 (31.57 %)	17 (42.50%)	23 (38.98%)
≥50%	13 (68.42%)	23 (57.50%)	36 (61.02%)
RISK OF RECURRENCE			
Low/Intermediate Risk	4 (21.05%)	18 (45.00%)	22 (37.29%)
High Risk	15 (78.95%)	22 (55.00%)	37 (62.71%)

USC UNIVERSIDADE DE SANTIAGO DE COMPOSTELA

Of note, the concordance agreement was higher in patients with a more aggressive phenotype :high-risk of recurrence (70.27%; Kappa Cohen=0.45); high myometrial infiltration (61.11%; Kappa Cohen=0.32); non-endometrioid histology (73.33%; Kappa Cohen=0.44) and patients previously classified as positive for ctDNA (n=18) based on the presence of patient-specific somatic point mutations or CNV (76.47%;Kappa Cohen=0.5; Figure 5C). We also focused on the detection rate in patients classified as MSI-H (n=43) based on the ddPCR panel applied in UAs, showing that 60.46% had≥1 marker altered when interrogating the corresponding cfDNA (Figure 6A). Furthermore, when patients were categorized based on their clinic-pathologic features, a clear correlation between the per-centage of detection and the more aggressive phenotypes was found. Thus, 70.83% of patients with high risk of recurrence showed at least one mononucleotide marker altered and three mononucleotide markers altered in 54.16%, respectively (Figure 6A). Overall, higher positivity was detected in patients with high myometrial infiltration, high grade, NEEC histology and higher FIGO stages (Figure 6A). Of note, these ctDNA detection percentages were higher than previously reported in the literature in nonmetastatic EC. Besides, patients with high-risk tumours showed higher levels of VAFs although the cfDNA levels were comparable between low and high-risk tumours (Figure 7A,B). In addition, a good correlation between the VAF of point mutations, CNVs and the MSI markers (n=8, Figure 5B) was found.

USC UNIVERSIDADE DE SANTIAGO DE COMPOSTELA

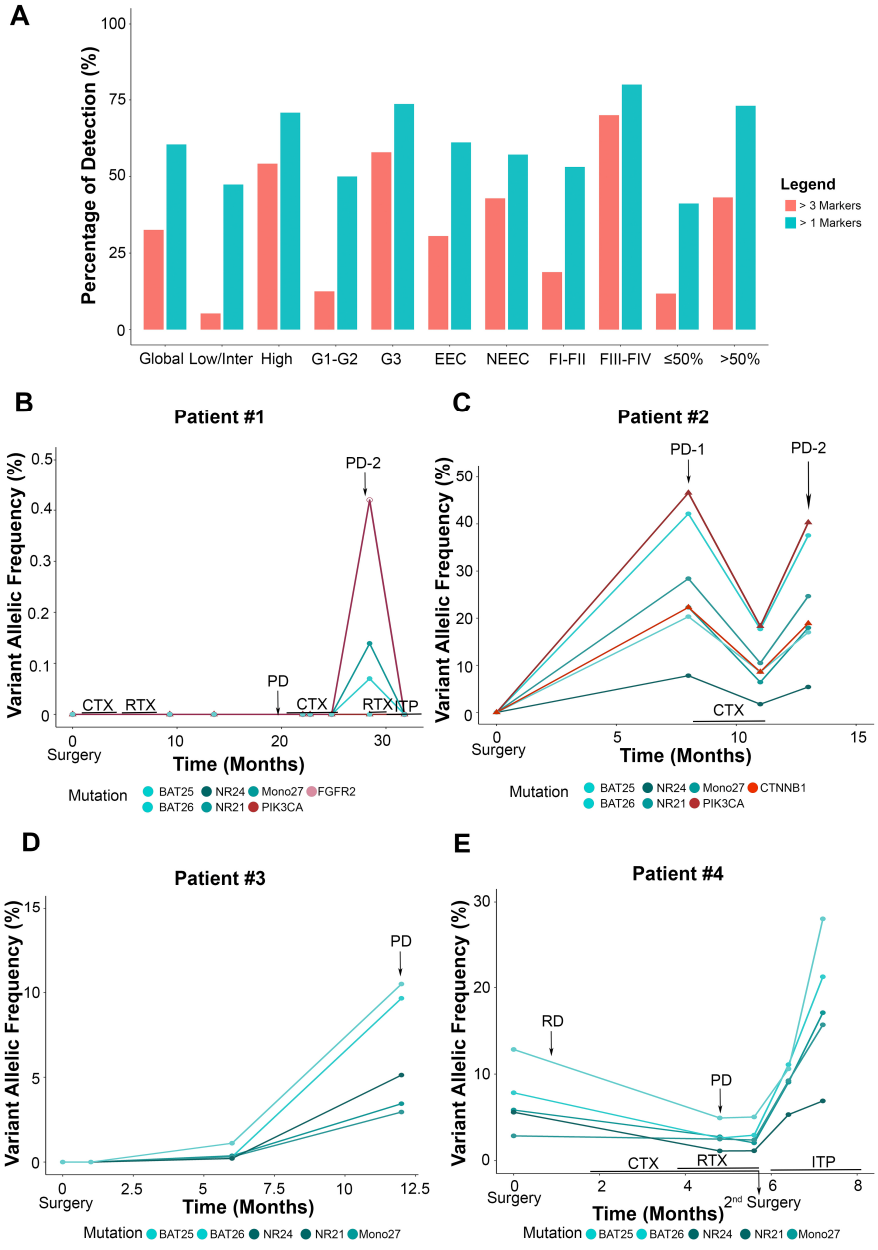


Figure 6: A. Percentage of detection of MSI markers altered on the cfDNA isolated from plasma in 40 patients classified as MSI-H based on the UAs analysis and

USC UNIVERSIDADE DE SANTIAGO DE COMPOSTELA

according to the tumour characteristics. At least three MSI markers altered (red)and one altered (green) were used as the threshold. **B.** ctDNA kinetics in patient no. 1 showcasing the value of the MSI assay to detect progression disease. **C.** ctDNA dynamics inpatient no. 2 mirrored the tumour evolution in response to therapy. **D.** ctDNA evolution in patient no. 3 showed potential to detect early progression. **E.** ctDNA levels in patient no. 4 evidence the potential of the MSI assay to detect residual disease and progression. CTX, chemotherapy treatment; ITP, immunotherapy; PD, progressive disease; RD, residual disease; RTX, radiotherapy treatment.

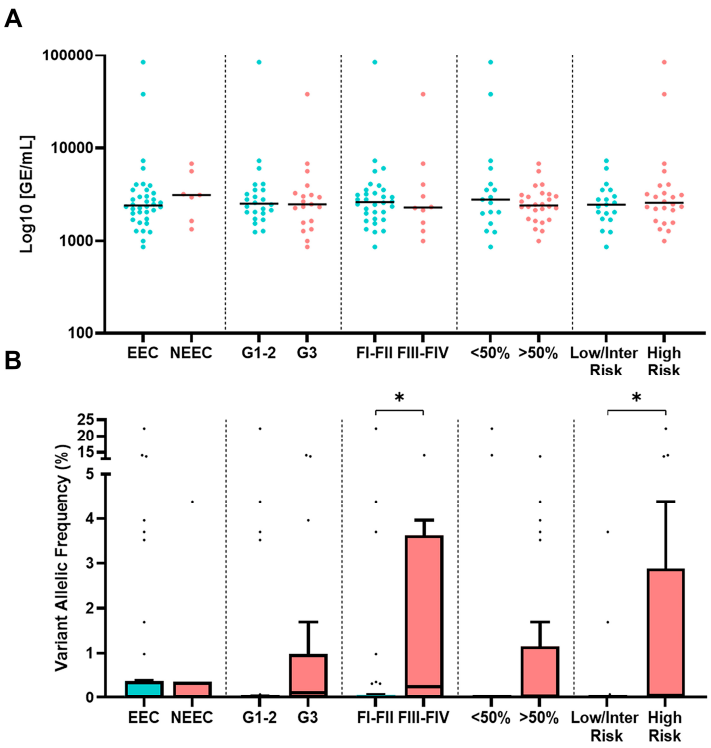


Figure 7: **A.** Distribution of the cfDNA concentration (GE/mL) between the different clinico-pathological variables. **B**. Distribution of the ctDNA variant allelic frequency (%) determined with the MSI test according to the different clinico-pathological variables. *p-value <0.05.

USC UNIVERSIDADE DE SANTIAGO DE COMPOSTELA

Furthermore, to assess the potential of the MSI assay to monitor the disease evolution, longitudinal samples from 15 patients were analysed. Of note, 6 patients had a pMMR/MSS tumour profile and were included to evaluate the potential shift to MSI during the disease evolution. All 6 patients were negative for the presence of ctDNA and remained as MSS in all longitudinal samples, including the four progressions. From the remaining 9 patients, classified as MSI-H, 5 were negative during the longitudinal analysis while 4 progressed after surgery, being the MSI markers detectable after disease progression in all cases (Table 3). Patient no. 1 underwent surgery in 2019 and received post-surgery Carboplatin-Paclitaxel combined therapy and radiotherapy. Nevertheless, a lung progression was detected by CT-scan 20 months later. Patient was then treated with chemotherapy but showed only partial response with a final tumour progression at brain level. Two MSI markers were detectable after this second progression (Figure 6B). Patient no. 2 was operated and 9 months later showed peritoneal progression and was treated with chemotherapy. As shown in Figure 6C, although the levels at surgery for the MSI markers and two specific point mutations in *CTNNB1* and *PIK3CA* were negative, they increased at progression disease and decrease when treatment started. A lung progression was detected after 4 months of treatment and the MSI markers increased again. In the case no. 3 the levels of ctDNA became detectable using the MSI assay 6 months after surgery, becoming more prominent at 12 months post-surgery, indicating an early progression of the disease which was con-firmed by image (Figure 6D). Finally, patient no. 4, was initially diagnosed and underwent surgery in 2020; however, a vaginal lesion was detected shortly after surgery. The patient was treated with chemotherapy and radiotherapy but showed a bad response with the appearance of an abdominal lesion, after the second surgery the patient was subjected to Pembrolizumab treatment; however, as seen by the ctDNA

USC UNIVERSIDADE DE SANTIAGO DE COMPOSTELA

kinetics the patient showed no response to treatment. The MSI markers were positive in all samples collected after surgery indicative of persistent disease (Figure 6E).

USC UNIVERSIDADE DE SANTIAGO DE COMPOSTELA

Table 3: Clinico-pathological features of the EC patients included in the analysis of longitudinal samples and their clinical course. (EEC: Endometrial Endometrioid Carcinoma, PD: Progression Disease).

ID	Histology	Grade	FIGO Stage	Myometrial Infiltration	Mutationes	MMR/MSI status	Clinical course
#1	EEC	3	IB	>50%	*PIK3CA, FGFR2*	dMMR/ MSI-H	Two PD after surgery.
#2	EEC	2	II	<50%	*PIK3CA, CTNNB1*	dMMR/ MSI-H	Two PD after surgery
#3	Mixed	3	IIC1	>50%	*ARID1A, FBXW7, PTEN, RB1*	dMMR/ MSI-H	Early PD
#4	EEC	3	IIIC	<50%	*AIRD1A, NBN, MSH2, NFE2L2, PIK3R1, PTEN, TP53*	dMMR/ MSI-H	PD after surgery
#5	NEEC	3	IIIC2	>50%	*PTEN, TP53*	pMMR/ MSS	Slow PD After Surgery
#6	EEC	3	IB	>50%	*MLH1, PIK3CA, PTEN*	dMMR/ MSI-H	No PD
#7	NEEC	3	IA	<50%	*FBXW7, TP53, CCNE1, PPP2R1A*	pMMR/ MSS	No PD
#8	EEC	3	IIIC2	>50%	*PIK3R1, MET, PTEN, TP53*	pMMR/ MSI-H	No PD
#9	EEC	3	IVB	>50%	*PIK3CA, PTEN, FGFR2, MAX, SMARCA4*	dMMR/ MSI-H	No PD
#10	EEC	3	IIIC1	>50%	*ARID1A, PIK3CA, PIK3R1, PTEN, TP53*	pMMR/ MSS	No PD
#11	EEC	3	IB	>50%	*TP53, PPP2R1A, PIK3CA*	pMMR/ MSS	Two PD after surgery
#12	NEEC	3	II	<50%	*TP53, PIK3CA*	pMMR/ MSS	PD after surgery
#13	NEEC	2	IA	<50%	*PIK3CA, TRET, TP53*	pMMR/ MSS	PD after surgery
#14	EEC	2	IA	<50%	*MLH1, NRAS, PIK3CA, KRAS, ARID1A, NOTCH1, PTEN, ATM, SLX4, CREBBP, FANCA, CFK12*	dMMR/ MSI-H	No PD
#15	EEC	2	II	<50%	*No Data*	dMMR/ MSI-H	No PD

USC UNIVERSIDADE DE SANTIAGO DE COMPOSTELA

4.3.4 | Discussion

MSI determination is becoming crucial in solid tumours, as it favours the hereditary screening and provides valuable information for the tumour prognosis and immunotherapy selection (275,286). In fact, results of KEYNOTE-028 (NCT02054806) demonstrated that Pembrolizumab was active in advanced PD-L1 positive EC patients progressing after standard therapy (287)providing robust data supporting the use of immunotherapy in EC.

Current strategies for EC diagnosis and molecular characterization are based on the analysis of solid tumour tissue at surgery (11) with the limitations inherent to this sample. Our study was novel to apply a highly sensitive approach, based on ddPCR, to interrogate the MSI status in UAs. The commercial assay employed includes five nucleotide markers (BAT25, BAT26, NR21, NR24 and MONO27) which has been previously applied in EC and other tumours with high accuracy (283) and sensitivity, since they can detect as little as 2bp difference without requiring paired normal sample (288). To validate our approach, the UAs from a total cohort of 90 patients with EC were interrogated using the ddPCR assay, being 64.44% classified as MSI-H after the analysis. In 8 of the 34 of these MSI-H tumours we found a genetic cause of the MSI status, being the remaining cases probably associated to epigenetic regulation, in line with the percentages expected of sporadic and Lynch-associated MSI tumours (289,290). Importantly, this patients' cohort was enriched in MMR deficient tumours with the purpose to technically validate our analytic approach, therefore, the results obtained should be interpreted taking into account that in a real-world cohort the rate of MSI tumours will be about the 30% (290). The cohort is also enriched in high-risk tumours since they have a greater clinical interest as potential future recurrent cases that could be treated and monitored based on our

USC UNIVERSIDADE DE SANTIAGO DE COMPOSTELA

non-invasive approach. To interrogate the accuracy of our approach the results obtained with the MSI panel in the UAs were compared to the MMR status determined by IHC in the corresponding solid biopsy, and a high global agreement (96.67%) was observed between both strategies for all the patients, showing the great value of UAs for the MSI testing in EC. We only observed three discordant cases, classified as pMMR by the IHC and as MSI-H by the ddPCR-based approach. The correlation between the MSI and MMR assessment is normally high; however, about 3% to 11% of MSI-H tumours can show conventional MMR staining and localization due to preserved antigenicity and compensation mechanisms (279,291). Although these discrepancies are relatively low, there may be different clinical behaviours between the group characterized by MSI testing and the group identified by IHC. We confirmed the MSI-H status of these three discordant cases by applying the ddPCR assay in FFPE tissues, evidencing the additional value of assessing MSI to characterize EC; moreover, significantly higher VAFs were found in the UA when compared to the FFPE. Our study demonstrated a total concordance of the MSI assessment in solid tissue samples and UAs, supporting the use of UAs for the MSI determination, as a highly sensitive, fast, cost effective and non-invasive diagnostic strategy for the accurate molecular stratification of EC patients. Although our workflow includes the UAs collection at surgery, this sample could be obtained by the gynaecologists without the need of special care and provides relevant information to confirm the diagnostic and surgical management of the patient. For example, in a recent work, a small NGS panel including 60 genes and 17 microsatellite markers was successfully applied to liquid-based cytology specimens obtained for EC screening and the corresponding FFPE tissues in seven patients, showing the same MSI profile (292). Although MMR/MSI alteration is normally an early event in EC generation, mosaicism

USC UNIVERSIDADE DE SANTIAGO DE COMPOSTELA

has been described in the expression of MMR proteins in about 3% to 5% of the tumours (280,293) together with MSI status shifts during tumour progression (205). The analysis of the MSI panel in the UAs can have a special value in these cases.

To complement our non-invasive approach, we also applied the test on cfDNA isolated from plasma samples. Our study allowed us to explore the feasibility to monitor MSI markers in longitudinal samples during tumour evolution. Notably, we were able to detect at least one of the MSI markers altered in 60.46% of the cases classified as MSI-H in the UAs which can be considered as indicators of the ctDNA content. These results are really promising, taking into consideration that we applied the test to a cohort of non-metastatic patients, who normally have low levels of ctDNA (91). Actually, Silveira et al employed another ddPCR-based strategy (which covers BAT-26, ACVR2A and DEFB105A/B) in plasma samples from a cohort of six patients with advanced EC, being 50% of the cases classified as unstable based on the cfDNA analysis. Therefore, our data supports the great potential of this technology to be applied in advanced and non-advanced tumours candidates for immunotherapy in which the primary tumour or the metastasis can be inaccessible, such as pancreatic, gastric, prostate or ovarian cancer (294). NGS based strategies have also been recently applied on cfDNA to characterize MSI in different tumour types and showed the same benefit from immunotherapy in patients classified as MSI-H in tissue samples and cfDNA (295). Although this strategy has the advantage of providing more information regarding the genomic landscape of the tumour, including a higher number of MSI loci, it is less sensitive than ddPCR-based assays (296–298).

USC UNIVERSIDADE DE SANTIAGO DE COMPOSTELA

In addition to providing a more complete view of tumour heterogeneity, the opportunity to interrogate the status of MSI in cfDNA of EC patients represents a valuable tool to monitor tumour evolution without the need to have a broad knowledge about each patient-specific genetic alteration, making the analysis ctDNA more cost-effective and less time-consuming than other strategies. In fact, we monitored the MSI panel in plasma samples from 15 EC patients, including four patients who showed tumour progression. One of these cases was characterized by an early progressive disease, being the MSI markers detect-able prior to the disease recurrence, and reflecting the tumour response to treatment and its fast evolution after recurrence. Interestingly, a second case also showed an increment of the MSI markers 6 months after surgery and only few months later was considered under clinical and radiological progression. Additionally, the MSI panel positivity, although lower, was detected 6 months after the tumour resection in a patient with residual disease who was treated with immunotherapy after progression. Besides, no MSI positivity was found in the longitudinal samples of patients with a good post-surgery evolution. These data reflects the potential of the MSI assessment by ddPCR in cfDNA to anticipate the disease recurrence and monitor the tumour evolution as it has been recently shown in other tumour types such as CRC (294). Therefore, our results, together with previous preliminary data obtained by NGS (229), support that cfDNA analyses assessing the MSI status could open new opportunities for a personalized follow-up and immunotherapy selection in EC patients and other immune-responsive tumours.

4.3.5 | Conclusions

In summary, our study is pioneer in demonstrating the accuracy of MSI evaluation in UAs from EC patients using a highly sensitive and robust

USC UNIVERSIDADE DE SANTIAGO DE COMPOSTELA

ddPCR-based assay. This approach allows a comprehensive tumour genotyping without the need for invasive procedures and can be easily implemented for the clinical diagnostic of EC. Furthermore, our results also demonstrate the value of the assay to interrogate the MSI status on cfDNA from EC patients, opening new options to make a dynamic characterization of this therapeutic-relevant molecular alteration and to monitor the tumour evolution in the context of both localized and metastatic solid tumours candidates to receive immuno-therapy. These promising results obtained in a cohort enriched in MSI-H tumours represent the basis to a further validation in larger cohort of patients and longitudinal samples.

USC UNIVERSIDADE DE SANTIAGO DE COMPOSTELA

4.4 | CHAPTER IV

Unveiling Endometrial Cancer Prognosis: Integrating cfDNA and ctDNA for Predictive and follow up Analysis

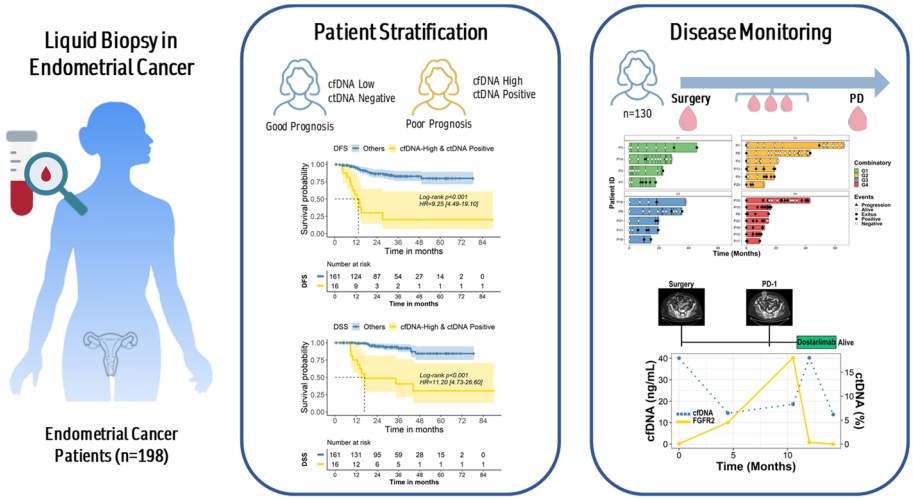
Results from this chapter have been presented at the ESGO meeting in Barcelona, 2024.

USC
UNIVERSIDADE DE SANTIAGO DE COMPOSTELA

CHAPTER IV

Unveiling Endometrial Cancer Prognosis: Integrating cfDNA and ctDNA for Predictive Analysis

GRAPHICAL ABSTRACT



Keywords: endometrial cancer, liquid biopsy, cfDNA, ctDNA, prognostic, disease monitoring

USC UNIVERSIDADE DE SANTIAGO DE COMPOSTELA

CHAPTER IV

Unveiling Endometrial Cancer Prognosis: Integrating cfDNA and ctDNA for Predictive Analysis

ABSTRACT

Introduction: In the past years, there has been a rise on advanced EC patients resulting in an increase on the mortality rates. To overcome this trend, it is essential to improve the stratification of the risk of post-surgery recurrence and to anticipate the development of disease relapse and resistance to treatment. Liquid biopsy analyses represent a promising tool to address these clinical challenges however the best strategy to efficiently applied them to improve EC management must be better defined. Therefore, the study aimed to determine the clinical value of cfDNA/ctDNA monitoring in patients with localized and recurrent disease.

Material & Methods: Plasma samples and the UA from 198 patients with localized EC were collected in different Spanish hospitals at surgery and also throughout the course of the disease (n=130). Total cfDNA was isolated from all plasma samples, quantified and analysed for the presence of ctDNA based on the mutational profile found on the UAs.

Results: The genetic characterization of UAs obtained at surgery allowed the identification of pathogenetic variants in the 95,45% of the tumours and ctDNA levels could be monitored in the 89,4% of the patients. High levels of cfDNA and detectable levels of ctDNA at baseline correlated with poor prognosis, for both DFS (Log-rank test p-value<0.0001; HR=9.25; 95% CI [4.49-19.10]) and DSS (Log-rank test p-value<0.0001; HR=11.20; 95% CI [4.73-26.60]). Importantly, this approach remains clinically significant when stratifying patients based on histology, grade or the global risk classification, highlighting its additional value to identify patient with a fast and poor evolution. In fact, cfDNA/ctDNA levels served to identify the patient who showed an early disease relapse among the tumours classified as intermediate-high-high risk of recurrence. Moreover, longitudinal analyses of cfDNA and ctDNA proved to be a

USC UNIVERSIDADE DE SANTIAGO DE COMPOSTELA

powerful asset to identify patients undergoing relapse, since ctDNA levels were detected months prior to the arisen of any clinical evidence.

Conclusion: This study represents the most comprehensive study on cfDNA/ctDNA characterization in EC and demonstrates the high value of this characterization to improve the risk stratification and anticipate the disease relapse in patients with localized disease. Besides, the dynamic ctDNA assessment showed utility to complement the standard of care strategies to monitor the disease evolution and the development of resistance to the treatment. Implementation of cfDNA/ctDNA monitoring into the clinical routine will provide a unique opportunity for improving EC management.

USC UNIVERSIDADE DE SANTIAGO DE COMPOSTELA

4.4.1| Introduction

Minimally invasive biomarkers are a necessity in the clinical context. They allow for the dynamic characterization of the disease providing important information in real time with minimal invasiveness and discomfort for the patients (299). In the past years, there has been a clear rise on advanced EC patients resulting in an increase on the mortality rates (8,237). Moreover, currently available therapeutic approaches for EC patients have shown limited efficiency on advanced EC patients (17). Nevertheless, regardless of the numerous advances in the field of gynaecological cancer, risk stratification remains an unsolved question for EC and the treatment paradigm has barely changed over the past years (8,11). Tumour heterogeneity and early tumour dissemination are postulated as key milestones to overcome in order to improve patient management (212,300). This clinical paradigm highlights the need to find a prognostic biomarker that helps to identify those patients with worse clinical prognosis as well as biomarkers that would allow to monitor the evolution of the disease during the treatment. In this study, we report the value to employ the cfDNA quantification and the ctDNA analyses not only as prognostic biomarkers but also its value as a follow up tool in a vast cohort of EC patients.

The analysis of circulating biomarkers such as cfDNA and ctDNA among others, allows for the sequential collection of samples with minimal discomfort for the patients, obtaining valuable in real time information (80,299,301–304). Although few studies have been published focusing on the value of liquid biopsy-based approaches in EC, promising results have been found (305,306). For instance, higher levels of cfDNA have been associated to EC patients with poor clinical outcome (168,228,294,307–310). Moreover, Bolivar et al have shown that high levels of cfDNA correlate with worse DFS

USC UNIVERSIDADE DE SANTIAGO DE COMPOSTELA

and DSS times (309). Regarding the value of ctDNA, around 30-40% of patients with EC have shown detectable levels of ctDNA, with poor clinical outcome patients having higher levels of detectable alteration, as shown on Chapter III (91,173). Moreover, some studies have shown that ctDNA levels analysed in longitudinal samples allow not only to monitor the disease, as evidenced by Ashley et al where cfDNA isolated from longitudinal samples collected from EC patients were subjected to NGS and correlated with clinical outcome (228). But also, to predict prognosis and even assess therapy efficiency (228,311). Nonetheless studies on larger multicentre cohorts are needed to validate these results.

In the current chapter we present a liquid-based pipeline that focuses on the quantification of cfDNA and ctDNA and determine its value to improve the current risk stratification of EC patients. Importantly, this approach not only allows for the identification of the subset of patients with the worst clinical outcome based on the levels of cfDNA and ctDNA, but also allows to identify patients with high risk of relapse regardless of their clinical characteristics.

4.4.2 | Material & Methods

4.4.2.1 | Patients inclusion and sample collection

A total of 198 patients with EC were recruited between January 2018 and June 2022 at the Gynaecology Department of Vall d'Hebron University Hospital (Barcelona, Spain), the MD Anderson Cancer Center (Madrid, Spain), the University Clinical Hospital of Santiago de Compostela (Santiago de Compostela, Spain) and the University Hospital La Fe (Valencia, Spain).

Peripheral blood samples were collected as previously described in the M&M section of the thesis. Plasma was isolated by a two-step centrifugation. Longitudinal peripheral blood samples were collected every 6 months until

USC UNIVERSIDADE DE SANTIAGO DE COMPOSTELA

tumour relapse and at different time points through the disease based on the clinicians' criteria.

4.4.3 | Results

4.4.3.1 | Clinicopathologic Characteristics of the cohort

A total of 198 patients with EC and with at least 6 months of post-surgery follow up have been prospectively included in the study. Clinical characteristics are summarised in Table 1. The cohort included patients with endometrioid (76%) and non-endometrioid carcinomas (24%), Grade 1-3 (40%, 18%, 42%, respectively), FIGO stage I-IV (65%, 15%, 15%, 4.7%, respectively) tumours from all TCGA groups (POLE 7,7%, MSI 39%, NSMP 27%, HCN 26%) classified accordingly with the updated ESMO/ESGO consensus (8). A total of 37 (19%) patients underwent tumour progression with a median DFS of 13.9 months [2.6-49.2]. A total of 24 (12%) patients perished due to the disease, showing the global cohort a median DSS of 19.1 months [8.6-45.7]. The UAs from all the patients were subjected to NGS as previously described (Chapter I). With this strategy we identified pathogenic mutation in 189 of the patients (95.46%) and we could design effective assays to monitor the ctDNA based on the presence of these variants in 177 patients. Of these patients, 130 (65.66%) had follow up samples available to study the value of longitudinal cfDNA/ctDNA monitoring in EC (Figure 1).

USC UNIVERSIDADE DE SANTIAGO DE COMPOSTELA

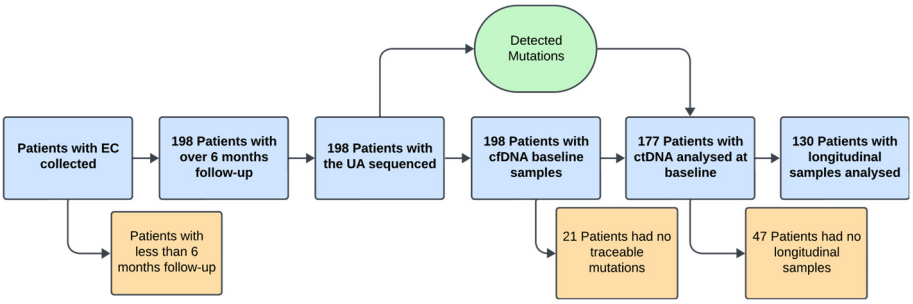


Figure 1: Design of the cfDNA and ctDNA analyses in the cohort of endometrial cancer patients. Consort diagram showing the number of patients excluded at each time point of the study.

Table 1: Clinical characteristics of the studied cohort.

CLINICAL VARIABLES	*N=198*	CLINICAL VARIABLES	*N=198*
Age	181	**Lymphovascular Space Infiltration**	171
Median (IQR)	67 (58-73)	No	137 (80%)
Histology	196	Yes	34 (20%)
NEEC	48 (24%)	**TCGA**	194
EEC	148 (76%)	POLE	15 (7.7%)
Tumour Grade	197	MSI	76 (27%)
Grade 1	78 (40%)	NSMP	53 (27%)
Grade 2	36 (18%)	HCN	50 (26%)
Grade 3	83 (42%)	**cfDNA Concentration (ng/mL)**	198
FIGO Stage	193	Median (IQR)	15 (10,24)
I	126 (65%)	**ctDNA Positivity**	177
II	29 (15%)	Detected	52 (29%)
III	29 (15%)	**Relapse**	198
IV	9 (4.7%)	No relapse	161 (81%)
Myometrial Infiltration	195	Relapse	37 (19%)
<50%	103 (53%)	**Exitus**	198
>50%	92 (47%)	No	174 (88%)
		Yes	24 (12%)

USC UNIVERSIDADE DE SANTIAGO DE COMPOSTELA

4.4.3.2 | Pre-surgery cfDNA levels has prognostic value in EC patients

The total cfDNA concentration was evaluated to determine its association with the clinico-pathologic characteristics and the disease aggressiveness. Total cfDNA was isolated from plasma samples (3-5mL) obtained at the time of tumour resection and quantified using Qubit fluorometry. The total cfDNA concentration at surgery ranged between 3.62-366.80 ng/mL with a mean value at 21.94 ng/mL and a median of 15.12 ng/mL. Higher levels of cfDNA correlate with traditional high risk of recurrence markers, although not statistically significance was found (Mann Whitney test p-value>0.05) (Figure 2A-H). Accordingly, significant higher pre-surgery cfDNA levels were found in patients who showed disease relapse or perished due to the disease (Mann Whitney test p-value<0.01) (Figure 2I-J). A cut-off at 25ng/mL was stablished to group patients into high or low cfDNA levels and explore the utility of cfDNA as a predictor of the clinical outcome. Following this strategy 20.70% (41/198) of patients showed high pre-surgery cfDNA levels (Figure 2J). These patients had a significantly shorter DFS (Log-rank test p-value<0.0001; HR=3.91; 95% CI [2.04-7.51]) and DSS (Log-rank test p-value<0.0001; HR=6.54; 95% CI [2.83-15.10]) than those with low levels of pre-surgery cfDNA (Figure 2L-M, respectively). Moreover, multivariant analyses showed that cfDNA levels had independent value compared to the remaining traditionally used clinical variables according to DFS (Log-rank test p-value=0.008; HR=2.98; 95% CI [1.35-6.61]) and DSS (Log-rank test p-value<0.001; HR=9.13; 95% CI [2.82-29.50]) (Table 2).

USC UNIVERSIDADE DE SANTIAGO DE COMPOSTELA

Table 2: cfDNA analyses identify the patients with the worst clinical outcome.

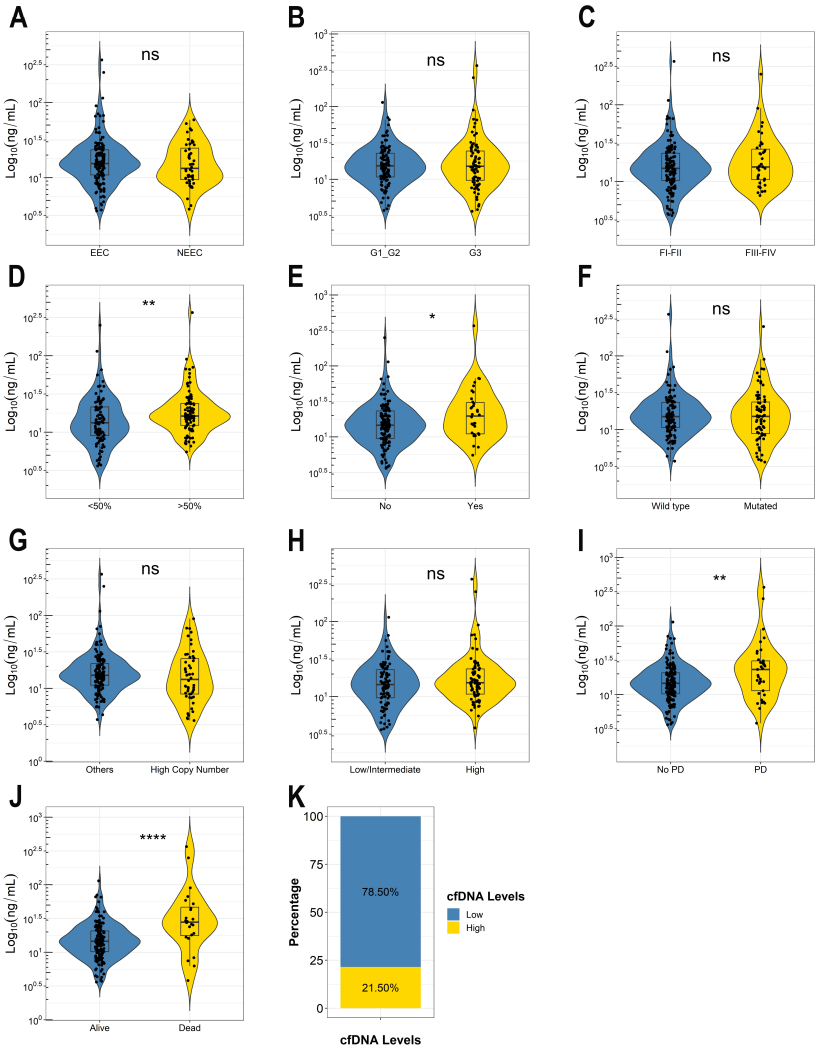
Variable	Univariate				Multivariate			
	HR 95% CI[2]		p-val	q-val[3]	HR 95% CI[2]		p-val	q-val[3]
Disease Free Survival								
Histology	3.72	1.95,7.11	<0.001	<0.001	2.16	0.83, 5.65	0.10	0.37
Grade	5.42	247,11.9	<0.001	<0.001	1.84	0.58, 5.81	0.30	0.37
FIGO Stage	4.04	2.10, 7.79	<0.001	<0.001	1.68	0.68, 4.17	0.26	0.37
Myometrial infiltration	2.36	1.16, 4.77	0.013	0.015	1.31	0.49, 3.51	0.60	0.60
LVSI	4.26	2.17, 8,38	<0.001	<0.001	1.72	0.65, 4.55	0.28	0.37
MSI Status	0.62	0.30, 1.27	0.21	0.21				
TP53 Status	4.08	1.90, 8.75	<0.001	<0.001	1.66	0.60, 4.57	0.32	0.37
cfDNA	3.91	2.04, 7.51	<0.001	<0.001	2.98	1.35, 6.61	0.008	0.058
Disease Specific Survival								
Histology	4.46	1.95,10.2	<0.001	<0.001	1.05	0.34,3.32	0.93	0.93
Grade	16.4	3.84,70.2	<0.001	<0.001	4.75	0.85,26.5	0.056	0.13
FIGO Stage	7.10	3.07,16.4	<0.001	<0.001	4.35	1.30,14.6	0.015	0.054
Myometrial infiltration	2.54	1.00,16.4	0.038	0.043	1.28	0.31,5.35	0.73	0.93
LVSI	4.90	2.07,11.6	<0.001	<0.001	0.86	0.23,3.25	0.83	0.93
MSI Status	0.52	0.20,1.35	0.16	0.16				
TP53 Status	9.32	2.74,31.6	<0.001	<0.001	3.05	0.72,12.9	0.11	0.19
cfDNA	6.54	2.83,15.1	<0.001	<0.001	9.13	2.82,29.5	0.001	0.001

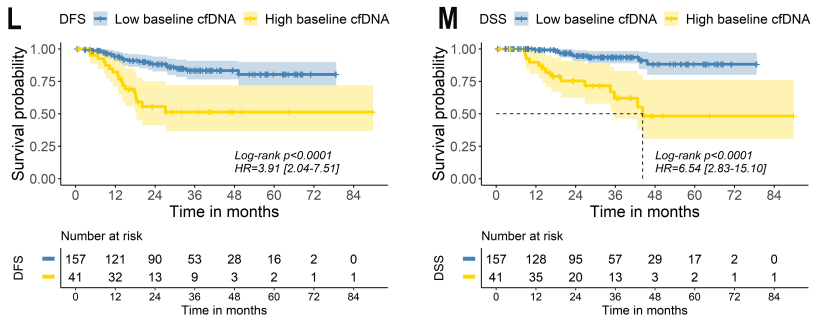
[1]U/D: undetermined

[2]HR 95% CI: Hazard Ratio 95% confidence interval

[3]False discovery rate for multiple testing

USC UNIVERSIDADE DE SANTIAGO DE COMPOSTELA





USC UNIVERSIDADE DE SANTIAGO DE COMPOSTELA

Figure 2: The value of pre-surgery cfDNA to identify patients with poor clinical outcome**. A-J.** Violin plots of the pre-surgery cfDNA levels (Log_{10} ng/mL) according to the clinicopathologic variables of the tumours. Statistical significance was assessed based on Mann–Whitney U test **p<0.01. **K.** Classification of the patients as low or high pre-surgery cfDNA based on the cut point (25 ng/mL). **L-M**. Kaplan Meier curves showing DFS (**L**) and DSS (**M**) based on pre-surgery cfDNA levels. Univariate Cox proportional-hazards model was used to estimate HR and log-rank test to report p-value.

Moreover, the potential correlation between cfDNA levels and standard blood biomarkers used in the clinical context for gynaecological tumours such as CA-125 or CEA was studied in part of the cohort. Importantly, cfDNA levels showed independence of CA-125 and CEA levels (Spearman R<0.1). Besides, no correlation between cfDNA levels and leucocytes count was found, indicating that DNA released by leucocytes has not a main impact on the total cfDNA levels in our cohort as was published in other studies (312). Furthermore, to ensure that the results of the value of cfDNA and ctDNA were not being biased towards tumour size or volume we performed a comparison of cfDNA levels and ctDNA positivity with tumour length (Figure 3A-C, respectively) and with tumour volume (Figure 3B-D, respectively).

USC UNIVERSIDADE DE SANTIAGO DE COMPOSTELA

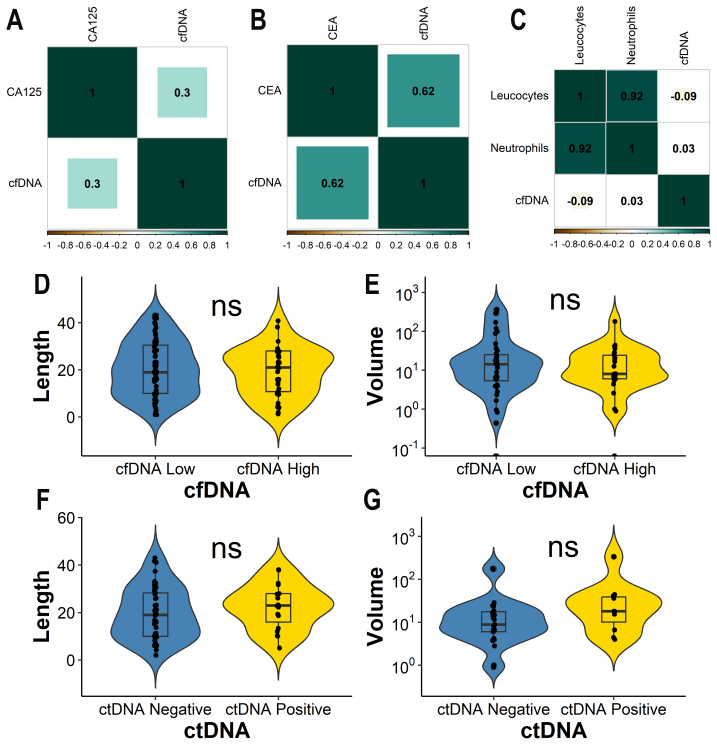


Figure 3: Pre-surgery cfDNA and ctDNA levels showed independence of other variables. **A-C.** Spearman Correlation of the cfDNA levels with other biomarkers such as CA-125 (**A**), CEA (**B**) or PBMCs (**C**). **D-G.** Violin plots of the length of the tumour (cm) with the cfDNA levels (**D**) and ctDNA (**F**) and of the tumour volume (cm^2) with the cfDNA levels (**E**) and ctDNA (**G**). Statistical significance was assessed based on Mann–Whitney U. ns p-value>0.05.

4.4.3.3 | CtDNA as a minimally invasive prognostic tool in EC patients

The levels of ctDNA were determined in a total of 177 patients using personalized ddPCR assays based on the mutational profile found in the UA and also a specific assay for detecting MSI markers in patients with unstable tumours as was previously described in chapter III (91,168). Following this approach, 52/177 (29.38%) patients showed detectable levels of ctDNA

USC UNIVERSIDADE DE SANTIAGO DE COMPOSTELA

(Figure 4K) with a VAF in a range from 0.01-39.10%, an average of 4.08% and a median of 0.44%. Pre-surgery ctDNA positivity was significantly associated with higher levels of cfDNA (Mann Whitney, p-value<0.01) being this association partially explained by a lower cfDNA input used for the ddPCR in patients with low cfDNA (Figures 5A and B). However, pre-surgery cfDNA levels and ctDNA VAF were no correlated in those patients with detectable ctDNA levels (Spearman R≤0.2) (Figure 4L). On the other side, higher detection rates and VAFs were determined in tumours with clinico-pathological features associated with high risk, more specifically in patients with high grade, FIGO III-IV, over 50% myometrial infiltration or LVSI (Mann Whitney, p-value<0.01) (Figure 4A-H). These data confirmed that high risk EC tumours shed into circulation higher ctDNA contents.

With the aim to understand if pre-surgery ctDNA can provide additional information to predict the disease evolution we grouped the patient in positive and negative for the ctDNA presence and performed survival analyses. Of note, patients with detectable levels of ctDNA showed significantly shorter DFS (Log-rank test p-value<0.001; HR=3.63; 95% CI [1.80-7.30]) and DSS (Log-rank test p-value<0.01; HR=3.91; 95% CI [1.57-9.74]) when compared to the patients with undetectable ctDNA (Figure 3M-N, respectively) (Table 3).

USC UNIVERSIDADE DE SANTIAGO DE COMPOSTELA

Table 3: ctDNA analyses allows for the identification of the patients with poor clinical outcome.

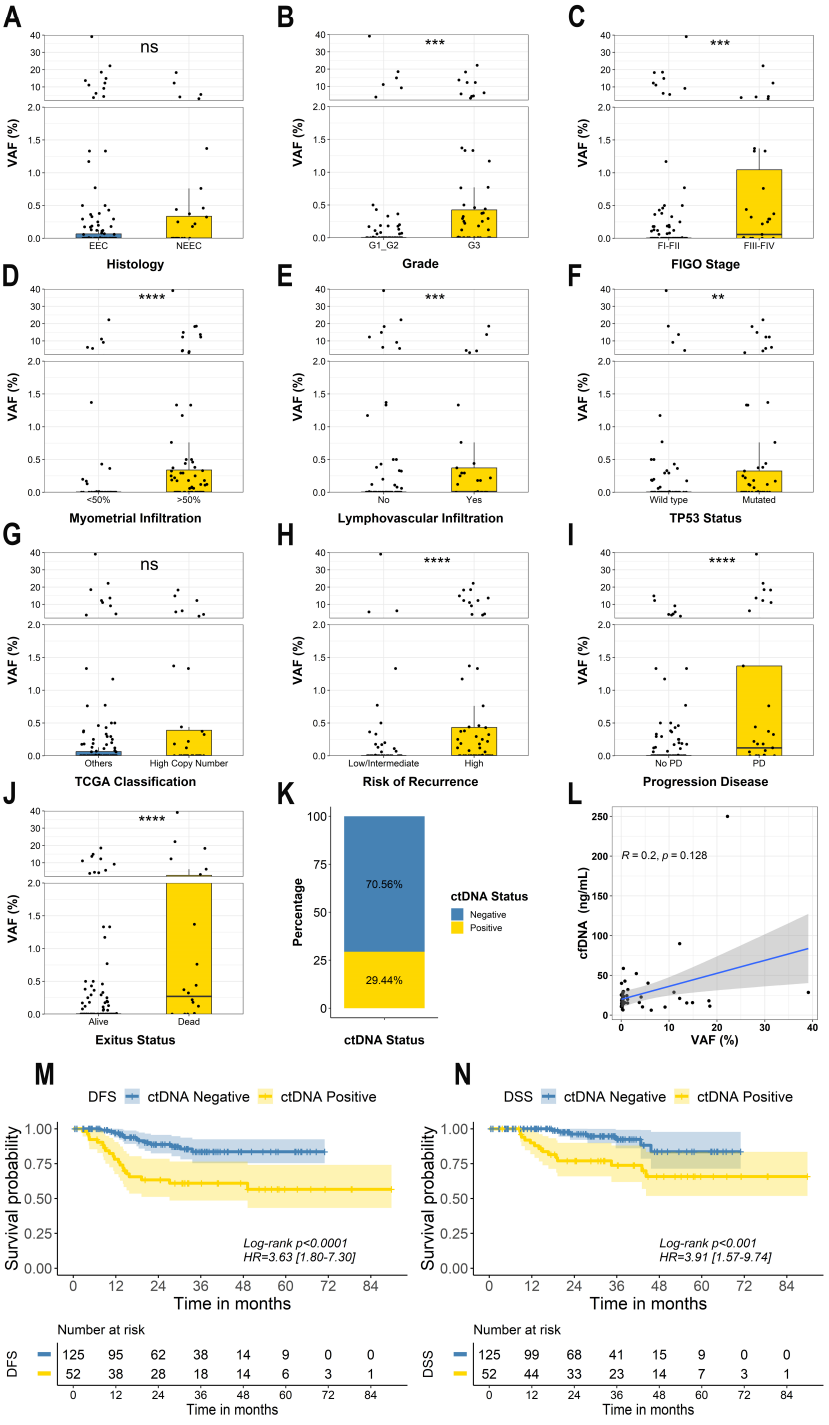
Variable	Univariate				Multivariate			
	HR 95% CI[2]		p-val	q-val[3]	HR 95% CI[2]		p-val	q-val[3]
Disease Free Survival								
Histology	3.72	1.95,7.11	<0.001	<0.001	2.57	0.99,6.69	0.047	0.16
Grade	5.42	247,11.9	<0.001	<0.001	1.26	0.37,4.25	0.71	0.75
FIGO Stage	4.04	2.10, 7.79	<0.001	<0.001	1.25	0.44,3.51	0.68	0.75
Myometrial infiltration	2.36	1.16, 4.77	0.013	0.015	0.85	0.30,2.35	0.75	0.75
LVSI	4.26	2.17, 8,38	<0.001	<0.001	2.38	0.83,6.79	0.10	0.24
MSI Status	0.62	0.30, 1.27	0.21	0.21				
TP53 Status	4.08	1.90, 8.75	<0.001	<0.001	1.33	0.45,3.99	0.61	0.75
ctDNA	3.63	1.80,7.30	<0.001	<0.001	2.70	1.12,6.46	0.025	0.16
Disease Specific Survival								
Histology	4.46	1.95,10.2	<0.001	<0.001	2.11	0.71,6.31	0.18	0.35
Grade	16.4	3.84,70.2	<0.001	<0.001	2.56	0.39,16.9	0.31	0.39
FIGO Stage	7.10	3.07,16.4	<0.001	<0.001	2.25	0.66,7.65	0.19	0.35
Myometrial infiltration	2.54	1.00,16.4	0.038	0.043	0.55	0.14,2.15	0.39	0.39
LVSI	4.90	2.07,11.6	<0.001	<0.001	2.32	0.62,8.72	0.20	0.35
MSI Status	0.52	0.20,1.35	0.16	0.16				
TP53 Status	9.32	2.74,31.6	<0.001	<0.001	2.07	0.45,9.58	0.33	0.39
ctDNA	3.91	1.57,9.74	0.002	0.003	3.40	1.18,9.77	0.018	0.13

[1]*U/D: undetermined*

[2]*HR 95% CI: Hazard Ratio 95% confidence interval*

[3]*False discovery rate for multiple testing*

USC UNIVERSIDADE DE SANTIAGO DE COMPOSTELA



USC UNIVERSIDADE DE SANTIAGO DE COMPOSTELA

Figure 4: Prognostic value of ctDNA analyses in EC patients**. A-J** Box plots representing the median variant allelic frequency (VAF %) of the alterations found in the ctDNA between the clinical variables. Statistical significance was assessed based on Mann–Whitney U test *p<0.05, **p<0.01, ****p<0.001. **K** Percentage of patients with positive and negative levels of ctDNA. **L**. Spearman correlation between the cfDNA levels at baseline (ng/mL) and the ctDNA VAFs (%). **M-N**. Kaplan Meier curves showing DFS (**M**) and OS (**N**) in patients with positive vs negative levels of ctDNA. Univariate Cox proportional-hazard model was used to estimate HR and log-rank test to report p-value.

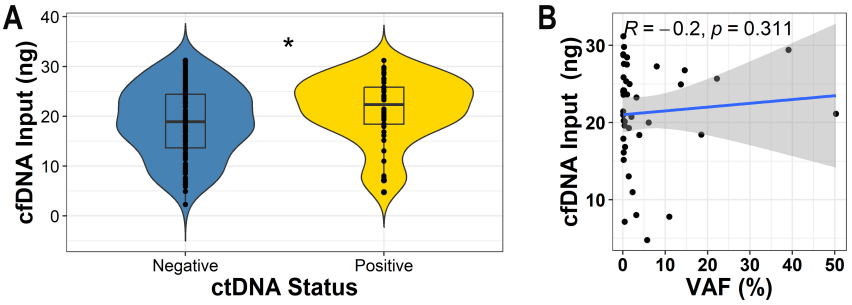


Figure 5: Correlation between the DNA input used for the ddPCR and the detection ctDNA**. A.** Violin plot of the DNA input (ng) used in the ddPCR between patients with detectable and non-detectable levels of ctDNA (Wilcoxon-rank test p<0.05) **B.** Correlation of ctDNA levels (VAF=%) and cfDNA input used in the ddPCR**.**

4.4.3.4| Combinatory analyses of cfDNA and ctDNA identified the patients with the worst clinical outcome

Since data obtained with the cfDNA and the ctDNA could provide complementary information we wated to explore if combining both factor we could improve our capacity to anticipate the EC evolution. With this purpose patients were classified according to the cfDNA levels and the presence/absence of ctDNA at surgery. Using this approach 4 groups were made: 'Group 1' cfDNA-Low/ctDNA-Negative (58.76%); 'Group 2' cfDNA-Low/ctDNA-Positive (20.34%); 'Group 3' cfDNA-High/ctDNA-Negative (11.86%)

USC UNIVERSIDADE DE SANTIAGO DE COMPOSTELA

and ‘Group 4’ cfDNA-High/ctDNA-Positive (9.04%). Clinical characteristics of the patients included in each group are summarised on Table 4. As seen on Figure 6A-B there is a clear worse prognosis associated to the presence of cfDNA and ctDNA.

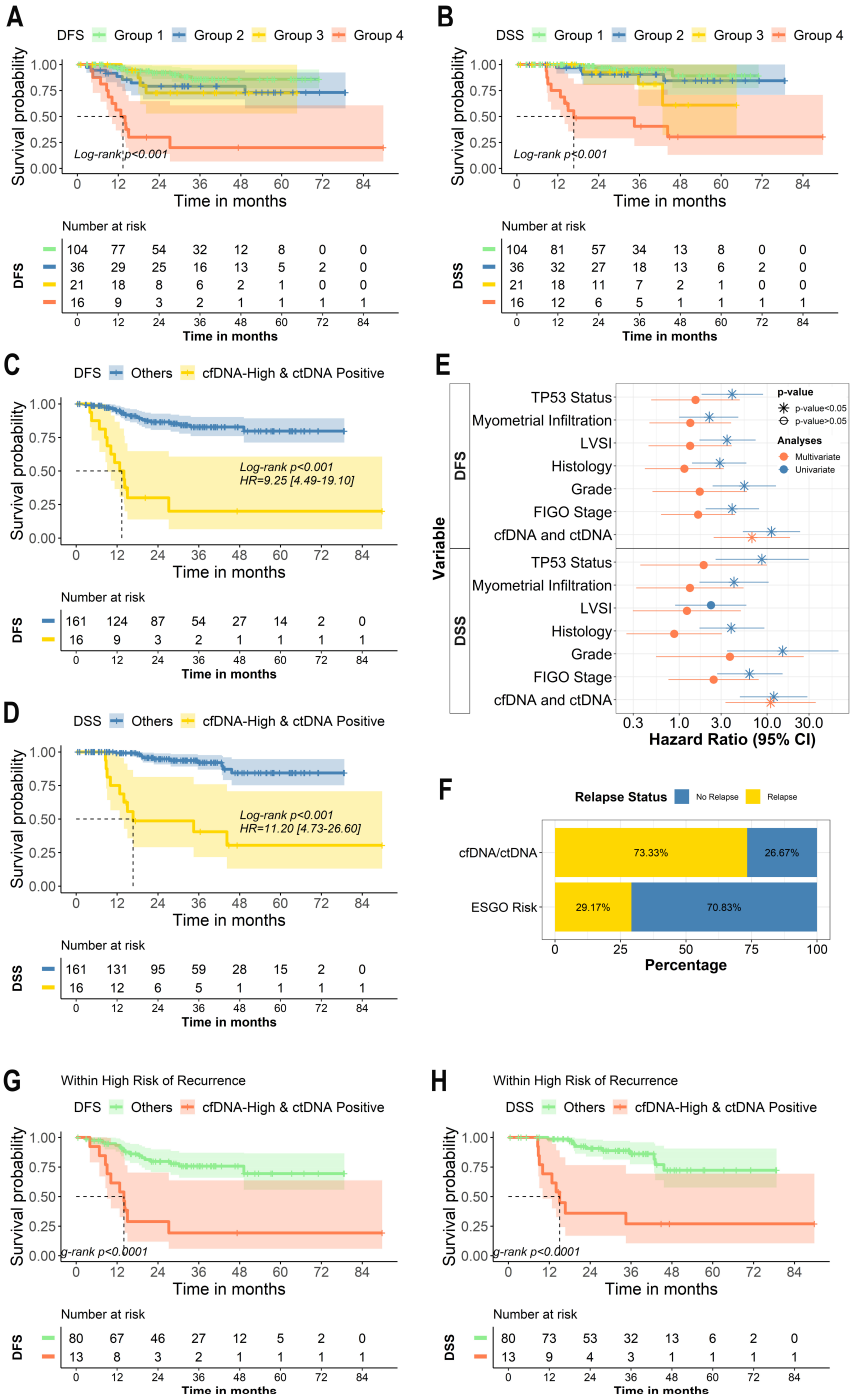
USC UNIVERSIDADE DE SANTIAGO DE COMPOSTELA

Table 4: Summary of the clinico-pathological features associated to the different groups based on the combinatory approach.

Variable	Group 1 N=104	Group 2 N=36	Group 3 N=21	Group 4 N=16	p-value[1]
Histology					0.061
Endometrioid	79 (77%)	30 (83%)	18 (86%)	8 (50%)	
Non Endometrioid	23 (23%)	6 (17%)	3 (14%)	8 (59%)	
Tumour Grade					**0.011**
Low Grade	66 (64%)	18 (50%)	15 (71%)	4 (25%)	
High Grade	37 (36%)	18 (50%)	6 (29%)	12 (75%)	
FIGO Stage					**<0.001**
I/II	84 (85%)	25 (74%)	20 (95%)	7 (44%)	
III/IV	15 (15%)	9 (26%)	1 (5%)	9 (56%)	
LVSI					**<0.001**
No	84 (81%)	16 (44%)	15 (71%)	7 (43%)	
Yes	9 (9.7%)	10 (38%)	5 (25%)	6 (46%)	
Myometrial Infiltration					**<0.001**
<50%	69 (67%)	7 (20%)	11 (55%)	6 (38%)	
>50%	34 (33%)	28 (80%)	9 (45%)	10 (63%)	
TCGA					
POLE	9 (8.80%)	3 (8.30%)	2 (11%)	0 (0%)	
MSI	41 (40%)	19 (53%)	7 (37%)	7 (44%)	
NSMP	31 (30%)	7 (19%)	6 (32%)	1 (6.3%)	
HCN	21 (21%)	7 (19%)	4 (21%)	8 (50%)	
Relapse Status					**<0.001**
No Relapse	95 (91%)	28 (78%)	17 (81%)	4 (25%)	
Relapse	9 (8.7%)	8 (22%)	4 (19%)	12 (75%)	
Death of disease					**<0.001**
No	100 (96%)	32 (89%)	18 (86%)	5 (31%)	
Yes	4 (3.8%)	4 (11%)	3 (14%)	11 (69%)	

[1]Kruskal-Wallis rank sum test; Fisher's exact test; Pearson's Chi-squared test

USC UNIVERSIDADE DE SANTIAGO DE COMPOSTELA



USC UNIVERSIDADE DE SANTIAGO DE COMPOSTELA

Figure 6: Combinatory analyses of cfDNA and ctDNA identify the patients with the worst clinical outcome**. A-B** Kaplan Meier curves showing DFS (**A**) and DSS (**B**) in patients according to the pre-surgery levels of cfDNA and ctDNA. **C-D** Kaplan Meier curves showing DFS (**C**) and DSS (**D**) in patients according to the pre-surgery high levels of cfDNA and detectable levels of ctDNA. **E.** Graphical representation of the univariate (blue) and multivariate (red) Cox proportional-hazard models. P-value<0.05 is represented with the * symbol. **F.** Bar plot with the early relapse status according to the combinatory approach and the ESGO risk classification. **G-H** Kaplan Meier curves showing DFS (**G**) and DSS (**H**) in patients according to the pre-surgery high levels of cfDNA and detectable levels of ctDNA in patients with high risk of recurrence according to the ESGO stratification.

Patients in group 4 (cfDNA-High/ctDNA-Positive) had a clear worse evolution in terms of DFS (Log-rank test p-value<0.0001; HR=9.25; 95% CI [4.49-19.10]) and DSS (Log-rank test p-value<0.0001; HR=11.20; 95% CI [4.73-26.60]) when compared to the remaining groups (Figure 6C-D, respectively). Patients of group 3 (cfDNA-low/ctDNA-Positive) showed poorer survival rates than patient of group 1 (cfDNAlow/ctDNA negative) but similar with the group 2 (cfDNAhigh/ctDNA negative) (Figure 6A-B). This result could be associated with the presence of potential false ctDNA negative patients included in group 2 due to the limitations of the ddPCR approach although cfDNA high levels indicate an aggressive disease.

Highlighting the aggressiveness of the tumours characterized by high cfDNA and ctDNA positivity, 75% of patients showed disease relapse and 69% died during the study follow-up as a result of the disease. Of note 73% these patients (group4) showed a relapse within the first year after the surgery while only the 30% of the tumours classified as intermediate/high risk of recurrence showed an early relapse (Figure 6F). Importantly, this combinatory approach showed complete independence over the traditionally risk factors and the molecular subtype (Figure 6E). Besides, this combinatory

USC UNIVERSIDADE DE SANTIAGO DE COMPOSTELA

approach remains clinically significant when stratifying patients based on histology, grade or the FIGO stage (Figure 7A-D). And even more importantly, the presence of high levels of pre-surgery cfDNA and the ctDNA positivity in patients classified as intermediate/high risk of recurrence based on ESGO-ENTRO-ESP criteria clearly discriminate those with a very indolent disease. Therefore, the analysis of liquid biopsy in the group of moderate/high risk complements the tools to anticipate the disease relapse (Figure 6G-H).

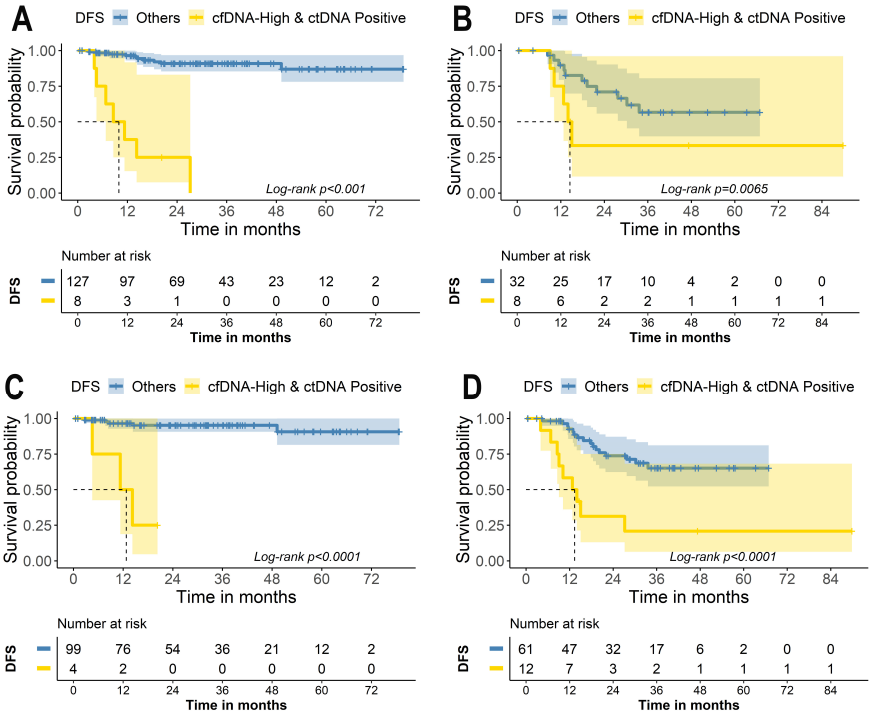


Figure 7: The clinical relevance of the combination of cfDNA and ctDNA analyses remains even within the more aggressive EC subtypes. **A-H** Kaplan Meier curves showing PFS and OS on patients with high baseline levels of cfDNA and detectable levels of ctDNA on patients with endometrioid EC (**A**) and non-endometrioid histology

USC UNIVERSIDADE DE SANTIAGO DE COMPOSTELA

(**B**) and patients with low grade (G1-G2) (**C**) and high grade (G3) (**D**). A log-rank test was used to report p-value.

4.4.3.5 | CfDNA and ctDNA as a monitoring tool for EC

To explore the value of cfDNA and ctDNA monitoring as a surrogate of the EC burden, a total of 372 longitudinal blood samples were analysed in a subset of 130 patients. From these patients, 22 showed disease progression (Figure 8). Although significant reduction on the cfDNA levels were found after surgical resection at 6 and 24 months (Wilcoxon signed-rank test) (Figure 9); the dynamics of cfDNA levels in the longitudinal samples did not show value to monitor the disease reappearance in our cohort of patients.

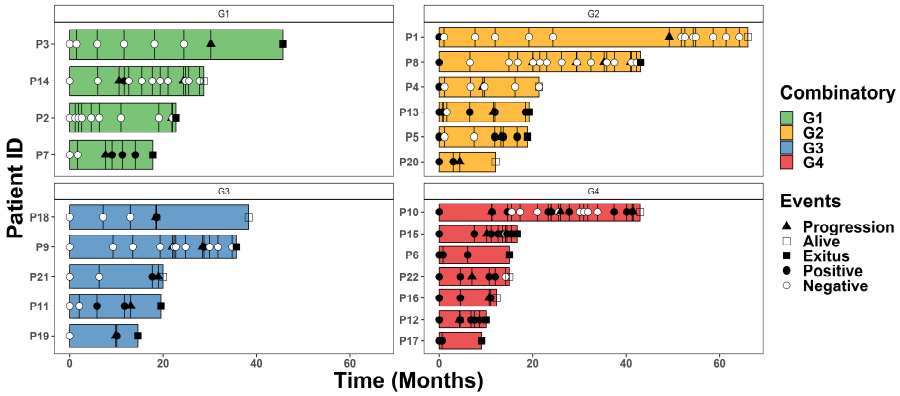


Figure 8: Swimmer plot of the patients that underwent relapse regardless of the availability of samples 6 months prior to the relapse.

USC UNIVERSIDADE DE SANTIAGO DE COMPOSTELA

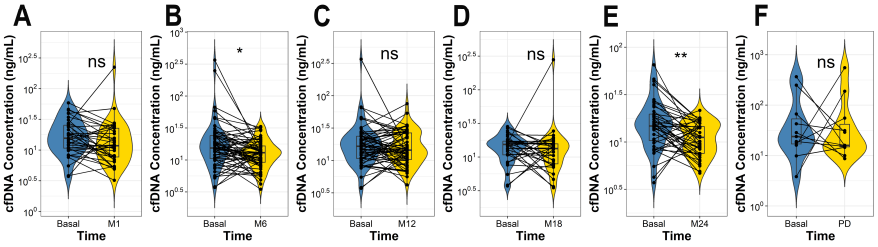


Figure 9: Longitudinal analysis of cfDNA in EC patients. Violin plots of the cfDNA levels within the entire population (**A-F**) when compared between baseline and different time points: **A**. 1-month post-surgery, **B**. 6 months post-surgery, **C**. 12 months post-surgery, **D**. 18 months post-surgery, **E**. 24 months post-surgery and **F**. at progression disease. Wilcoxon signed-rank test was used to assess statistical significance between paired samples *p<0.05.

Notably, the analyses of the specific tumour fraction through longitudinal samples allowed for the identification of the disease recurrence months before (4.68±2.98) the clinical confirmation of relapse, mainly in patients with detectable pre-surgery ctDNA (80%, 8/10) (Figure 10A). However, in 4/22 (18.18%) of all patients who showed recurrent disease the ctDNA was not detectable with the ddPCR approach. Most of these patients were also ctDNA negative at surgery, showing the need to improve the sensitivity of the ctDNA detection to monitor tumours which are low shedders.

Importantly, longitudinal analyses of ctDNA proved to be a powerful asset to identify patients undergoing an early relapse, as reflected the patient #1 described in Figure 10B. This patient was diagnosed with an Endometrioid FIGO Stage IB tumour, positive for a pathogenic mutation in *FGFR2* in the pre-surgery cfDNA (0.06%), which was found increased 5 months after surgery (4.52%) and two months later a relapse at abdominal level was clinically confirmed (18%). The patient started to receive Dostarlimab and the ctDNA strongly decreased (0.38%) in line with the partial response defined

USC UNIVERSIDADE DE SANTIAGO DE COMPOSTELA

based on CT-Scan. The patient is currently in response (0%) and being monitored by means of the ctDNA together the image assessment.

Longitudinal analyses also allow for the dynamic characterization of the disease in response to therapy pressure (Figure 10C-D). For example, in Figure 10C is represented the case of a 69-year-old patient that was diagnosed with EC of serous histology of high grade and FIGO IIIA. NGS analyses of the UA showed alterations within the *PPP2R1A* and *TP53* genes and they were followed through the course of the disease. The patient had high levels of cfDNA at surgery as well as detectable levels of ctDNA. According to clinical guidelines the patient was treated with Carboplatin-Paclitaxel combined therapy and radiotherapy. Afterwards, the cfDNA/ctDNA levels were measured again, finding detectable levels of alteration after surgery that were indicative of early progression disease (0.29%). Shortly after, the patient was confirmed to have a disease relapse at the liver through CT-Scan and showed a spike on ctDNA levels (16.90%). After the recurrence, patient was treated with a more aggressive regimen of chemotherapy. Two plasma samples were collected to monitor the response to the therapy, and although there was an initial reduction on ctDNA levels, they started to increase again, and the patient showed progressive disease with peritoneal affectation and entered PS-ECOG 4 and could no longer be treated.

Another example is reflected on Figure 10D, a 58 year old patient diagnosed with a mixed histology phenotype (initially diagnosed as endometrioid), grade 2, FIGO IB tumour that showed high levels of cfDNA and really high levels of ctDNA at surgery. NGS analyses of the UA showed alterations within the *KRAS* gene and this alteration was followed through the course of the disease. After a year, patient showed symptoms compatible with a disease relapse at the lungs. At this moment ctDNA was positive confirming

USC UNIVERSIDADE DE SANTIAGO DE COMPOSTELA

the recurrence of the disease. Due to the nature of the relapse the patient was closely monitored throughout the course of the disease, and the cfDNA/ctDNA kinetics reflects the evolution of the disease and the response to therapy, being able to identify the resurge of the disease prior to clinical evidence. Thanks to this approach, clinicians have been able to adjust the treatment and anticipate CT-Scans according to the tumour kinetics. It is important to note that traditionally clinical variables identified this patient as being of intermediate risk, but our combinatory approach of cfDNA and ctDNA analyses classified it as of being of high risk of recurrence, reinforcing the additional value of liquid biopsy to anticipate the disease relapse.

USC UNIVERSIDADE DE SANTIAGO DE COMPOSTELA

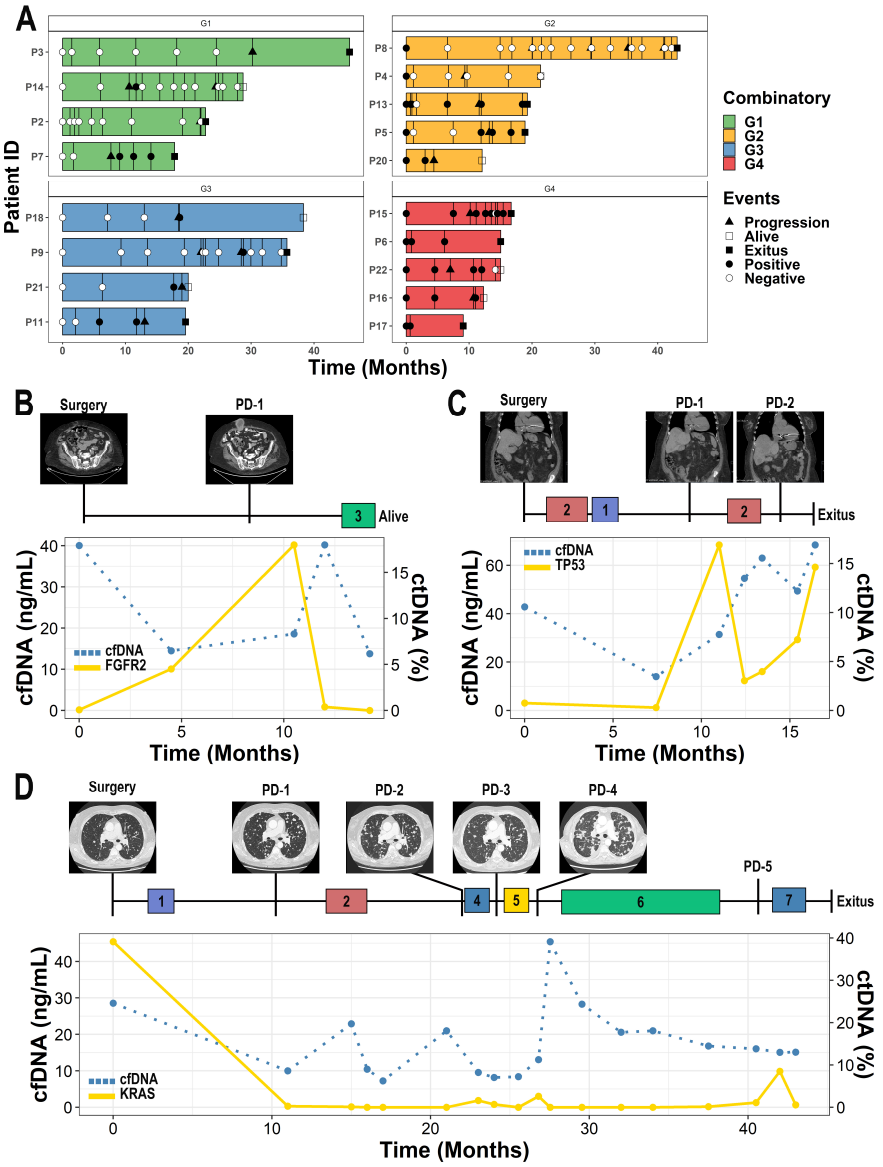


Figure 10: The longitudinal analyses of cfDNA and ctDNA allow for early detection of disease progression and accurately reflect the disease kinetics in response to treatment. **A.** Swimmer plot of the *18* patients that underwent tumour progression divided based on the combinatory approach with longitudinal samples collected at

USC UNIVERSIDADE DE SANTIAGO DE COMPOSTELA

least 6 months prior to the relapse (cfDNA and ctDNA). **B-D**. Example figures of the cfDNA (blue dotted line) and ctDNA kinetics (yellow line) in patients with advanced disease. 1. Radiotherapy, 2. Carboplatin-Paclitaxel, 3. Dostarlimab, 4. Exemestane. 5. Doxorrubicine and Avastin. 6. Lenvatinib and Pembrolizumab, 7. Topotecan and Bevacizumab.

4.4.4 | Discussion

To our knowledge, the present study represents the largest multicentre study conducted on EC that asses the value of cfDNA and ctDNA as minimally invasive biomarkers to, not only predict patient outcome, but also the largest data set where longitudinal samples were analysed to determine the value of liquid biopsy on EC. We have shown that cfDNA and ctDNA metrics can help to identify patients with shorter DFS and OS. In addition, we have shown that close follow-up of ctDNA in patients with poor prognosis allows for the early detection of the disease relapse.

Although, cfDNA origin is still unclear, multiple release pathways have been proposed, such as through apoptosis, necrosis, NETosis or from extracellular vesicles, among others (58,313). Most of the plasma cfDNA found in healthy people is thought to be derived by nucleated blood cells, such as neutrophils and lymphocytes (58). CfDNA levels are influenced by multiple factors such as age, metabolic activity, immune processes and disease, such as cancer (314). In patients with different solid tumour types cfDNA levels are found increased in comparison with healthy people and has been associated with poor prognosis in advanced stages (60,315) and, apart from the contribution of the tumour derived cfDNA in this increment, the neoplastic transformation may have systemic effect on cell turnover or DNA clearance associated with the cfDNA dynamic (60). In the present study we have shown that pre-surgery assessment of cfDNA levels correlates with worse clinical outcome, being a robust independent prognostic biomarker for

USC UNIVERSIDADE DE SANTIAGO DE COMPOSTELA

EC patients. We found a trend to have higher levels of cfDNA in high grade and myometrial/lymph vascular invasion as it was previously described by our group and other groups with different methodologies (91,228,316). These high cfDNA levels in high-risk tumours can be partially explained by a high ctDNA release but also other systemic mechanism which are more intensely regulated in advanced stages of the disease. In our study we did not find correlation between cfDNA and the pre-surgery levels of different blood cells population but we couldn't rule out the impact of this population on the cfDNA content without the application of more specific analyses to characterize the cfDNA origin in our EC population. Nevertheless, data presented clearly pointed to the cfDNA analysis as simple and cost-effective biomarker with prognostic value at surgery.

Indeed, when we specifically analyse the ctDNA fraction through personalized ddPCR assays which tracked MSI markers or pathogenic alterations (SNVs or CNVs) identified in the UAs, we found detectable levels in the 38% of the global cohort of patients, being this positivity more frequent in high grade (41.10%) or infiltrative tumours (46.91%). Regarding the molecular EC subtypes, *TP53* mutant tumours also showed higher detection of pre-surgery ctDNA. VAFs were found higher in tumours with high-risk characteristics. These data are in line with previous studies which demonstrated a high ctDNA content linked to high risk or advanced endometrial tumours (91,228,309,317). Accordingly, we found that patients with detectable levels of ctDNA at surgery had significantly shorter DFS and DSS times, although with no independent value over the rest of clinical variables, probably due to the strong correlation with the other risk factors under study.

USC UNIVERSIDADE DE SANTIAGO DE COMPOSTELA

Nonetheless, the combination of both cfDNA and ctDNA data at surgery allowed for the identification of a group of patients, with high levels of cfDNA and detectable levels of ctDNA, that showed an extremely poor clinical outcome. Although this group represents the 10% of the global cohort of patients analysed in our study, most of them developed an early relapse within the first year after surgery. The combined analysis of the pre-surgery cfDNA and ctDNA served to discriminate the risk of recurrence independently the histology, the FIGO stage, the grade or the molecular subtype. In fact, our approach served to identify the patients with a very aggressive evolution within the group of intermediate high/ high risk tumours. Moreover, this approach allowed for the identification of patients with initially good clinical outcome as in fact, being of poor prognosis. Therefore, our approach not only allows for the identification of the subset of patients with the worst clinical outcome but also allows to identify patients with high risk of relapse regardless of their clinical characteristics. It is important to mention that patients with low levels of cfDNA and detectable levels of ctDNA at surgery showed a poor evolution in comparison with the patients with low cfDNA and undetectable ctDNA. However, this group was not so clinically relevant in comparison with the high cfDNA and positive ctDNA. We hypothesize that high cfDNA levels are indicating local or systemic changes associated with the tumour aggressiveness, non-directly linked to the ctDNA release, but impacting on the disease biology.

Therefore, our data clearly demonstrate the clinical interest of the cfDNA/ctDNA analysis at surgery to improve the risk stratification. Ideally the determination of pre-surgery ctDNA through tumour informed or non-informed strategies would help to better stratify the risk of recurrence in all EC patients who undergo surgery. However, we consider especially relevant the ctDNA assessment in patients with high cfDNA or other risk factor, since

USC UNIVERSIDADE DE SANTIAGO DE COMPOSTELA

the ctDNA presence will be a key tool to define the cohort of patients that would benefit from a closer follow-up or an intensification of the adjuvant treatment.

Notably, the ctDNA monitoring represents a valuable approach to detect the presence of minimal residual disease, anticipate the disease relapse and evaluate the response to the therapy in advanced EC stages as the present study and other works have evidenced (91,228,229). From the total cohort of patients included in the study, we monitored the cfDNA and ctDNA levels in longitudinal plasma samples from 130 patients. Globally, the cfDNA dynamic lack value to accurately mirror the tumour burden although in specific cases cfDNA levels changed accordingly with the tumour evolution. This result could be explained by the addition of other factors such as the adjuvant therapy that can modify systemically the cfDNA release into circulation (318). Of note, for the follow-up context ctDNA monitoring showed high value to track the disease evolution. Post-surgery ctDNA was only detected in cases with MRD or recurrent disease. Specially in cases with positive levels of pre-surgery ctDNA, the ctDNA kinetics served to detect the relapse months before the clinical/radiological confirmation, providing an opportunity to start the treatment of advanced disease earlier and accounting with the molecular information of the tumour clones that are driving the recurrent disease. The clinical relevance of the post-surgery ctDNA monitoring has been well documented in other tumour types like colorectal, lung or breast tumours (319–322) and also in EC longitudinal ctDNA assessment by NGS and ddPCR has been successfully applied to detect the disease advance (91,228,229). Our study represents the larger cohort of EC patients monitored with ctDNA so far, and robustly demonstrate the benefit of this strategy to make a more personalize and precise disease follow-up. Regardless of these positive results, our approach has some limitations since ctDNA pre/post-surgery

USC UNIVERSIDADE DE SANTIAGO DE COMPOSTELA

detection was not efficient in around 20% of patients who showed disease relapse. To this regards it's important to mention that our approach prioritise sensitivity by analysing the most predominant alterations found in the primary tumour of each patient; nonetheless, it may not be the predominant clone being released into the bloodstream and the arisen of new mutations within tumour evolution is not taken into consideration. Other technologies, such as panel-based strategies circumvent this limitation at the cost of sensitivity, as the one discussed on chapter I (228,229).

4.4.5 | Conclusions

Overall, the study demonstrated the value of cfDNA and ctDNA analyses as prognostic tools in the largest EC cohort published so far. High levels of cfDNA and detectable levels of ctDNA at surgery strongly correlated with poor prognosis and served to identify the patients that suffered an early relapse independently of the established risk factors currently used to manage EC. Additionally, the longitudinal ctDNA assessment allowed for the early identification of recurrences and the development of resistance to the treatment. Implementation of this approach into the clinic with the traditionally used risk variables would translate into a much better management of the patients reducing over treatment and allowing the identification of those patients who should be closely monitored. Although still far, the implementation of liquid biopsy into the clinic could improve greatly the management of the EC patients.

USC UNIVERSIDADE DE SANTIAGO DE COMPOSTELA

4.5 | CHAPTER V

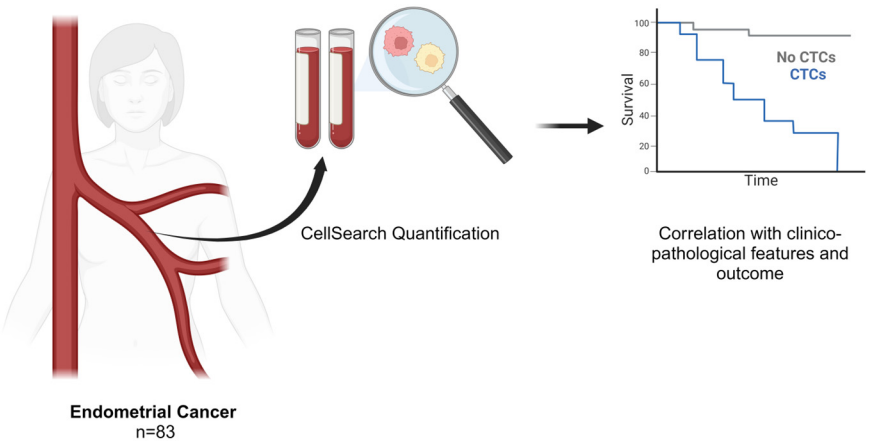
CTCs as Prognostic Biomarkers in Endometrial Cancer: Findings from a Multicentred Study

USC
UNIVERSIDADE DE SANTIAGO DE COMPOSTELA

CHAPTER V

CTCs as Prognostic Biomarkers in Endometrial Cancer: Findings from a Multicentred Study

Graphical Abstract:



Created with BioRender.com

Keywords: endometrial cancer, liquid biopsy, CTCs, prognostic, biomarker

USC UNIVERSIDADE DE SANTIAGO DE COMPOSTELA

CHAPTER V

CTCs as Prognostic Biomarkers in Endometrial Cancer: Findings from a Multicentred Study

Abstract:

CTCs have a key role in the metastatic cascade, yet their clinical relevance in EC remains unclear. This study aimed to bridge this gap by analysing CTCs in 83 EC patients, assessing their correlation with clinico-pathological features and prognostic implications.

Our analysis revealed a CTC positivity rate of 21.69% among EC patients, with CTC counts ranging from 1 to 80 per 7.5mL of blood. Notably, higher CTC levels were associated with more aggressive tumour phenotypes, such as higher grade, advanced FIGO stages, and increased myometrial and LVSI. Importantly, patients with detectable CTCs exhibited significantly shorter DFS and DSS. Subsequent subgroup analysis using a 2 CTC cutoff further confirmed the prognostic significance of CTC presence, with consistent findings in both DFS and DSS. However, despite these associations, CTCs did not maintain independent prognostic significance in multivariate analyses.

Nonetheless, our study showcases the adverse prognostic implications of CTC presence in EC, suggesting their potential utility as complementary prognostic markers. Further research is needed to further validate the role of CTC involvement in EC progression and their role in guiding personalized treatment strategies for EC patients.

USC UNIVERSIDADE DE SANTIAGO DE COMPOSTELA

4.5.1 | Introduction

CTCs are cells that have intravasated into the bloodstream from either primary or metastatic locations and have a principal role within the metastatic cascade. Due to their biological importance multiple studies have focused on the clinical significance of CTCs as a tool to improve the prognosis and anticipate the response to treatment. The clinical and biological interest of CTCs has been well documented on multiple cancer types, such as breast, lung, prostate or colorectal (86–88).

In the context of EC, only few studies that have evaluated the clinical significance of CTCs. However, the limited research conducted indicates that the presence of CTCs in the bloodstream is linked to more aggressive phenotypes (89–91,115). Most of the conducted studies analysed limited cohort sizes, therefore the conclusions obtained are lack of high clinical impact. For instance, Bogani and collaborators found a 7% prevalence of positive CTCs in grade 3 EC patients, with associations noted between CTC presence and deep myometrial infiltration and positive lymph nodes in patients with endometrioid histologic subtype (116). Our group also showed higher CTC levels in high-risk EC patients. Moreover, gene-expression profiling characterized a high CTC-plasticity phenotype with stemness and EMT features which demonstrated an advantage in the promotion of metastasis in an *in vivo* mouse model of CTC dissemination and homing (90).

Given the potential clinical relevance and impact on prognosis of CTC enumeration, we screened in 83 EC patients for epithelial CTCs using the CellSearch system and examined the correlation between the number of CTCs and different clinico-pathological features as well as clinical outcome to determine their value as a prognostic and predictive biomarker.

USC UNIVERSIDADE DE SANTIAGO DE COMPOSTELA

4.5.2 | Material & Methods

4.5.2.1 | Patients inclusion

A total of 83 patients with EC were recruited between January 2018 and June 2022 at the Gynaecology Department of Vall d'Hebron University Hospital (Barcelona, Spain), the MD Anderson Cancer Center (Madrid, Spain), the University Clinical Hospital of Santiago de Compostela (Santiago de Compostela, Spain) and the Bellvitge University Hospital (Barcelona, Spain).

4.5.2.2 | Sample collection and processing

Peripheral blood samples were collected using CellSave Preservative tubes (Silicon Biosystems Inc, Huntington Valley, USA). They were used for CTC isolation with the CellSearch system (Menarini, Sylicon Biosystems, Bologna, Italy). This system allows for the isolation and enumeration of EpCAM-positive CTCs. After CTC isolation with the CellSearch Epithelial Circulating Tumor Cell Kit (Menarini, Silicon Biosystems Inc), cells were labeled with phycoerythrin-conjugated anti-CK antibodies, allophycocyanin-conjugated anti-CD45 antibodies, and 4,6-diamino-2-phenylindole (DAPI) to stain the nuclei. The CellTracks Analyzer (Menarini, Silicon Biosystems, Bologna, Italy) was used to acquire digital images of the three different fluorescent dyes with a 12-bit camera; the images were reviewed by trained operators to determine the CTC count.

4.5.3 | Results

4.5.3.1 | Cohort characteristics

The cohort included 83 patients with EC with the clinical characteristics summarised in Table 1. The cohort included patients with EEC and NEEC, Grade 1-3, FIGO stage I-IV patients from all TCGA groups (POLE, MSI, NSMP,

USC UNIVERSIDADE DE SANTIAGO DE COMPOSTELA

HCN) classified accordingly with the updated ESMO/ESGO consensus (8). A total of 21 (25%) patients underwent tumour progression with a median PFS of 25.7 months [2.6-63.3]. A total of 18 (22%) patients perished due to the disease, with a median OS of 31.1 months [3.7-63.3]. It is important to highlight that this cohort is enriched on patients of intermediate/high and high risk of recurrence according to the ESMO/ESGO consensus (11), therefore is not representative of a real-world EC cohort daily managed in the participating hospitals.

USC UNIVERSIDADE DE SANTIAGO DE COMPOSTELA

Table 1: Clinico-pathological features of the studied cohort according to the presence of CTCs in 7.5mL of blood.

Variable	N	Negative n=65[1]	Positive n=18[1]	p-value[2]
Age	83			0.3
Median (IQR)		68 (59,75)	72 (61,78)	
Histology	81			0.5
EEC		40 (63%)	10 (56%)	
NEEC		23(37%)	8 (44%)	
Tumour Grade	81			0.4
G1		7 (11%)	2 (11%)	
G2		21 (33%)	3 (17%)	
G3		35 (56%)	13 (72%)	
FIGO Stage	82			**0.042**
I-II		48 (75%)	9 (50%)	
III-IV		16 (25%)	9 (50%)	
Myometrial infiltration	79			0.2
<50%		25 (40%)	4 (24%)	
>50%		37 (60%)	13 (76%)	
Lymphovascular Space Invasion	69	11 (20%)	7 (54%)	**0.030**
TCGA	79			0.3
POLE		5 (8.1%)	0 (0%)	
MSI		19 (31%)	4 (24%)	
NSMP		15 (24%)	2 (12%)	
HCN		23 (37%)	11 (65%)	
cfDNA Concentration (ng/mL)	78			0.070
Median (IQR)		16 (11,24)	25 (15,32)	
ctDNA Positivity	64	16 (33%)	12 (75%)	**0.004**
Number of CTCs	83			**<0.001**
Median (IQR)		0 (0-0)	3 (2-4)	
Recurrent Disease	83			**0.012**
No relapse		53 (82%)	9 (50%)	
Relapse		12 (18%)	9 (50%)	
Exitus	83			**0.020**
Alive		55 (85%)	10 (56%)	
Dead		10 (15%)	8 (44%)	

[1]N (%)

[2]Wilcoxon rank sum test; Pearson Chi-squared test; Fisher's exact test

4.5.3.2 | CTCs correlation with clinico-pathological features

The EpCAM positive CTC population was analysed in peripheral blood samples collected at surgery using the CellSearch technology, the reference

USC UNIVERSIDADE DE SANTIAGO DE COMPOSTELA

method for CTC enumeration of epithelial cells. Out of 83 patients, 21.69% tested positive for CTCs, with counts ranging from 1 to 80 CTCs per 7.5mL of blood. Most patients had less than 5 CTCs (77.78%). The positivity rate was consistent between patients with EEC or NEEC histology. However, higher rates of positivity were observed in tumours of high grade (72%), advanced FIGO stages (50%), patients classified as high-copy number (65%), with over 50% of myometrial infiltration (76%), and with LVSI (54%). Additionally, patients who experienced relapse or deceased had significantly higher positivity rates and CTC counts.

Upon examining the interaction of CTCs with other experimental variables, it was found that patients with CTCs exhibited higher levels of cfDNA and were more likely to be positive for ctDNA, potentially indicating a more aggressive tumour phenotype. This finding coincided with shorter DFS and DSS.

USC UNIVERSIDADE DE SANTIAGO DE COMPOSTELA

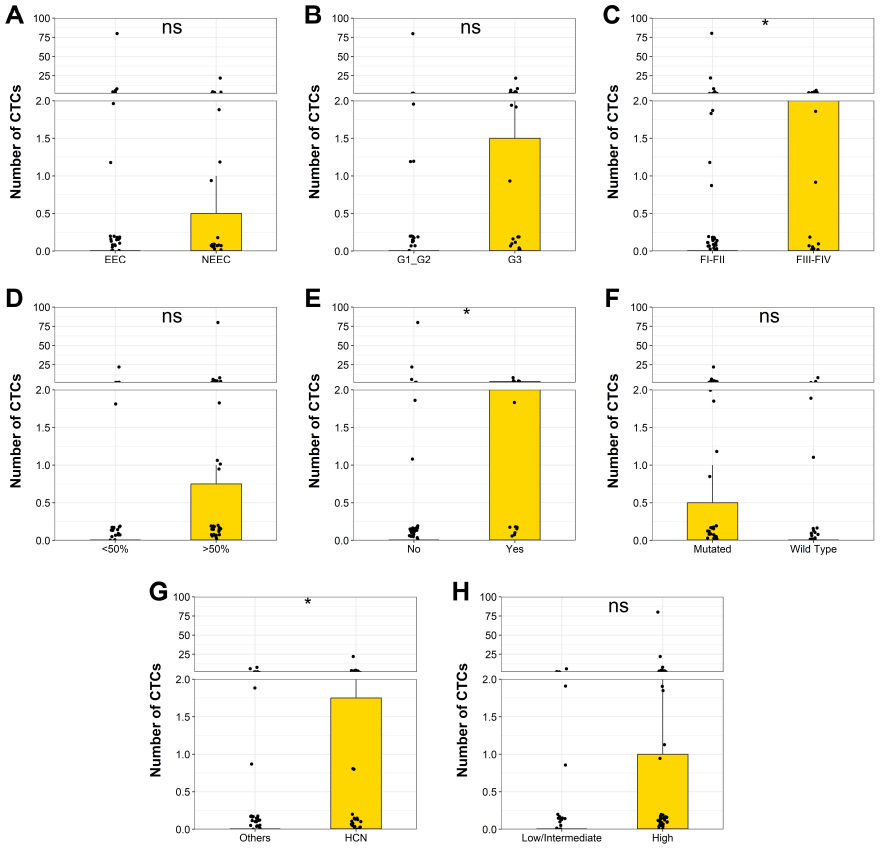


Figure 1: CTCs are associated with more aggressive phenotypes. **A-H** Boxplot of the number of CTCs across different clinico-pathological features: histology (**A**), grade (**B**), FIGO stage (**C**), myometrial infiltration (**D**), LVSI (**E**), p53 Status (**F**), TCGA Classification (**G**) and risk of recurrence (**H**). Wilcoxon signed-rank test was used to determine statistical significance *p-value<0.05.

Next, we evaluated the potential prognostic significance of CTCs. Patients were divided into two groups based on their CTC status: those with positive CTC levels and those with negative levels. As shown in Figure 2A-B, individuals with detectable CTCs had shorter DFS (HR:2.82 [1.18,6.71]; p-value=0.025) and DSS (HR:2.89 [1.11,7.54], p-value=0.036). Furthermore, to

USC UNIVERSIDADE DE SANTIAGO DE COMPOSTELA

strengthen the reliability of our findings, we established a cutoff of 2 CTCs to further differentiate patients into high and low CTCs levels. Subsequent Kaplan-Meier analyses revealed consistent results in both DFS (HR: 2.86 [1.18,6.95]; p-value=0.028) and DSS (HR: 3.60 [1.37,9.43]; p-value=0.012) (Figure 2C-D, respectively). While the presence of CTCs did not maintain significance as an independent prognostic biomarker within the multivariate analyses employing the Cox proportional hazards model (Table 2), it remains evident that the presence of CTCs serves as an unfavourable prognostic indicator in EC.

USC UNIVERSIDADE DE SANTIAGO DE COMPOSTELA

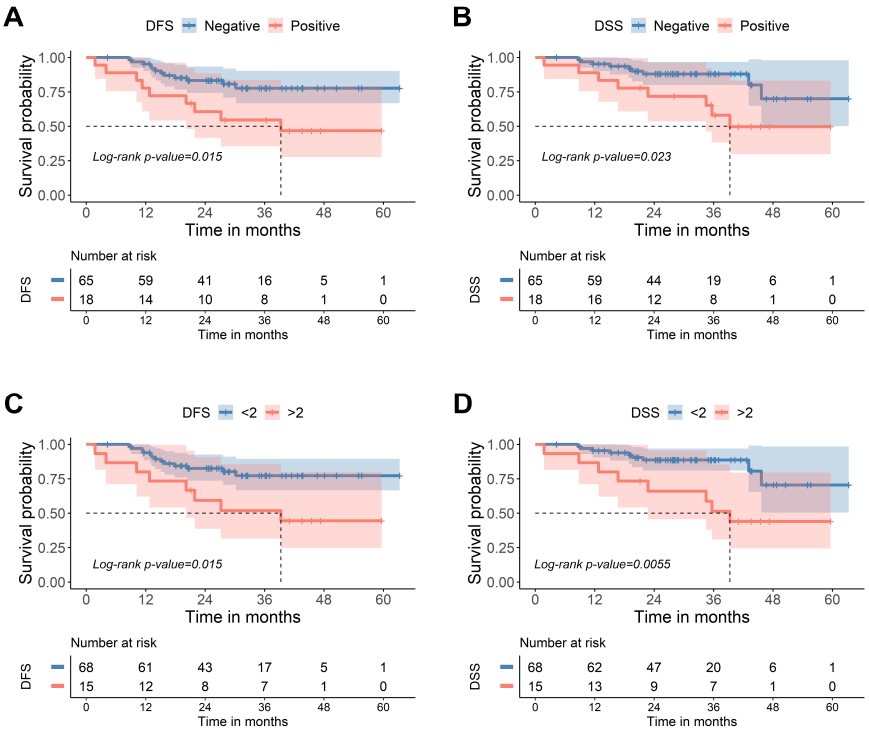


Figure 2: The presence of CTCs is directly linked to shorter DFS and DSS**. A-B.** Kaplan Meier representation of the DFS (**A**) and DSS (**B**) according to the presence of CTCs. **C-D.** Kaplan-Meier representation according to the presence of ≥2 CTCs/7,5mL of blood, showing significant shorter DFS (**C**) and DSS (**D**)**.**

USC UNIVERSIDADE DE SANTIAGO DE COMPOSTELA

Table 2: Cox-regression model of the value of CTCs in DFS and DSS.

Variable	Univariate				Multivariate			
	HR 95% CI[2]		p-val	q-val[3]	HR 95% CI[2]		p-val	q-val[3]
Disease Free Survival								
Histology	2.14	0.91,5.05	0.08	0.12	3.58	1.07,12.10	0.03	0.12
Grade	5.64	1.65,19.2	**<0.001**	**0.008**	2.93	0.32,26.7	0.29	0.41
FIGO Stage	2.96	1.25,7.00	**0.017**	**0.033**	1.62	0.58,4.53	0.36	0.41
Myometrial infiltration	1.88	0.69,5.14	0.19	0.19				
LVSI	3.10	1.28,7.52	**0.016**	**0.033**	3.00	1.02,8.83	0.048	0.12
MSI Status	0.42	0.14,1.28	0.10	0.12				
TP53 Status	3.98	1.16,13.70	**0.012**	**0.033**	1.71	0.45,6.51	0.41	0.41
CTCs	2.82	1.18,6.71	**0.025**	**0.040**	2.78	0.99,7.86	0.058	0.12
Disease Specific Survival								
Histology	2.27	0.87,5.92	0.094	0.13	3.26	0.87,12.10	0.069	0.15
Grade	7.20	1.64,31.60	**0.001**	**0.007**	*U/D*[1]	*U/D*[1]	*U/D*[1]	*U/D*[1]
FIGO Stage	3.46	1.33,9.01	**0.012**	**0.033**	1.54	0.48,4.94	0.47	0.47
Myometrial infiltration	1.80	0.59,5.54	0.28	0.29				
LVSI	3.03	1.12,8.17	**0.032**	**0.057**	2.88	0.81,10.2	0.10	0.15
MSI Status	0.55	0.18,1.73	0.29	0.29				
TP53 Status	10.30	1.36,78.7	**0.002**	**0.007**	3.69	0.45-30.3	0.16	0.19
CTCs	2.89	1.11,7.54	**0.036**	**0.057**	2.49	0.85,7.27	0.10	0.15

[1]*U/D: undetermined*

[2]*HR 95% CI: Hazard Ratio 95% confidence interval*

[3]*False discovery rate for multiple testing*

4.5.4 | Discussion

To our knowledge, this is one of the largest multicentre studies conducted on EC to determine the value of CTCs as minimally invasive prognostic biomarkers to predict patient outcome. Overall, although the rate of patients

USC UNIVERSIDADE DE SANTIAGO DE COMPOSTELA

with detectable CTCs was low, their detection allows for the identification of patients with shorter DFS and DSS.

It is important to remark that CTCs can intravasate into the bloodstream to generate new metastases, although their survival rate in circulation is limited due to the adverse environment in circulation. Therefore, they are key players in the dissemination of the disease. Multiple studies have shown that CTCs are indicative of poor prognosis in many solid tumours such as breast, colorectal and prostate tumours. In fact, in 2004 FDA approved the CTCs enumeration with the CellSearch in metastatic breast cancer and in 2007 and 2008, this approval was extended to colorectal and prostate cancer, respectively (178,323–325). While the prognostic relevance of CTCs has been well-established in these cancer types their significance in gynaecological tumours, particularly EC, has remained relatively limited. In line with previous studies, we found a low percentage of EC patients with detectable levels of CTCs (21,7%). Our group together the ENITEC (European Network for Individualized Treatment in EC) Consortium described in a pilot study a 22% of patients with detectable EpCAM positive CTCs (n = 32 high-risk EC) (90). Similarly, the 15% of EC showed detectable epithelial CTCs in a cohort of 40 patients, in which the presence of cervical involvement was a key factor associated with the CTCs detection (326). Opposite, by using the same isolation strategy Lemech et al. reported 60% CTC-positivity in 30 advanced EC patients, generally associated with NEEC versus EEC, higher tumour size and stage (327).

In our study we have seen that EC with phenotypic markers of aggressiveness present higher number of CTCs on the bloodstream. Specifically with more invasive phenotypes, such as, LVSI, myometrial infiltration and high grade. Which are inherently more aggressive and tend to

USC UNIVERSIDADE DE SANTIAGO DE COMPOSTELA

metastasise. But not only with clinical variables, but also experimental variables studied on previous chapters, such as cfDNA and ctDNA. Patients with CTCs tend to have higher levels of cfDNA and detectable levels of ctDNA, which is a further indicator of a subtype of EC with a more secretive phenotype. Moreover, since the presence of CTCs has been linked to more invasive phenotypes in our cohort, we decided to analyse the correlation of CTCs with prognosis. Significantly shorter DFS and DSS have been found on those patients with detectable CTCs, indicating a potential use of the CTC enumeration to complement the current risk tools. In line with our results, using the CellSearch system Fancini, et al reported that presence and counts of CTCs during laparoscopy, and the evaluation of their ER status, could help to predict the clinical outcome of these patients (115).

Although the relevant findings obtained with our study, it is important to highlight that one limitation of the study is associated with the use of the CellSearch system for the isolation of CTCs, since it only allows to enrich cells of epithelial origin with relative high expression of the EpCAM molecule in the cell-membrane. It should be noted that the CTCs are in a dynamic state, transitioning between epithelial and mesenchymal phenotypes (328,329)(cc; Cohen et al. Cancers 2023). Actually, a gene-expression profiling of EpCAM positive CTCs isolated from EC our group characterised a strong CTC-plasticity phenotype with stemness and EMT features that may provide an advantage in the promotion of metastasis for CTC dissemination and homing (90). Therefore, more complete studies that apply other technologies, such as non-epitope dependant could of interest to assess the presence of mesenchymal CTCs in the bloodstream of EC patients. In fact, Kolostova et al., demonstrated the feasibility of isolating CTCs from endometrial and cervical cancers to culture them in vitro for a short time by a non-antigen dependent technique (330). Using the same enrichment strategy, 92 EC patients with

USC UNIVERSIDADE DE SANTIAGO DE COMPOSTELA

localized disease were evaluated for the presence of CTCs, showing an improved detection rate compared to previous studies (331).

4.5.5 | Conclusions

In conclusion, our study represents a step forward in understanding the role of CTCs as prognostic biomarkers in EC. This multicentre study, among the largest conducted in the field, sheds light on the potential of CTCs in predicting patient outcomes. As demonstrated, the presence of CTCs in the bloodstream correlates with shorter DFS and DSS, highlighting their utility as indicators of disease progression and aggressiveness. The presence of CTCs and more aggressive tumour phenotypes, such as LVSI, deep myometrial infiltration, and high tumour grade could be an indicator of disease severity and metastatic potential.

Overall, our findings highlight the interest of CTCs as minimally invasive biomarkers for risk stratification and prognostication in EC patients, however the CTCs detection rates are still low. Further exploration of CTCs in larger and more diverse patient cohorts, coupled with advanced detection techniques, holds the potential to further our understanding of EC biology and ultimately improve clinical management strategies for this disease.

USC UNIVERSIDADE DE SANTIAGO DE COMPOSTELA

4.6|CHAPTER VI

Preclinical models in endometrial cancer

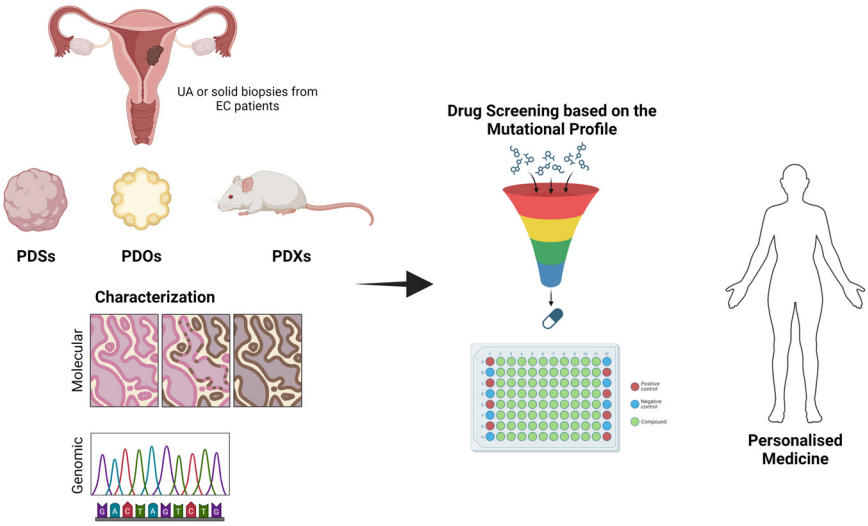
Part of the results from this chapter have been published as a case report in the international journal of molecular sciences (311)

USC
UNIVERSIDADE DE SANTIAGO DE COMPOSTELA

CHAPTER VI

Preclinical models in Endometrial cancer

Graphical Abstract:



Created with BioRender.com

Keywords: endometrial cancer, liquid biopsy, preclinical models, patient derived organoids, patient derived spheroids, patient derived xenografts, immunotherapy, targeted therapy

USC UNIVERSIDADE DE SANTIAGO DE COMPOSTELA

CHAPTER VI

Preclinical models in Endometrial cancer

Abstract:

Preclinical models play a pivotal role in biomedical research by bridging the gap between basic scientific discoveries and clinical applications. Within this context, personalized medicine has traditionally relied on *in vitro* and *in vivo* models, albeit with limitations such as lack of heterogeneity and complexity. This chapter focuses on two 3D models, PDSs and PDOs, which offer more realistic physiological features and heterogeneity than traditional 2D cultures.

Within this chapter, we aimed to optimize a pipeline for generating preclinical models from minimally invasive samples, specifically UAs, to identify effective treatments for EC patients upon relapse. Both PDSs and PDOs were successfully generated from UA or solid biopsies, characterized through IHC and NGS, and subjected to drug screening assays.

PDOs generated from UA or solid biopsies accurately recapitulated the tissue of origin, reflecting patient-specific molecular profiles and responses to treatment. Moreover, *in vitro* assays revealed significant efficacy of targeted therapies (e.g., BYL719, RAD001) compared to standard therapy (Carboplatin-Paclitaxel). Further validation *in vivo* demonstrated comparable therapeutic responses between standard and targeted therapies, with PDS-based PDX confirming the efficacy of immunotherapy.

In conclusion, within this chapter we showcase the clinical value of PDSs and PDOs in guiding personalized therapeutic strategies for EC patients, particularly utilizing minimally invasive samples like UA. These preclinical

USC UNIVERSIDADE DE SANTIAGO DE COMPOSTELA

models offer a cost-effective and reliable approach to identify and validate targeted therapies, paving the way for improved treatment outcomes in EC.

USC UNIVERSIDADE DE SANTIAGO DE COMPOSTELA

4.6.1 | Introduction

Preclinical models are essential tools in biomedical research, serving as a crucial bridge between basic science discoveries and clinical applications. These models encompass a diverse array of experimental systems, ranging from simple cell cultures to complex animal models, each offering unique insights into disease mechanisms, therapeutic targets, and treatment efficacy (137,156).

Traditionally, personalised medicine has focused on the generation of *in-vitro* and *in-vivo* models to study the disease with the main limitation being the lack of heterogeneity and more complex physiological characteristics from the human body (137,156). Within the current chapter we will focus on two 3D models that recapitulate, to some extent, more complex physiological features and allow for a more heterogeneous culture, the PDSs and PDOs. Whereas both culture methods allow for the generation of preclinical models that recapitulate the tumour of origin, each model comes with their own limitations and benefits.

PDSs represents a heterogeneous culture of cells in suspension conditioned without ECM, therefore, they cannot precisely recapitulate the tissue of origin but have a 3D structure and are more cost-efficient. In fact, multiple studies have shown the value of PDSs in oncological research for pharmacological studies or the study of the tumour microenvironment (142,150,332), even in EC patients (149,333,334).

PDOs bypass the previously mentioned limitations, since they are a more realistic heterogenous culture that can recapitulate the tissue of origin as they are cultured with conditioned media and ECM. This allows for more realistic drug screening assays to identify the most effective treatment in each patient according to their mutational profile (153,154). In the case of

USC UNIVERSIDADE DE SANTIAGO DE COMPOSTELA

gynaecological malignancies, PDOs have been successfully established from explants and tissue biopsies with a moderate success rate (155–159,335–337).

In this chapter, we focused on the generation of preclinical models, both PDSs and PDOs from tissue and minimally invasive samples of EC patients. The aim of the current chapter was to optimise a pipeline for the generation of this preclinical models that allowed for the identification of the most effective treatment that could be used at the time of patient relapse.

4.6.2 | Material & Methods

4.6.2.1 | Sample collection and processing

Both models (PDSs or PDOs) were generated from either the UA or solid biopsies as previously described (155,157,158). In brief, tissue was mechanically and chemically dissociated by mincing the tissue and incubation with DMEM-F12 (Lonza, Basel, Switzerland) with 1.25 U/mL of Dispase II (Sigma-Aldrich, St. Louis, MO, USA) and 0.4 mg/mL of Collagenase IV (ThermoFisher, Waltham, MA, USA) during 45m-1h at 37 ºC; next, cell chunks were dissociated into a single cell by incubation at 37 ºC with TrypLe (ThermoFisher, Waltham, MA, USA). For the PDSs generation, cells were seeded in suspension in Ultra-Low Attachment (ULA) plates with conditioned media (Table 1). For the PDOs generation, cells were seeded in BME (R&D Systems, Minneapolis, MN, USA) domes with conditioned medium as already described in the literature in a 70:30 ratio (157,158) (Table 2).

USC UNIVERSIDADE DE SANTIAGO DE COMPOSTELA

Table 1: List of compounds, concentration, and supplier for the spheroids culture medium.

Product	Concentration	Supplier	Catalog Number
DMEM/F12	-	Lonza	12-719F
B27 supplement	2%	ThermoFisher	17504044
Antibiotic-antimycotic	1%	ThermoFisher	15240062
EGF	8 nM	Peprotech	AF-100-15
b-FGF	0.1 nM	Peprotech	100-18B
Heparin Sodium	0.07%	Selleckchem	S1346

Table 2: List of compounds, concentration, and supplier for the organoid culture medium.

Product	Concentration	Supplier	Catalog Number
DMEM/F12	-	Lonza	12-719F
h-R-spondin1 (hRSPO1)	7.50 nM	Peprotech	120-38
h-noggin (hNOG)	2.17 nM	Peprotech	120-10C
B27 supplement	2%	ThermoFisher	17504044
N2 supplement	1%	ThermoFisher	17502048
Insulin-transferrin-selenium (ITS)	1%	ThermoFisher	41400045
GlutaMAX™ supplement	1%	ThermoFisher	35050061
Antibiotic-antimycotic	1%	ThermoFisher	15240062
Nicotinamide (NICO)	2 mM	Sigma-Aldrich	N0636
A83-01	0.6 µM	Sigma-Aldrich	SML0788
N-acetyl L-cysteine (NAC)	1.25 mM	Sigma-Aldrich	A7250
EGF	8 nM	Peprotech	AF-100-15
b-FGF	0.1 nM	Peprotech	100-18B
SB202190 (p38i)	10 µM	Sigma-Aldrich	S7067
17-β estradiol	1 nM	Sigma-Aldrich	E8875
Y-27632 *	10 µM	Selleckchem	S1049

USC UNIVERSIDADE DE SANTIAGO DE COMPOSTELA

4.6.2.2 | Preclinical models characterisation

To ensure the origin and reliability of the generated models, they were characterised by IHC and by NGS:

For IHC characterisation, PDS/PDOs were collected, fixed with 4% PFA (Ted Pella, Inc., Redding, CA, USA) for 24 h at 4 °C, and then embedded into 1% agar tissue-teks and stored in 70% ethanol until processed as previously described (338). The IHC characterization was performed at the Pathology Services from the hospital. Sections from FFPE tumour tissue (4 µm thick) were automatically stained in a Dako Omnis immunostainer (Dako-Agilent, Santa Clara, CA, USA).

For the NGS characterization, DNA was isolated using the QIAamp DNA mini kit (Thermo Fisher, Pleasanton, CA) according to the manufacturer's indications. The DNA was sequenced using the Oncomine Comprehensive Panel v3 (Thermo Fisher, Pleasanton, CA) following the previously described protocol in the material and methods section of the thesis.

4.6.2.3 | *In vitro* drug screening assays

To identify potential effective drugs on the basis of the mutational profile obtained from the targeted sequencing analysis, we performed an *in silico* study using the CTD (http://ctdbase.org/) and STITCH (http://stitch.embl.de/) compound databases. These databases contain peer-reviewed information about the effect of drugs on specific genes or signalling pathways, thus indicating the relationship between chemicals and proteins in the human context. In this analysis, we included the mutational status of each identified gene per case. The identified drugs were then discussed with the clinicians and the most relevant ones were used to treat PDS/PDO

USC UNIVERSIDADE DE SANTIAGO DE COMPOSTELA

models, and standard treatment (Carboplatin-Paclitaxel combined therapy) was included as a control.

For drug screening assays, cells from the generated PDS/PDOs were dissociated into single cells and seeded in a p96-well plate with depleted medium, after 48 h medium was supplemented with the specific treatment. Viability was assessed using the alamarBlue™ (AB) approach at 72 h (ThermoFisher, Waltham, MA, United States) according to the manufacturer's indication.

4.6.2.4 | *In vivo* studies

For implantation of the single cell PDSs, mice were housed and maintained under specific-pathogen-free conditions, and procedures were performed in accordance with institutional guidelines and approved by the Use Committee for Animal Care from the Universidad de Santiago de Compostela. Aseptic procedures were followed for all surgeries. Each 8-week-old female SCID-beige mouse (Janvier Labs, Le Genest Saint-Isle, France) was anesthetized with 2% isoflurane/air (Isoflo, Esteve Farma, Carnaxide, Portugal) and kept under anaesthesia for the entire procedure. The area was prepared for sterile surgery by shaving off the fur and scrubbing with a betadine solution and sterile 4×4 gauze. For the orthotopic implantation, a midline ventral incision was made in the skin and abdominal wall. Once open, the uterus was located and 50 µL of cell suspension (cell suspension in the Matrigel matrix (BD Biosciences) in a 1:2 ratio) was injected with a 30 G syringe. After the Matrigel was allowed to solidify, the syringe was removed and the uterus was returned to the abdominal cavity. The wound was closed with Ethicon VICRIL (Johnson & Johnson International, Diegem, Belgium) sutures. Buprenodale (Dechra, Dales Pharmaceuticals, Keighley Road, Skipton, UK) was used for postoperative analgesia.

USC UNIVERSIDADE DE SANTIAGO DE COMPOSTELA

The orthotopic tumours that developed in the uteri were minced into small pieces and placed subcutaneously in the flanks of 8-week-old female SCID-beige mice. For the preclinical studies, once the tumours reached a suitable size of 150–200 mm, they were randomly assigned to one of the four groups and treated with placebo or the specific treatments on the basis of the molecular alterations found in the UAs and a molecular tumour board consensus:

Group 1: Placebo (methylcellulose 0.5%; Sigma; n = 4) administered through oral gavage for 5 days on/2 days off until sacrifice.

Group 2: CarboTaxol (Carboplatin (50 mg/kg) and Paclitaxel (20 mg/kg) combined) therapy administered intraperitoneally once every week for 4 weeks (n=4).

Group 3: BYL719, (50 mg/kg; Achemblock, Burlingame, CA) dissolved in DMSO, administered through oral gavage in methylcellulose 0.5% (Sigma) for 5 days on/2 days off until sacrifice (n=4).

Group 4: RAD001 (10 mg/kg, Achemblock, Burlingame, CA) dissolved in DMSO, administered through oral gavage in methylcellulose 0.5% (Sigma) for 3 days on/4 days off until sacrifice (n=4).

To assess the immunotherapy efficacy, 8 week-old female NOD.Cg-Prkdc^{SCID} Il2rg^{tm1Wjl}/SzJ (NSG) mice (Charles River Laboratories, Wilmington, Massachusetts, United States) were used. Tumours generated on SCID mice where minced and implanted subcutaneously on the flank of 8 NSG mice. Once the tumour reached the appropriate size, 1x10^{7} human PBMC isolated from healthy donors using Ficoll 400 (Thermo Fisher, Pleasanton, CA) were injected intraperitoneally one day prior to the beginning of the experiments. The next day, mice were randomly assigned to one of two groups:

USC UNIVERSIDADE DE SANTIAGO DE COMPOSTELA

Group 1: placebo group (saline injection intraperitoneal weekly) (n=4).

Group 2: Pembrolizumab (KEYTRUDA) (10mg/kg, MedChemExdpress, NJ, USA) injected intraperitoneally weekly (n=4).

After 4 weeks all mice were sacrificed and whole blood was extracted through cardiac puncture and analysed on the BD FACSAria™ (BD Biosciences, Franklin Lakes, New Jersey, US) with PE anti-human CD45 Antibody (BioLegend, San Diego, California, US) to quantify the number of human-PBMCs found in circulation.

All mice were sacrificed after the tumour diameter reached 15 mm, the tumour volume exceeded 1200 mm^3, or the human endpoint criteria were met, according to the guidelines of Directive 2010/63/EU for the protection of animals used for scientific purposes, including assessment of appearance, body function, environment, and behaviour. Tumour size was measured with calipers (Rohs) twice per week. Tumour volume was calculated according to the following formula: $V = (W^2 \times L)/2$ where V is the tumour volume, W is the tumour width, and L is the tumour length.

4.6.3|Results

4.6.3.1|Patient derived spheroids (PDSs)

4.6.3.1.1|Generation and characterization

PDSs were generated from the UA of 10 EC patients of mostly EEC histology. However, only 1 model (10%) was successfully established and propagated through time. The generated model came from an EEC of high grade, FIGO stage IB with over 50% myometrial infiltration but no LVSI. The patient presented mutations in the *MLH1*, *PIK3CA* and *PTEN* genes.

USC UNIVERSIDADE DE SANTIAGO DE COMPOSTELA

To ensure the robustness of the model, we performed an IHQ and NGS characterization. As seen on Figure 1A, the generated PDSs present the same IHC profile, with a loss of expression of the *MLH1* and *PMS2* genes. The only discrepancy found was associated with the expression of progesterone which is higher on the PDSs when compared to the tissue of origin. As for the genetic analyses, the same mutations were found on *MLH1*, *PIK3CA* and *PTEN* in all samples included in the analyses (UA, FFPE and PDSs) (Figure 1B). These results further confirm the origin of the generated PDSs and the reliability of the approach.

4.6.3.1.2 | Drug screening assays

The mutational analysis of the UA was used to screen for specific therapies with bioinformatic tools that were later discussed on a tumour board. Based on those results, we selected the orally bioavailable BYL719 (Alpelisib) and RAD001 (Everolimus) inhibitors as therapeutic alternatives to target the altered *PIK3CA* the pathway. Moreover, the Pembrolizumab (Keytruda) monoclonal antibody was also selected due to the alterations found on the MMR pathway.

The effectiveness of the BYL719 and RAD001 treatments was compared to the standard therapy (Carboplatin-Paclitaxel combined therapy). Significant reduction (Mann Whitney p-value <0.001) on the cell viability was observed at the higher concentrations of the compounds (Figure 1C), obtaining over 50% of cell mortality. On the other hand, the standard treatment did not show that much effectiveness *in vitro*.

USC UNIVERSIDADE DE SANTIAGO DE COMPOSTELA

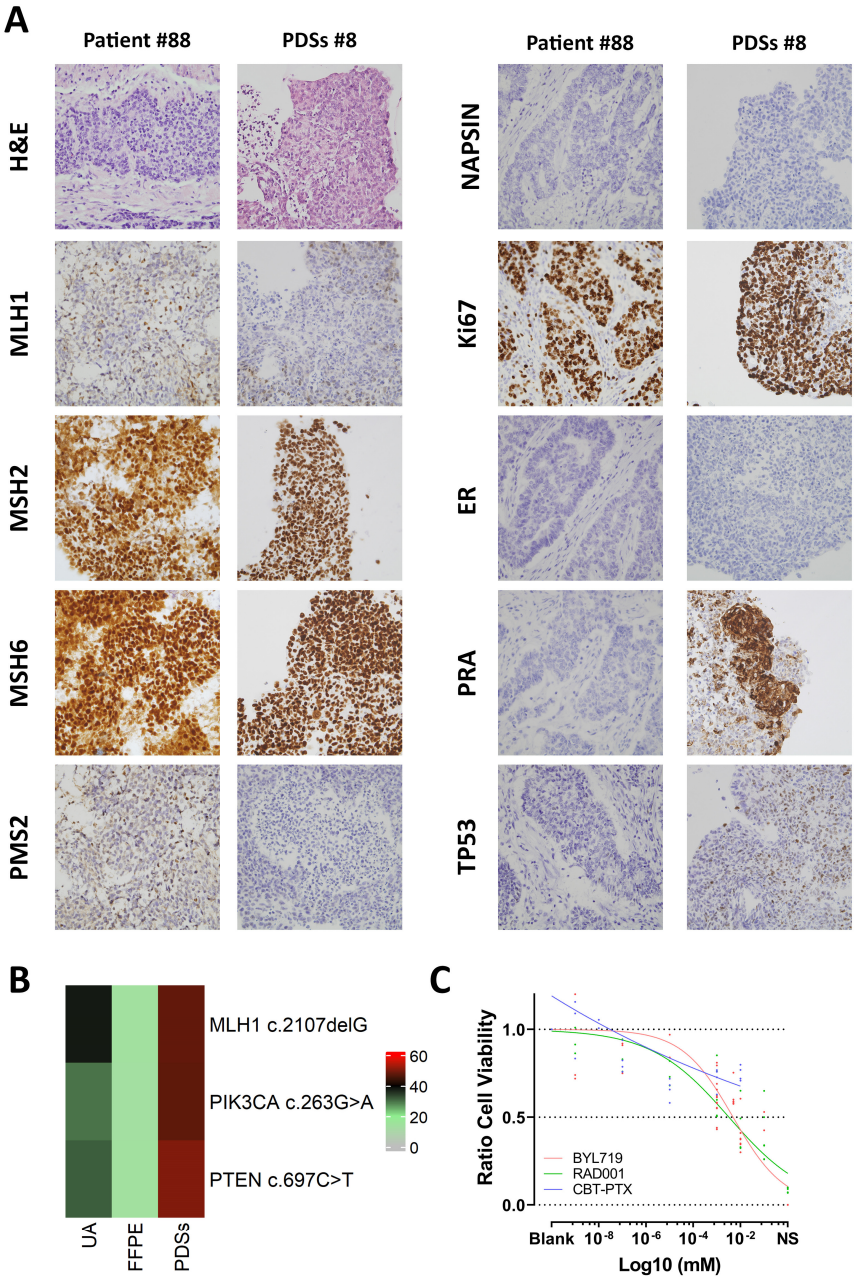


Figure 1: Characterisation and pharmacological studies of the generated PDSs from patient #88 **A.** IHC characterisation of the models using the most relevant

USC UNIVERSIDADE DE SANTIAGO DE COMPOSTELA

molecular markers in the clinical context. **B.** Heatmap of the genomic characterisation of the PDSs and compared to the UA and FFPE. **C.** Dose-response curves for the three different drugs tested in the model: BYL719 (red), RAD001 (green) and CBT-PTX (blue).

To further validate these results and complete a personalised pipeline, we decided to design a pilot preclinical study *in-vivo*. The PDSs were dissociated into single cell and injected into the uteri of an immunodeficient mice. After generation of the orthotopic tumour, subcutaneous passage was conducted in a series of mice (n = 16) for amplification and evaluation of therapy efficacy. Mice were equally distributed in four groups: a placebo control group (n=4), a control group treated with the standard Carboplatin/Paclitaxel therapy (weekly intraperitoneal injection for 4 weeks) (n=4), a group treated with daily oral administration of BYL719 (n=4), and a group treated with oral administration of RAD001 (three times a week) (n=4). The tumour was measured three times a week as specified in the section 4.6.2.4 of the chapter. No toxicity or adverse effects were observed during the timeframe of the study. As seen on Figure 2A, significant reduction in the tumour growth was observed after 14 days of treatment (2 way Anova p-value <0.001) with no differences between the SoC and the targeted therapies.

Moreover, since the patient presented alterations within the MMR pathway we evaluated the efficacy of immunotherapy in this model. Tumours generated on SCID mice where minced and implanted subcutaneously on the flank of 8 NSG mice. Once the tumour reached the appropriate size, $1x10^7$ PBMCs were injected intraperitoneally and randomly assigned to one of two groups: a placebo group (n=4) and the Pembrolizumab arm (n=4) the next day the administration of the monoclonal therapy of Pembrolizumab started. As seen on Figure 2B, the treatment with the monoclonal antibody Pembrolizumab was able to control the tumour growth reaching statistical significance at the end point (2way Anova, p-value <0.001). Moreover, the

USC UNIVERSIDADE DE SANTIAGO DE COMPOSTELA

effectiveness of the therapy was not linked to the percentage of humanised PBMCs on circulation since no statistical significance was found among the groups (Figure 2C).

These results reinforced the clinical value of the PDSs to identify potential therapies targeting specific molecular pathways in EC, and the generation of suitable preclinical models to validate the identified personalized therapies using a minimally invasive sample like the UA.

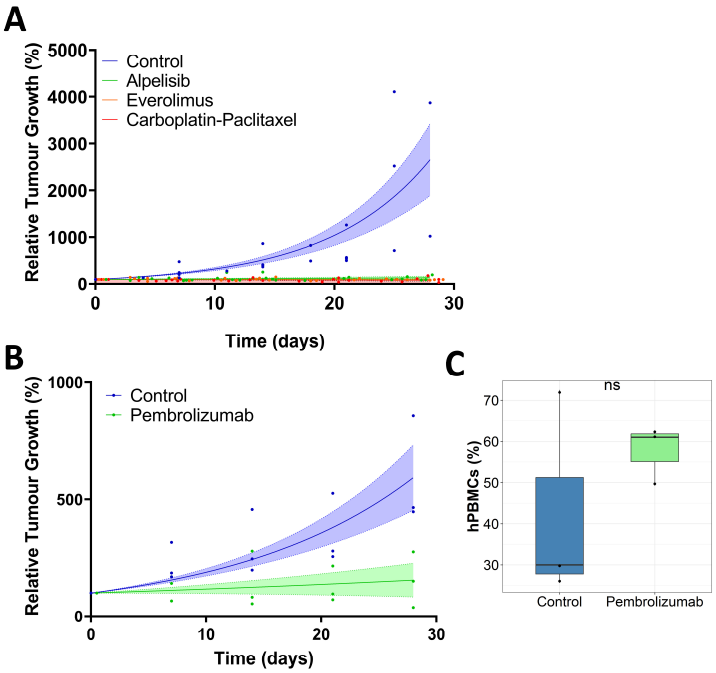


Figure 2: Targeted therapies and immunotherapy are effective in PDXs from EC patients**. A.** PDX tumour growth evolution in response to Carboplatin/Paclitaxel (weekly intraperitoneal injection for 4 weeks, n = 4), BYL719 (daily oral gavage; n = 4), RAD001 (oral gavage 3 days on/2 off, n=4) or control (methyl cellulose daily oral gavage; n = 4) treatment. **B.** PDX tumour growth evolution in response to Pembrolizumab (weekly intraperitoneal injection for 4 weeks, n = 4), or control (saline weekly intraperitoneal

USC UNIVERSIDADE DE SANTIAGO DE COMPOSTELA

injection for 4 weeks; n = 4) treatment. **C)** Boxplot of the distribution of human PBMCs in the PDX treated with Pembrolizumab or placebo.

4.6.3.2 | Patient derived organoids (PDOs)

Although PDSs can recapitulate the tissue of origin, the architecture of the tumour is lost since no ECM is provided for the generation of the models. Therefore, we decided to move into a more complex model, the PDOs. We successfully generated PDOs from a solid tissue biopsy and the UA of patients with EC.

4.6.3.2.1 | PDOs generated from solid biopsies

Results from this chapter have been previously published as a case report in the international journal of molecular sciences (311).

Although the main focus of the present work was the generation of preclinical models from minimally invasive samples one of the patients including for the ctDNA monitoring showed progression disease and although we had no UA-derived cells to generate the PDO model, we were successful in generating PDOs from abdominal metastases of this patient. The patient was diagnosed with a G1 EEC, apparently stage I clinically and by imaging (MRI), although with two nonspecific nodes <10 mm. A total abdominal hysterectomy, bilateral adnexectomy and lymphadenectomy were performed. A definitive pathology report showed mixed areas of a low-grade and a high-grade adenocarcinoma of the endometrium, infiltrating less than 50% of the myometrium, without vascular, perineural or cervical stroma invasion. IHC analysis showed deficient expression of MSH2 and MSH6 proteins, positive expression of the ER receptor (100%) and PR receptors (30%) and negative expression of HER2. Based on the above finding, she was diagnosed with a mixed tumour with low-grade and high-grade areas of an endometrioid adenocarcinoma of the endometrium, FIGO stage IIIC2, pT3bN0M0.

USC UNIVERSIDADE DE SANTIAGO DE COMPOSTELA

However, before starting adjuvant CTP and RTP, a lesion on the anterior side of the vagina, infiltrating the urethra was detected. She received 3 cycles of Carboplatin-Paclitaxel but evaluated as progression by image. Then, she received concomitant Cisplatin and RTP and determined again as clinical and imaging locoregional progression with the appearance of an implant in the abdominal wall, also confirmed by biopsy to be of endometrial carcinoma origin, that was also used for the generation of preclinical models (Figure 3). Then, she received 3 cycles of Pembrolizumab (17). Nevertheless, the patient underwent progressive disease and death in few months.

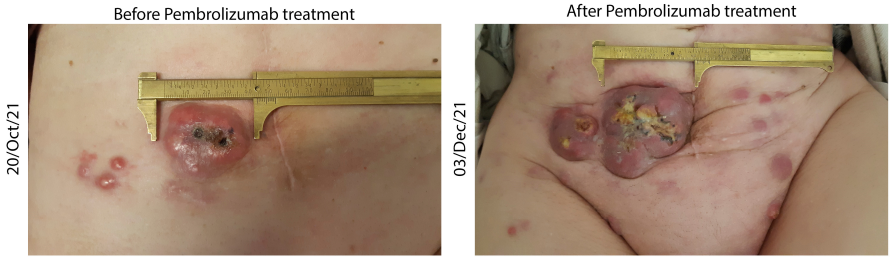


Figure 3: Representative images of the abdominal implants showing the rapid tumour progression during Pembrolizumab treatment.

The patient presented mutations in the following genes: *ARID1A, MSH2, NFE2L2, PIK3R1A, NBN, PTEN* and *TP53* (Figure 4A). Based on the alterations, the patient was classified as MSI-H due to the alterations found in *MSH2* (10); nevertheless, alterations in *TP53* and *NBN* are indicative of a poor prognosis of the patient, since alterations on *NBN* have been linked to cisplatin resistance in some cancer subtypes (339,340) and *TP53* is strongly associated with shorter progression-free survival and overall survival in EC (10,341). Moreover, the mutational landscape was later used to identify potential active therapies based on the found alterations. Due to the ambiguous molecular classification of the patient, the UA was further

USC UNIVERSIDADE DE SANTIAGO DE COMPOSTELA

characterised by analysing the status of 5 mononucleotide repeats (BAT25, BAT26, NR24, NR21 and Mono27) using the ddPCR-MSI panel described in Chapter III. Following this approach, over 20% of VAF was found in all 5 mononucleotide repeats; therefore, the patient was classified as MSI-H.

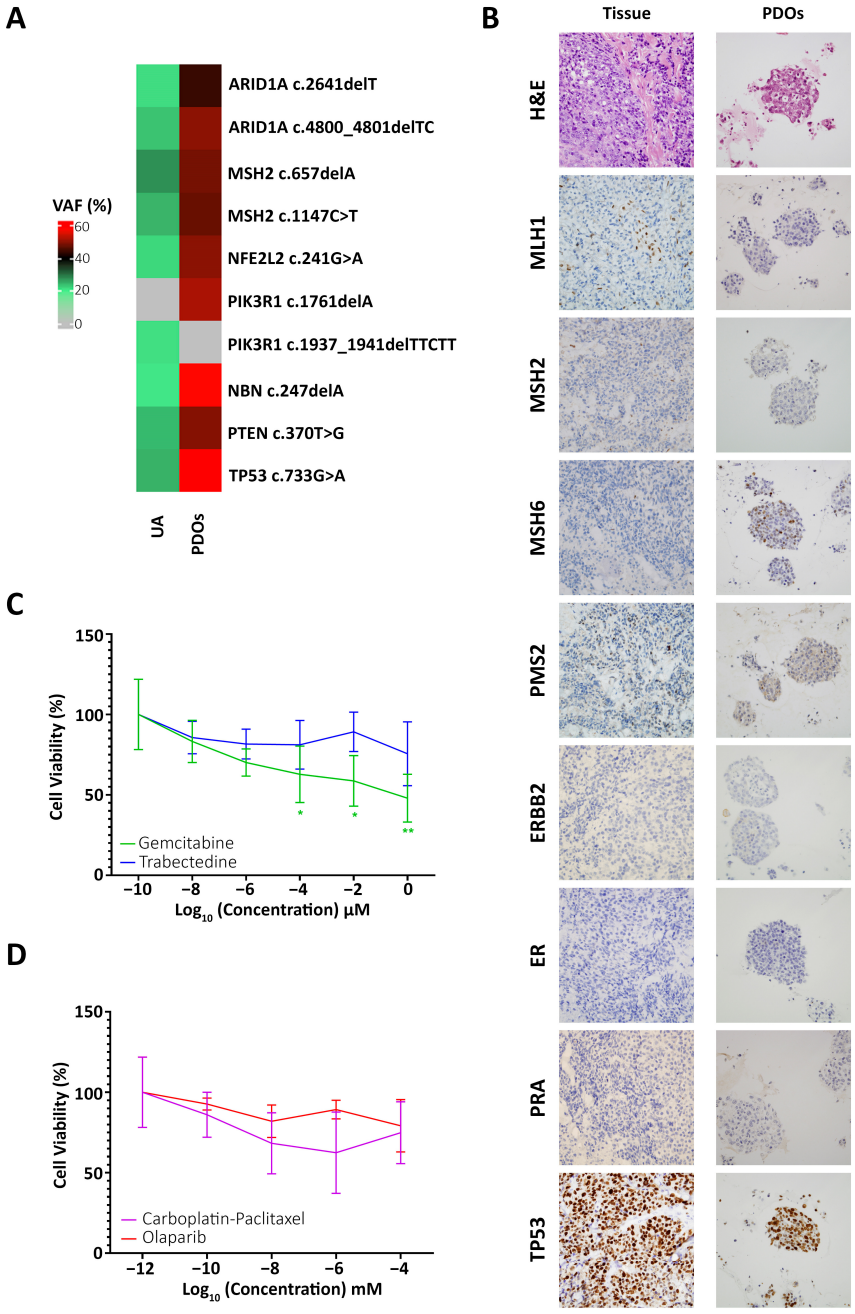
As was previously mentioned, PDOs were generated from the relapse tissue biopsy by mechanically and enzymatic dissociation and cultured with conditioned media that promotes cell proliferation and survival. In order to ensure that the generated PDOs accurately resemble the disease, they were characterised by IHC and NGS analysis and compared to the metastatic lesion. As for the molecular profile, the generated PDOs shared the same IHC expression as the peritoneal metastasis, with aberrant expression in the 4 MMR proteins, negative expression of HER2, ER and PRA negative and aberrant expression of TP53 (Figure 4B). As for the genetic landscape, the mutational profile of the PDOs was compared to the UA. Both samples shared the same mutations and MSI profile, but with higher percentages of alteration in the generated PDOs; only one discrepancy in the *PIK3R1A* gene was found, being the alteration found in a different codon; nevertheless, with the same clinical impact: a non-functional protein (Figure 4A).

After confirming that the PDOs resemble the tissue of origin, they were subjected to alternative therapies, based on the mutational profile the following compounds were selected: Carboplatin-Paclitaxel combined therapy, the standard of care, Olaparib, a Poly (ADP-ribose) polymerase inhibitor involved in DNA repair pathways; Trabectedin, an antineoplastic compound that has shown high efficiency on the treatment of advance ovarian and endometrial carcinomas harbouring ARID1A mutations (227); and Gemcitabine, another potent antineoplastic compound involved in DNA replication.

USC UNIVERSIDADE DE SANTIAGO DE COMPOSTELA

Cell viability was assessed in PDOs using AB after 72 h from the beginning of the assay. A statistically significant reduction in cell viability was found when PDOs were treated with Gemcitabine (two-way ANOVA; p-value <0.01) in contrast to the remaining therapies where no significant reduction in the cell viability was found (Figure 4C-D) just as in the patient, where tumour progression happened while the patient was being subjected to CTP and RTP treatment. These results suggest the efficacy of Gemcitabine as a potential treatment; nevertheless, due to the clinical impairment, it could not be administered to the patient.

USC UNIVERSIDADE DE SANTIAGO DE COMPOSTELA



USC UNIVERSIDADE DE SANTIAGO DE COMPOSTELA

Figure 4: A. Heatmap representation of the mutational profile of the UA and the generated PDOs showing the same mutational profile. **B.** Immunohistochemistry comparison between the tissue biopsy and the generated PDOs reflecting the same molecular profile. **C.** Cell viability analysis after the treatment with Gemcitabine (green) and Trabectedin (blue) showing a significant decrease in cell viability when treated with Gemcitabine. **D.** Cell viability analysis after the treatment with Carboplatin-Paclitaxel combined therapy (purple) and Olaparib (red) showing no significant reduction in cell viability. Two-way ANOVA * p-value < 0.05, ** p-value > 0.01.

Overall, the results obtained with these PDOs, although originated from a solid biopsy, served to validate the general protocols for PDOs generation and characterization and demonstrated the value of these models for identifying alternative therapies to treat the advanced disease, although unfortunately the evolution of the tumour was aggressive.

4.6.3.2.2| PDOs generated from the UA.

A protocol for PDOs generation from UAs was established. These PDOs were generated from UA by mechanically and enzymatic dissociation of the cell fraction and cultured with conditioned media that promotes cell proliferation and survival in a matrix of BME. In 21 out of 31 patients (67.74%) we were able to generate PDOs at passage 0, a summary of the clinical characteristics of the cohort can be found on Table 3. Of those, 10 models grew and amplified after passage [5-20] (47.62%). Nonetheless, 4 of those models were later on identified as being healthy tissue, not of tumour origin. Of the 6 generated tumour-PDOs 5 were of EEC and 1 of NEEC, the efficiency of PDOs generation on NEEC was notably lower (10%) when compared to EEC (95%). In 4 of these PDOs we performed a more complete molecular characterization and were included for further analyses. The clinico-pathological characteristics of the patients from who the PDOs were originated can be found in Table 4.

USC UNIVERSIDADE DE SANTIAGO DE COMPOSTELA

Table 3: Clinico-pathological features of the patients included for PDO generation within brackets is the number of PDOs successfully generated at passage 0.

CLINICAL VARIABLES	*N=31*	CLINICAL VARIABLES	*N=31*
Histology	31	**Lymphovascular Space Infiltration**	31
NEEC	10 (1)	No	29 (20)
EEC	21 (20)	Yes	2 (1)
Tumour Grade	31	**TCGA**	31
Grade 1	14 (16)	POLE	0 (0)
Grade 2	2 (1)	MSI	10 (8)
Grade 3	15 (4)	NSMP	9 (8)
FIGO Stage	31	HCN	12 (5)
I	26 (20)	**Relapse**	31
II	2 (0)	No relapse	26 (20)
III	2 (1)	Relapse	5 (1)
IV	1 (0)	**Exitus**	31
Myometrial Infiltration	31	No	27 (20)
<50%	19 (14)	Yes	4 (1)
>50%	12 (7)		

Table 4: Clinico-pathological features of the fully characterised PDOs.

ID	Histology	Grade	FIGO	Myometrial Infiltration	LVSI	TCGA	Risk	Relapse
BL160	Serous	G3	III	>50%	Yes	MSI	High	Yes
BL212	Endometrioid	G1	IB	>50%	No	NSMP	Intermediate	No
BL213	Endometrioid	G3	IA	<50%	No	NSMP	Intermediate	No
BL230	Endometrioid	G2	IA	<50%	No	MSI	Low	No

The PDOs presented different aspects such as cystic (Figure 5A) or dense morphologies (Figure 5B). In order to ensure that the generated PDOs accurately resemble the disease, they were characterised by IHC and NGS analysis and compared to the primary tumour. Starting with the IHC characterisation, the generated PDOs shared the same IHC expression as the

USC UNIVERSIDADE DE SANTIAGO DE COMPOSTELA

tissue of origin (Figure 5C-D) being able to accurately recapitulate the tissue of origin and maintain, for instance, the gland like structure in the endometrioid low grade cases (cystic organoids) (Figure 5C-D). Importantly, although the PDOs recapitulate the tissue of origin, at early passages we can find a heterogeneous cell culture that includes both healthy tissue (wild type expression of MLH1) and tumour (absence of MLH1 as can be seen in Figure 5C.

As for the genetic landscape, the mutational profile of the PDOs was compared to the UA using the same NGS-based panel (Figure 5E-F). On figure 5E we can see the genetic characterisation of the PDOs from the NEEC patient. The patient presented alterations in *TP53* and *PPP2R1A*, which correlate with the traditional molecular profile of NEEC tumours. On Figure 5F we have an example of the molecular profile of an EEC tumour. Both the UA and the PDOs presented the same mutations, *ARID1A*, *CTNNB1*, *PIK3CA*, *PIK3R1* and *PTEN*. Although in both cases, no discrepancies were observed between the PDOs and the UA, genetic landscape of the EEC PDOs clearly highlights the availability of many more therapeutic options when compared to the NEEC.

After confirming that the PDOs resemble the tissue of origin, they were subjected to alternative therapies, based on the mutational profile and the clinical translation, the following compounds were selected: Carboplatin-Paclitaxel combined therapy, the standard of care; Trabectedin, an antineoplastic compound that has shown high efficiency on the treatment of advance ovarian and endometrial carcinomas harbouring *ARID1A* mutations (227); Gemcitabine-Vinorelbine combined therapy, another potent antineoplastic compound involved in DNA replication; and Doxorubicin, an anthracycline that has shown effectiveness on EC treatment. The

USC UNIVERSIDADE DE SANTIAGO DE COMPOSTELA

concentration of the drugs on the following screenings was selected based on the highest concentration possible on plasma samples (342). Response to treatment was determined based on the response dose curves.

Cell viability was assessed in PDOs using AB after 72 h from the beginning of the assay. The least effective treatments were the CBT-PTX combined therapy (blue line) and the Doxorubicin (green line), whereas the combination of Gemcitabine and Vinorelbine (orange line) or the Trabectedin (red line) showed higher effectiveness to promote the cell death of the PDOs at lower dosage (Figure 6). Moreover, as seen on Figure 6A, the PDOs generated from the NEEC patients, the more aggressive phenotype, showed little reduction on cell viability when being treated by the different treatment regimens, which mirrors the tumour evolution of the patient.

Interestingly, the clinical evolution of patient #160, from how we successfully obtained PDOs, has been previously described on chapter IV. In brief, the patient (69-year-old) was diagnosed patient that with a serous tumour of high grade and classified a FIGO IIIA, she was treated Carboplatin-Paclitaxel combined therapy and radiotherapy after surgery. Nonetheless, early relapse was detected shortly after. After relapse, patient was treated with a more aggressive regimen of chemotherapy, but the patient showed progressive disease with peritoneal affectation and entered PS-ECOG 4 and could no longer be treated. Of note, PDOs obtained from this patient showed no response to Carboplatin-Paclitaxel but they showed a more positive response to Trabectedin or the combination of Vinorelbine-Gemcitabine (Figure 6).

USC UNIVERSIDADE DE SANTIAGO DE COMPOSTELA

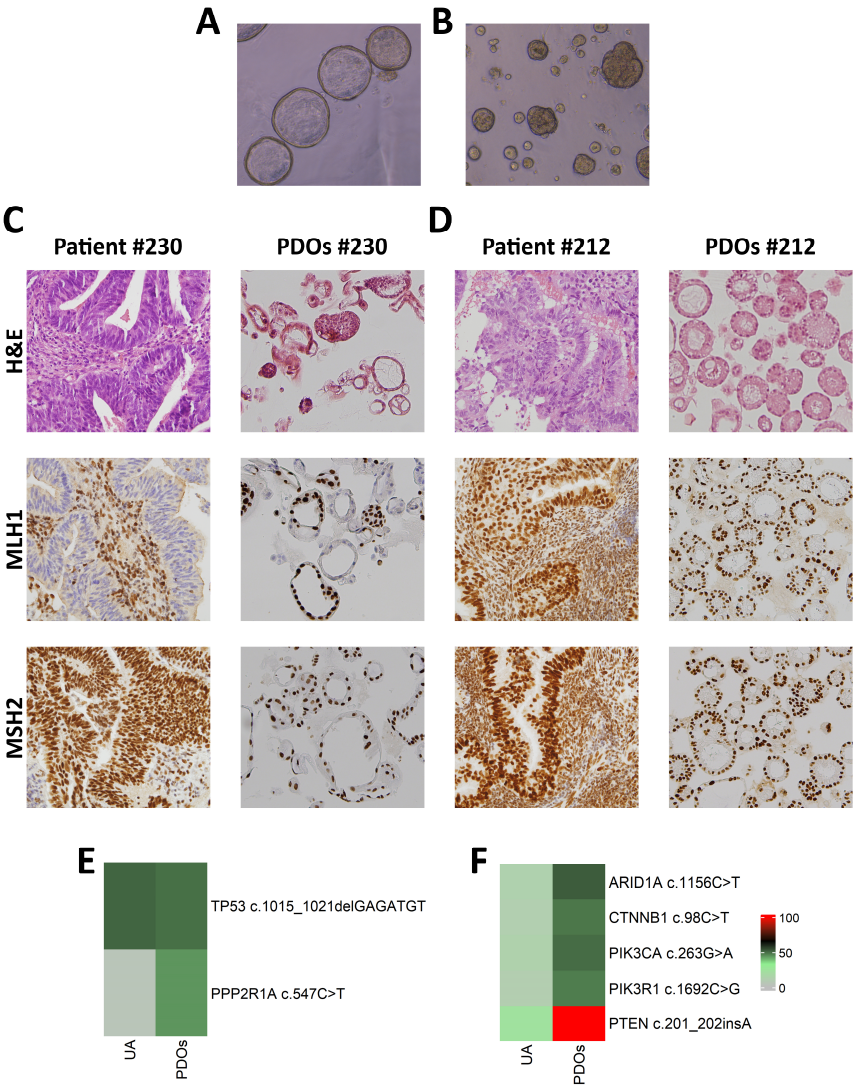


Figure 5: Characterisation of the PDOs. **A-B** Representative images of PDOs with (**A**) cystic or (**B**) dense morphology. **C-D** Example images of the UHC characterisation of the PDO models comparing the expression of different markers with the tissue of origin (**C**) Patient 230, (**D**) Patient 212. **E-F** Genomic characterisation of the PDOs generated form patient (**E**) 160 and (**F**) 212. Images at 40x.

USC UNIVERSIDADE DE SANTIAGO DE COMPOSTELA

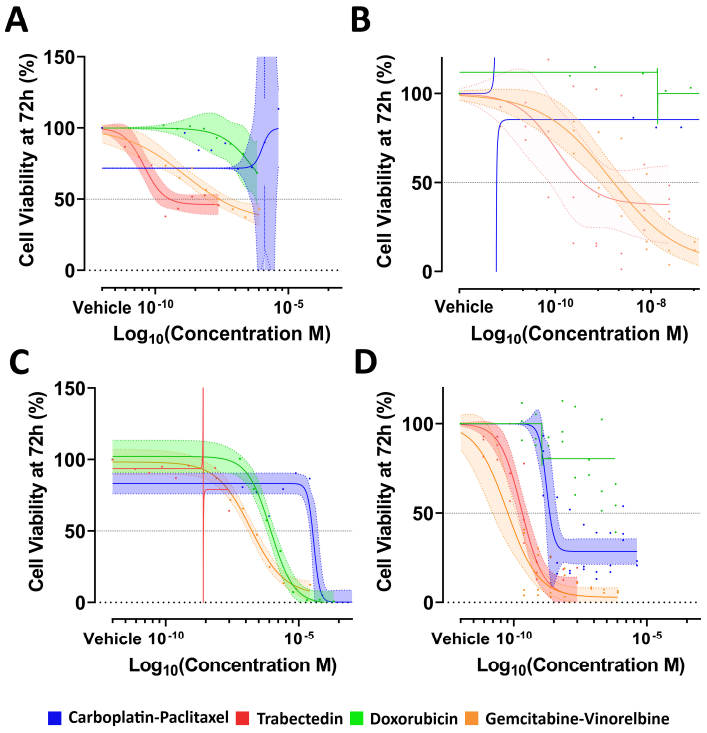


Figure 6: Dose-response curves of the different PDOs to the different chemotherapy regiments: Carboplatin-Paclitaxel (blue line), Trabectedin (red line) Doxorubicin (green line) and Gemcitabine-Vinorelbine (orange line) of the generated PDOs. **A.** PDOs #160 **B.** PDOs #212 **C.** PDOs BL230 and **D.** PDOs BL213.

These results reinforced the clinical value of the PDOs to identify potential therapies targeting specific molecular pathways in EC, and the generation of suitable preclinical models to validate the identified personalized therapies using a minimally invasive sample like the UA is feasible. Moreover, as seen on patient 160, the PDOs mimic the response found on the tumour of the patients.

USC UNIVERSIDADE DE SANTIAGO DE COMPOSTELA

4.6.4 | Discussion

Treatment strategies for EC are evolving with the development of molecular analysis and precision-based approaches. Preclinical models have arisen as a key element in personalised medicine, as they are a heterogeneous sample that recapitulates the tissue of origin and can be used to perform high-throughput pharmacological studies in order to identify alternative therapeutic options (154,336). In the case of EC, they have been successfully established from tumour biopsies and tissue explants (155,156,159,337). Results from this chapter showed the value of PDS and PDOs generation from EC solid and fluid samples to obtain reliable preclinical models that mimic the molecular landscape and the response to treatment showed by the tumours of origin therefore, that have great potential to be used to guide therapy selection.

First, we stablished a simpler model in the form of PDSs and, although the success rate was low (19%) the generated model could recapitulate most of the tumour characteristics although the models did not recapitulate the architecture of the tumour. The low success rate of this models could be due to the optimisation process that was undergoing at early stages of this line of research, which undoubtedly affected the success rate. Nonetheless, despite said limitations, the model accurately reflected clinico-pathological key features of the tumour. PDSs treated with specific inhibitors of the PIK/AKT/mTOR pathway exhibited better response rates *in vitro*. The higher response rate was not observed in the *in-vivo* model, where both the standard chemotherapy and the targeted therapies exhibited similar response rates. The discrepancies between *in vitro* an *in vivo* could be due to the different drug metabolism and drug distribution of the compound or other physiological conditions (343)(151). Moreover, we were able to use the PDS to

USC UNIVERSIDADE DE SANTIAGO DE COMPOSTELA

generate humanised PDX to screen for the effectiveness of another key therapeutic approach, immunotherapy. The PDX treated with Pembrolizumab showed an excellent tumour volume control when compared to its respective control group. Therefore, although PDSs cannot recapitulate the full characteristics of the tumour, they represent a valuable preclinical model since they are a cost-effective alternative to the PDOs that can accurately mimicked the tumour response *in vivo*.

Next, we established a protocol for PDOs generation as the most representative 3D culture model for the disease characterization and performing drug screening. Our main goal was the generation of PDOs from UAs obtained at surgery. Although a higher success rate was observed with the UAs derived PDOs (nearly 70%) and around 40% of those could be maintained through time. The higher success rate could be due to the changes on the cell culture media that provided further nourishment for the cells and promoted the generation of the PDOs. Nonetheless, the stablished PDOs are stable over time and retain the morphological features of the primary tumour through cryopreservation and passages, which ensures the utility of PDOs for therapy selection or drug discovery in EC. Interestingly, patients with phenotypic features associated with better clinical outcome presented higher success rate for establishment of the culture. Patients of EEC histology, lower grades, early FIGO stages were easier to established at passage 0 when compared to the more aggressive phenotypes. However, when it came down to the passage of the cultures, most of the PDOs were problematic to passage and most died off within the first two passages after seeding. Which in short, highlights the need for further optimisation and improvements for the proper establishment of the cultures. Although using a different approach, Berg et al have reported that the success rate for generation of PDOs from biopsies of SC is lower than EEC, further

USC UNIVERSIDADE DE SANTIAGO DE COMPOSTELA

highlighting the need of optimisation to cover the most aggressive subtype of EC (159).

Another important caveat of our approach that needs to be taken into consideration is the nature of the UA, although the UA is a minimally invasive sample that captures the intratumor heterogeneity, it also contains cells from healthy endometrium. Within our study, in 40% of the models that were successfully amplified through time, downstream characterisation revealed that the models were of healthy origin. To circumvent this limitation, more specific conditioned media that promote the growth of tumoral tissue, such as Nutlin-3a to select for TP53 mutated tumours (344), could help reduce the number of healthy PDOs generated from the UA. Regarding the intratumor heterogeneity, it would be interesting to evaluate how well the PDOs recapitulate this heterogeneity. Further studies delving into the genetic, epigenetic and transcriptomic profile of the PDOs compared to the UA and different areas of the primary tumour (and metastatic when available) would be of great value to tackle this question.

Based on the results from this Chapter, we have seen that PDOs recapitulate the molecular and genomic landscape of the primary tumour. The PDOs accurately reflect the genomic heterogeneity found in the UA with an enriched fraction on the mutations VAF. The genomic characterisation of the PDOs could help to identify minority clones within the tumour that could help guide the clinicians towards a more precise treatment regimen. Although within our work we mainly focus on chemotherapy regimens due to the easy translation into the clinic, other groups have shown that treatment tailored to the genomic profile of the PDOs is feasible (158,159). Moreover, Arias et al have shown that PDOs from another gynaecological malignancy (serous carcinomas) could be used to explore the difference mechanism behind

USC UNIVERSIDADE DE SANTIAGO DE COMPOSTELA

platinum resistance; by exposing the PDOs to different concentrations of the compound they generated resistant PDOs that were subjected to transcriptomic studies (345). But the clinical interest behind PDOs does not just reside behind the identification of the most effective treatment. Berg et al have shown that, by analysing the gene-expression of the organoids using a RNA-seq approach, the molecular signature obtained could be used to predict survival in EC patients (159). Which, in combination with the complete characterisation of the PDOs (WES, RNA-seq and IHC) further validates the clinical relevance and utility of the PDOs.

Although this work is pioneer on using the UA to generate preclinical models for EC, we only began to scratch the surface of what could be done and more optimisation is required until this could be properly implemented into the clinic. The most pressing manners being the problems behind the generation of NEEC PDOs and the lack of tumour microenvironment within the pharmacological studies that could yield biased results on the efficacy of the drugs.

4.6.5 | Conclusions

In conclusion, preclinical models are powerful asset in personalised medicine with great potential in EC. Our study is pioneer in using the UA as a reliable sample for the generation of preclinical models (PDSs and PDOs) that recapitulate the tissue of origin and mimic the response of the tumour. These models have great value to capture the ITH and serve as preclinical tool to select alternative therapies and overcome the therapy resistance.

USC UNIVERSIDADE DE SANTIAGO DE COMPOSTELA

5 | OVERALL DISCUSSION

USC
UNIVERSIDADE
DE SANTIAGO
DE COMPOSTELA

OVERALL DISCUSSION

Over the past years, precision medicine has been the gold standard in the fight against cancer; running away from the 'one size fits all' mentality and moving forward into a tailored medicine approach that could improve diagnoses or therapy selection, which in turn would translate into higher survival rates. Precision medicine is possible thanks to the combination of: genomic studies, to elucidate the genomic landscape that could help predict the risk of recurrence or treatment response; high throughput imaging analyses to characterise diseases at a molecular level; targeted therapies for specific molecular pathways or genetic mutations implicated in a disease, therefore maximizing efficacy and reducing adverse effects; or for instance, using computational predictive models that generate predictive signatures for disease progression or response to therapy, among others (346,347).

Precision medicine has the potential to revolutionise healthcare by offering more effective and personalised treatments, improving patient outcomes, and reducing healthcare costs. In line with this premise, in the present doctoral dissertation we have explored and described the value of liquid biopsy-based strategies that allowed for a minimally invasive genomic characterization of the disease as well as the identification of circulating biomarkers that further improved the stratification of EC patients and the disease monitoring. Moreover, we also explored the feasibility and accuracy of primary 3D cultures generation from UAs to test the activity of traditional and novel therapies.

Within the current thesis we have focused on patients with EC and evaluated how, through liquid biopsy analyses, we could improve patient management and care. EC, although usually associated with good clinical outcomes, has a non-neglectable 20% of patients that undergo tumour

USC UNIVERSIDADE DE SANTIAGO DE COMPOSTELA

relapse after the curative surgery. This subset of patients have extremely poor prognosis and usually do not respond to traditional treatments (3,9) with the 5-year survival expectancy dropping to a mere 10-30% (236,237). Overall, we included 202 patients from different Spanish Hospitals to evaluate the clinical applicability of different liquid biopsy analyses with the aim to: a) deeply characterise the disease through the UA genetic profiling (**Chapter I-III**); b) improve patient stratification (**Chapter IV-V**); c) analyse tumour kinetics using circulating biomarkers (**Chapter I, III and IV**); and d) generate preclinical models to assess therapy efficiency (**Chapter VI**).

Within the first chapters we provided a comprehensive overview of the value of the UA as a minimally invasive sample in gynaecological malignancies, specifically in the context of EC. In **Chapter I**, we performed a comprehensive characterization of the genomic landscape of 202 EC patients and identified potential key genes linked to progression disease that could be used as alternative therapeutic targets.

In line with previous studies we described that patients harbouring *TP53* mutations presented a significantly shorter DFS and DSS (8,10,15), and that patients with *POLE* mutations showed an extremely favourable prognosis (8,10,15). These results further validate the robustness of the UA as a reliable sample to assess the genetic landscape of EC patients. Moreover, we were able to identify patients with ITH. Over 30% of patients (66 out of 202) presented genes with multi hit alterations. ITH is one of the main obstacles that personalised medicine wants to tackle, since the heterogeneity within the tumour could lead to variations in treatment responses, making it difficult to develop targeted therapies that effectively eradicate all cancer cells (211). Therefore, being able to identify patients with ITH through the sequencing of the UA would be of relevant value to improve our understanding about the

USC UNIVERSIDADE DE SANTIAGO DE COMPOSTELA

clinical and the therapeutic impact of the molecular heterogeneity, especially in tumours with favourable prognostic which show an aggressive evolution and poor therapy responses.

To this regard it is also important to highlight that genomic alterations represent and guide only partially the tumour biology. Actually, epigenetic deregulation is one of the main drivers of oncogenesis. In EC, epigenetic alterations are closely related to patient prognosis (238). Therefore, in **Chapter II**, we characterised the methylome of 57 EC patients through the analysis of UAs. With this approach we identified a differential methylome profile between EEC and NEEC. The exploratory analyses of the methylome in the UA proved to be feasible and allowed for the identification of potential novel pathways related in EC relapse, the calcium signalling pathway and the GABAergic pathway.

These pathways have been previously described in other tumour types for their implication in cancer progression as being promoters of cell proliferation, invasion, dissemination and immune system evasion (248,249,264,251–256,261,262). Nonetheless, there are no therapeutic options available that are approved within the clinical context to target these pathways. It is important to highlight, that results from this chapter have been the basis for opening new lines of work to elucidate the role of these pathway in EC development and aggressiveness and as real treatment targets.

These potential therapeutic targets would help to complement the therapeutic strategies currently available to treat EC which are essentially, chemotherapy, hormone blockade and Immunotherapy. This last treatment has become a good option to treat solid tumours with overexpression of PD-L1, aberrant expression of one of the components of the MMR or if they are

USC UNIVERSIDADE DE SANTIAGO DE COMPOSTELA

MSI (36) in the primary tumour. Usually, these biomarkers are determined through IHC analyses of the primary tumour. However, MSI status can be interrogated using plasma cfDNA though NGS-based strategies such as the FoundationOne Liquid CDx, which was approved for different solid tumours (77,78). Nonetheless, NGS-based approaches require high cfDNA input, and complex bioinformatic analyses make the clinical applicability of WGS or WES strategies limited on cfDNA clinical studies. In **Chapter III**, we technically validated a ddPCR-based panel that interrogates the status of 5 MSI markers in minimally invasive samples (UAs) and evaluated its concordance and accuracy when compared to the SoC, IHC characterization of the MMR proteins in FFPE. We found a high concordance (96.67%) between the analysis of MSI markers in UAs and the SoC regardless of the clinico-pathological features. Thus, demonstrating a fast, accurate and cheaper alternative to NGS-based strategies that could be easily implemented into the clinic that tackles the mosaicism found on patients and bypass limitations of the IHC. Both techniques are complementary of each other and should be looked as a whole.

Moreover, we also evaluated the performance of the assay on cfDNA samples. A good overall concordance (70.27%) was obtained when comparing the performance of the ddPCR assay on UAs and cfDNA in high-risk tumours. However, in this case, the concordance was lower, which is expected taking into account the limitations related to the ctDNA content. Low shedder tumours or tumour localised in areas, such as the brain, would inherently have lower levels of ctDNA in circulation (348) and, regardless of the low LoD offered by the ddPCR, could yield false negative results. Therefore, analyses of the cfDNA to assess the MSI status should be considered within the context of high-risk patients or advanced disease; in the remaining cases, the UA would be preferable. This test is highly relevant in the context of

USC UNIVERSIDADE DE SANTIAGO DE COMPOSTELA

monitorisation, since it allows for the follow up of the disease without the need of big panels or the need for a complex knowledge of the mutational landscape of each patient. Importantly, this approach is not limited to EC tumours, but could also be easily implemented in other tumour types such as colorectal cancer where MSI also plays a huge role. Moreover, following that premise, this study has allowed the accreditation of the technique with the normative references of ISO and is now part of the liquid biopsy portfolio with diagnostic purposes available in our hospital.

Overall, results from these first chapters highlight the utility of the UA to perform multiple types of molecular studies. The characterization of the UA could open new avenues for the management of the disease, by allowing for a deep characterization prior to the surgical resection of the tumour. For instance, this could translate into a more effective planification of the surgery disease; data from the genomic characterization could allow for the escalation or de-escalation based on the presence of *POLE* or *TP53* alterations. Moreover, it could help in the identification of neoadjuvant targeted therapies based on the genomic landscape of the patients.

On the other hand, liquid biopsy should play a key role for improving the risk stratification in EC. Accurate risk stratification remains an unsolved question in EC, since about 20% of patients classified post-surgery as low risk face recurrence disease. Although included in the risk classification system, molecularly guided management of EC lags behind most other cancers. Besides, the development of new clinical tools that combine clinical-pathologic, radiologic, and molecular characteristics to accurately predict the risk of recurrence is essential to better treat, and thus improve, the survival of these patients. In **Chapters IV-V** we combined different circulating

USC UNIVERSIDADE DE SANTIAGO DE COMPOSTELA

biomarkers into a prognostic model to improve the risk stratification as well as patient care.

Previous studies have shown that the presence of ctDNA is linked to shorter DFS in various tumour types (349–352). In **Chapter IV** we evaluated the pre-surgical levels of cfDNA and ctDNA in a cohort of 198 patients through a fluorometric quantification of the cfDNA and a ddPCR-based approach for the ctDNA. Our results showed that the combination of these two circulating biomarkers had great independent prognostic value over traditionally used clinico-pathological features. Although this group only represents 10% of the global cohort analysed in our study, most of them developed an early relapse within the first year after surgery. Moreover, this approach allowed for the identification of patients with initially good clinical outcome as of poor prognosis. Therefore, our approach not only allows for the identification of the subset of patients with the worst clinical outcome but also allows to identify patients with high risk of relapse regardless of their clinical characteristics.

CfDNA levels are influenced by multiple factors such as age, metabolic activity, immune processes and disease, such as cancer (314,353). These high cfDNA levels in high-risk tumours can be partially explained by a high ctDNA release but also other systemic mechanisms which are more intensely regulated in advanced stages of the disease (60). Although in our study we did not find correlation between cfDNA and the pre-surgery levels of different blood cells population, more specific analyses of the specific origin of the cfDNA should be conducted to rule out the impact of this population on the total cfDNA content. We hypothesize that high cfDNA levels are indicating local or systemic changes associated with the tumour aggressiveness, non-directly linked to the ctDNA release, but impacting on the disease biology,

USC UNIVERSIDADE DE SANTIAGO DE COMPOSTELA

such as the own tumour microenvironment, the immune system or changes in the metabolic activity of nearby cells.

In addition to the cfDNA and the ctDNA, in **Chapter V** we quantified the presence of CTCs in circulation in a cohort of 90 patients through an epitope dependant technology, the CellSearch. We found a low percentage of patients with detectable levels of CTCs (21,7%) linked to phenotypic markers of aggressiveness Interestingly, not only with clinical variables, but also experimental variables studied on other chapters, such as cfDNA and ctDNA. Patients with CTCs tend to have higher levels of cfDNA and detectable levels of ctDNA, which is indicative of a subtype of EC with a more secretive phenotype. Moreover, significantly shorter DFS and DSS have been found on those patients with detectable CTCs, indicating a potential use of the CTC enumeration to complement the current risk tools. In line with our results, other groups have reported that, using the CellSearch system, the presence and counts of CTCs could help to predict the clinical outcome of these patients (115). Nonetheless, it is important to highlight that the quantification of CTCs using the CellSearch system only allows for the enrichment of epithelial cells with relative high expression of the EpCAM molecule in the cell-membrane, and CTCs are in a dynamic state, transitioning between epithelial and mesenchymal phenotypes (328,329). More complete studies that apply other technologies, such as non-epitope dependant, could be of interest to assess the presence of mesenchymal CTCs in the bloodstream of EC patients.

Overall, in **Chapter IV** and **Chapter V** we have seen the clinical utility of different circulating biomarkers with great potential to identify patients of poor prognosis at surgery The implementation of circulating biomarkers into the clinic is already a reality for other tumours where, for instance, the

USC UNIVERSIDADE DE SANTIAGO DE COMPOSTELA

analyses of cfDNA can help guide treatment selection for CRC patients (349,350). The results of the thesis are relevant to advance in the real application of these circulating biomarkers also in endometrial tumours. A potential model that could be implemented would start with the characterisation of the cfDNA prior to surgery, by a simple quantification of the levels of the cfDNA we would have an initial idea of the prognosis of the patient. Patients with low levels could be followed using the traditional risk stratification, however, patients with high levels of cfDNA should be more closely monitored. At the time of surgical resection, the UA would be collected and sequenced (to assess the mutational landscape) and another blood sample could be collected for: i) the quantification of CTCs, as an additional prognostic biomarker and, ii) ctDNA assessment based on the mutations of the patient. If the patient has detectable levels of ctDNA and/or detected CTCs a closer follow up could be performed every 3-5 months. Patients with negative levels of ctDNA or CTCs could be followed using the traditional risk stratification.

Another milestone in the EC management is the lack of non-invasive and accurate diagnostic methods. There are no screening programmes and very often the diagnostic process starts when symptoms, such as abnormal uterine bleeding, occur (43). Therefore, non-invasive and accurate methods for EC detection and disease monitoring, especially in high-risk population, are needed. In the present thesis we evaluated the clinical utility of cfDNA and ctDNA dynamics using two distinct technologies: an NGS-based approach (**Chapter I**) and a ddPCR-based approach (**Chapter III** and **Chapter IV**). Through the NGS-based approach of **Chapter I** we evaluated the clinical utility of a small, targeted NGS panel in an exploratory cohort of 18 patients of mainly advanced disease. Although alterations were detected in 68.75% of the samples, our cohort was notably enriched with patients exhibiting highly

USC UNIVERSIDADE DE SANTIAGO DE COMPOSTELA

aggressive phenotypes who have experienced relapse. Therefore, any conclusions drawn from this study should be contextualized within the predominantly advanced-stage disease setting. Moreover, a large number of alterations found on the cfDNA with this approach were not found on the UA and could potentially be due to clonal haematopoiesis, such as alterations in *GNAS* and this limitation should also be taken into consideration. Nonetheless, in line with previous studies, this approach allowed for the identification of patient-specific genetic information and to monitor clonal evolution over time without sequencing the primary tumour (71,228,229).

On the other hand, on **Chapter III** and **Chapter IV** we utilised a personalised ddPCR-based approach according to the specific alterations found on the UAs (previously identified on **Chapter I** and **Chapter III**). The kinetics of the ctDNA levels mimicked the tumour dynamics. Overall, we explored the value of longitudinal analyses of cfDNA and ctDNA in 130 patients. The results from this thesis demonstrate that ctDNA monitoring represents a valuable approach to detect the presence of MRD, anticipate the disease relapse and evaluate the response to the therapy in advanced EC stages as the present study and other works have evidenced in CRC, breast and even EC (91,228,229). Importantly, post-surgery ctDNA was only detected in cases with MRD or recurrent disease. In some cases, the ctDNA was detected months before the clinical/radiological confirmation. This occurred mainly in patients with detectable ctDNA levels at surgery. Early detection of the disease relapse provides an opportunity to start the treatment of advanced disease earlier and even guide therapy selection according to the specific subclones identified thanks to the genetic characterization of UAs at surgery and the ctDNA at the disease relapse.

USC UNIVERSIDADE DE SANTIAGO DE COMPOSTELA

It is important to highlight that our study represents the largest cohort of EC patients monitored with ctDNA so far, and robustly demonstrates the benefit of this strategy to make a more personalised and precise disease follow-up. Nonetheless, the path to personalised medicine is still unclear. Should sensitivity be prioritised over specificity or the other way around? Both strategies, the NGS-based approach and the ddPCR-based approach provide useful information and have their own limitations. An appealing option with potential clinical utility would be to analyse the kinetics of the disease using a personalised ddPCR-based approach combined with an NGS-based strategy at the time of relapse to assess the arise of potential novel alterations that could help guide therapeutic options.

Last, but not least, we wanted to help clinicians on the identification of the most effective treatments for advanced EC patients. In **Chapter VI** we explored the feasibility and clinical utility of preclinical models generated from minimally invasive samples. Within this Chapter we have optimised a novel pipeline that allows for the processing of the UA to generate two different preclinical models, PDSs and PDOs. In line with previously published works, results from these chapters show that both approaches could be used to generate robust models that recapitulate the tissue of origin (155,157,159,337). Moreover, pharmacological studies showed that the models recapitulate the response found on the primary tumour and allowed for the identification of more effective therapies. Sadly, due to the rapid progression of the disease, patients could not benefit from it. Nonetheless, these models could be used to obtain information on a large number of compounds prior to relapse, which is a huge advantage to the traditional murine models. Moreover, these models offer the possibility of more complex drug screening for instance, cell therapy with TCR or CAR-T could be easily tested as previously demonstrated (354).

USC UNIVERSIDADE DE SANTIAGO DE COMPOSTELA

Although we had low success rate on the generation on some of the models, mainly due to the first step of the protocol optimisation and the difficulty behind the generation of preclinical models from NEEC subtypes, the results obtained prove the potential clinical utility of preclinical models to improve the management of EC. PDSs/PDOs could be generated at the time of surgical resection, characterised, biobanked and thawed at the time of relapse to screen for potential therapies that could be used on the second line of treatment. Indeed, discrepancies between the primary tumour and the metastases are expected and, ideally, PDSs/PDOs would be generated from the metastatic tissue. However, tissue availability is not always feasible, and this could be a good alternative to offer a more personalised option to those patients.

Furthermore, these models will be a valuable tool to study and better understand the molecular mechanism associated with the resistance to different drugs, the mechanism behind relapse and to screen for novel therapeutic avenues.

To sum up, within the current thesis we explored the clinical utility of different liquid biopsy techniques in the context of localised and advanced EC disease with the objective to improve patient management. We have described the UA as a valuable sample that recapitulates the tissue of origin and captures the ITH, not only at a genetic level, but also the methylome and the MSI status is captured. Moreover, we have explored the clinical utility of three different circulating biomarkers: cfDNA, ctDNA and CTCs that have helped identify patients with worse clinical outcome. Furthermore, the kinetics of cfDNA and ctDNA have allowed for the identification of MRD, anticipate the disease relapse and evaluate the response to therapy. Lastly, we have generated reliable preclinical models from UAs that recapitulate the

USC UNIVERSIDADE DE SANTIAGO DE COMPOSTELA

tissue of origin and under treatment, mirrored the response found on patients.

It is extremely important to highlight that, this personalised pipeline based on liquid biopsy, has already been implemented in our hospital to complement the standard tools employed for the tumour characterization, the risk stratification and the disease follow-up, representing a real and useful tool in the clinical practice of our hospital that we would like to translate into a more generalized use of liquid biopsy in other hospitals. The integration of our liquid-biopsy-based pipeline into the clinic is feasible and in combination with tumour boards would translate into a much more efficient management of EC patients through personalised medicine.

USC UNIVERSIDADE DE SANTIAGO DE COMPOSTELA

6|CONCLUSIONS

USC
UNIVERSIDADE
DE SANTIAGO
DE COMPOSTELA

CONCLUSIONS

From the present doctoral dissertation, the following conclusions have been extracted:

From the present doctoral dissertation, the following conclusions have been extracted:

1. The Uterine Aspirate (UA) is a minimally invasive and reliable sample that can be used for the genomic and epigenomic characterization of Endometrial Cancer (EC), capturing the intra tumour molecular heterogeneity.
2. The use of a targeted NGS-based approach on UAs yields comparable results to WES studies performed in solid biopsies, representing a good tool for the molecular classification of EC and to predict the tumour prognosis.
3. The use of a targeted NGS/based approach on cfDNA samples allows for the identification of novel mutations arisen through tumour evolution that could be used as alternative therapeutic targets in patients with advanced EC.
4. The UA from serous tumours show a specific methylation signature, with predominantly hypomethylated CpGs compared to endometrioid tumours. This signature is associated with the promotion of neuroactive ligand-receptor interaction, cAMP and calcium signalling pathways.
5. The MSI testing in minimally invasive samples (UA and cfDNA) from EC patients by ddPCR represents a valuable clinical tool, that provides additional information to identify the unstable tumours than SoC and monitor the evolution of the disease.
6. The detection of high levels of cfDNA and detectable levels of ctDNA at surgery serves to identify tumours with a more aggressive phenotype,

USC UNIVERSIDADE DE SANTIAGO DE COMPOSTELA

associated with significantly shorter DFS and DSS times and disease relapse within the first two years after surgical resection. This prognostic value is independent and add value to the current risk stratification tools.

7. Longitudinal analyses of ctDNA mirror tumour kinetics and enable the identification of early relapses prior to any clinical or radiologic evidence.
8. The presence of CTCs at surgery in localized EC is linked to an aggressive disease in terms of poor DFS and DSS, although its prognostic value is more limited than the combined analysis of cfDNA/ctDNA.
9. Preclinical models generated from minimally invasive biopsies are a powerful asset in personalised medicine for EC. PDSs and PDOs derived from UA recapitulate the histologic and genetic profile of the tissue of origin, mimicking the response of the tumour to different pharmacological regimens.
10. Combined application of UAs and blood biomarkers characterization, together with personalized therapy testing in PDOs/PDSs generated from UAs, represents a comprehensive and valuable strategy to anticipate the disease evolution and guide therapy selection in patients with endometrial tumours.

USC UNIVERSIDADE DE SANTIAGO DE COMPOSTELA

7 | BIBLIOGRAPHY

USC
UNIVERSIDADE
DE SANTIAGO
DE COMPOSTELA

BIBLIOGRAPHY

1. Santucci C, Mignozzi S, Malvezzi M, Boffetta P, Collatuzzo G, Levi F, et al. European cancer mortality predictions for the year 2024 with focus on colorectal cancer. Ann Oncol. 2024;35(3):308–16.

2. Purdie DM, Green AC. Epidemiology of endometrial cancer. Best Pract Res Clin Obstet Gynaecol. 2001;15(3):341–54.

3. Amant F, Moerman P, Neven P, Timmerman D, Van Limbergen E, Vergote I. Endometrial cancer. Lancet. 2005;366(9484):491–505.

4. Siegel RL, Miller KD, Wagle NS, Jemal A. Cancer statistics, 2023. CA Cancer J Clin. 2023;73(1):17–48.

5. Raglan O, Kalliala I, Markozannes G, Cividini S, Gunter MJ, Nautiyal J, et al. Risk factors for endometrial cancer: An umbrella review of the literature. Int J Cancer. 2019;145(7):1719–30.

6. Hernandez A V., Pasupuleti V, Benites-Zapata VA, Thota P, Deshpande A, Perez-Lopez FR. Insulin resistance and endometrial cancer risk: A systematic review and meta-analysis. Eur J Cancer. 2015;51(18):2747–58.

7. Lokuhetty D, White V WR. Female Genital Tumours 5th Edition, Volume 4. 5th Editio. 2020. 632 p.

8. Berek JS, Matias-Guiu X, Creutzberg C, Fotopoulou C, Gaffney D, Kehoe S, et al. FIGO staging of endometrial cancer: 2023. Int J Gynecol Obstet. 2023;162(2):383–94.

9. del Carmen MG, Birrer M, Schorge JO. Uterine papillary serous cancer: A review of the literature. Gynecol Oncol. 2012 Dec;127(3):651–61.

10. Getz G, Gabriel SB, Cibulskis K, Lander E, Sivachenko A, Sougnez C, et al. Integrated genomic characterization of endometrial carcinoma. Nature. 2013;497(7447):67–73.

11. Concin N, Matias-Guiu X, Vergote I, Cibula D, Mirza MR, Marnitz S, et al. ESGO/ESTRO/ESP guidelines for the management of patients with endometrial carcinoma. Int J Gynecol Cancer. 2021;31(1):12–39.

12. Oaknin A, Bosse TJ, Creutzberg CL, Giornelli G, Harter P, Joly F, et al. Endometrial cancer: ESMO Clinical Practice Guideline for diagnosis, treatment and follow-up. Ann Oncol. 2022;33(9):860–77.

USC UNIVERSIDADE DE SANTIAGO DE COMPOSTELA

13. Siegenthaler F, Epstein E, Büchi CA, Gmür A, Saner FACM, Rau TT, et al. Prognostic value of lymphovascular space invasion according to the molecular subgroups in endometrial cancer. Int J Gynecol Cancer. 2023;33(11):1702–7.

14. Kommoss S, McConechy MK, Kommoss F, Leung S, Bunz A, Magrill J, et al. Final validation of the ProMisE molecular classifier for endometrial carcinoma in a large population-based case series. Ann Oncol. 2018;29(5):1180–8.

15. Talhouk A, McConechy MK, Leung S, Yang W, Lum A, Senz J, et al. Confirmation of ProMisE: A simple, genomics-based clinical classifier for endometrial cancer. Cancer. 2017;123(5):802–13.

16. Vipat S, Gupta D, Jonchhe S, Anderspuk H, Rothenberg E, Moiseeva TN. The non-catalytic role of DNA polymerase epsilon in replication initiation in human cells. Nat Commun. 2022;13(1).

17. Wang Q, Peng H, Qi X, Wu M, Zhao X. Targeted therapies in gynecological cancers: a comprehensive review of clinical evidence. Signal Transduct Target Ther. 2020;5(1).

18. Karpel H, Slomovitz B, Coleman RL, Pothuri B. Biomarker-driven therapy in endometrial cancer. Int J Gynecol Cancer. 2023;33(3):343–50.

19. Valerie Beral, Diana Bull GRMWSC. Endometrial cancer and hormone-replacement therapy in the Million Women Study. Lancet. 2005;365(9470):1543–51.

20. Mahdi H, Ray-Coquard I, Lorusso D, Mirza MR, Monk BJ, Slomovitz B. Evolving treatment paradigms in metastatic or recurrent low-grade endometrial cancer: When is hormonal-based therapy the preferred option? Int J Gynecol Cancer. 2023;33(11):1675–81.

21. Chaudhry P, Asselin E. Resistance to chemotherapy and hormone therapy in endometrial cancer. Endocr Relat Cancer. 2009;16(2):363–80.

22. Covens AL, Filiaci V, Gersell D, Lutman C V., Bonebrake A, Lee YC. Phase II study of fulvestrant in recurrent/metastatic endometrial carcinoma: A Gynecologic Oncology Group Study. Gynecol Oncol. 2011;120(2):185–8.

23. Chen JLY, Huang Y Sen, Huang CY, Hsu CY, Lan KH, Cheng WF, et al. Impact of adjuvant radiotherapy on the survival of women with

USC UNIVERSIDADE DE SANTIAGO DE COMPOSTELA

optimally resected stage III endometrial cancer in the era of modern radiotherapy: A retrospective study. Radiat Oncol. 2020;15(1).

24. Harkenrider MM, Abu-Rustum N, Albuquerque K, Bradfield L, Bradley K, Dolinar E, et al. Radiation Therapy for Endometrial Cancer: An American Society for Radiation Oncology Clinical Practice Guideline. Pract Radiat Oncol. 2023;13(1):41–66.

25. Boothe D, Wolfson A, Christensen M, Francis S, Werner TL, Gaffney DK. Lymphovascular invasion in endometrial cancer: Prognostic value and implications on adjuvant radiation therapy use. Am J Clin Oncol Cancer Clin Trials. 2019;42(7):549–54.

26. de Boer SM, Powell ME, Mileshkin L, Katsaros D, Bessette P, Haie-Meder C, et al. Adjuvant chemoradiotherapy versus radiotherapy alone for women with high-risk endometrial cancer (PORTEC-3): final results of an international, open-label, multicentre, randomised, phase 3 trial. Lancet Oncol. 2018;19(3):295–309.

27. Hogberg T, Signorelli M, De Oliveira CF, Fossati R, Lissoni AA, Sorbe B, et al. Sequential adjuvant chemotherapy and radiotherapy in endometrial cancer-Results from two randomised studies. Eur J Cancer. 2010;46(13):2422–31.

28. Abal M, Andreu J, Barasoain I. Taxanes: Microtubule and Centrosome Targets, and Cell Cycle Dependent Mechanisms of Action. Curr Cancer Drug Targets. 2005;3(3):193–203.

29. Geisberg CA, Sawyer DB. Mechanisms of anthracycline cardiotoxicity and strategies to decrease cardiac damage. Curr Hypertens Rep. 2010;12(6):404–10.

30. Homesley HD, Filiaci V, Gibbons SK, Long HJ, Cella D, Spirtos NM, et al. A randomized phase III trial in advanced endometrial carcinoma of surgery and volume directed radiation followed by cisplatin and doxorubicin with or without paclitaxel: A Gynecologic Oncology Group study. Gynecol Oncol. 2009;112(3):543–52.

31. Stevens GHJ, Robles L. Neuromuscular complications. Support Oncol (Expert Consult - Online Print). 2011;283–91.

32. Muggia FM, Blessing JA, Method M, Miller DS, Johnson GA, Lee RB, et al. Evaluation of vinorelbine in persistent or recurrent squamous cell carcinoma of the cervix: A Gynecologic Oncology Group study. Gynecol Oncol. 2004;92(2):639–43.

USC UNIVERSIDADE DE SANTIAGO DE COMPOSTELA

33. Szucs Z, Jones RL. Introduction to Systemic Antineoplastic Treatments for Cardiologists. Clin Cardio-oncology. 2016;15–38.

34. Grisham RN, Adaniel C, Hyman DM, Ma W, Iasonos A, Aghajanian C, et al. Gemcitabine for advanced endometrial cancer: A retrospective study of the memorial sloan-kettering cancer center experience. Int J Gynecol Cancer. 2012;22(5):807–11.

35. Mirza MR, Chase DM, Slomovitz BM, dePont Christensen R, Novák Z, Black D, et al. Dostarlimab for Primary Advanced or Recurrent Endometrial Cancer. N Engl J Med. 2023;388(23):2145–58.

36. O'Malley DM, Bariani GM, Cassier PA, Marabelle A, Hansen AR, De Jesus Acosta A, et al. Pembrolizumab in Patients With Microsatellite Instability–High Advanced Endometrial Cancer: Results From the KEYNOTE-158 Study. J Clin Oncol. 2022 Mar 1;40(7):752–61.

37. Cicala CM, Musacchio L, Scambia G, Lorusso D. Dostarlimab: From preclinical investigation to drug approval and future directions. Hum Vaccines Immunother. 2023;19(1).

38. Oaknin A, Bosse TJ, Creutzberg CL, Giornelli G, Harter P, Joly F, et al. Endometrial cancer: ESMO Clinical Practice Guideline for diagnosis, treatment and follow-up ☆. Ann Oncol. 2022;33(9):860–77.

39. Quaresmini D, Guida M. Antiangiogenic drugs as chemosensitizer in melanoma. In: Antiangiogenic Drugs as Chemosensitizers in Cancer Therapy. Elsevier; 2022. p. 93–109.

40. Passarelli A, Ventriglia J, Pisano C, Cecere SC, Napoli M Di, Rossetti S, et al. The way to precision medicine in gynecologic cancers: The first case report of an exceptional response to alpelisib in a PIK3CA-mutated endometrial cancer. Front Oncol. 2023 Jan 13;12.

41. Roncolato F, Lindemann K, Willson ML, Martyn J, Mileshkin L. Pi3K/AKT/mTOR inhibitors for advanced or recurrent endometrial cancer. Cochrane Database Syst Rev. 2019;2019(10).

42. Morales JC, Li L, Fattah FJ, Dong Y, Bey EA, Patel M, et al. Review of poly (ADP-ribose) polymerase (PARP) mechanisms of action and rationale for targeting in cancer and other diseases. Crit Rev Eukaryot Gene Expr. 2014;24(1):15–28.

43. Colombo N, Creutzberg C, Amant F, Bosse T, González-Martón A, Ledermann J, et al. ESMO-ESGO-ESTRO consensus conference on endometrial cancer: Diagnosis, treatment and follow-up. Ann Oncol.

USC UNIVERSIDADE DE SANTIAGO DE COMPOSTELA

2016;27(1):16–41.

44. Costas L, Frias-Gomez J, Guardiola M, Benavente Y, Pineda M, Pavón MÁ, et al. New perspectives on screening and early detection of endometrial cancer. Int J Cancer. 2019 Dec 15;145(12):3194–206.

45. Urick ME, Bell DW. Clinical actionability of molecular targets in endometrial cancer. Nat Rev Cancer. 2019;19(9):510–21.

46. Le DT, Durham JN, Smith KN, Wang H, Bartlett BR, Aulakh LK, et al. Mismatch repair deficiency predicts response of solid tumors to PD-1 blockade. Science. 2017;357(6349):409–13.

47. Marín-Jimenez JA, García-Muler S, Matías-Gui X, Piulats JM. Facts and Hopes in Immunotherapy of Endometrial Cancer. Clin Cancer Res. 2022;28(22):4849–60.

48. Jerzak KJ, Duska L, MacKay HJ. Endocrine therapy in endometrial cancer: An old dog with new tricks. Gynecol Oncol. 2019;153(1):175–83.

49. van Weelden WJ, Lalisang RI, Bulten J, Lindemann K, van Beekhuizen HJ, Trum H, et al. Impact of hormonal biomarkers on response to hormonal therapy in advanced and recurrent endometrial cancer. Am J Obstet Gynecol. 2021;225(4):407.e1-407.e16.

50. Pijnenborg JMA, Van Weelden WJ, Reijnen C, Xanthoulea S, Romano A. Redefining the Position of Hormonal Therapy in Endometrial Cancer in the Era of Molecular Classification. J Clin Oncol. 2024;42(1):8–12.

51. Romani C, Capoferri D, Reijnen C, Lonardi S, Ravaggi A, Ratti M, et al. L1CAM expression as a predictor of platinum response in high-risk endometrial carcinoma. Int J Cancer. 2022;151(4):637–48.

52. Razavi P, Li BT, Brown DN, Jung B, Hubbell E, Shen R, et al. High-intensity sequencing reveals the sources of plasma circulating cell-free DNA variants. Nat Med. 2019;25(12):1928–37.

53. Batool SM, Yekula A, Khanna P, Hsia T, Gamblin AS, Ekanayake E, et al. The Liquid Biopsy Consortium: Challenges and opportunities for early cancer detection and monitoring. Cell Reports Med. 2023;4(10).

54. Graham Brock, Elena Castellanos-Rizaldos, Lan Hu, Christine Coticchia JS. Liquid biopsy for cancer screening, patient stratification and monitoring. 2018;1–11.

55. Hirahata T, ul Quraish R, Quraish A ul, ul Quraish S, Naz M, Razzaq

USC UNIVERSIDADE DE SANTIAGO DE COMPOSTELA

MA. Liquid Biopsy: A Distinctive Approach to the Diagnosis and Prognosis of Cancer. Cancer Inform. 2022;21.

56. Smit DJ, Pantel K. Circulating tumor cells as liquid biopsy markers in cancer patients. Mol Aspects Med. 2024;96.

57. Schwarzenbach H, Hoon DSB, Pantel K. Cell-free nucleic acids as biomarkers in cancer patients. Nat Rev Cancer. 2011;11(6):426–37.

58. Moss J, Magenheim J, Neiman D, Zemmour H, Loyfer N, Korach A, et al. Comprehensive human cell-type methylation atlas reveals origins of circulating cell-free DNA in health and disease. Nat Commun. 2018;9(1).

59. Kustanovich A, Schwartz R, Peretz T, Grinshpun A. Life and death of circulating cell-free DNA. Cancer Biol Ther. 2019;20(8):1057–67.

60. Mattox AK, Douville C, Wang Y, Popoli M, Ptak J, Silliman N, et al. The Origin of Highly Elevated Cell-Free DNA in Healthy Individuals and Patients with Pancreatic, Colorectal, Lung, or Ovarian Cancer. Cancer Discov. 2023;13(10):2166–79.

61. Alborelli I, Generali D, Jermann P, Cappelletti MR, Ferrero G, Scaggiante B, et al. Cell-free DNA analysis in healthy individuals by next-generation sequencing: a proof of concept and technical validation study. Cell Death Dis. 2019;10(7).

62. Yu SCY, Lee SWY, Jiang P, Leung TY, Chan KCA, Chiu RWK, et al. High-resolution profiling of fetal DNA clearance from maternal plasma by massively parallel sequencing. Clin Chem. 2013;59(8):1228–37.

63. Diehl F, Schmidt K, Choti MA, Romans K, Goodman S, Li M, et al. Circulating mutant DNA to assess tumor dynamics. Nat Med. 2008;14(9):985–90.

64. Thierry AR, El Messaoudi S, Gahan PB, Anker P, Stroun M. Origins, structures, and functions of circulating DNA in oncology. Cancer Metastasis Rev. 2016;35(3):347–76.

65. Mouliere F, Chandrananda D, Piskorz AM, Moore EK, Morris J, Ahlborn LB, et al. Enhanced detection of circulating tumor DNA by fragment size analysis. Sci Transl Med. 2018;10(466).

66. Surani A. Circulating tumour DNA: a minimally invasive biomarker for tumour detection and stratification. Br J Pharm. 2016;1(1).

67. Radic M, Kaplan MJ. Extracellular chromatin traps interconnect cell

USC UNIVERSIDADE DE SANTIAGO DE COMPOSTELA

biology, microbiology, and immunology. Front Immunol. 2013;4(JUN).

68. van der Leest P, Boonstra PA, Elst A Ter, van Kempen LC, Tibbesma M, Koopmans J, et al. Comparison of circulating cell-free dna extraction methods for downstream analysis in cancer patients. Cancers (Basel). 2020;12(5).

69. Sorber L, Zwaenepoel K, Deschoolmeester V, Roeyen G, Lardon F, Rolfo C, et al. A Comparison of Cell-Free DNA Isolation Kits: Isolation and Quantification of Cell-Free DNA in Plasma. J Mol Diagnostics. 2017;19(1):162–8.

70. Jennings L, Van Deerlin VM, Gulley ML. Recommended principles and practices for validating clinical molecular pathology tests. Arch Pathol Lab Med. 2009;133(5):743–55.

71. Lee JS, Cho EH, Kim B, Hong J, Kim YG, Kim Y, et al. Clinical Practice Guideline for Blood-based Circulating Tumor DNA Assays. Ann Lab Med. 2024;44(3):195–209.

72. Pascual J, Attard G, Bidard FC, Curigliano G, De Mattos-Arruda L, Diehn M, et al. ESMO recommendations on the use of circulating tumour DNA assays for patients with cancer: a report from the ESMO Precision Medicine Working Group. Ann Oncol. 2022;33(8):750–68.

73. Cisneros-Villanueva M, Hidalgo-Pérez L, Rios-Romero M, Cedro-Tanda A, Ruiz-Villavicencio CA, Page K, et al. Cell-free DNA analysis in current cancer clinical trials: a review. Br J Cancer. 2022;

74. Kim JO, Shin JY, Kim SR, Shin KS, Kim J, Kim MY, et al. Evaluation of two egfr mutation tests on tumor and plasma from patients with non-small cell lung cancer. Cancers (Basel). 2020;12(4).

75. Vollbrecht C, Hoffmann I, Lehmann A, Merkelbach-Bruse S, Fassunke J, Wagener-Ryczek S, et al. Proficiency testing of PIK3CA mutations in HR+/HER2-breast cancer on liquid biopsy and tissue. Virchows Arch. 2023;482(4):697–706.

76. Shirley M. Epi proColon® for Colorectal Cancer Screening: A Profile of Its Use in the USA. Mol Diagnosis Ther. 2020;24(4):497–503.

77. Woodhouse R, Li M, Hughes J, Delfosse D, Skoletsky J, Ma P, et al. Clinical and analytical validation of foundation one liquid CDx, a novel 324-Gene cfDNA-based comprehensive genomic profiling assay for cancers of solid tumor origin. PLoS One. 2020;15(9 September).

USC UNIVERSIDADE DE SANTIAGO DE COMPOSTELA

78. Cahn F, Revon-riviere G, Min V, Rome A, Filaine P, Pelletier A, et al. Blood-Derived Liquid Biopsies Using Foundation One® Liquid CDx for Children and Adolescents with High-Risk Malignancies: A Monocentric Experience. Cancers (Basel). 2022;14(11).

79. Bauml JM, Li BT, Velcheti V, Govindan R, Curioni-Fontecedro A, Dooms C, et al. Clinical validation of Guardant360 CDx as a blood-based companion diagnostic for sotorasib. Lung Cancer. 2022;166:270–8.

80. Alix-Panabières C, Pantel K. Liquid biopsy: From discovery to clinical application. Cancer Discov. 2021;11(4):858–73.

81. Pantel K, Alix-Panabières C. Crucial roles of circulating tumor cells in the metastatic cascade and tumor immune escape: biology and clinical translation. J Immunother Cancer. 2022;10(12).

82. Micalizzi DS, Maheswaran S, Haber DA. A conduit to metastasis: Circulating tumor cell biology. Genes Dev. 2017;31(18):1827–40.

83. Eslami-S Z, Cortés-Hernández LE, Alix-Panabières C. The Metastatic Cascade as the Basis for Liquid Biopsy Development. Front Oncol. 2020;10:1055.

84. Lusby R, Dunne P, Tiwari VK. Tumour invasion and dissemination. Biochem Soc Trans. 2022;50(3):1245–57.

85. Hanahan D. Hallmarks of Cancer: New Dimensions. Cancer Discov. 2022;12(1):31–46.

86. Aceto N, Bardia A, Miyamoto DT, Donaldson MC, Wittner BS, Spencer JA, et al. Circulating tumor cell clusters are oligoclonal precursors of breast cancer metastasis. Cell. 2014;158(5):1110–22.

87. Abdalla TSA, Meiners J, Riethdorf S, König A, Melling N, Gorges T, et al. Prognostic value of preoperative circulating tumor cells counts in patients with UICC stage I-IV colorectal cancer. PLoS One. 2021;16(6 June).

88. Foy V, Lindsay CR, Carmel A, Fernandez-Gutierrez F, Krebs MG, Priest L, et al. EPAC-lung: European pooled analysis of the prognostic value of circulating tumour cells in small cell lung cancer. Transl Lung Cancer Res. 2021;10(4):1653–65.

89. Fehm T, Becker S, Bachmann C, Beck V, Gebauer G, Banys M, et al. Detection of disseminated tumor cells in patients with gynecological cancers. Gynecol Oncol. 2006;103(3):942–7.

USC UNIVERSIDADE DE SANTIAGO DE COMPOSTELA

90. Alonso-Alconada L, Muinelo-Romay L, Madissoo K, Diaz-Lopez A, Krakstad C, Trovik J, et al. Molecular profiling of circulating tumor cells links plasticity to the metastatic process in endometrial cancer. Mol Cancer. 2014;13(1).

91. Casas-Arozamena C, Díaz E, Moiola CP, Alonso-Alconada L, Ferreiros A, Abalo A, et al. Genomic profiling of uterine aspirates and cfDNA as an integrative liquid biopsy strategy in endometrial cancer. J Clin Med. 2020;9(2).

92. Nagrath S, Sequist L V., Maheswaran S, Bell DW, Irimia D, Ulkus L, et al. Isolation of rare circulating tumour cells in cancer patients by microchip technology. Nature. 2007;450(7173):1235–9.

93. Riethdorf S, O'Flaherty L, Hille C, Pantel K. Clinical applications of the CellSearch platform in cancer patients. Adv Drug Deliv Rev. 2018;125:102–21.

94. Andree KC, van Dalum G, Terstappen LWMM. Challenges in circulating tumor cell detection by the CellSearch system. Mol Oncol. 2016;10(3):395–407.

95. Wang Z, Sun N, Liu H, Chen C, Ding P, Yue X, et al. High-Efficiency Isolation and Rapid Identification of Heterogeneous Circulating Tumor Cells (CTCs) Using Dual-Antibody-Modified Fluorescent-Magnetic Nanoparticles. ACS Appl Mater Interfaces. 2019;11(43):39586–93.

96. Descamps L, Roy D Le, Deman AL. Microfluidic-Based Technologies for CTC Isolation: A Review of 10 Years of Intense Efforts towards Liquid Biopsy. Int J Mol Sci. 2022;23(4).

97. Drucker A, Teh EM, Kostyleva R, Rayson D, Douglas S, Pinto DM. Comparative performance of different methods for circulating tumor cell enrichment in metastatic breast cancer patients. PLoS One. 2020;15(8 August).

98. Ferreira MM, Ramani VC, Jeffrey SS. Circulating tumor cell technologies. Mol Oncol. 2016;10(3):374–94.

99. Miller MC, Robinson PS, Wagner C, O'Shannessy DJ. The Parsortix™ Cell Separation System—A versatile liquid biopsy platform. Cytom Part A. 2018;93(12):1234–9.

100. Morgan TM, Lange PH, Vessella RL. Detection and characterization of circulating and disseminated prostate cancer cells. Front Biosci. 2007;12(8):3000–9.

USC UNIVERSIDADE DE SANTIAGO DE COMPOSTELA

101. Varmazyari V, Habibiyan H, Ghafoorifard H, Ebrahimi M, Ghafouri-Fard S. A dielectrophoresis-based microfluidic system having double-sided optimized 3D electrodes for label-free cancer cell separation with preserving cell viability. Sci Rep. 2022;12(1).

102. Tay RY, Fernández-Gutiérrez F, Foy V, Burns K, Pierce J, Morris K, et al. Prognostic value of circulating tumour cells in limited-stage small-cell lung cancer: analysis of the concurrent once-daily versus twice-daily radiotherapy (CONVERT) randomised controlled trial. Ann Oncol. 2019;30(7):1114–20.

103. Jin F, Zhu L, Shao J, Yakoub M, Schmitt L, Reißfelder C, et al. Circulating tumour cells in patients with lung cancer universally indicate poor prognosis. Eur Respir Rev. 2022;31(166).

104. Pang S, Li H, Xu S, Feng L, Ma X, Chu Y, et al. Circulating tumour cells at baseline and late phase of treatment provide prognostic value in breast cancer. Sci Rep. 2021;11(1):13441.

105. Gradilone A, Naso G, Raimondi C, Cortesi E, Gandini O, Vincenzi B, et al. Circulating tumor cells (CTCs) in metastatic breast cancer (MBC): Prognosis, drug resistance and phenotypic characterization. Ann Oncol. 2011;22(1):86–92.

106. Cieślikowski WA, Antczak A, Nowicki M, Zabel M, Budna-Tukan J. Clinical relevance of circulating tumor cells in prostate cancer management. Biomedicines. 2021;9(9).

107. Lu YJ, Wang P, Peng J, Wang X, Zhu YW, Shen N. Meta-analysis Reveals the Prognostic Value of Circulating Tumour Cells Detected in the Peripheral Blood in Patients with Non-Metastatic Colorectal Cancer. Sci Rep. 2017;7(1).

108. Wang C, Zhang Z, Chong W, Luo R, Myers RE, Gu J, et al. Improved prognostic stratification using circulating tumor cell clusters in patients with metastatic castration-resistant prostate cancer. Cancers (Basel). 2021;13(2):1–13.

109. Krol I, Schwab FD, Carbone R, Ritter M, Picocci S, De Marni ML, et al. Detection of clustered circulating tumour cells in early breast cancer. Br J Cancer. 2021;125(1):23–7.

110. Aceto N. Bring along your friends: Homotypic and heterotypic circulating tumor cell clustering to accelerate metastasis. Biomed J. 2020;43(1):18–23.

USC UNIVERSIDADE DE SANTIAGO DE COMPOSTELA

111. Cohen SJ, Punt CJA, Iannotti N, Saidman BH, Sabbath KD, Gabrail NY, et al. Prognostic significance of circulating tumor cells in patients with metastatic colorectal cancer. Ann Oncol. 2009;20(7):1223–9.

112. Bendahl PO, Belting M, Gezelius E. Longitudinal Assessment of Circulating Tumor Cells and Outcome in Small Cell Lung Cancer: A Sub-Study of RASTEN—A Randomized Trial with Low Molecular Weight Heparin. Cancers (Basel). 2023;15(12).

113. Gerratana L, Davis AA, Zhang Q, Basile D, Rossi G, Strickland K, et al. Longitudinal Dynamics of Circulating Tumor Cells and Circulating Tumor DNA for Treatment Monitoring in Metastatic Breast Cancer. JCO Precis Oncol. 2021;(5):943–52.

114. Capuozzo M, Ferrara F, Santorsola M, Zovi A, Ottaiano A. Circulating Tumor Cells as Predictive and Prognostic Biomarkers in Solid Tumors. Cells. 2023;12(22).

115. Francini S, Duraes M, Rathat G, Macioce V, Mollevi C, Pages L, et al. Circulating Tumor Cell Detection by Liquid Biopsy during Early-Stage Endometrial Cancer Surgery: A Pilot Study. Biomolecules. 2023;13(3).

116. GIORGIO BOGANI, MINETTA C. LIU, SEAN C. DOWDY, WILLIAM A. CLIBY, SARAH E. KERR, KIMBERLY R. KALLI, et al. Detection of Circulating Tumor Cells in High-risk Endometrial Cancer. Anticancer Res. 2015;35:683–8.

117. Maritschnegg E, Heitz F, Pecha N, Bouda J, Trillsch F, Grimm C, et al. Uterine and Tubal Lavage for Earlier Cancer Detection Using an Innovative Catheter: A Feasibility and Safety Study. Int J Gynecol Cancer. 2018;28(9):1692–8.

118. Zuber TJ. Endometrial biopsy. Am Fam Physician. 2001;63(6):1131–5.

119. Blobel CP. Remarkable roles of proteolysis on and beyond the cell surface. Curr Opin Cell Biol. 2000;12(5):606–12.

120. Arribas J, Borroto A. Protein ectodomain shedding. Chem Rev. 2002;102(12):4627–37.

121. Martinez-Garcia E, Lesur A, Devis L, Cabrera S, Matias-Guiu X, Hirschfeld M, et al. Targeted proteomics identifies proteomic signatures in liquid biopsies of the endometrium to diagnose endometrial cancer and assist in the prediction of the optimal surgical treatment. Clin Cancer Res. 2017;23(21):6458–67.

USC UNIVERSIDADE DE SANTIAGO DE COMPOSTELA

122. Barnabas GD, Bahar-Shany K, Sapoznik S, Helpman L, Kadan Y, Beiner M, et al. Microvesicle proteomic profiling of uterine liquid biopsy for ovarian cancer early detection. Mol Cell Proteomics. 2019;18(5):865–75.

123. Niklasson O, Skude G, Marsal K, Casslén B. Diagnosis of endometrial cancer in patients with postmenopausal bleeding by analysis of the lactate dehydrogenase isoenzyme activity profile in uterine fluid. Gynecol Oncol. 2004;93(2):385–9.

124. Perez-Sanchez C, Colas E, Cabrera S, Falcon O, Sanchez-Del-Río A, García E, et al. Molecular diagnosis of endometrial cancer from uterine aspirates. Int J Cancer. 2013;133(10):2383–91.

125. Liu J, Sun H, Wang X, Yu Q, Li S, Yu X, et al. Increased exosomal microRNA-21 and microRNA-146a levels in the cervicovaginal lavage specimens of patients with cervical cancer. Int J Mol Sci. 2014;15(1):758–73.

126. Colas E, Perez C, Cabrera S, Pedrola N, Monge M, Castellvi J, et al. Molecular markers of endometrial carcinoma detected in uterine aspirates. Int J Cancer. 2011;129(10):2435–44.

127. Casado-Vela J, Rodriguez-Suarez E, Iloro I, Ametzazurra A, Alkorta N, García-Velasco JA, et al. Comprehensive proteomic analysis of human endometrial fluid aspirate. J Proteome Res. 2009;8(10):4622–32.

128. Roman-Canal B, Moiola CP, Gatius S, Bonnin S, Ruiz-Miró M, González E, et al. Ev-associated miRNAs from peritoneal lavage are a source of biomarkers in endometrial cancer. Cancers (Basel). 2019;11(6).

129. Łaniewski P, Cui H, Mahnert ND, Mourad J, Borst MP, Willmott L, et al. Protein biomarkers in cervicovaginal lavages for detection of endometrial cancer. Biomark Res. 2022;10(1).

130. Nair N, Camacho-Vanegas O, Rykunov D, Dashkoff M, Camacho SC, Schumacher CA, et al. Genomic Analysis of Uterine Lavage Fluid Detects Early Endometrial Cancers and Reveals a Prevalent Landscape of Driver Mutations in Women without Histopathologic Evidence of Cancer: A Prospective Cross-Sectional Study. PLoS Med. 2016;13(12).

131. Mota A, Colás E, García-Sanz P, Campoy I, Rojo-Sebastián A, Gatius S, et al. Genetic analysis of uterine aspirates improves the diagnostic value and captures the intra-tumor heterogeneity of endometrial cancers. Mod Pathol. 2017;30(1):134–45.

USC UNIVERSIDADE DE SANTIAGO DE COMPOSTELA

132. Chao A, Wu KY, Lin CY, Lee YS, Huang HJ, Tang YH, et al. Towards less invasive molecular diagnostics for endometrial cancer: massively parallel sequencing of endometrial lavage specimens in women attending for an office hysteroscopy. J Mol Med. 2022;100(9):1331–9.

133. Ghezelayagh TS, Kohrn BF, Fredrickson J, Manhardt E, Radke MR, Katz R, et al. Uterine Lavage Identifies Cancer Mutations and Increased TP53 Somatic Mutation Burden in Individuals with Ovarian Cancer . Cancer Res Commun. 2022;2(10):1282–92.

134. Žilovič D, Vaicekauskaitė I, Čiurlienė R, Sabaliauskaitė R, Jarmalaitė S. Uterine Cavity Lavage Mutation Analysis in Lithuanian Ovarian Cancer Patients. Cancers (Basel). 2023;15(3).

135. Bats AS, Blons H, Narjoz C, Le Frere-Belda MA, Laurent-Puig P, Lecuru F. Microsatellite instability analysis in uterine cavity washings to detect endometrial cancer in lynch syndrome. Anticancer Res. 2014;34(6):3211–6.

136. Yap J, Salamonsen LA, Jobling T, Nicholls PK, Dimitriadis E. Interleukin 11 is upregulated in uterine lavage and endometrial cancer cells in women with endometrial carcinoma. Reprod Biol Endocrinol. 2010;8.

137. Nyen T Van, Moiola CP, Colas E, Annibali D, Amant F. Modeling endometrial cancer: Past, present, and future. Int J Mol Sci. 2018;19(8).

138. Katt ME, Placone AL, Wong AD, Xu ZS, Searson PC. In vitro tumor models: Advantages, disadvantages, variables, and selecting the right platform. Front Bioeng Biotechnol. 2016;4(FEB).

139. Anton D, Burckel H, Josset E, Noel G. Three-dimensional cell culture: A breakthrough in vivo. Int J Mol Sci. 2015;16(3):5517–27.

140. Kapałczyńska M, Kolenda T, Przybyła W, Zajączkowska M, Teresiak A, Filas V, et al. 2D and 3D cell cultures – a comparison of different types of cancer cell cultures. Arch Med Sci. 2018;14(4):910–9.

141. Nyen T Van, Moiola CP, Colas E, Annibali D, Amant F. Modeling endometrial cancer: Past, present, and future. Int J Mol Sci. 2018;19(8).

142. Calpe B, Kovacs WJ. High-throughput screening in multicellular spheroids for target discovery in the tumor microenvironment. Expert Opin Drug Discov. 2020;15(8):955–67.

USC UNIVERSIDADE DE SANTIAGO DE COMPOSTELA

143. Caleb Jensen, Yong Teng. Is It Time to Start Transitioning From 2D to 3D Cell Culture? Front Mol Biosci. 2020;7(33).

144. Francesco Pampaloni, Emmanuel G. Reynaud, Ernst Stelzer. The third dimension bridges the gap between cell culture and live tissue. Nat Rev Mol Cell Biol. 2007;8:839–45.

145. Nguyen DT, Famiglietti JE, Smolchek RA, Dupee Z, Diodati N, Pedro DI, et al. 3D In Vitro Platform for Cell and Explant Culture in Liquid-Like Solids. Cells. 2022;11(6).

146. Sakalem ME, De Sibio MT, da Costa FA da S, de Oliveira M. Historical evolution of spheroids and organoids, and possibilities of use in life sciences and medicine. Biotechnol J. 2021;16(5).

147. Rasouli M, Safari F, Kanani MH, Ahvati H. Principles of Hanging Drop Method (Spheroid Formation) in Cell Culture. 2024;

148. Salinas-Vera YM, Valdés J, Pérez-Navarro Y, Mandujano-Lazaro G, Marchat LA, Ramos-Payán R, et al. Three-Dimensional 3D Culture Models in Gynecological and Breast Cancer Research. Front Oncol. 2022;12.

149. Collins A, Miles GJ, Wood J, MacFarlane M, Pritchard C, Moss E. Patient-derived explants, xenografts and organoids: 3-dimensional patient-relevant pre-clinical models in endometrial cancer. Gynecol Oncol. 2020;156(1):251–9.

150. Surina, Tanggis, Suzuki T, Hisata S, Fujita K, Fujiwara S, et al. Patient-derived spheroids and patient-derived organoids simulate evolutions of lung cancer. Heliyon. 2023;9(3).

151. Muguruma M, Teraoka S, Miyahara K, Ueda A, Asaoka M, Okazaki M, et al. Differences in drug sensitivity between two-dimensional and three-dimensional culture systems in triple-negative breast cancer cell lines. Biochem Biophys Res Commun. 2020;533(3):268–74.

152. Sato T, Vries RG, Snippert HJ, Van De Wetering M, Barker N, Stange DE, et al. Single Lgr5 stem cells build crypt-villus structures in vitro without a mesenchymal niche. Nature. 2009;459(7244):262–5.

153. LeSavage BL, Suhar RA, Broguiere N, Lutolf MP, Heilshorn SC. Next-generation cancer organoids. Nat Mater. 2022;21(2):143–59.

154. Hofer M, Lutolf MP. Engineering organoids. Nat Rev Mater. 2021;6(5):402–20.

USC UNIVERSIDADE DE SANTIAGO DE COMPOSTELA

155. Turco MY, Gardner L, Hughes J, Cindrova-Davies T, Gomez MJ, Farrell L, et al. Long-term, hormone-respTurco MY, Gardner L, Hughes J, Cindrova-Davies T, Gomez MJ, Farrell L, Hollinshead M, Marsh SGE, Brosens JJ, Critchley HO, et al. Long-term, hormone-responsive organoid cultures of human endometrium in a chemically defined medium. N. Nat Cell Biol. 2017;19(5):568–77.

156. Lõhmussaar K, Boretto M, Clevers H. Human-Derived Model Systems in Gynecological Cancer Research. Trends in Cancer. 2020;6(12):1031–43.

157. Boretto M, Cox B, Noben M, Hendriks N, Fassbender A, Roose H, et al. Development of organoids from mouse and human endometrium showing endometrial epithelium physiology and long-term expandability. Dev. 2017;144(10):1775–86.

158. Boretto M, Maenhoudt N, Luo X, Hennes A, Boeckx B, Bui B, et al. Patient-derived organoids from endometrial disease capture clinical heterogeneity and are amenable to drug screening. Nat Cell Biol. 2019;21(8):1041–51.

159. Berg HF, Hjelmeland ME, Lien H, Espedal H, Fonnes T, Srivastava A, et al. Patient-derived organoids reflect the genetic profile of endometrial tumors and predict patient prognosis. Commun Med. 2021;1(1):1–14.

160. Abdolahi S, Ghazvinian Z, Muhammadnejad S, Saleh M, Asadzadeh Aghdaei H, Baghaei K. Patient-derived xenograft (PDX) models, applications and challenges in cancer research. J Transl Med. 2022;20(1).

161. Okada S, Vaeteewoottacharn K, Kariya R. Application of highly immunocompromised mice for the establishment of patient-derived xenograft (PDX) models. Cells. 2019;8(8).

162. Villafranca-Magdalena B, Masferrer-Ferragutcasas C, Lopez-Gil C, Rubia EC de la, Rebull M, Parra G, et al. Genomic Validation of Endometrial Cancer Patient-Derived Xenograft Models as a Preclinical Tool. Int J Mol Sci. 2022;23(11).

163. Peille AL, Vuaroqueaux V, Wong SS, Ting J, Klinger K, Zeitouni B, et al. Evaluation of molecular subtypes and clonal selection during establishment of patient-derived tumor xenografts from gastric adenocarcinoma. Commun Biol. 2020;3(1).

164. Sengal AT, Bonazzi V, Smith D, Moiola CP, Lourie R, Rogers R, et al. Endometrial cancer PDX-derived organoids (PDXOs) and PDXs with

USC UNIVERSIDADE DE SANTIAGO DE COMPOSTELA

FGFR2c isoform expression are sensitive to FGFR inhibition. npj Precis Oncol. 2023;7(1).

165. Mota A, Oltra SS, Selenica P, Moiola CP, Casas-Arozamena C, López-Gil C, et al. Intratumor genetic heterogeneity and clonal evolution to decode endometrial cancer progression. Oncogene. 2022;41(13):1835–50.

166. Steinkamp MP, Lagutina I, Brayer KJ, Schultz F, Burke D, Pankratz VS, et al. Humanized Patient-derived Xenograft Models of Disseminated Ovarian Cancer Recapitulate Key Aspects of the Tumor Immune Environment within the Peritoneal Cavity. Cancer Res Commun. 2023;3(2):309–24.

167. Liu Y, Wu W, Cai C, Zhang H, Shen H, Han Y. Patient-derived xenograft models in cancer therapy: technologies and applications. Signal Transduct Target Ther. 2023;8(1).

168. Casas-Arozamena C, Moiola CP, Vilar A, Bouso M, Cueva J, Cabrera S, et al. Noninvasive detection of microsatellite instability in patients with endometrial cancer. Int J Cancer. 2023;152(10):2206–17.

169. Foundation RCTR. R: A Language and Environment for Statistical Computing. Vol. 0, Study R. 2017. p. https://www.R-project.org.

170. Ammar R. Package ' randomcoloR '. Cran. 2019.

171. Robin X, Turck N, Hainard A, Tiberti N, Lisacek F, Sanchez JC, et al. pROC: An open-source package for R and S+ to analyze and compare ROC curves. Vol. 12, BMC Bioinformatics. 2011.

172. Milton Bache S, Wickham H, Bache SM, Wickham H, Milton Bache S, Wickham H. Magrittr: a forward-pipe operator for R. Cran.R-Project.Org. 2014.

173. Xu S, Chen M, Feng T, Zhan L, Zhou L, Yu G. Use ggbreak to Effectively Utilize Plotting Space to Deal With Large Datasets and Outliers. Front Genet. 2021;12.

174. Garrett G, Hadley W. Dates and Times Made Easy with lubridate. Vol. 40, Journal of Statistical Software. 2011. p. 1–25.

175. Sing T, Sander O, Beerenwinkel N, Lengauer T. ROCR: Visualizing classifier performance in R. Bioinformatics. 2005;21(20):3940–1.

176. Zuguang Gu, Roland Eils, Matthias Schlesner. Complex heatmaps reveal patterns and correlations in multidimensional genomic data.

USC UNIVERSIDADE DE SANTIAGO DE COMPOSTELA

Bioinformatics. 2016;

177. Sjoberg DD, Whiting K, Curry M, Lavery JA, Larmarange J. Reproducible Summary Tables with the gtsummary Package. R J. 2021;13(1):570–80.

178. Evans MJ, Barton P, Niwa S, Soga M, Seibold S, Tsuchiya K, et al. Ggpubr: “ggplot2” based publication ready plots . Vol. 0, R package version. 2018. p. 2-.

179. Therneau Terry. A Package for Survival Analysis in R . R package version 3.5-0. 2023.

180. Kassambara A. Rstatix: Pipe-Friendly Framework for Basic Statistical Tests. 2021.

181. Taiyun W, Simko V. R package “corrplot”: Visualization of a Correlation Matrix . 2021. Ava

182. Kassambara A, Kosinski M, Biecek P, Scheipl F. Survminer: Drawing Survival Curves Using “Ggplot2”. . 2021.

183. Jessica Weiss and Wei Xu. swimplot: Tools for Creating Swimmers Plots using “ggplot2.” 2021;

184. Kassambara A, Mundt F, Kassambara, A.; Mundt F. Factoextra: extract and visualize the results of multivariate data analyses. URL http://www.sthda.com/english/rpkgs/factoextra BugReports. 2017. p. 1–76.

185. Wickham H. ggplot2: Elegant Graphics for Data Analysis. Ggplot2. 2009;

186. Larmarange J. _labelled: Manipulating Labelled Data_ . R package version 2.9.1. 2022.

187. Wickham H. forcats: Tools for Working with Categorical Variables (Factors). R package version 0.5.1. . 2023. p. https://CRAN.R-project.org/package=forcat.

188. Lê S, Josse J, Husson F. FactoMineR: An R package for multivariate analysis. J Stat Softw. 2008;25(1):1–18.

189. Wickham H. stringr: simple, consistent wrappers for common string operations. R package. 2023;

190. Müller K, Wickham H. tibble: Simple Data Frames..

USC UNIVERSIDADE DE SANTIAGO DE COMPOSTELA

Https://Tibble.Tidyverse.Org/,. 2023.

191. Wickham H, Averick M, Bryan J, Chang W, McGowan L, François R, et al. Welcome to the Tidyverse. J Open Source Softw. 2019;4(43):1686.

192. Neuwirth E, Brewer CA. RColorBrewer: ColorBrewer palettes. R package version. 2011. p. https://cran.R-project.org/package=RColorBrewer.

193. Wickham H. readxl: Read Excel Files. 2016.

194. Pedersen TL. patchwork: The Composer of Plots . Cran. 2020.

195. Wickham H, Francois R. dplyr: A Grammar of Data Manipulation . 2018.

196. Henry L, Wickham H. Purrr: Functional programming tools. R package version 0.3.2. 2019.

197. Wickham H, Hester J, Francois R. readr: Read Rectangular Text Data. R package version 1.1.1. 2017. p. https://CRAN.R-project.org/package=readr.

198. Wickham H. scales: Scale Functions for Visualization. 2016.

199. Wickham H, Vaughan D, Girlich M. tidyr: Tidy Messy Data . R package version 1.3.0. 2023.

200. Wiesweg M. survivalAnalysis: High-Level Interface for Survival Analysis and Associated Plots. 2019.

201. Corr B, Cosgrove C, Spinosa D, Guntupalli S. Endometrial cancer: molecular classification and future treatments. BMJ Med. 2022;1(1):e000152.

202. Jumaah AS, Salim MM, Sahib Al-Haddad H, McAllister KA, Yasseen AA. The frequency of POLE-mutation in endometrial carcinoma and prognostic implications: A systemic review and meta-analysis. J Pathol Transl Med. 2020;54(6):471–9.

203. Jumaah AS, Al-Haddad HS, McAllister KA, Yasseen AA. The clinicopathology and survival characteristics of patients with POLE proofreading mutations in endometrial carcinoma: A systematic review and meta-analysis. PLoS One. 2022;17(2 February).

204. Vermij L, Léon-Castillo A, Singh N, Powell ME, Edmondson RJ, Genestie C, et al. p53 immunohistochemistry in endometrial cancer: clinical and

USC UNIVERSIDADE DE SANTIAGO DE COMPOSTELA

molecular correlates in the PORTEC-3 trial. Mod Pathol. 2022;35(10):1475–83.

205. Ashley CW, Da Cruz Paula A, Kumar R, Mandelker D, Pei X, Riaz N, et al. Analysis of mutational signatures in primary and metastatic endometrial cancer reveals distinct patterns of DNA repair defects and shifts during tumor progression. Gynecol Oncol. 2019;152(1):11–9.

206. Harbour JW, Luo RX, Dei Santi A, Postigo AA, Dean DC. Cdk phosphorylation triggers sequential intramolecular interactions that progressively block Rb functions as cells move through G1. Cell. 1999;98(6):859–69.

207. Berry JL, Polski A, Cavenee WK, Dryja TP, Linn Murphree A, Gallie BL. The RB1 story: Characterization and cloning of the first tumor suppressor gene. Genes (Basel). 2019;10(11).

208. Liang L, Wang H, Shi H, Li Z, Yao H, Bu Z, et al. A Designed Peptide Targets Two Types of Modifications of p53 with Anti-cancer Activity. Cell Chem Biol. 2018;25(6):761-774.e5.

209. Arena G, Riscal R, Linares LK, Le Cam L. MDM2 controls gene expression independently of p53 in both normal and cancer cells. Cell Death Differ. 2018;25(9):1533–5.

210. Bohlman S, Manfredi JJ. p53-independent effects of Mdm2. Subcell Biochem. 2014;85:235–46.

211. Ramón y Cajal S, Sesé M, Capdevila C, Aasen T, De Mattos-Arruda L, Diaz-Cano SJ, et al. Clinical implications of intratumor heterogeneity: challenges and opportunities. J Mol Med. 2020;98(2):161–77.

212. Mota A, Colás E, García-Sanz P, Campoy I, Rojo-Sebastián A, Gatius S, et al. Genetic analysis of uterine aspirates improves the diagnostic value and captures the intra-tumor heterogeneity of endometrial cancers. Mod Pathol. 2017;30(1):134–45.

213. Lindemann K, Kildal W, Kleppe A, Tobin KAR, Pradhan M, Isaksen MX, et al. Impact of molecular profile on prognosis and relapse pattern in low and intermediate risk endometrial cancer. Eur J Cancer. 2024;200.

214. McAlpine JN, Chiu DS, Nout RA, Church DN, Schmidt P, Lam S, et al. Evaluation of treatment effects in patients with endometrial cancer and POLE mutations: An individual patient data meta-analysis. Cancer. 2021;127(14):2409–22.

USC UNIVERSIDADE DE SANTIAGO DE COMPOSTELA

215. Ye C , Ma Y , Zhang Q , li G ZW. Prognostic Analysis of PTEN Mutation in Endometrial Carcinoma. Eur PMC. 2022;

216. Gbelcová H, Gergely L, Šišovský V, Straka, Böhmer D, Pastoráková A, et al. PTEN mutations as predictive marker for the high-grade endometrial cancer development in slovak women. Physiol Res. 2022;71:S125–35.

217. Salvesen HB, Stefansson I, Kalvenes MB, Das S, Akslen LA. Loss of PTEN expression is associated with metastatic disease in patients with endometrial carcinoma. Cancer. 2002;94(8):2185–91.

218. Travaglino A, Raffone A, Raimondo D, Reppuccia S, Ruggiero A, Arena A, et al. Prognostic significance of CTNNB1 mutation in early stage endometrial carcinoma: a systematic review and meta-analysis. Arch Gynecol Obstet. 2022;306(2):423–31.

219. Ledinek Ž, Sobočan M, Knez J. The Role of CTNNB1 in Endometrial Cancer. Dis Markers. 2022;2022.

220. Costigan DC, Dong F, Nucci MR, Howitt BE. Clinicopathologic and immunohistochemical correlates of CTNNB1 mutated endometrial endometrioid carcinoma. Int J Gynecol Pathol. 2020;39(2):119–27.

221. Kurnit KC, Kim GN, Fellman BM, Urbauer DL, Mills GB, Zhang W, et al. CTNNB1 (beta-catenin) mutation identifies low grade, early stage endometrial cancer patients at increased risk of recurrence. Mod Pathol. 2017;30(7):1032–41.

222. Green AK, Feinberg J, Makker V. A Review of Immune Checkpoint Blockade Therapy in Endometrial Cancer. Am Soc Clin Oncol Educ B. 2020;(40):238–44.

223. Watanabe T, Nanamiya H, Kojima M, Nomura S, Furukawa S, Soeda S, et al. Clinical relevance of oncogenic driver mutations identified in endometrial carcinoma. Transl Oncol. 2021;14(3).

224. Linn P, Kohno S, Sheng J, Kulathunga N, Yu H, Zhang Z, et al. Targeting RB1 loss in cancers. Cancers (Basel). 2021;13(15).

225. Zoumpoulidou G, Alvarez-Mendoza C, Mancusi C, Ahmed RM, Denman M, Steele CD, et al. Therapeutic vulnerability to PARP1,2 inhibition in RB1-mutant osteosarcoma. Nat Commun. 2021;12(1).

226. Alaseem AM. Advancements in MDM2 inhibition: Clinical and pre-clinical investigations of combination therapeutic regimens. Saudi

USC UNIVERSIDADE DE SANTIAGO DE COMPOSTELA

Pharm J. 2023;31(10).

227. Takeda T, Banno K, Okawa R, Yanokura M, Iijima M, Iriekunitomi H, et al. ARID1A gene mutation in ovarian and endometrial cancers (Review). Oncol Rep. 2016;35(2):607–13.

228. Ashley CW, Selenica P, Patel J, Wu M, Nincevic J, Lakhman Y, et al. High-Sensitivity Mutation Analysis of Cell-Free DNA for Disease Monitoring in Endometrial Cancer. Clin Cancer Res. 2023;29(2):410–21.

229. Moss EL, Gorsia DN, Collins A, Sandhu P, Foreman N, Gore A, et al. Utility of Circulating Tumor DNA for Detection and Monitoring of Endometrial Cancer Recurrence and Progression. Cancers (Basel). 2020 Aug 10;12(8).

230. Chan Hiu Ting, Chin Yoon Ming, Nakamura Yusuke, Low Siew-Kee. Clonal Hematopoiesis in Liquid Biopsy: From Biological Noise to Valuable Clinical Implications. Cancers (Basel). 2020;

231. Fabre MA, de Almeida JG, Fiorillo E, Mitchell E, Damaskou A, Rak J, et al. The longitudinal dynamics and natural history of clonal haematopoiesis. Nature. 2022;606(7913):335–42.

232. Emily Mitchell, Michael Spencer Chapman, Nicholas Williams, Kevin J. Dawson, Nicole Mende, Emily F. Calderbank, Hyunchul Jung, Thomas Mitchell, Tim H. H. Coorens, David H. Spencer, Heather Machado, Henry Lee-Six, Megan Davies, Daniel Hayler, Margarete A. …Peter J. Campbell. Clonal dynamics of haematopoiesis across the human lifespan. Nature. 2022

233. Vasseur D, Arbab A, Giudici F, Marzac C, Michiels S, Tagliamento M, et al. Genomic landscape of liquid biopsy mutations in TP53 and DNA damage genes in cancer patients. npj Precis Oncol. 2024;8(1).

234. Kar SP, Quiros PM, Gu M, Jiang T, Mitchell J, Langdon R, et al. Genome-wide analyses of 200,453 individuals yield new insights into the causes and consequences of clonal hematopoiesis. Nat Genet. 2022;54(8):1155–66.

235. Pich O, Reyes-Salazar I, Gonzalez-Perez A, Lopez-Bigas N. Discovering the drivers of clonal hematopoiesis. Nat Commun. 2022;13(1).

236. Llauradó M, Ruiz A, Majem B, Ertekin T, Colás E, Pedrola N, et al. Molecular bases of endometrial cancer: New roles for new actors in the diagnosis and the therapy of the disease. Mol Cell Endocrinol.

USC UNIVERSIDADE DE SANTIAGO DE COMPOSTELA

2012;358(2):244–55.

237. Siegel RL, Miller KD, Fuchs HE, Jemal A. Cancer statistics, 2022. CA Cancer J Clin. 2022;72(1):7–33.

238. Zhang B, Xing X, Li J, Lowdon RF, Zhou Y, Lin N, et al. Comparative DNA methylome analysis of endometrial carcinoma reveals complex and distinct deregulation of cancer promoters and enhancers. BMC Genomics. 2014 Dec 6;15(1):868.

239. Xu T, Ding H, Chen J, Lei J, Zhao M, Ji B, et al. Research Progress of DNA Methylation in Endometrial Cancer. Biomolecules. 2022 Jul 4;12(7):938.

240. Smith ZD, Meissner A. DNA methylation: roles in mammalian development. Nat Rev Genet. 2013 Mar 12;14(3):204–20.

241. Greenberg MVC, Bourc'his D. The diverse roles of DNA methylation in mammalian development and disease. Nat Rev Mol Cell Biol. 2019;20(10):590–607.

242. Seeber LMS, Zweemer RP, Marchionni L, Massuger LFAG, Smit VTHBM, van Baal WM, et al. Methylation profiles of endometrioid and serous endometrial cancers. Endocr Relat Cancer. 2010 Sep;17(3):663–73.

243. Makabe T, Arai E, Hirano T, Ito N, Fukamachi Y, Takahashi Y, et al. Genome-wide DNA methylation profile of early-onset endometrial cancer: its correlation with genetic aberrations and comparison with late-onset endometrial cancer. Carcinogenesis. 2019 Jul 4;40(5):611–23.

244. Beinse G, Borghese B, Métairie M, Just PA, Poulet G, Garinet S, et al. Highly Specific Droplet-Digital PCR Detection of Universally Methylated Circulating Tumor DNA in Endometrial Carcinoma. Clin Chem. 2022 Jun 1;68(6):782–93.

245. Müller F, Scherer M, Assenov Y, Lutsik P, Walter J, Lengauer T, et al. RnBeads 2.0: comprehensive analysis of DNA methylation data. Genome Biol. 2019 Dec 14;20(1):55.

246. Garcia-Moreno A, López-Domínguez R, Villatoro-García JA, Ramirez-Mena A, Aparicio-Puerta E, Hackenberg M, et al. Functional Enrichment Analysis of Regulatory Elements. Biomedicines. 2022;10(3).

247. Colaprico A, Silva TC, Olsen C, Garofano L, Garolini D, Cava C, et al.

USC UNIVERSIDADE DE SANTIAGO DE COMPOSTELA

TCGAbiolinks: An R/Bioconductor package for integrative analysis with GDC data. 2023

248. Neman J, Termini J, Wilczynski S, Vaidehi N, Choy C, Kowolik CM, et al. Human breast cancer metastases to the brain display GABAergic properties in the neural niche. Proc Natl Acad Sci U S A. 2014;111(3):984–9.

249. Zhang X, Zhang R, Zheng Y, Shen J, Xiao D, Li J, et al. Expression of gamma-aminobutyric acid receptors on neoplastic growth and prediction of prognosis in non-small cell lung cancer. J Transl Med. 2013;11(1):1–10.

250. Wei B, Zhu Y, Yang P, Han Y, Wang S, Wang X, et al. GABAB1e promotes the malignancy of human cancer cells by targeting the tyrosine phosphatase PTPN12. iScience. 2021;24(11):103311.

251. Huang D, Wang Y, Thompson JW, Yin T, Alexander PB, Qin D, et al. Cancer-cell-derived GABA promotes β-catenin-mediated tumour growth and immunosuppression. Nat Cell Biol. 2022;24(2):230–41.

252. Bhattacharya D, Gawali VS, Kallay L, Toukam DK, Koehler A, Stambrook P, et al. Therapeutically leveraging GABAA receptors in cancer. Exp Biol Med. 2021;246(19):2128–35.

253. TERUNUMA M. Diversity of structure and function of GABAB receptors: a complexity of GABAB-mediated signaling. Proc Japan Acad Ser B. 2018 Dec 11;94(10):390–411.

254. Nicholson-Guthrie CS, Guthrie GD, Sutton GP, Baenziger JC. Urine GABA levels in ovarian cancer patients: Cancer Lett. 2001 Jan;162(1):27–30.

255. Sung HY, Yang SD, Ju W, Ahn JH. Aberrant epigenetic regulation of GABRP associates with aggressive phenotype of ovarian cancer. Exp Mol Med. 2017;49(5):1–9.

256. KRISHEK BJ, MOSS SJ, SMART TG. A Functional Comparison of the Antagonists Bicuculline and Picrotoxin at Recombinant GABA A Receptors. Neuropharmacology. 1996;35(9–10):1289–98.

257. Takehara A, Hosokawa M, Eguchi H, Ohigashi H, Ishikawa O, Nakamura Y, et al. γ-aminobutyric acid (GABA) stimulates pancreatic cancer growth through overexpressing GABAA receptor π subunit. Cancer Res. 2007;67(20):9704–12.

USC UNIVERSIDADE DE SANTIAGO DE COMPOSTELA

258. Ippolito JE, Merritt ME, Bäckhed F, Moulder KL, Mennerick S, Manchester JK, et al. Linkage between cellular communications, energy utilization, and proliferation in metastatic neuroendocrine cancers. Proc Natl Acad Sci. 2006 Aug 15;103(33):12505–10.

259. Abdul M, Mccray SD, Hoosein NM. Expression of gamma-aminobutyric acid receptor (subtype A) in prostate cancer. Acta Oncol (Madr). 2008 Jan 8;47(8):1546–50.

260. Solorzano SR, Imaz-Rosshandler I, Camacho-Arroyo I, García-Tobilla P, Morales-Montor G, Salazar P, et al. GABA promotes gastrin-releasing peptide secretion in NE/NE-like cells: Contribution to prostate cancer progression. Sci Rep. 2018 Jul 6;8(1):10272.

261. Wu L, Lian W, Zhao L. Calcium signaling in cancer progression and therapy. FEBS J. 2021 Nov 28;288(21):6187–205.

262. Huang T, Zhou J, Wang J. Calcium and calcium-related proteins in endometrial cancer: opportunities for pharmacological intervention. Int J Biol Sci. 2022;18(3):1065–78.

263. Shen B, Hao J, Lin Y, Li X, Yang X, Huang T, et al. Estrogen-Induced Extracellular Calcium Influx Promotes Endometrial Cancer Progress by Regulating Lysosomal Activity and Mitochondrial ROS. Front Med. 2022 Feb 10;9.

264. Jones CA, Hazlehurst LA. Role of Calcium Homeostasis in Modulating EMT in Cancer. Biomedicines. 2021 Sep 11;9(9):1200.

265. Tian X, Wang J, Jiang L, Jiang Y, Xu J, Feng X. Chemokine/GPCR Signaling-Mediated EMT in Cancer Metastasis. J Oncol. 2022;2022.

266. Jean-Charles PY, Kaur S, Shenoy SK. G Protein-Coupled Receptor Signaling Through β-Arrestin-Dependent Mechanisms. J Cardiovasc Pharmacol. 2017;70(3):142–58.

267. Li J, Wang AS, Wang S, Wang CY, Xue S, Li WY, et al. Death-inducer obliterator 1 (DIDO1) silencing suppresses the growth of bladder cancer cells through decreasing SAPK/JNK signaling cascades. Neoplasma. 2020;67(05):1074–84.

268. Zhang Y, Jiang J, Zhang J, Shen H, Wang M, Guo Z, et al. CircDIDO1 inhibits gastric cancer progression by encoding a novel DIDO1-529aa protein and regulating PRDX2 protein stability. Mol Cancer. 2021 Dec 12;20(1):101.

USC UNIVERSIDADE DE SANTIAGO DE COMPOSTELA

269. Kurnit KC, Westin SN, Coleman RL. Microsatellite instability in endometrial cancer: New purpose for an old test. Cancer. 2019;125(13):2154–63.

270. Li K, Luo H, Huang L, Luo H, Zhu X. Microsatellite instability: a review of what the oncologist should know. Cancer Cell Int. 2020 Dec 13;20(1):16.

271. Garrido-Ramos M. Satellite DNA: An Evolving Topic. Genes (Basel). 2017 Sep 18;8(9):230.

272. Eshleman JR, Markowitz SD. Mismatch repair defects in human carcinogenesis. Hum Mol Genet. 1996 Sep;5(Supplement_1):1489–94.

273. Giardiello FM, Allen JI, Axilbund JE, Boland CR, Burke CA, Burt RW, et al. Guidelines on Genetic Evaluation and Management of Lynch Syndrome: A Consensus Statement by the US Multi-Society Task Force on Colorectal Cancer. Gastroenterology. 2014 Aug;147(2):502–26.

274. Tafe LJ, Riggs ER, Tsongalis GJ. Lynch Syndrome Presenting as Endometrial Cancer. Clin Chem. 2014 Jan 1;60(1):111–21.

275. Le DT, Durham JN, Smith KN, Wang H, Bartlett BR, Aulakh LK, et al. Mismatch repair deficiency predicts response of solid tumors to PD-1 blockade. Science (80-). 2017 Jul 28;357(6349):409–13.

276. Oaknin A, Tinker A V., Gilbert L, Samouëlian V, Mathews C, Brown J, et al. Clinical Activity and Safety of the Anti–Programmed Death 1 Monoclonal Antibody Dostarlimab for Patients With Recurrent or Advanced Mismatch Repair–Deficient Endometrial Cancer. JAMA Oncol. 2020 Nov 1;6(11):1766.

277. Stelloo E, Nout RA, Osse EM, Jürgenliemk-Schulz IJ, Jobsen JJ, Lutgens LC, et al. Improved risk assessment by integrating molecular and clinicopathological factors in early-stage endometrial cancer-combined analysis of the PORTEC cohorts. Clin Cancer Res. 2016;22(16):4215–24.

278. Rodriguez-Bigas MA, Boland CR, Hamilton SR, Henson DE, Jass JR, Khan PM, et al. A National Cancer Institute Workshop on Hereditary Nonpolyposis Colorectal Cancer Syndrome: meeting highlights and Bethesda guidelines. J Natl Cancer Inst. 1997;89(23):1758–62.

279. Stelloo E, Jansen AML, Osse EM, Nout RA, Creutzberg CL, Ruano D, et al. Practical guidance for mismatch repair-deficiency testing in endometrial cancer. Ann Oncol Off J Eur Soc Med Oncol.

USC UNIVERSIDADE DE SANTIAGO DE COMPOSTELA

2017;28(1):96–102.

280. Evrard C, Tachon G, Randrian V, Karayan-Tapon L, Tougeron D. Microsatellite instability: Diagnosis, heterogeneity, discordance, and clinical impact in colorectal cancer. Cancers (Basel). 2019;11(10).

281. Umar A, Boland CR, Terdiman JP, Syngal S, Chapelle A d. l., Ruschoff J, et al. Revised Bethesda Guidelines for Hereditary Nonpolyposis Colorectal Cancer (Lynch Syndrome) and Microsatellite Instability. JNCI J Natl Cancer Inst. 2004 Feb 18;96(4):261–8.

282. Suraweera N, Duval A, Reperant M, Vaury C, Furlan D, Leroy K, et al. Evaluation of tumor microsatellite instability using five quasimonomorphic mononucleotide repeats and pentaplex PCR. Gastroenterology. 2002 Dec;123(6):1804–11.

283. Boldrin E, Piano MA, Alfieri R, Mazza M, Vassallo L, Scapinello A, et al. Msi analysis in solid and liquid biopsies of gastroesophageal adenocarcinoma patients: A molecular approach. Int J Mol Sci. 2021;22(14).

284. Wong YF, Cheung TH, Lo KWK, Yim SF, Chan LKY, Buhard O, et al. Detection of microsatellite instability in endometrial cancer: advantages of a panel of five mononucleotide repeats over the National Cancer Institute panel of markers. Carcinogenesis. 2006 May 1;27(5):951–5.

285. Libera L, Craparotta I, Sahnane N, Chiaravalli AM, Mannarino L, Cerutti R, et al. Targeted gene sequencing of Lynch syndrome–related and sporadic endometrial carcinomas. Hum Pathol. 2018 Nov;81:235–44.

286. Gómez-Raposo C, Merino Salvador M, Aguayo Zamora C, García de Santiago B, Casado Sáenz E. Immune checkpoint inhibitors in endometrial cancer. Crit Rev Oncol Hematol. 2021;161.

287. Ott PA, Bang YJ, Berton-Rigaud D, Elez E, Pishvaian MJ, Rugo HS, et al. Safety and antitumor activity of pembrolizumab in advanced programmed death ligand 1–positive endometrial cancer: Results from the KEYNOTE-028 study. J Clin Oncol. 2017;35(22):2535–41.

288. Wu X, Snir O, Rottmann D, Wong S, Buza N, Hui P. Minimal microsatellite shift in microsatellite instability high endometrial cancer: a significant pitfall in diagnostic interpretation. Mod Pathol. 2019;32(5):650–8.

289. Kaneko E, Sato N, Sugawara T, Noto A, Takahashi K, Makino K, et al.

USC UNIVERSIDADE DE SANTIAGO DE COMPOSTELA

MLH1 promoter hypermethylation predicts poorer prognosis in mismatch repair deficiency endometrial carcinomas. J Gynecol Oncol. 2021;32(6).

290. Zighelboim I, Goodfellow PJ, Gao F, Gibb RK, Powell MA, Rader JS, et al. Microsatellite Instability and Epigenetic Inactivation of MLH1 and Outcome of Patients With Endometrial Carcinomas of the Endometrioid Type. J Clin Oncol. 2007 May 20;25(15):2042–8.

291. Müller A, Giuffre G, Edmonston TB, Mathiak M, Roggendorf B, Heinmöller E, et al. Challenges and pitfalls in HNPCC screening by microsatellite analysis and immunohistochemistry. J Mol Diagn. 2004 Nov;6(4):308–15.

292. Akahane T, Kitazono I, Yanazume S, Kamio M, Togami S, Sakamoto I, et al. Next-generation sequencing analysis of endometrial screening liquid-based cytology specimens: A comparative study to tissue specimens. BMC Med Genomics. 2020;13(1).

293. Watkins JC, Nucci MR, Ritterhouse LL, Howitt BE, Sholl LM. Unusual mismatch repair immunohistochemical patterns in endometrial carcinoma. Am J Surg Pathol. 2016;40(7):909–16.

294. Silveira AB, Bidard FC, Kasperek A, Melaabi S, Tanguy ML, Rodrigues M, et al. High-Accuracy Determination of Microsatellite Instability Compatible with Liquid Biopsies. Clin Chem. 2020;66(4):606–13.

295. Willis J, Lefterova MI, Artyomenko A, Kasi PM, Nakamura Y, Mody K, et al. Validation of microsatellite instability detection using a comprehensive plasma-based genotyping panel. Clin Cancer Res. 2019;25(23):7035–45.

296. Wang Z, Zhao X, Gao C, Gong J, Wang X, Gao J, et al. Plasma-based microsatellite instability detection strategy to guide immune checkpoint blockade treatment. J Immunother Cancer. 2020 Nov 10;8(2):e001297.

297. Cai Z, Wang Z, Liu C, Shi D, Li D, Zheng M, et al. Detection of Microsatellite Instability from Circulating Tumor DNA by Targeted Deep Sequencing. J Mol Diagnostics. 2020 Jul;22(7):860–70.

298. Gilson P, Merlin JL, Harlé A. Detection of Microsatellite Instability: State of the Art and Future Applications in Circulating Tumour DNA (ctDNA). Cancers (Basel). 2021 Mar 24;13(7).

299. Siravegna G, Marsoni S, Siena S, Bardelli A. Integrating liquid biopsies

USC UNIVERSIDADE DE SANTIAGO DE COMPOSTELA

into the management of cancer. Nat Rev Clin Oncol. 2017;14(9):531–48.

300. Mota A, Oltra SS, Selenica P, Moiola CP, Casas-Arozamena C, López-Gil C, et al. Intratumor genetic heterogeneity and clonal evolution to decode endometrial cancer progression. Oncogene. 2022 Mar 25;41(13):1835–50.

301. Chen Q, Zhang ZH, Wang S, Lang JH. Circulating cell-free DNA or circulating tumor dna in the management of ovarian and endometrial cancer. Onco Targets Ther. 2019;12:11517–30.

302. Reichert ZR, Morgan TM, Li G, Castellanos E, Snow T, Dall'Olio FG, et al. Prognostic value of plasma circulating tumor DNA fraction across four common cancer types: a real-world outcomes study. Ann Oncol. 2023;34(1):111–20.

303. Nakamura Y, Okamoto W, Kato T, Esaki T, Kato K, Komatsu Y, et al. Circulating tumor DNA-guided treatment with pertuzumab plus trastuzumab for HER2-amplified metastatic colorectal cancer: a phase 2 trial. Nat Med. 2021 Nov 11;27(11):1899–903.

304. Wan JCM, Stephens D, Luo L, White JR, Stewart CM, Rousseau B, et al. Genome-wide mutational signatures in low-coverage whole genome sequencing of cell-free DNA. Nat Commun. 2022;13(1):1–12.

305. Blitzer GC, Zhao SG, Bradley KA, Hartenbach EM. The role of ctDNA in endometrial cancer: A tool for risk stratification and disease monitoring. Gynecol Oncol. 2023 Aug;

306. Shen Y, Shi R, Zhao R, Wang H. Clinical application of liquid biopsy in endometrial carcinoma. Med Oncol. 2023;40(3):1–6.

307. Cicchillitti L, Corrado G, de Angeli M, Mancini E, Baiocco E, Patrizi L, et al. Circulating cell-free DNA content as blood based biomarker in endometrial cancer. Oncotarget. 2017;8(70):115230–43.

308. Dobrzycka B, Terlikowski SJ, Mazurek A, Kowalczuk O, Niklinska W, Chyczewski L, et al. Circulating free DNA, p53 antibody and mutations of KRAS gene in endometrial cancer. Int J Cancer. 2010;127(3):612–21.

309. Bolivar AM, Luthra R, Mehrotra M, Chen W, Barkoh BA, Hu P, et al. Targeted next-generation sequencing of endometrial cancer and matched circulating tumor DNA: identification of plasma-based, tumor-associated mutations in early stage patients. Mod Pathol.

USC UNIVERSIDADE DE SANTIAGO DE COMPOSTELA

2019;32(3):405–14.

310. Feng W, Jia N, Jiao H, Chen J, Chen Y, Zhang Y, et al. Circulating tumor DNA as a prognostic marker in high-risk endometrial cancer. J Transl Med. 2021;19(1):1–11.

311. Casas-Arozamena C, Cortegoso A, Piñeiro-Perez R, Abalo A, Arias E, Sampayo V, et al. Improving the Management of Endometrial Cancer Patients through the Use of Liquid Biopsy Analyses: A Case Report. Int J Mol Sci. 2022;23(15):1–11.

312. Trulson I, Stahl J, Margraf S, Scholz M, Hoecherl E, Wolf K, et al. Cell-Free DNA in Plasma and Serum Indicates Disease Severity and Prognosis in Blunt Trauma Patients. Diagnostics. 2023;13(6).

313. Grabuschnig S, Bronkhorst AJ, Holdenrieder S, Rodriguez IR, Schliep KP, Schwendenwein D, et al. Putative origins of cell-free DNA in humans: A review of active and passive nucleic acid release mechanisms. Int J Mol Sci. 2020;21(21):1–24.

314. Madsen AT, Hojbjerg JA, Sorensen BS, Winther-Larsen A. Day-to-day and within-day biological variation of cell-free DNA. EBioMedicine. 2019;49:284–90.

315. Mondelo-Macía P, García-González J, Abalo A, Mosquera-Presedo M, Aguín S, Mateos M, et al. Plasma cell-free DNA and circulating tumor cells as prognostic biomarkers in small cell lung cancer patients. Transl Lung Cancer Res. 2022;11(10):1995–2009.

316. Vizza E, Corrado G, De Angeli M, Carosi M, Mancini E, Baiocco E, et al. Serum DNA integrity index as a potential molecular biomarker in endometrial cancer. J Exp Clin Cancer Res. 2018;37(1).

317. Grassi T, Harris FR, Smadbeck JB, Murphy SJ, Block MS, Multinu F, et al. Personalized tumor-specific DNA junctions to detect circulating tumor in patients with endometrial cancer. PLoS One. 2021;16(6 June).

318. Qiu B, Guo W, Zhang F, Lv F, Ji Y, Peng Y, et al. Dynamic recurrence risk and adjuvant chemotherapy benefit prediction by ctDNA in resected NSCLC. Nat Commun. 2021;12(1).

319. Diehn M, Alizadeh AA, Adams HP, Lee JJ, Klassen S, Palma JF, et al. Early prediction of clinical outcomes in resected stage II and III colorectal cancer (CRC) through deep sequencing of circulating tumor DNA (ctDNA). J Clin Oncol. 2017;35(15_suppl):3591–3591.

USC UNIVERSIDADE DE SANTIAGO DE COMPOSTELA

320. Tie J, Cohen JD, Wang Y, Christie M, Simons K, Lee M, et al. Circulating tumor dna analyses as markers of recurrence risk and benefit of adjuvant therapy for stage III colon cancer. JAMA Oncol. 2019;5(12):1710–7.

321. Gale D, Heider K, Ruiz-Valdepenas A, Hackinger S, Perry M, Marsico G, et al. Residual ctDNA after treatment predicts early relapse in patients with early-stage non-small cell lung cancer. Ann Oncol. 2022;33(5):500–10.

322. Garcia-Murillas I, Chopra N, Comino-Méndez I, Beaney M, Tovey H, Cutts RJ, et al. Assessment of Molecular Relapse Detection in Early-Stage Breast Cancer. JAMA Oncol. 2019;5(10):1473–8.

323. Cristofanilli M, Hayes DF, Budd GT, Ellis MJ, Stopeck A, Reuben JM, et al. Circulating tumor cells: A novel prognostic factor for newly diagnosed metastatic breast cancer. J Clin Oncol. 2005;23(7):1420–30.

324. De Bono JS, Scher HI, Montgomery RB, Parker C, Miller MC, Tissing H, et al. Circulating tumor cells predict survival benefit from treatment in metastatic castration-resistant prostate cancer. Clin Cancer Res. 2008;14(19):6302–9.

325. Cohen SJ, Punt CJA, Iannotti N, Saidman BH, Sabbath KD, Gabrail NY, et al. Relationship of circulating tumor cells to tumor response, progression-free survival, and overall survival in patients with metastatic colorectal cancer. J Clin Oncol. 2008;26(19):3213–21.

326. Ni T, Sun X, Shan B, Wang J, Liu Y, Gu SL, et al. Detection of circulating tumour cells may add value in endometrial cancer management. Eur J Obstet Gynecol Reprod Biol. 2016;207:1–4.

327. Lemech CR, Ensell L, Paterson JC, Eminowicz G, Lowe H, Arora R, et al. Enumeration and Molecular Characterisation of Circulating Tumour Cells in Endometrial Cancer. Oncology. 2016;91(1):48–54.

328. Abreu M, Cabezas-Sainz P, Pereira-Veiga T, Falo C, Abalo A, Morilla I, et al. Looking for a Better Characterization of Triple-Negative Breast Cancer by Means of Circulating Tumor Cells. J Clin Med. 2020 Jan 27;9(2):353.

329. Cohen EN, Jayachandran G, Gao H, Peabody P, McBride HB, Alvarez FD, et al. Phenotypic Plasticity in Circulating Tumor Cells Is Associated with Poor Response to Therapy in Metastatic Breast Cancer Patients. Cancers (Basel). 2023;15(5).

USC UNIVERSIDADE DE SANTIAGO DE COMPOSTELA

330. Kolostova K, Spicka J, Matkowski R, Bobek V. Isolation, primary culture, morphological and molecular characterization of circulating tumor cells in gynecological cancers. Am J Transl Res. 2015;7(7):1203–13.

331. Kiss I, Kolostova K, Matkowski R, Jędryka M, Czekański A, Pavlasek J, et al. Correlation between disease stage and the presence of viable circulating tumor cells in endometrial cancer. Anticancer Res. 2018;38(5):2983–7.

332. Hamilton G, Rath B. Applicability of tumor spheroids for in vitro chemosensitivity assays. Expert Opin Drug Metab Toxicol. 2019;15(1):15–23.

333. Kiyohara Y, Yoshino K, Kubota S, Okuyama H, Endo H, Ueda Y, et al. Drug screening and grouping by sensitivity with a panel of primary cultured cancer spheroids derived from endometrial cancer. Cancer Sci. 2016;107(4):452–60.

334. Cao M, Liu Z, You D, Pan Y, Zhang Q. TMT-based quantitative proteomic analysis of spheroid cells of endometrial cancer possessing cancer stem cell properties. Stem Cell Res Ther. 2023;14(1).

335. Gibson WJ, Hoivik EA, Halle MK, Taylor-Weiner A, Cherniack AD, Berg A, et al. The genomic landscape and evolution of endometrial carcinoma progression and abdominopelvic metastasis. Physiol Behav. 2017;176(5):139–48.

336. Lõhmussaar K, Oka R, Espejo Valle-Inclan J, Smits MHH, Wardak H, Korving J, et al. Patient-derived organoids model cervical tissue dynamics and viral oncogenesis in cervical cancer. Cell Stem Cell. 2021;28(8):1380-1396.e6.

337. Maru Y, Tanaka N, Itami M, Hippo Y. Efficient use of patient-derived organoids as a preclinical model for gynecologic tumors. Gynecol Oncol. 2019;154(1):189–98.

338. Wörsdörfer P, Rockel A, Alt Y, Kern A, Ergün S. Generation of Vascularized Neural Organoids by Co-culturing with Mesodermal Progenitor Cells. STAR Protoc. 2020;1(1).

339. Wokołorczyk D, Kluźniak W, Huzarski T, Gronwald J, Szymiczek A, Rusak B, et al. Mutations in ATM, NBN and BRCA2 predispose to aggressive prostate cancer in Poland. Int J Cancer. 2020 Nov 15;147(10):2793–800.

USC UNIVERSIDADE DE SANTIAGO DE COMPOSTELA

340. Wu Z, Li S, Tang X, Wang Y, Guo W, Cao G, et al. Copy Number Amplification of DNA Damage Repair Pathways Potentiates Therapeutic Resistance in Cancer. Theranostics. 2020;10(9):3939–51.

341. Santoro A, Angelico G, Travaglino A, Inzani F, Arciuolo D, Valente M, et al. New Pathological and Clinical Insights in Endometrial Cancer in View of the Updated ESGO/ESTRO/ESP Guidelines. Cancers (Basel). 2021 May 26;13(11):2623.

342. Liston DR, Davis M. Clinically relevant concentrations of anticancer drugs: A guide for nonclinical studies. Clin Cancer Res. 2017;23(14):3489–98.

343. Yadav J, El Hassani M, Sodhi J, Lauschke VM, Hartman JH, Russell LE. Recent developments in in vitro and in vivo models for improved translation of preclinical pharmacokinetics and pharmacodynamics data. Drug Metab Rev. 2021;53(2):207–33.

344. Yokota E, Iwai M, Yukawa T, Yoshida M, Naomoto Y, Haisa M, et al. Clinical application of a lung cancer organoid (tumoroid) culture system. npj Precis Oncol. 2021;5(1).

345. Arias-Diaz AE, Ferreiro-Pantin M, Barbazan J, Perez-Beliz E, Ruiz-Bañobre J, Casas-Arozamena C, et al. Ascites-Derived Organoids to Depict Platinum Resistance in Gynaecological Serous Carcinomas. Int J Mol Sci. 2023;24(17).

346. Akhoon N. Precision medicine: A new paradigm in therapeutics. Int J Prev Med. 2021;12(1).

347. König IR, Fuchs O, Hansen G, von Mutius E, Kopp M V. What is precision medicine? Eur Respir J. 2017;50(4).

348. Rhrissorrakrai K, Utro F, Levovitz C, Parida L. Lesion Shedding Model: unraveling site-specific contributions to ctDNA. Brief Bioinform. 2023;24(2).

349. Dasari A, Morris VK, Allegra CJ, Atreya C, Benson AB, Boland P, et al. ctDNA applications and integration in colorectal cancer: an NCI Colon and Rectal–Anal Task Forces whitepaper. Nat Rev Clin Oncol. 2020;17(12):757–70.

350. Kotani D, Oki E, Nakamura Y, Yukami H, Mishima S, Bando H, et al. Molecular residual disease and efficacy of adjuvant chemotherapy in patients with colorectal cancer. Nat Med. 2023;29(1):127–34.

USC UNIVERSIDADE DE SANTIAGO DE COMPOSTELA

351. Prat A, Brasó-Maristany F, Martínez-Sáez O, Sanfeliu E, Xia Y, Bellet M, et al. Circulating tumor DNA reveals complex biological features with clinical relevance in metastatic breast cancer. Nat Commun. 2023;14(1).

352. Cullinane C, Fleming C, O'Leary DP, Hassan F, Kelly L, O'Sullivan MJ, et al. Association of Circulating Tumor DNA with Disease-Free Survival in Breast Cancer: A Systematic Review and Meta-analysis. JAMA Netw Open. 2020;3(11).

353. Bettegowda C, Sausen M, Leary RJ, Kinde I, Wang Y, Agrawal N, et al. Detection of circulating tumor DNA in early- and late-stage human malignancies. Sci Transl Med. 2014;6(224).

354. Dekkers JF, Alieva M, Cleven A, Keramati F, Wezenaar AKL, van Vliet EJ, et al. Uncovering the mode of action of engineered T cells in patient cancer organoids. Nat Biotechnol. 2023;41(1):60–9.

USC UNIVERSIDADE DE SANTIAGO DE COMPOSTELA

APPENDICES

USC
UNIVERSIDADE
DE SANTIAGO
DE COMPOSTELA

Appendix 1: Index of figures and Tables

A. Index of figures

1| Introduction

Figure 1: Representative immunohistochemistry haematoxylin and eosin slides of endometrial tumours 43

Figure 2: Diagram of the molecular classification and recommendations for molecular profiling in EC 47

Figure 3: Graphical representation of the most relevant pathways in EC carcinogenesis and the targetable elements 59

Figure 4: Summary of the main clinical challenges and the chapters where said challenges are tackled 61

Figure 5: Limitations and advantages of liquid and solid biopsies 63

Figure 6: Release mechanism of cfDNA 66

Figure 7: The metastatic cascade 70

Figure 8: Key differences between the different types of cell cultures 78

3|Material & Methods

Figure 1: Limit of detection for the ddPCR assays 90

4|Results

4.1| Precision Oncology in Endometrial Cancer: NGS Perspectives on Minimally Invasive Samples

Figure 1: Clinico-pathological features of the studied cohort 100

Figure 2: Heatmap representative of the top 15 alterations found in the UA 103

Figure 3: Distribution of the most prevalent mutations according to histology .. 105

Figure 4: The TCGA classification allows for the stratification of EC patients 106

Figure 5: Patients with *TP53* mutated present significantly shorted DFS independently of the FIGO Stage 107

USC UNIVERSIDADE DE SANTIAGO DE COMPOSTELA

Figure 6: Genomic distribution in the NSMP molecular subtype 108

Figure 7: Genomic alterations in advanced disease 109

Figure 8: Summary of the quality metrics for the NGS analyses of the cfDNA ... 112

Figure 9: Heatmap with the found alterations in cfDNA and correspondence with tissue 113

Figure 10: The longitudinal analyses of ctDNA through an NGS targeted approach allows to monitor the disease evolution 115

4.2| Epigenetic regulation in Endometrial Carcinoma: Insights from Methylome Profiling

Figure 1: Quality metrics of the methylome studies in the UA 128

Figure 2: NEEC present a differential methylome profile. 130

Figure 3: Validation of the array through pyrosequencing 132

4.3| Non-invasive detection of microsatellite instability in patients with endometrial cancer

Figure 1: Overview of the ddPCR and IHC assay 143

Figure 2: Correlation between the UA and FFPE VAFs using the ddPCR assay ... 145

Figure 3: Concordance between the SoC and the UA 148

Figure 4: Differential mutational landscape in dMMR and pMMR patients 150

Figure 5: Concordance between the UA and the cfDNA 152

Figure 6: Sensitivity and specificity of the ddPCR assay for identification of patients and follow up the disease. 155

Figure 7: Distribution of the cfDNA and ctDNA levels according to clinico-pathological features 156

4.4| Unveiling Endometrial Cancer Prognosis: Integrating cfDNA and ctDNA for Predictive and follow up Analysis

Figure 1: Design of the cfDNA and ctDNA analyses in the cohort of endometrial cancer patients. 172

USC UNIVERSIDADE DE SANTIAGO DE COMPOSTELA

Figure 2: The value of pre-surgery cfDNA to identify patients with poor clinical outcome. 175

Figure 3: cfDNA and ctDNA levels are independent of tumour length or volume in endometrial cancer 177

Figure 4: The value of pre-surgery ctDNA to identify patients with poor clinical outcome. 180

Figure 5: Correlation between ddPCR DNA input and the detection of alterations. 181

Figure 6: Combinatory analyses of cfDNA and ctDNA identify the patients with the worst clinical outcome. 183

Figure 7: The clinical relevance of the combination of cfDNA and ctDNA analyses remains even within the more aggressive endometrial cancer subtypes. 185

Figure 8: Swimmer plot of the patients that underwent relapse regardless of the availability of samples 6 months prior to the relapse. 186

Figure 9: Longitudinal analysis of cfDNA in endometrial cancer patients. 187

Figure 10: The longitudinal analyses of cfDNA and ctDNA allow for early detection of disease progression and accurately reflect the disease kinetics in response to treatment. 190

4.5| CTCs as Prognostic Biomarkers in Endometrial Cancer: Findings from a Multicentred Study

Figure 1: CTCs are associated with more aggressive phenotypes. 204

Figure 2: The presence of CTCs is directly linked to shorter DFS and DSS. 206

4.6| Preclinical models in Endometrial cancer

Figure 1: Characterisation and pharmacological studies of the generated PDSs from patient #88. 223

Figure 2: Targeted therapies and immunotherapy are effective in PDXs from EC patients. 225

USC UNIVERSIDADE DE SANTIAGO DE COMPOSTELA

Figure 3: Representative images of the abdominal implants showing the rapid tumour progression during pembrolizumab treatment. 227

Figure 4: Characterisation and pharmacological studies of the generated PDOs from patient #127 230

Figure 5: Characterisation of the PDOs. 235

Figure 6: Dose-response curves of the different PDOs to the different chemotherapy regiments 236

USC UNIVERSIDADE DE SANTIAGO DE COMPOSTELA

B. Index of Tables

1| Introduction

Table 1: 2023 FIGO staging of cancer of the endometrium 49

Table 2: Definition of prognostic 51

Table 3: Summary of the ESGO recommended treatments to treat EC 56

3| Material & Methods

Table 1: Summary of the packages used for the statistical analysis in R. 91

4|Results

4.1| Precision Oncology in Endometrial Cancer: NGS Perspectives on Minimally Invasive Samples

Table 1: Summary of the most relevant clinico-pathological features of the cohort 101

Table 2: Comparison of the SNPs and CNAs found in the UA through the targeted panel with the TCGA available data 104

Table 3: Summary of the hazards ratio and p-values obtained with the Cox-proportional regression model 107

4.2| Epigenetic regulation in Endometrial Carcinoma: Insights from Methylome Profiling

Table 1: Summary of the most relevant clinico-pathological features of the cohort included in the cfDNA analyses 125

4.3| Non-invasive detection of microsatellite instability in patients with endometrial cancer

Table 1: Summary of the most relevant clinico-pathological features of the cohort 147

Table 2: Summary of the most relevant clinico-pathological features of the studied cohort in the cfDNA analyses 153

USC UNIVERSIDADE DE SANTIAGO DE COMPOSTELA

Table 3: Summary of the most relevant clinico-pathological features of the patients where longitudinal analyses was performed with the cfDNA 159

4.4| Unveiling Endometrial Cancer Prognosis: Integrating cfDNA and ctDNA for Predictive and follow up Analysis

Table 1: Summary of the most relevant clinico-pathological features of the cohort..... 172

Table 2: Univariate and multivariate analyses of the pre-surgical levels of cfDNA with the most relevant clinico-pathological features of the cohort..... 174

Table 3: Univariate and multivariate analyses of the pre-surgical levels of ctDNA with the most relevant clinico-pathological features of the cohort..... 179

Table 4: Summary of the most relevant clinico-pathological features of the cohort according to the combinatory approach. 182

4.5| CTCs as Prognostic Biomarkers in Endometrial Cancer: Findings from a Multicentred Study

Table 1: Summary of the most relevant clinico-pathological features of the cohort according to the presence of CTCs..... 202

Table 2: Univariate and multivariate analyses of the presence of CTCs with the most relevant clinico-pathological features of the cohort..... 207

4.6| Preclinical models in Endometrial cancer

Table 1: Specific composition of the media used to the culture of PDSs. 217

Table 2: Specific composition of the media used to the culture of PDOs..... 217

Table 3: Summary of the most relevant clinico-pathological features of the patients included for PDOs generation 232

Table 4: Summary of the most relevant clinico-pathological features of generated PDOs 232

USC UNIVERSIDADE DE SANTIAGO DE COMPOSTELA

Appendix 2: List of Publications

1| Improving the Management of Endometrial Cancer Patients through the Use of Liquid Biopsy Analyses: A Case Report.

Carlos Casas-Arozamena[#], Alexandra Cortegoso[#], Raquel Piñeiro-Perez, Alicia Abalo, Efigenia Arias, Victoria Sampayo, Ana Vilar, Marta Bouso, Eva Diaz, Gema Moreno-Bueno, Rafael López-López, Laura Muinelo-Romay, Miguel Abal*, Juan Cueva*.

[#]These authors contributed equally to this work/* Corresponding.

Int J Mol Sci, 2022; 1;23(15):8539

ISSN 1661-6596

MDPI, 1-August-2022

Full text available: https://www.mdpi.com/1422-0067/23/15/8539

Permissions- This is an open access article distributed under the terms of the Creative Commons CC-BY license which permits unrestricted use, distribution, and reproduction in any medium, provided the original work is properly cited.

Journal citation reports (JCR) category rank (2022): Q1 (66/285) Biochemistry & Molecular Biology

Journal Impact Factor (2022): 5.6

Contribution to this work: I, Carlos Casas Arozamena, was involved in conceptualization, methodology, investigation , data curation, software, writing, original draft and analysis of the data. Particularly, I performed patient sample processing, nuclei acid isolation, ddPCR assays, PDOs generation, drug screening assays, statistical analyses and manuscript writing.

USC UNIVERSIDADE DE SANTIAGO DE COMPOSTELA

2| Noninvasive detection of microsatellite instability in patients with endometrial cancer

Carlos Casas-Arozamena, Cristian Pablo Moiola, Ana Vilar, Marta Bouso, Juan Cueva, Silvia Cabrera, Victoria Sampayo, Efigenia Arias, Alicia Abalo, Ángel García, Ramón Manuel Lago-Lestón, Sara Oltra, Eva Díaz, Juan Ruiz-Bañobre, Rafael López-López, Gema Moreno-Bueno, Antonio Gil-Moreno, Eva Colás, Miguel Abal, Laura Muinelo-Romay*

* Corresponding.

Int J Cancer, 2023; 152(10):2206-2217

ISSN: 0020-7136

WILEY, 17-January-2023

Full text available: https://onlinelibrary.wiley.com/doi/10.1002/ijc.34435

Permissions- This is an open access article under the terms of the Creative Commons Attribution-NonCommercial-NoDerivs License, which permits use and distribution in any medium, provided the original work is properly cited, the use is non-commercial and no modifications or adaptations are made.

Journal citation reports (JCR) category rank (2023): Q1 (52/241) Oncology

Journal Impact Factor (2022): 6.4

Contribution to this work: I, Carlos Casas Arozamena, was involved in conceptualization, methodology, investigation , data curation, software, writing, original draft and analysis of the data. Particularly, I performed cell culture, patient sample processing, nuclei acid isolation, ddPCR assays, statistical analyses and manuscript writing.

USC UNIVERSIDADE DE SANTIAGO DE COMPOSTELA

Appendix 3: Ethical considerations and attached permissions

1| Images use

Unless clarified, all the images presented in this thesis have been produced by the author. In the case of images reused or adapted from other manuscripts, permission has been granted by the publishers, and the legal use has been clarified at the bottom of the corresponding figures.

In addition, the free resource Flaticon.com and BioRender (BioRender.com) were employed. Publications rights have been obtained for all figures under the student plan.

2| Human cell culture

All cancer lines used in this work were acquired from commercially available resources (American Tissue Culture Collection, ATCC) and cultured in the conditions recommended by the manufacturers and only used for the research purposes specifically described. All experiments within this doctoral dissertation were performed with mycoplasma-free cells. All human cell lines have been authenticated using STR (or SNP) profiling within the last 3 years.

3| Patient's samples

The studies were carried out according to the rules of the Declaration of Helsinki of 1975, revised in 2013, and according to the standards for good clinical practice and other local ethical laws and regulations. Informed consent forms, approved by the pertinent ethical committees, were signed by all patients prior to sample collection (Autonomic Galician Ethical Committee Code 2017/430 and 2021/143).

USC UNIVERSIDADE DE SANTIAGO DE COMPOSTELA

4| Animal Studies

Mice were housed and maintained under specific-pathogen-free conditions, and procedures were performed in accordance with institutional guidelines and approved by the Use Committee for Animal Care from the Universidad de Santiago de Compostela. Mice studies were approved by the appropriate ethical committee (code 15012/2021/010).

USC UNIVERSIDADE DE SANTIAGO DE COMPOSTELA

5 | Attached permissions

a. Publications and Licensing rights for images

Print

JOHN WILEY AND SONS LICENSE TERMS AND CONDITIONS

Apr 08, 2024

This Agreement between Mr. Carlos Casas Arozamena ("You") and John Wiley and Sons ("John Wiley and Sons") consists of your license details and the terms and conditions provided by John Wiley and Sons and Copyright Clearance Center.

License Number	5764160836567
License date	Apr 08, 2024
Licensed Content Publisher	John Wiley and Sons
Licensed Content Publication	Biotechnology Journal
Licensed Content Title	Historical evolution of spheroids and organoids, and possibilities of use in life sciences and medicine
Licensed Content Author	Miriane de Oliveira, Felipe Allan da Silva da Costa, Maria Teresa De Sibio, et al
Licensed Content Date	Jan 25, 2021
Licensed Content Volume	16
Licensed Content Issue	5
Licensed Content Pages	13
Type of Use	Dissertation/Thesis
Requestor type	University/Academic
Format	Print and electronic
Portion	Figure/table
Number of figures/tables	1
Will you be translating?	No
Title of new work	PERSONALISED MEDICINE IN ENDOMETRIAL CANCER THROUGH THE USE OF LIQUID BIOPSY
Institution name	Universidade Santiago de Compostela
Expected presentation date	Jun 2024
Portions	Figure 2
Requestor Location	Mr. Carlos Casas Arozamena Augusto Gonzalez Besada nº1 6ºG Pontevedra, Galicia 36001 Spain Attn: Mr. Carlos Casas Arozamena
Publisher Tax ID	EU826007151
Total	**0.00 USD**
Terms and Conditions	

TERMS AND CONDITIONS

This copyrighted material is owned by or exclusively licensed to John Wiley & Sons, Inc. or one of its group companies (each a"Wiley Company") or handled on behalf of a society with which a Wiley Company has exclusive publishing rights in relation to a particular work (collectively "WILEY"). By clicking "accept" in connection with completing this licensing transaction, you agree that the following terms and conditions apply to this transaction (along with the billing and payment terms and conditions established by the Copyright Clearance Center Inc., ("CCC's Billing and Payment terms and conditions"), at the time that you opened your RightsLink account (these are available at any time at http://myaccount.copyright.com).

USC UNIVERSIDADE DE SANTIAGO DE COMPOSTELA

49 Spadina Ave. Suite 200
Toronto ON M5V 2J1 Canada
www.biorender.com

Confirmation of Publication and Licensing Rights

April 8th, 2024
Science Suite Inc.

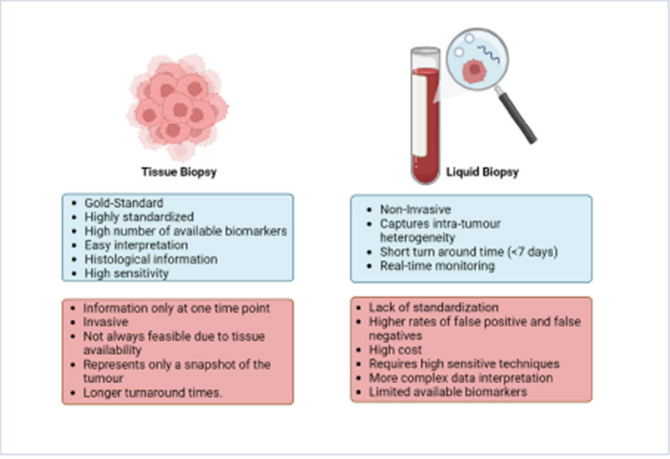
Subscription: *Student Plan*
Agreement number: *LS26OBBP4Q*
Journal name: *N/A*

To whom this may concern,

This document is to confirm that Carlos Casas arozamena has been granted a license to use the BioRender content, including icons, templates and other original artwork, appearing in the attached completed graphic pursuant to BioRender's Academic License Terms. This license permits BioRender content to be sublicensed for use in journal publications.

All rights and ownership of BioRender content are reserved by BioRender. All completed graphics must be accompanied by the following citation: "Created with BioRender.com".

BioRender content included in the completed graphic is not licensed for any commercial uses beyond publication in a journal. For any commercial use of this figure, users may, if allowed, recreate it in BioRender under an Industry BioRender Plan.



For any questions regarding this document, or other questions about publishing with BioRender refer to our BioRender Publication Guide, or contact BioRender Support at support@biorender.com.

USC UNIVERSIDADE DE SANTIAGO DE COMPOSTELA

49 Spadina Ave. Suite 200
Toronto ON M5V 2J1 Canada
www.biorender.com

Confirmation of Publication and Licensing Rights

April 8th, 2024
Science Suite Inc.

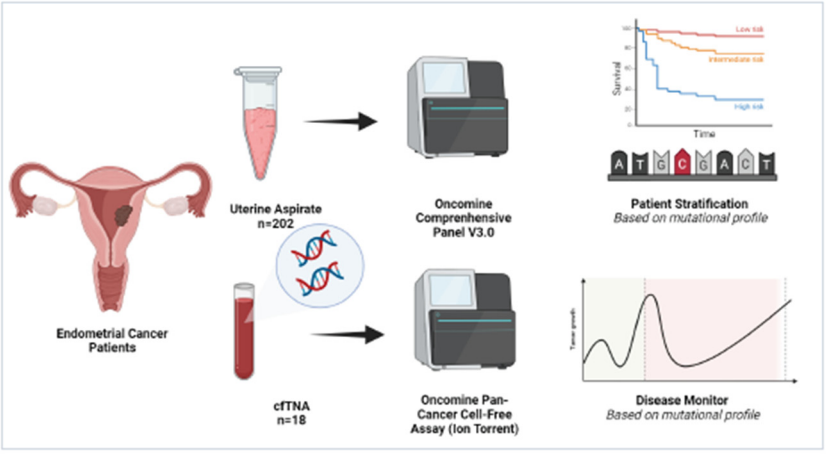
Subscription:	*Student Plan*
Agreement number:	*AZ26OBE092*
Journal name:	*N/A*

To whom this may concern,

This document is to confirm that Carlos Casas arozamena has been granted a license to use the BioRender content, including icons, templates and other original artwork, appearing in the attached completed graphic pursuant to BioRender's Academic License Terms. This license permits BioRender content to be sublicensed for use in journal publications.

All rights and ownership of BioRender content are reserved by BioRender. All completed graphics must be accompanied by the following citation: "Created with BioRender.com".

BioRender content included in the completed graphic is not licensed for any commercial uses beyond publication in a journal. For any commercial use of this figure, users may, if allowed, recreate it in BioRender under an Industry BioRender Plan.



For any questions regarding this document, or other questions about publishing with BioRender refer to our BioRender Publication Guide, or contact BioRender Support at support@biorender.com.

USC UNIVERSIDADE DE SANTIAGO DE COMPOSTELA

49 Spadina Ave. Suite 200
Toronto ON M5V 2J1 Canada
www.biorender.com

Confirmation of Publication and Licensing Rights

April 8th, 2024
Science Suite Inc.

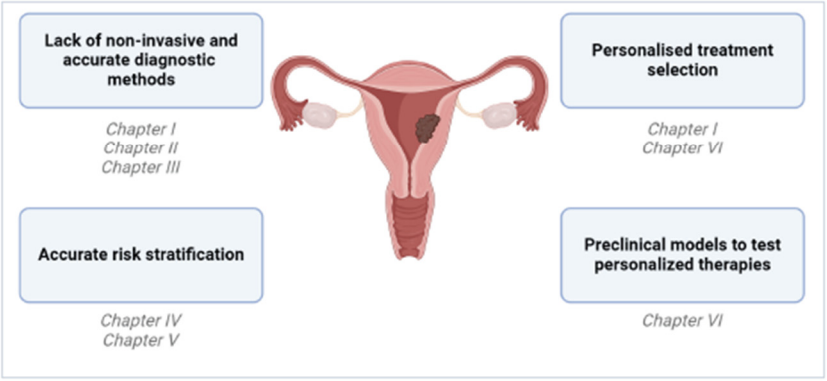
Subscription:	*Student Plan*
Agreement number:	*CF26OBCGN3*
Journal name:	*N/A*

To whom this may concern,

This document is to confirm that Carlos Casas arozamena has been granted a license to use the BioRender content, including icons, templates and other original artwork, appearing in the attached completed graphic pursuant to BioRender's Academic License Terms. This license permits BioRender content to be sublicensed for use in journal publications.

All rights and ownership of BioRender content are reserved by BioRender. All completed graphics must be accompanied by the following citation: "Created with BioRender.com".

BioRender content included in the completed graphic is not licensed for any commercial uses beyond publication in a journal. For any commercial use of this figure, users may, if allowed, recreate it in BioRender under an Industry BioRender Plan.



For any questions regarding this document, or other questions about publishing with BioRender refer to our BioRender Publication Guide, or contact BioRender Support at support@biorender.com.

USC UNIVERSIDADE DE SANTIAGO DE COMPOSTELA

49 Spadina Ave. Suite 200
Toronto ON M5V 2J1 Canada
www.biorender.com

Confirmation of Publication and Licensing Rights

April 8th, 2024
Science Suite Inc.

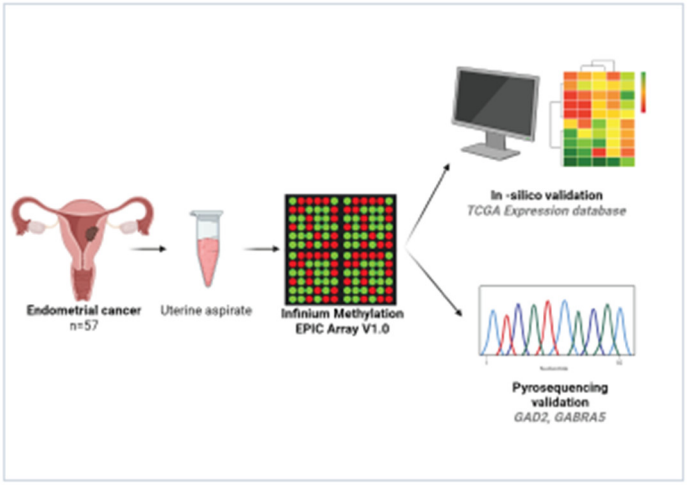
Subscription:	*Student Plan*
Agreement number:	*KE26O9UGKB*
Journal name:	*N/A*

To whom this may concern,

This document is to confirm that Carlos Casas arozamena has been granted a license to use the BioRender content, including icons, templates and other original artwork, appearing in the attached completed graphic pursuant to BioRender's Academic License Terms. This license permits BioRender content to be sublicensed for use in journal publications.

All rights and ownership of BioRender content are reserved by BioRender. All completed graphics must be accompanied by the following citation: "Created with BioRender.com".

BioRender content included in the completed graphic is not licensed for any commercial uses beyond publication in a journal. For any commercial use of this figure, users may, if allowed, recreate it in BioRender under an Industry BioRender Plan.



For any questions regarding this document, or other questions about publishing with BioRender refer to our BioRender Publication Guide, or contact BioRender Support at support@biorender.com.

USC UNIVERSIDADE DE SANTIAGO DE COMPOSTELA

49 Spadina Ave. Suite 200
Toronto ON M5V 2J1 Canada
www.biorender.com

Confirmation of Publication and Licensing Rights

April 8th, 2024
Science Suite Inc.

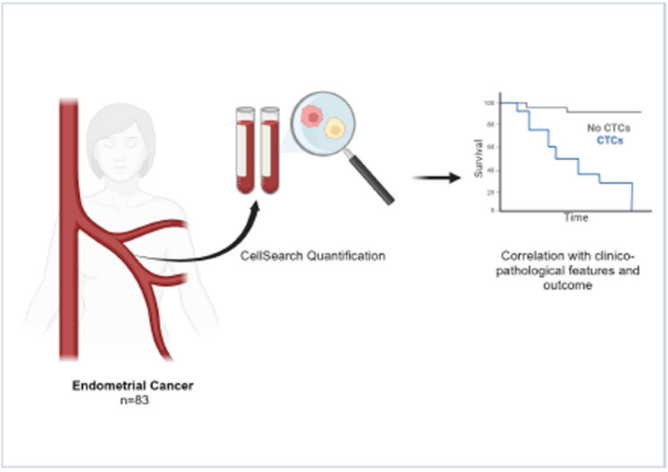
Subscription:	*Student Plan*
Agreement number:	*XX26O9UHFL*
Journal name:	*N/A*

To whom this may concern,

This document is to confirm that Carlos Casas arozamena has been granted a license to use the BioRender content, including icons, templates and other original artwork, appearing in the attached completed graphic pursuant to BioRender's Academic License Terms. This license permits BioRender content to be sublicensed for use in journal publications.

All rights and ownership of BioRender content are reserved by BioRender. All completed graphics must be accompanied by the following citation: "Created with BioRender.com".

BioRender content included in the completed graphic is not licensed for any commercial uses beyond publication in a journal. For any commercial use of this figure, users may, if allowed, recreate it in BioRender under an Industry BioRender Plan.



For any questions regarding this document, or other questions about publishing with BioRender refer to our BioRender Publication Guide, or contact BioRender Support at support@biorender.com.

USC UNIVERSIDADE DE SANTIAGO DE COMPOSTELA

49 Spadina Ave. Suite 200
Toronto ON M5V 2J1 Canada
www.biorender.com

Confirmation of Publication and Licensing Rights

April 8th, 2024
Science Suite Inc.

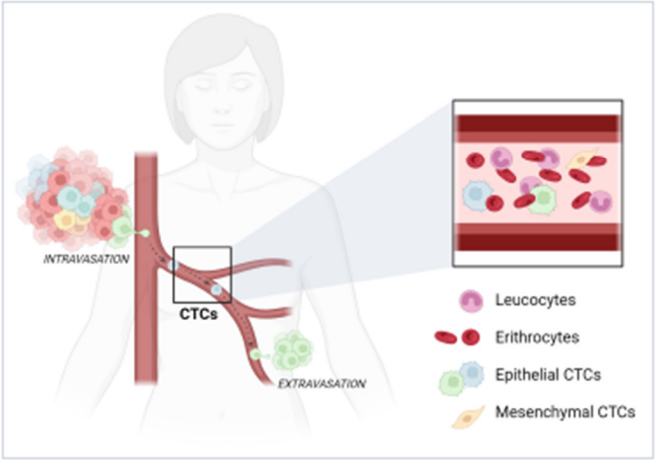
Subscription:	***Student Plan***
Agreement number:	***JK26O9UIBD***
Journal name:	***N/A***

To whom this may concern,

This document is to confirm that Carlos Casas arozamena has been granted a license to use the BioRender content, including icons, templates and other original artwork, appearing in the attached completed graphic pursuant to BioRender's Academic License Terms. This license permits BioRender content to be sublicensed for use in journal publications.

All rights and ownership of BioRender content are reserved by BioRender. All completed graphics must be accompanied by the following citation: "Created with BioRender.com".

BioRender content included in the completed graphic is not licensed for any commercial uses beyond publication in a journal. For any commercial use of this figure, users may, if allowed, recreate it in BioRender under an Industry BioRender Plan.



For any questions regarding this document, or other questions about publishing with BioRender refer to our BioRender Publication Guide, or contact BioRender Support at support@biorender.com.

USC UNIVERSIDADE DE SANTIAGO DE COMPOSTELA

49 Spadina Ave. Suite 200
Toronto ON M5V 2J1 Canada
www.biorender.com

Confirmation of Publication and Licensing Rights

April 8th, 2024
Science Suite Inc.

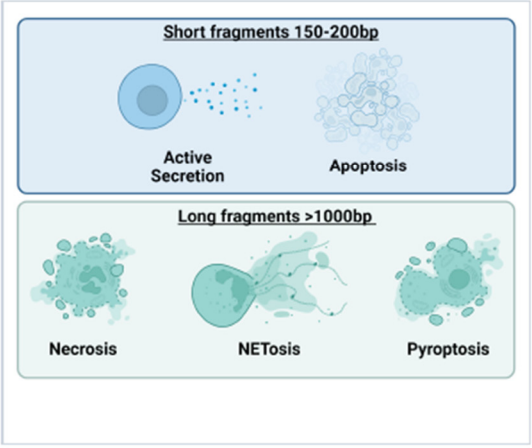
Subscription:	*Student Plan*
Agreement number:	*WL26O9UJRB*
Journal name:	*N/A*

To whom this may concern,

This document is to confirm that Carlos Casas arozamena has been granted a license to use the BioRender content, including icons, templates and other original artwork, appearing in the attached completed graphic pursuant to BioRender's Academic License Terms. This license permits BioRender content to be sublicensed for use in journal publications.

All rights and ownership of BioRender content are reserved by BioRender. All completed graphics must be accompanied by the following citation: "Created with BioRender.com".

BioRender content included in the completed graphic is not licensed for any commercial uses beyond publication in a journal. For any commercial use of this figure, users may, if allowed, recreate it in BioRender under an Industry BioRender Plan.



For any questions regarding this document, or other questions about publishing with BioRender refer to our BioRender Publication Guide, or contact BioRender Support at support@biorender.com.

USC UNIVERSIDADE DE SANTIAGO DE COMPOSTELA

49 Spadina Ave. Suite 200
Toronto ON M5V 2J1 Canada
www.biorender.com

Confirmation of Publication and Licensing Rights

April 8th, 2024
Science Suite Inc.

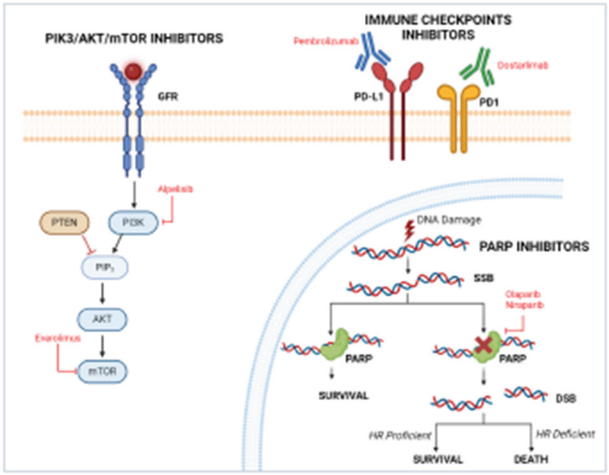
Subscription: *Student Plan*
Agreement number: *MF26OBCY4U*
Journal name: *N/A*

To whom this may concern,

This document is to confirm that Carlos Casas arozamena has been granted a license to use the BioRender content, including icons, templates and other original artwork, appearing in the attached completed graphic pursuant to BioRender's Academic License Terms. This license permits BioRender content to be sublicensed for use in journal publications.

All rights and ownership of BioRender content are reserved by BioRender. All completed graphics must be accompanied by the following citation: "Created with BioRender.com".

BioRender content included in the completed graphic is not licensed for any commercial uses beyond publication in a journal. For any commercial use of this figure, users may, if allowed, recreate it in BioRender under an Industry BioRender Plan.



For any questions regarding this document, or other questions about publishing with BioRender refer to our BioRender Publication Guide, or contact BioRender Support at support@biorender.com.

USC UNIVERSIDADE DE SANTIAGO DE COMPOSTELA

49 Spadina Ave. Suite 200
Toronto ON M5V 2J1 Canada
www.biorender.com

Confirmation of Publication and Licensing Rights

April 8th, 2024
Science Suite Inc.

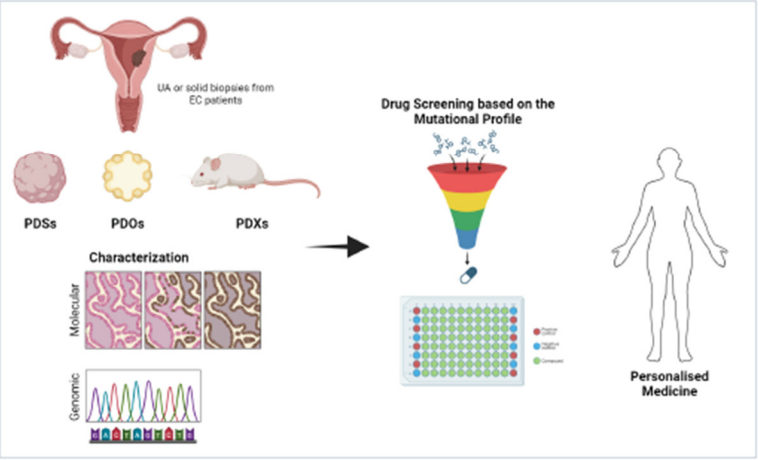
Subscription:	*Student Plan*
Agreement number:	*IY26OA2LBM*
Journal name:	*N/A*

To whom this may concern,

This document is to confirm that Carlos Casas arozamena has been granted a license to use the BioRender content, including icons, templates and other original artwork, appearing in the attached completed graphic pursuant to BioRender's Academic License Terms. This license permits BioRender content to be sublicensed for use in journal publications.

All rights and ownership of BioRender content are reserved by BioRender. All completed graphics must be accompanied by the following citation: "Created with BioRender.com".

BioRender content included in the completed graphic is not licensed for any commercial uses beyond publication in a journal. For any commercial use of this figure, users may, if allowed, recreate it in BioRender under an Industry BioRender Plan.



For any questions regarding this document, or other questions about publishing with BioRender refer to our BioRender Publication Guide, or contact BioRender Support at support@biorender.com.

USC UNIVERSIDADE DE SANTIAGO DE COMPOSTELA

b. Favourable report (Clinical research ethics committee of Galica CEIC).

XUNTA DE GALICIA
CONSELLERÍA DE SANIDADE
Secretaría Xeral Técnica

Secretaría Técnica
Comité Autonómico de Ética da Investigación de Galicia
Secretaría Xeral. Consellería de Sanidade
Edificio Administrativo San Lázaro
15703 SANTIAGO DE COMPOSTELA
Tel: 881546425. Correo-e: ceic@sergas.es

galicia

DICTAMEN DEL COMITÉ DE ÉTICA DE LA INVESTIGACIÓN DE SANTIAGO-LUGO

Guillermo José Prada Ramallal, Secretario del Comité de Ética de la Investigación de Santiago-Lugo,

CERTIFICA:

Que este Comité evaluó en su reunión del día 18 de enero de 2018 el estudio:

Título: Aproximaciones al manejo de la enfermedad avanzanda en cáncer de endometrio a través de la identificación de biomarcadores en biopsia líquida
Promotor: Miguel Abal Posada
Tipo de estudio: Outros
Versión:
Código del Promotor:
Código de Registro: 2017/530

Y, tomando en consideración las siguientes cuestiones:

- La pertinencia del estudio, teniendo en cuenta el conocimiento disponible, así como los requisitos legales aplicables, y en particular la Ley 14/2007, de investigación biomédica, el Real Decreto 1716/2011, de 18 de noviembre, por el que se establecen los requisitos básicos de autorización y funcionamiento de los biobancos con fines de investigación biomédica y del tratamiento de las muestras biológicas de origen humana, y se regula el funcionamiento y organización del Registro Nacional de Biobancos para investigación biomédica, la ORDEN SAS/3470/2009, de 16 de diciembre, por la que se publican las Directrices sobre estudios Postautorización de Tipo Observacional para medicamentos de uso humano, y la Circular nº 07/2004, de investigaciones clínicas con productos sanitarios.
- La idoneidad del protocolo en relación con los objetivos del estudio, justificación de los riesgos y molestias previsibles para el sujeto, así como los beneficios esperados.
- Los principios éticos da Declaración de Helsinki vigente.
- Los Procedimientos Normalizados de Trabajo del Comité.

Emite un dictamen **FAVORABLE** para la realización del estudio **por el/la investigador/a del centro**:

Centros	Investigadores Principales
C.H. Universitario de Santiago	Ana Vilar Lagares, Juan F. Cueva Bañuelos

En Santiago de Compostela, a 23 de enero 2018.

El Secretario del Comité Territorial de Ética de la Investigación de Santiago Lugo,

guillermo.jose.prada.ramallal@sergas.es
2018.01.24 11:10:51 +02'00'

Guillermo José Prada Ramallal

USC UNIVERSIDADE DE SANTIAGO DE COMPOSTELA

XUNTA DE GALICIA
CONSELLERÍA DE SANIDADE
Secretaría Xeral Técnica

Secretaría Técnica
Comité Autonómico de Ética da Investigación de Galicia
Secretaría Xeral. Consellería de Sanidade
Edificio Administrativo San Lázaro
15703 SANTIAGO DE COMPOSTELA
Tel: 881546425. Correo-e: ceic@sergas.es

galicia

Guillermo José Prada Ramallal, Secretario del Comité de Ética de la Investigación de Santiago-Lugo,

HACE CONSTAR QUE:

1.- El Comité Territorial de Ética de la Investigación de Santiago-Lugo cumple tanto en su composición como en sus PNTs los requisitos legales vigentes (RD 1090/2015 de ensayos clínicos, y la Ley 14/2007 de Investigación Biomédica).

2.- La composición actual del Comité Territorial de Ética de la Investigación de Santiago-Lugo es:

- **Juan Manuel Vázquez Lago (Presidente).** Médico especialista en Medicina Preventiva y Salud Pública. Área de Gestión Integrada de Santiago.
- **Pilar Rodríguez Ledo (Vicepresidenta).** Médico especialista en Medicina Familiar y Comunitaria. Área de Gestión Integrada de Lugo.
- **Guillermo José Prada Ramallal (Secretario).** Médico especialista en Farmacología Clínica. Área de Gestión Integrada de Santiago. Fundación Ramón Domínguez.
- **Lorenzo Armenteros del Olmo (Vicesecretario).** Médico especialista en Medicina Familiar y Comunitaria. Área de Gestión Integrada de Lugo.
- **Francisco Campos Pérez.** Biólogo. Instituto de Investigación Sanitaria de Santiago de Compostela.
- **Rosana Castelo Domínguez.** Farmacéutica de Atención Primaria. Área de Gestión Integrada de Santiago.
- **Ricardo García Martínez.** Licenciado en Derecho. Área de Gestión Integrada de Lugo.
- **Jaime Gulín Dávila**. Farmacéutico especialista en Farmacia Hospitalaria. Área de Gestión Integrada de Lugo.
- **Victor Herrán Carreira.** Paciente. ADIL-Asociación de Diabéticos Lucense.
- **María Jesús Lamas Díaz.** Farmacéutica especialista en Farmacia Hospitalaria. Área de Gestión Integrada de Santiago.
- **Carlos Rodríguez Moreno.** Médico especialista en Farmacología Clínica. Área de Gestión Integrada de Santiago.
- **Rafael Carlos Vidal Pérez.** Médico especialista en Cardiología. Área de Gestión Integrada de Lugo.
- **María Jesús Wandosell Picatoste.** Enfermera. Área de Gestión Integrada de Santiago.

Para que conste donde proceda, y a petición del promotor/investigador, en Santiago de Compostela, a 23 de enero de 2018.

El Secretario del Comité Territorial de Ética de la Investigación de Santiago Lugo,

XUNTA DE GALICIA SECRETARÍA XERAL TÉCNICA COMITÉS DE ÉTICA DA INVESTIGACIÓN CONSELLERÍA DE SANIDADE

guillermo.jose.prada.ramallal@sergas.es
2018.01.24 11:10:53 +02'00'

Guillermo José Prada Ramallal

USC UNIVERSIDADE DE SANTIAGO DE COMPOSTELA

XUNTA DE GALICIA
CONSELLERÍA DE SANIDADE
Secretaría Xeral Técnica

SERVIZO GALEGO de SAÚDE | Xerencia do Servizo Galego de Saúde

galicia

DICTAMEN DEL COMITÉ DE ÉTICA DE LA INVESTIGACIÓN DE SANTIAGO-LUGO

Ana Estany Gestal, Secretaria del Comité de Ética de la Investigación de Santiago-Lugo,

CERTIFICA:

Que este Comité evaluó en su reunión del día 23 de marzo de 2021 el estudio:

Título: Estrategia dual de biopsia líquida en cáncer de endometrio: evaluación del riesgo de recurrencia y terapia personalizada
Versión: 1.0
Promotor/a: Juan Fernando Cueva Bañuelos, Ana Vilar Lagares
Investigador/a: Juan Fernando Cueva Bañuelos
Código de Registro: 2021/143

Y que este Comité, tomando en consideración la pertinencia del estudio, el conocimiento disponible, los requisitos legales aplicables y los Procedimientos Normalizados de Trabajo del Comité, emite un dictamen **FAVORABLE** para la realización del citado estudio.

Documento asinado dixitalmente por:
Ana Estany Gestal (31/03/2021 12:53)
https://sede.xunta.gal/csv?idcve=SAOC-W4G4-BOAH-OF4O-TC4P-0X4R-BYPP-Z161-7188-0192-19

NOTA: Se le recuerda que en el caso de que en este estudio se recluten pacientes, el equipo investigador debe tener disponible el Documento de Consentimiento Informado (Hojas de Información y Hojas de Firma) tanto en *galego* como en castellano en el momento de comenzar el reclutamiento.

Xacobeo 2021

USC UNIVERSIDADE DE SANTIAGO DE COMPOSTELA

XUNTA DE GALICIA
CONSELLERÍA DE SANIDADE
Secretaría Xeral Técnica

SERVIZO GALEGO de SAÚDE | Xerencia do Servizo Galego de Saúde

galicia

Y HACE CONSTAR QUE:

1.- El Comité Territorial de Ética de la Investigación de Santiago-Lugo cumple tanto en su composición como en sus PNTs los requisitos legales vigentes.

2.- La composición actual del Comité Territorial de Ética de la Investigación de Santiago-Lugo es:

Presidenta
Pilar Rodríguez Ledo. Médico especialista en Medicina Familiar y Comunitaria.

Vicepresidenta
María Mercedes Rodicio García. Médico especialista en Pediatría.

Secretaria
Ana Estany Gestal. Licenciada en Farmacia.

Vicesecretaria
Catalina Caamaño Isorna. Farmacéutica de Atención Primaria.

Vocales
Francisco Campos Pérez. Licenciado en Biología.
Jesús Fernández Álvarez. Miembro lego.
Ricardo García Martínez. Licenciado en Derecho.
Jaime Gulín Dávila. Farmacéutico especialista en Farmacia Hospitalaria.
Jesús Prego Domínguez. Enfermero.
Lorenzo Armenteros del Olmo. Médico especialista en Medicina Familiar y Comunitaria.
Eva Marcos Doldán. Analista-programadora.
Carlos Rodríguez Moreno. Médico especialista en Farmacología Clínica.
Juan Manuel Vázquez Lago. Médico especialista en Medicina Preventiva y Salud Pública.

Para que conste donde proceda, y a petición de quien proceda, en Santiago de Compostela,

La Secretaria del Comité Territorial de Ética de la Investigación de Santiago Lugo,

Documento asinado dixitalmente por:
Ana Estany Gestal (31/03/2021 12:53)
https://sede.xunta.gal/cve?dove=5AOC-W4G4-8DAH-QF4O-TCAP-0X4R-BY9P-Z161-7188-0192-19

Xacobeo 2021

USC UNIVERSIDADE DE SANTIAGO DE COMPOSTELA

c. Favourable report for animal studies

XUNTA DE GALICIA
CONSELLERÍA DO MEDIO RURAL

Xefatura Territorial
Sº de Gandaría
Edificio administrativo Monelos, 4º andar
Rúa Vicente Ferrer, Nº 2
15008 A Coruña
Tfno.: 981 184 565
Correo electrónico: servizo.gandaria.a.coruna@xunta.gal

galicia

RESOLUCIÓN DE AUTORIZACIÓN DE PROXECTO DE EXPERIMENTACIÓN ANIMAL

Expediente núm.: 15012/2021/010
Persoa solicitante: Anxo Vidal Figueroa
Forma de inicio: solicitude da persoa interesada

Data de inicio do expediente: 16.4.2021
Procedemento: resolución de autorización

ANTECEDENTES

A persoa solicitante presentou con data 16.4.2021 unha solicitude para a realización do proxecto de experimentación animal (entrada no Rexistro Electrónico da Xunta de Galicia 2021/879794), cuxos datos se detallan a continuación:

Denominación do proxecto: Modelos animais para o estudo e tratamento do cancro e a metástase en oncoloxía médica traslacional

Nome do centro usuario: Centro de Biomedicina Experimental (CEBEGA) da Universidade de Santiago de Compostela
Persoa responsable do proxecto: Alba Ferreirós López
Establecemento onde se realizarán os procedementos do proxecto (ou lugar xeográfico no caso de traballos de campo): Centro de Biomedicina Experimental (CEBEGA)

Clasificación do proxecto : Tipo I ☐ Tipo II ☐ Tipo III ☒

CONSIDERACIÓNS LEGAIS E TÉCNICAS

1 O Real decreto 53/2013, de 1 de febreiro (BOE 34, do 8 de febreiro), polo que se establecen as normas básicas aplicables para a protección dos animais utilizados en experimentación e outros fins científicos, incluíndo a docencia, establece no seu artigo 33 as condicións de autorizacións dos proxectos con animais de experimentación.

2 O artigo 88 da Lei 39/2015, de 1 de outubro, do procedemento administrativo común das administracións públicas (BOE 236, do 2 de outubro de 2015) establece que a resolución que poña fin o procedemento decidirá todas as cuestións expostas polos interesados e aquelas outras derivadas deste.

CVE: P9HxV4KY8
Verificación: https://sede.xunta.gal/cve

Xacobeo 21·22

USC UNIVERSIDADE DE SANTIAGO DE COMPOSTELA

XUNTA DE GALICIA
CONSELLERÍA DO MEDIO RURAL

Xefatura Territorial
Sº de Gandaría
Edificio administrativo Monelos, 4º andar
Rúa Vicente Ferrer, Nº 2
15008 A Coruña
Tfno.: 981 184 565
Correo electrónico: servizo.gandaria.a.coruna@xunta.gal

galicia

3 O Servizo de Gandaría da Coruña revisou a documentación achegada na solicitude e o resultado favorable da avaliación do proxecto realizada polo órgano habilitado, a Sección de Experimentación Animal do Comité de Bioética da Universidade de Santiago de Compostela.

Esta xefatura territorial é competente para ditar unha resolución, de conformidade co Decreto 149/2018, do 5 de decembro, polo que se establece a estrutura orgánica da Consellería do Medio Rural e se modifica parcialmente o Decreto 177/2016, do 15 de decembro, polo que se fixa a estrutura orgánica da Vicepresidencia e das consellerías da Xunta de Galicia (DOG 235, do 11 de novembro).

De acordo con todo o indicado, RESOLVO:

1 Autorizar o proxecto solicitado.

2 O proxecto precisa someterse a unha avaliación retrospectiva aos tres anos tras a súa aprobación (segundo indica o informe do órgano habilitado).

3 A autorización deste proxecto terá unha duración de cinco anos e unha vez transcorrido este tempo deberá ser renovada.

A citada autorización é unicamente válida nas condicións que figuran no expediente. Ante calquera cambio significativo no proxecto que poida ter efectos negativos sobre o benestar dos animais, deberá solicitar a confirmación da autorización ao Servizo Provincial de Gandaría.

Esta autorización poderá ser suspendida no caso de que o proxecto non se leve a cabo de acordo coas condicións de autorización e retirala, previo expediente tramitado ao que se lle dará audiencia.

Contra a presente resolución, que non pon fin á vía administrativa, poderá interpoñer un recurso de alzada ante o conselleiro de Medio Rural. O prazo comezará a contar dende o día seguinte ao da recepción desta resolución. Todo isto, segundo o disposto nos artigos 121 e 122 da citada Lei 39/2015.

Mediante este escrito notificaselle a Anxo Vidal Figueroa esta resolución segundo o esixido no artigo 40.1 da antedita Lei 39/2015.

Asinado por: SANTOS MANEIRO, JOSE MANUEL
Cargo: Xefe Territorial
Data e hora: 22/04/2021 14:01:14

CME: FIIHVU4X8
Verificación: https://sede.xunta.gal/csv

Xacobeo 21·22

USC UNIVERSIDADE DE SANTIAGO DE COMPOSTELA

d. Training certificate for animal experimentation



O REITOR
DA UNIVERSIDADE DE SANTIAGO DE COMPOSTELA
(EL RECTOR DE LA UNIVERSIDAD DE SANTIAGO DE COMPOSTELA)

CONSIDERANDO QUE

don **CARLOS CASAS AROZAMENA** con DNI/PASAPORTE 77480593X, superou os estudos correspondentes ao Curso de Formación de 6,5 ECTS, organizado pola VICERREITORÍA DE INVESTIGACIÓN E INNOVACIÓN, durante o ano académico 2019-2020, expide o presente

Diploma de Aproveitamento no
PROGRAMA DE FORMACIÓN DE
CAPACITACIÓN PARA A REALIZACIÓN DAS FUNCIÓNS A+B+C EN EXPERIMENTACIÓN ANIMAL: CURSO TRONCAL PARA ROEDORES E LAGOMORFOS

O presente diploma, propio da Universidade de Santiago de Compostela, expídese ao abeiro do artigo 34.1 da Lei orgánica 4/2007, de 12 de abril.

*Don **Carlos Casas Arozamena**, con DNI/PASAPORTE 77480593X, superó los estudios correspondientes al Curso de Formación de 6,5 ECTS, organizado por la VICERRECTORÍA DE INVESTIGACIÓN E INNOVACIÓN, durante el año académico 2019-2020, expide el presente Diploma de Aprovechamiento en el PROGRAMA DE FORMACIÓN DE **FORMACIÓN DE CAPACITACIÓN PARA LA REALIZACIÓN DE LAS FUNCIONES A+B+C EN EXPERIMENTACIÓN ANIMAL: CURSO TRONCAL PARA ROEDORES Y LAGOMORFOS.***

El presente diploma, propio de la Universidad de Santiago de Compostela, se expide al amparo del artículo 34.1 de la Ley Orgánica 4/2007, de 12 de abril.

Santiago de Compostela, a 12 de junio de 2020

Santiago de Compostela, a 12 de xuño de 2020

O reitor,
El rector,

Antonio López Díaz

CLAVE ALFANUMÉRICA: USC-10860-FC
NÚMERO DE REXISTRO: 202010860-FC

Documento expedido en papel de seguridade reactivo ó borrado químico con filamentos luminiscentes e sélo en seco.
Documento expedido en papel de seguridad reactivo al borrado químico con filamentos luminiscentes y sello en seco.

CLAVE ALFANUMÉRICA: USC-10860-FC **NÚMERO DE REXISTRO: 202010860-FC**

FORMACIÓN CONTINUA

Reverso do Diploma de Aproveitamento no PROGRAMA DE FORMACIÓN EN FORMACIÓN DE CAPACITACIÓN PARA A REALIZACIÓN DAS FUNCIÓNS A+B+C EN EXPERIMENTACIÓN ANIMAL: CURSO TRONCAL PARA ROEDORES E LAGOMORFOS, expedido a don **CARLOS CASAS AROZAMENA**, con DNI/PASAPORTE 77480593X, superado no ano académico 2019-2020.

*Reverso del Diploma de Aprovechamiento en el PROGRAMA DE FORMACIÓN EN FORMACIÓN DE CAPACITACIÓN PARA LA REALIZACIÓN DE LAS FUNCIONES A+B+C EN EXPERIMENTACIÓN ANIMAL: CURSO TRONCAL PARA ROEDORES Y LAGOMORFOS, expedido a don **Carlos Casas Arozamena**, con DNI/PASAPORTE 77480593X, superado en el año académico 2019-2020.*

CONTIDOS DO CURSO	ECTS*	CONTENIDOS DEL CURSO
Lexislación nacional	0,1	Legislación nacional
Ética, benestar animal e as 3 Rs	0,2	Ética, bienestar animal y las Rs
Bioloxía básica nivel 1	0,4	Biología básica nivel 1
Coidado, saúde e manexo dos animais nivel 1	0,5	Cuidado, salud y manejo de los animales nivel 1
Recoñecemento da dor, sufrimento e angustia	0,3	Reconocimiento del dolor, sufrimiento y angustia
Métodos incruentos de sacrificio nivel 1	0,2	Métodos incruentos de sacrificio nivel 1
Bioloxía básica nivel 2	0,4	Biología básica nivel 2
Métodos incruentos de sacrificio nivel 2	0,4	Métodos incruentos de sacrificio nivel 2
Procedementos mínimamente invasivos sen anestesia nivel 1	0,6	Procedimientos mínimamente invasivos sin anestesia nivel 1
Procedementos mínimamente invasivos sen anestesia nivel 2	1	Procedimientos mínimamente invasivos sin anestesia nivel 2
Anestesia para procedementos menores	0,5	Anestesia para procedimientos menores
Anestesia avanzada para intervencións quirúrxicas ou procedementos prolongados	1,2	Anestesia avanzada para intervenciones quirúrgicas o procedimientos prolongados
Principios da cirurxía	0,7	Principios da cirugía

Este Diploma expídese unha vez verificado que o interesado reúne os requisitos para a súa obtención.
Este Diploma se expide una vez verificado que el interesado reúne los requisitos para su obtención.

A xefa da Sección de Títulos,
La jefa de la Sección de Títulos,

María Salomé García Rielo

Este diploma queda asentado co número USC-10860-FC do Libro de Rexistro Número 5 de Expedición e Entrega de Diplomas de Formación Continua co nº de expediente **202010860-FC**.

Este diploma queda asentado con el número USC-10860-FC del Libro de Registro Número 5 de Expedición y Entrega de Diplomas de Formación Continua con el nº de expediente **202010860-FC**

Santiago de Compostela, 26 de xuño de 2020

A xefa do Negociado de Títulos,
La jefa del Negociado de Títulos,

María das Mercedes Alonso Pequeño

(*) 1 ECTS (European Credit Transfer and Accumulation System) equivale a 25 horas de traballo total do alumno. No caso de realizar prácticas en empresas, cada 25 horas de presenza na entidade equivale a 1 ECTS
1 ECTS (European Credit Transfer and Accumulation System) equivale a 25 horas de trabajo total del alumno. En el caso de realizar prácticas en empresas, cada 25 horas de presencia en la entidad equivale a 1 ECTS

USC UNIVERSIDADE DE SANTIAGO DE COMPOSTELA

d. Rights and permissions for articles

JOHN WILEY AND SONS LICENSE TERMS AND CONDITIONS

Apr 08, 2024

This Agreement between Mr. Carlos Casas Arozamena ("You") and John Wiley and Sons ("John Wiley and Sons") consists of your license details and the terms and conditions provided by John Wiley and Sons and Copyright Clearance Center.

License Number	5764161298267
License date	Apr 08, 2024
Licensed Content Publisher	John Wiley and Sons
Licensed Content Publication	International Journal of Cancer
Licensed Content Title	Noninvasive detection of microsatellite instability in patients with endometrial cancer
Licensed Content Author	Gema Moreno-Bueno, Antonio Gil-Moreno, Laura Muinelo-Romay, et al
Licensed Content Date	Jan 24, 2023
Licensed Content Volume	152
Licensed Content Issue	10
Licensed Content Pages	12
Type of Use	Dissertation/Thesis
Requestor type	Author of this Wiley article
Format	Print and electronic
Portion	Full article
Will you be translating?	No
Title of new work	PERSONALISED MEDICINE IN ENDOMETRIAL CANCER THROUGH THE USE OF LIQUID BIOPSY
Institution name	Universidade Santiago de Compostela
Expected presentation date	Jun 2024
Requestor Location	Mr. Carlos Casas Arozamena Augusto Gonzalez Besada nº1 6ºG Pontevedra, Galicia 36001 Spain Attn: Mr. Carlos Casas Arozamena
Publisher Tax ID	EU826007151
Total	**0.00 USD**
Terms and Conditions	

TERMS AND CONDITIONS

This copyrighted material is owned by or exclusively licensed to John Wiley & Sons, Inc. or one of its group companies (each a"Wiley Company") or handled on behalf of a society with which a Wiley Company has exclusive publishing rights in relation to a particular work (collectively "WILEY"). By clicking "accept" in connection with completing this licensing transaction, you agree that the following terms and conditions apply to this transaction (along with the billing and payment terms and conditions established by the Copyright Clearance Center Inc., ("CCC's Billing and Payment terms and conditions"), at the time that you opened your RightsLink account (these are available at any time at http://myaccount.copyright.com).

USC UNIVERSIDADE DE SANTIAGO DE COMPOSTELA

Appendix 4: NGS sequencing of the UA samples from Chapter III.

Code	MS Status	GENE	NUCLEOTIDE CHANGE	PROTEIN CHANGE	GAIN/LOSS	VAF (%)
Patient #1	MSI-H	**CTNNB1**	c.121A>G	p.Thr41Ala	Gain	44.29
		RNF43	c.1585C>T	p.Arg529Trp	Unknown	48.62
		PTEN	c.442G>A	p.Ala148Thr	Loss	47.94
Patient #2	MSI-H	**ARID1A**	c.6343C>T	p.Gln2115Ter	Loss	14.30
		FBXW7	c.1514G>T	p.Arg505Leu	Loss	42.65
		PTEN	c.813delT	p.His272ThrfsTer4	Loss	45.13
		RB1	c.2359C>T	p.Arg787Ter	Loss	9.15
Patient #3	MSI-H	**ARID1A**	c.2641delT	p.Ser881GlnfsTer10	loss	21.45
		ARID1A	c.4800_4801delTC	p.Pro1601Ter	Loss	23.4
		MSH2	c.657delA	p.Gly220GlufsTer4	Loss	27.37
		MSH2*	c.1147C>T	p.Arg383Ter	Loss	24.62
		NFE2L2	c.241G>A	p.Gly81Ser	Gain	21.9
		PIK3R1	c.1937_1941delTTCTT	p.Phe646CysfsTer6	Loss	21.27
		NBN	c.247delA	p.Met83CysfsTer9	Loss	20.67
		PTEN	c.370T>G	p.Cys124Gly	Loss	24.15
		TP53	c.733G>A	p.Gly245Ser	Loss	24.75

Code	MS Status	GENE	NUCLEOTIDE CHANGE	PROTEIN CHANGE	GAIN/LOSS	VAF (%)
Patient #4	MSI-H	**CTNNB1**	c.98C>G	p.Ser33Cys	Gain	34.48
		PIK3CA	c.1634A>C	p.Glu545Ala	Gain	25.00
Patient #5	MSI-H	**ARID1A**	c.6583_6584insC	p.Leu2195ProfsTer30	Loss	14.31
		PIK3CA	c.1030G>A	p.Val344Met	Gain	13.01
		PIK3CA	c.3140A>G	p.His1047Arg	Gain	17.09
		KRAS	c.38G>A	p.Gly13Asp	Gain	14.13
		TP53	c.743G>A	p.Arg248Gln	Gain	12.81
		SMARCA4	c.2917C>T	p.Arg973Trp	Loss	11.27
Patient #6	MSI-H	**BRAF**	c.1406G>A	p.Gly469Glu	gain	31.23
		PTEN	c.955_956delAC	p.Thr319PhefsTer5	loss	30.86
		ATM	c.1369C>T	p.Arg457Ter	loss	35.77
		KRAS	c.38G>A	p.Gly13Asp	gain	29.49
		TP53	c.844C>T	p.Arg282Trp	loss	35.63
		NF1	c.943C>T	p.Gln315Ter	loss	31.15
Patient #7	MSI-H	**NRAS**	c.35G>A	p.Gly12Asp	gain	45.37
		MSH6	c.3013C>T	p.Arg1005Ter	Loss	6.73
		CTNNB1	c.122C>T	p.Thr41Ile	gain	46.07
		PTEN	c.388C>G	p.Arg130Gly	Loss	91.03

Code	MS Status	GENE	NUCLEOTIDE CHANGE	PROTEIN CHANGE	GAIN/LOSS	VAF (%)
Patient #8	MSI-H	**ARID1A**	c.2132C>G	p.Ser711Ter	Loss	33.02
		PIK3R1	c.1732_1735delGACCinsCCA	p.Asp578ProfsTer4	Loss	61.28
		PTEN	c.388C>G	p.Arg130Gly	Loss	41.45
		KRAS	c.35G>A	p.Gly12Asp	Gain	37.96
Patient #9	MSI-H	**PIK3CA**	c.3140A>G	p.His1047Arg	gain	34.65
		KRAS	c.35G>C	p.Gly12Ala	gain	38.37
Patient #10	MSI-H	**PMS2**	c.1261C>T	p.Arg421Ter	Loss	41.05
		TP53	c.707A>G	p.Tyr236Cys	Loss	69.57
		PPP2R1A	c.544C>T	p.Arg182Trp	gain	41.20
Patient #11	MSI-H	**ARID1A**	c.6472C>T	p.Arg2158Ter	Loss	38.80
		PIK3CA	c.1633G>A	p.Glu545Lys	Gain	76.84
		FBXW7	c.1394G>A	p.Arg465His	Loss	36.93
		KRAS	c.35G>A	p.Gly12Asp	Gain	33.05
Patient #12	MSI-H	**PIK3CA**	c.1034A>T	p.Asn345Ile	Gain	30.75
		PTEN	c.416delT	p.Leu139fs	Loss	55.39
		FGFR2	c.1647T>A	p.Asn549Lys	Loss	59.23
		MAX	c.83A>G	p.His28Arg	Gain	26.81
		SMARCA4	c.2917C>T	p.Arg973Trp	Loss	6.10

Code	MS Status	GENE	NUCLEOTIDE CHANGE	PROTEIN CHANGE	GAIN/LOSS	VAF (%)
Patient #13	MSI-H	**PIK3R1**	c.2113C>T	p.Gln705Ter	Loss	26.05
		MET	c.504G>T	p.Glu168Asp	Gain	49.68
		PTEN	c.367C>T	p.His123Tyr	Loss	29.86
		PTEN	c.445_446insT	p.Gln149fs	Loss	30.47
		TP53	c.730G>T	p.Gly244Cys	Loss	5.00
Patient #14	MSI-H	**PIK3CA**	c.3062A>G	p.Tyr1021Cys	GAIN	20.15
		ERBB2	c.2524G>A	p.Val842Ile	GAIN	20.50
		GNAS	c.601C>T	p.Arg201Cys	Gain	21.20
		MSH2	c.1363G>T	p.Glu455Ter	Loss	20.30
		RB1	c.1548G>A	p.Trp516Ter	Loss	19.97
		PTEN	c.85delT	p.Tyr29IlefsTer25	Loss	22.90
		FGFR2	c.913G>A	p.Gly305Arg	Gain	19.35
Patient #15	MSI-H	**PTEN**	c.389G>C	p.Arg130Pro	Loss	20.40
Patient #16	MSI-H	**MSH2**	p.Arg680Ter	c.2038C>T	Loss	49.27
		FBXW7	p.Arg224Ter	c.670C>T	Loss	20.52
		PTEN	p.Gln245Ter	c.733C>T	Loss	20.13
		CDKN1B	p.Pro137fs	c.410delC	Loss	20.18
		MAP2K1	p.Pro124Ser	c.370C>T	Gain	23.66
Patient #17	MSI-H	**KRAS**	c.175G>A	p.Ala59Thr	Gain	25.20

Code	MS Status	GENE	NUCLEOTIDE CHANGE	PROTEIN CHANGE	GAIN/LOSS	VAF (%)
Patient #18	MSI-H	**MLH1**	c.2035G>T	p.Glu679Ter	Loss	16.78
		CTNNB1	c.94G>A	p.Asp32Asn	Gain	6.26
		PIK3CA	c.263G>A	p.Arg88Gln	Gain	15.96
		PIK3R1	c.1519G>T	p.Glu507Ter	Loss	16.15
		PTEN	c.373A>G	p.Lys125Glu	Loss	15.41
		PTEN	c.462C>A	p.Phe154Leu	Loss	16.51
		ATM	c.742C>T	p.Arg248Ter	Loss	15.02
		POLE	c.857C>G	p.Pro286Arg	Loss	16.80
		RB1	c.709G>T	p.Glu237Ter	Loss	13.78
		SLX4	c.4523C>T	p.Ser1508Leu	Unknown	14.98
Patient #19	MSI-H	**PIK3CA**	c.1634A>G	p.Glu545Gly	Gain	19.68
		PTEN	c.388C>G	p.Arg130Gly	Loss	39.91
		FGFR1	c.495_497delTGA	p.Asp166del	Gain	13.28
		PPP2R1A	c.547C>T	p.Arg183Trp	Gain	42.38
Patient #20	MSI-H	**PTEN**	c.388C>T	p.Arg130Ter	Loss	84.43
Patient #21	MSI-H	**MTOR**	c.6644C>T	p.Ser2215Phe	Gain	36.29
		PIK3CA	c.3129G>T	p.Met1043Ile	Gain	38.27
		PTEN	c.144C>A	p.Asn48Lys	Loss	39.97

Code	MS Status	GENE	NUCLEOTIDE CHANGE	PROTEIN CHANGE	GAIN/LOSS	VAF (%)
Patient #21	MSI-H	**PTEN**	c.389delG	p.Arg130fs	Loss	40.61
		KRAS	c.38G>A	p.Gly13Asp	Gain	39.29
Patient #22	MSI-H	**ARID1A**	c.4003C>T	p.Arg1335Ter	Loss	22.31
		PIK3CA	c.1636C>A	p.Gln546Lys	Gain	26.13
		PIK3R1	c.1669C>T	p.Arg557Ter	Loss	37.66
		PTEN	c.367C>G	p.His123Asp	Loss	35.91
		PTEN	c.388C>G	p.Arg130Gly	Loss	34.72
		TP53	c.817C>T	p.Arg273Cys	Loss	4.57
		TP53	c.583A>T	p.Ile195Phe	Loss	4.11
		TP53	c.430C>T	p.Gln144Ter	Loss	7.69
Patient #23	MSI-H	**MLH1**	c.2107delG	p.Glu703LysfsTer80	Loss	38.02
		PIK3CA	c.263G>A	p.Arg88Gln	Gain	29.70
		PTEN	c.697C>T	p.Arg233Ter	Loss	31.53
Patient #24	MSS	**ARID1A**	c.2248C>T	p.Arg750Ter	Loss	84.67
		ATR	c.760G>T	p.Glu254Ter	Loss	5.06
		FBXW7	c.2065C>T	p.Arg689Trp	Loss	35.22
		PIK3R1	c.1042C>T	p.Arg348Ter	Loss	36.69
		PIK3R1	c.1381C>T	p.Arg461Ter	Loss	77.27
		RAD50,TH2LCRR	c.3424G>T	p.Glu1142Ter	Loss	41.48

Code	MS Status	GENE	NUCLEOTIDE CHANGE	PROTEIN CHANGE	GAIN/LOSS	VAF (%)
Patient #24	MSS	**ATM**	c.829G>T	p.Glu277Ter	Loss	37.24
		POLE	c.857C>G	p.Pro286Arg	Loss	42.26
		BRCA2	c.289G>T	p.Glu97Ter	Loss	37.51
		RB1	c.967G>T	p.Glu323Ter	Loss	38.83
		NF1	c.1570G>T	p.Glu524Ter	Loss	40.19
		NF1	c.4084C>T	p.Arg1362Ter	Loss	43.86
		PPP2R1A	c.547C>T	p.Arg183Trp	Gain	36.87
Patient #25	MSS	**CTNNB1**	c.95A>T	p.Asp32Val	Gain	23.00
		PIK3CA	c.331A>G	p.Lys111Glu	Gain	37.25
		PIK3R1	c.1710_1711insT	p.Ile571fs	Loss	43.31
		PIK3R1	c.1743delG	p.Met582fs	Loss	43.37
		PTEN	c.389G>A	p.Arg130Gln	Loss	32.75
		PTEN	c.923delG	p.Arg308fs	Loss	57.59
Patient #26	MSI-L	**FBXW7**	c.1393C>T	p.Arg465Cys	Loss	29.85
		TP53	c.832C>T	p.Pro278Ser	Loss	17.95
		CCNE1	copy number mean (9,81)		Gain	5%:8.32. 95%:11.57
		PPP2R1A	c.767C>T	p.Ser256Phe	Gain	26.22
Patient #27	MSS	**PIK3CA**	copy number mean (5,7)		Gain	5%:4.81. 95%:6.75

Code	MS Status	GENE	NUCLEOTIDE CHANGE	PROTEIN CHANGE	GAIN/LOSS	VAF (%)
Patient #28	MSS	**ARID1A**	c.1513_1514delCA	p.Gln505fs	Loss	26.28
		CTNNB1	c.133_135delTCT	p.Ser45del	Gain	27.76
		PTEN	c.217G>T	p.Glu73Ter	Loss	25.51
Patient #29	MSS	**ARID1A**	c.3283C>T	p.Gln1095Ter	Loss	38.98
		PTEN	c.62delT	p.Phe21fs	Loss	39.70
		PTEN	c.388C>T	p.Arg130Ter	Loss	43.62
		FGFR2	c.1647T>A	p.Asn549Lys	Gain	40.10
Patient #30	MSS	**ARID1A**	c.5965C>T	p.Arg1989Ter	Loss	43.57
		CTNNB1	c.110C>T	p.Ser37Phe	Gain	39.61
		PIK3CA	c.3129G>T	p.Met1043Ile	Gain	40.10
		FBXW7	c.1972C>T	p.Arg658Ter	Loss	42.61
		PIK3R1	c.1042C>T	p.Arg348Ter	Loss	87.16
		PTEN	c.19G>T	p.Glu7Ter	Loss	43.37
		CREBBP	c.3955C>T	p.Arg1319Ter	Loss	34.18
Patient #31	MSS	**NRAS**	c.182A>G	p.Gln61Arg	Gain	12.61
		TP53	c.610G>T	p.Glu204Ter	Loss	28.47
Patient #32	MSS	**PIK3R1**	p.Asp560His	c.1678G>C	Loss	4.40
		TP53	p.Gly266Glu	c.797G>A	Loss	67.33

Code	MS Status	GENE	NUCLEOTIDE CHANGE	PROTEIN CHANGE	GAIN/LOSS	VAF (%)
Patient #33	MSS	**BRAF**	c.1742A>G	p.Asn581Ser	Gain	45.60
		WHSC1L1(1) - FGFR1(2)	Gene fusion		Gain	2927 counts
		PTEN	c.916delA	p.Ile306Ter	Loss	50.17
		RB1	c.2087_2090delGAGA	p.Arg696fs	Loss	13.15
Patient #34	MSS	**PIK3CA**	c.3129G>T	p.Met1043Ile	Gain	37.96
		RICTOR	copy number mean (5.78)		Gain	5%:5.06. 95%:6.6
		TP53	c.722C>G	p.Ser241Cys	Loss	74.55
		PPP2R1A	c.767C>A	p.Ser256Tyr	Gain	29.34
Patient #35	MSS	**CCND3**	copy number mean (5,28)		Gain	5%:4.49. 95%:6.21
		MYC	copy number mean (29,63)		Gain	5%:25.39. 95%:34.58
		CCNE1	copy number mean (4,79)		Gain	5%:4.07. 95%:5.63
		AKT2	copy number mean (23,18)		Gain	5%:19.86. 95%:27.05
		PPP2R1A	c.536C>G	p.Pro179Arg	Gain	66.48
Patient #36	MSS	**TP53**	c.613T>G	p.Y205D	Loss	19.66
		PIK3CA	c.323G>A	p.Arg108His		53.23
Patient #37	MSS	**CTNNB1**	c.94G>C	p.Asp32His	Gain	44.30
		ESR1	c.1610A>C	p.Tyr537Ser	Gain	20.14
Patient #38	MSS	**PIK3CA**	copy number mean (8.66)		Gain	

Code	MS Status	GENE	NUCLEOTIDE CHANGE	PROTEIN CHANGE	GAIN/LOSS	VAF (%)
Patient #39	MSS	**CTNNB1**	c.110C>T	p.Ser37Phe	Gain	28.90
		PIK3CA	c.3127A>G	p.Met1043Val	Gain	30.47
		ESR1	c.1610A>C	p.Tyr537Ser	Gain	33.03
		PTEN	c.511C>T	p.Gln171Ter	Loss	27.29
		FGFR2	c.755C>G	p.Ser252Trp	Gain	31.97
Patient #40	MSS	**PTEN**	c.81_82insT	p.Ile28fs	Loss	37.04
		TP53	c.569C>T	p.Pro190Leu	Loss	74.76
Patient #41	MSS	**NOTCH2**	c.5356C>T	p.Arg1786Ter	Loss	25.83
		XPO1	c.1711G>A	p.Glu571Lys	Gain	17.87
		PIK3CA	c.1030G>A	p.Val344Met	Gain	35.36
		PIK3CA	c.3062A>G	p.Tyr1021Cys	Gain	37.67
		FBXW7	c.979G>T	p.Glu327Ter	Loss	36.67
		PIK3R1	c.1042C>T	p.Arg348Ter	Loss	33.41
		PIK3R1	c.1156C>T	p.Arg386Ter	Loss	33.87
		PTEN	c.101C>T	p.Ala34Val	Loss	32.72
		PTEN	c.545T>G	p.Leu182Ter	Loss	36.62
		PTEN	c.697C>T	p.Arg233Ter	Loss	9.80
		ATM	c.9022C>T	p.Arg3008Cys	Loss	32.12
		FANCI	c.1447G>T	p.Glu483Ter	Loss	6.68
		TP53	c.1024C>T	p.Arg342Ter	Loss	12.42

Code	MS Status	GENE	NUCLEOTIDE CHANGE	PROTEIN CHANGE	GAIN/LOSS	VAF (%)
Patient #41	MSS	**NF1**	c.532G>T	p.Glu178Ter	Loss	34.37
		NF1	c.7348C>T	p.Arg2450Ter	Loss	34.53
		MSH2	c.2272G>A	p.Asp758Asn	Unknown/potential pathogenic	8.85
		POLE	c.4942G>A	p.Glu1648Lys	Loss	34.15

Appendix 5: Quality statistics for the NGS sequencing of the cfDNA samples.

Patient ID	Number of mapped reads	Percent reads on target	Average base coverage depth	Uniformity of base coverage	Amplicon Read Coverage						Target Base Coverage				
					% Assigned to amplicon reads	Average reads per amplicon	Uniformity of amplicon coverage	Amplicons with at least 500 reads	Amplicon reading end to end	Amplicon base composition bias	Percentage base reads on target	Average base coverage depth	Uniformity of base coverage	Target base coverage at 500x	Percent end to end reads
41-PD	17042699	96.38%	56240	98.69%	96.38%	60388	98.90%	100%	97.79%	0.551	52.00%	56240	98.69%	100%	94.40%
41-PD2	18154072	94.49%	55614	98.21%	94.49%	63067	99.26%	100%	95.22%	0.358	51.03%	55614	98.21%	100%	90.33%
63-PD3b	17450033	92.70%	51942	97.67%	92.70%	59500	98.53%	100%	94.49%	0.530	50.76%	51942	97.67%	100%	87.97%
63-PD4	15143546	95.77%	51316	98.08%	95.77%	53322	98.53%	100%	97.79%	0.820	52.74%	51316	98.08%	100%	94.21%
67-PD	13757586	93.69%	44111	98.36%	93.69%	47389	98.90%	100%	94.85%	0.610	51.60%	44111	98.36%	100%	92.24%
67-PD2	16021455	86.87%	43453	98.31%	86.87%	51169	98.53%	100%	92.28%	0.430	47.79%	43453	98.31%	100%	84.57%
79-A	11073530	89.24%	30592	98.17%	89.24%	36330	98.16%	100%	93.38%	0.471	48.38%	30592	98.17%	100%	85.20%
79-PD5	10867885	84.50%	26847	98.39%	84.50%	33762	98.90%	100%	91.18%	0.211	46.14%	26847	98.39%	100%	79.28%
132-F	11874239	94.65%	37376	98.15%	94.65%	41319	98.16%	100%	95.96%	0.770	51.74%	37376	98.15%	100%	90.94%
136-PD2	13583786	93.07%	40779	98.19%	93.07%	46478	98.53%	100%	94.12%	0.569	50.85%	40779	98.19%	100%	88.87%

Patient ID	Number of mapped reads	Percent reads on target	Average base coverage depth	Uniformity of base coverage	Amplicon Read Coverage						Target Base Coverage				
					% Assigned to amplicon reads	Average reads per amplicon	Uniformity of amplicon coverage	Amplicons with at least 500 reads	Amplicon reading end to end	Amplicon base composition bias	Percentage base reads on target	% Assigned to amplicon reads	Average reads per amplicon	Target base coverage at 500x	Percent end to end reads
136-PD3	18121732	93.01%	55452	98.41%	93.01%	61966	99.26%	100%	95.96%	0.368	50.48%	55452	98.41%	100%	90.54%
141-PD	24579399	92.25%	78922	97.84%	92.25%	83365	98.16%	100%	95.96%	0.882	50.63%	78.922	97.84%	100%	92.78%
199-PD	15168082	94.00%	49353	99.34%	94.00%	52421	99.63%	100%	95.59%	0.262	52.01%	49353	99.34%	100%	92.16%
160-PD1	10985334	92.09%	31689	98.67%	92.09%	37191	98.90%	100%	93.01%	0.297	50.64%	31689	98.67%	100%	85.19%
160-PD2	15129024	96.64%	52196	98.31%	96.64%	53750	98.53%	100%	98.16%	0.839	53.11%	52196	98.31%	100%	95.08%
005-PD	10588839	93.64%	32474	97.86%	93.64%	36454	98.90%	100%	94.49%	0.398	51.36%	32474	97.86%	100%	88.98%
10PD	18986185	95.70%	61451	96.02%	95.70%	66800	97.06%	100%	97.43%	0.914	51.74%	61451	96.02%	100%	94.01%
24A	22346110	95.72%	75726	96.67%	95.72%	78643	97.06%	100%	98.16%	0.948	52.81%	75726	96.67%	100%	94.57%
24PD	20609972	95.81%	69524	96.94%	95.81%	72600	97.43%	100%	98.16%	0.690	52.42%	69524	96.94%	100%	94.86%
63PD	19150110	94.91%	63286	95.21%	94.91%	66823	96.32%	100%	97.79%	1.146	51.56%	63286	95.21%	100%	95.54%
134A	21913843	92.15%	69389	95.39%	92.16%	74239	96.69%	100%	91.43%	1.123	50.13%	69389	95.39%	100%	94.05%
141A	19202513	91.37%	58561	95.21%	91.37%	64508	96.32%	100%	95.22%	0.968	49.60%	58561	95.21%	100%	92.35%

Patient ID	Number of mapped reads	Percent reads on target	Average base coverage depth	Uniformity of base coverage	Amplicon Read Coverage						Target Base Coverage				
					% Assigned to amplicon reads	Average reads per amplicon	Uniformity of amplicon coverage	Amplicons with at least 500 reads	Amplicon reading end to end	Amplicon base composition bias	Percentage base reads on target	Average base coverage depth	Uniformity of base coverage	Target base coverage at 500x	Percent end to end reads
160A	18754654	95.32%	65456	96.83%	95.32%	65723	97.79%	100%	97.79%	0.774	53.15%	65456	96.83%	100%	94.60%
199A	25700607	94.02%	79825	96.93%	94.02%	88840	97.79%	100%	94.85%	0.858	51.55%	79825	96.93%	100%	90.34%
219A	21534178	95.08%	69784	96.02%	95.08%	75271	97.06%	100%	95.59%	0.890	52.35%	69784	96.02%	100%	92.51%
36A	26460530	96.66%	94667	98.47%	96.66%	94030	98.90%	100%	98.90%	0.602	53.80%	94667	98.47%	100%	96.17%
88A	17565858	88.36%	54672	97.42%	88.36%	57060	98.16%	100%	98.16%	0.798	48.16%	54672	97.42%	100%	95.19%
67A	12478661	88.89%	36947	97.86%	88.89%	40783	98.53%	100%	94.12%	0.567	48.92%	36947	97.86%	100%	89.28%
121A	16648223	94.06%	55967	97.83%	94.06%	57572	98.53%	100%	98.16%	0.867	51.62%	55967	97.83%	100%	95.60%
132A	18467984	91.45%	58683	97.62%	91.45%	62093	97.79%	100%	95.96%	1.141	50.41%	58683	97.62%	100%	92.64%
136-PD	17026668	93.45%	53186	96.11%	93.45%	58500	96.69%	100%	95.22%	0.988	51.09%	53186	96.11%	100%	91.30%
127Cx-B	20530265	94.65%	68532	97.80%	94.65%	71437	98.53%	100%	98.16%	0.854	52.09%	68532	97.80%	100%	94.11%

Appendix 6: Alterations found on the NGS sequencing of the cfDNA samples.

ID	Gene	AA Chg	Mol Freq %	Genotype	Ref Allele	Mut Molecular Cov.	WT Mol Counts	Raw Read Depth	QC Test (LoD) %	Transcript ID
05-PD	none detected								0.1757-0.2727	
10-PD	none detected								0.0790-0.1454	
121-A	none detected								0.1246-0.1960	
127-PD	TP53	p.R273C	5.48	G/A	G	103	1776	33956	0.23	NM_000546.6
127-PD	TP53	p.P250L	0.24	G/A	G	11	4632	76187	0.09	NM_000546.6
127-PD	TP53	p.G245S	9.41	C/T	C	437	4206	76187	0.09	NM_000546.6
127-PD	TP53	p.L137Q	1.66	A/T	A	43	2551	61440	0.12	NM_000546.6
127PD	GNAS	p.R201C	0.08	C/T	C	4	5294	65301	0.08	NM_000516.7
132-A	APC	p.S1465WfsTer3	0.11	GAAAAG/GAAA	GAAAAG	1	888	49523	0.48	NM_000038.6
132-A	TP53	p.Q331HfsTer6	2.19	ACC/ACCA	ACC	24	1072	52935	0.27	NM_000546.6
132-PD	PIK3CA	p.E545K	12.82	G/A	G	389	2645	30311	0.14	NM_006218.4
132-PD	TP53	p.V157_A159del	3.42			58	1638	29345	0.18	NM_000546.6
134-A	none detected								0.1199-0.2247	

ID	Gene	AA Chg	Mol Freq %	Genotype	Ref Allele	Mut Molecular Cov.	WT Mol Counts	Raw Read Depth	QC Test (LoD) %	Transcript ID
136-PD	TP53	p.V216M	0.29	C/T	C	6	2055	51879	0.21	NM_000546.6
136-PD	GNAS	p.R201C	0.22	C/T	C	5	2292	52570	0.19	NM_000516.7
136-PD	PIK3CA	p.N345I	0.25	A/T	A	3	1212	26883	0.35	NM_006218.4
136-PD	RET	p.A883S	0.40	AGC/ATC	AGC	5	1234	22374	0.35	NM_020975.6
136-PD	TP53	p.R273H	0.66	C/T	C	5	751	17969	0.57	NM_000546.6
136-PD2	TP53	p.V216M	0.15	C/T	C	5	3412	53976	0.13	NM_000546.6
136-PD2	GNAS	p.R201C	0.08	C/T	C	3	3653	51021	0.12	NM_000516.7
141-A	TP53	p.G262V	0.61	C/A	C	3	488	22080	0.87	NM_000546.6
141-A	TP53	p.R248Q	0.32	C/T	C	5	1580	65232	0.27	NM_000546.6
141-PD	KRAS	p.G12V	0.18	ACC/AAC	ACC	6	3385	68204	0.13	NM_033360.4
141-PD	TP53	p.G262V	0.28	C/A	C	3	1082	34675	0.39	NM_000546.6
160-A	GNAS	p.R201C	0.12	C/T	C	5	4061	64699	0.11	NM_000516.7
160-PD	GNAS	p.R201C	0.29	C/T	C	7	2446	34677	0.17	NM_000516.7
160-PD2	GNAS	p.R201C	0.23	C/T	C	15	6489	58264	0.08	NM_000516.7
199-A	TP53	p.L194R	0.12	A/C	A	3	2464	84441	0.17	NM_000546.6
199-PD	FGFR2	p.S252W	9.94	G/C	G	280	2538	63921	0.15	NM_000141.5

ID	Gene	AA Chg	Mol Freq %	Genotype	Ref Allele	Mut Molecular Cov.	WT Mol Counts	Raw Read Depth	QC Test (LoD) %	Transcript ID
199-PD	TP53	p.V157F	0.15	C/A	C	3	1989	52844	0.21	NM_000546.6
219-A	TP53	p.Q331HfsTer6	1.54	ACC/ACCA	ACC	20	1279	64224	0.23	NM_000546.6
24-PD	FBXW7	p.R505C	48.79	G/A	G	1827	1918	57244	0.11	NM_033632.3
24-PD	TP53	p.G266R	67.89	C/T	C	1448	685	42243	0.20	NM_000546.6
24-A	FBXW7	p.R505C	1.51	G/A	G	32	2086	85167	0.20	NM_033632.3
24-A	TP53	p.G266R	6.42	C/T	C	58	845	64224	0.47	NM_000546.6
24-A	TP53	p.Q331HfsTer6	1.28	ACC/ACCA	ACC	21	1626	40214	0.23	NM_000546.6
36-A	TP53	p.G244S	0.10	C/T	C	5	5247	137682	0.08	NM_000546.6
36-A	TP53	p.Y220C	0.14	T/C	T	6	4177	74164	0.10	NM_000546.6
36-A	GNAS	p.R201H	0.07	G/A	G	4	5783	93473	0.08	NM_000516.7
41-PD	CTNNB1	p.T41A	21.21	A/G	A	1796	6670	59347	0.08	NM_001904.4
41-PD	PIK3CA	p.H1047L	45.21	A/T	A	4024	4876	60316	0.08	NM_006218.4
41-PD	TP53	p.R213=	51.74	T/C	T	4846	4520	61509	0.10	NM_000546.6
41-PD2	CTNNB1	p.T41A	18.92	A/G	A	983	4212	62748	0.08	NM_001904.4
41-PD2	PIK3CA	p.H1047L	38.99	A/T	A	2184	3418	63029	0.08	NM_006218.4
199-PD	TP53	p.V157F	0.15	C/A	C	3	1989	52844	0.21	NM_000546.6
219-A	TP53	p.Q331HfsTer6	1.54	ACC/ACCA	ACC	20	1279	64224	0.23	NM_000546.6

ID	Gene	AA Chg	Mol Freq %	Genotype	Ref Allele	Mut Molecular Cov.	WT Mol Counts	Raw Read Depth	QC Test (LoD) %	Transcript ID
41-PD2	TP53	p.R213=	50.28	T/C	T	2878	2846	62659	0.11	NM_000546.6
63-PD	none detected								0.1469-0.2985	
63-PD3	none detected								0.2022-0.3327	
63-PD4	TP53	p.V272M	0.38	C/T	C	6	1580	28115	0.27	NM_000546.6
63-PD4	TP53	p.Y220C	0.11	T/C	T	3	2661	40135	0.16	NM_000546.6
67-A	PIK3CA	p.E545A	0.42	A/C	A	8	1892	26051	0.23	NM_006218.4
67-A	FGFR2	p.N549K	1.32	A/T	A	34	2546	38360	0.17	NM_000141.5
67-PD	PIK3CA	p.E545A	2.09	A/C	A	75	3521	38141	0.12	NM_006218.4
67-PD	FGFR2	p.N549K	4.19	A/T	A	132	3015	43538	0.14	NM_000141.5
67-PD2	none detected								0.2524-0.3762	
79-A	APC	p.S1465WfsTer3	0.08	GAAAAG/GAAA	GAAAAG	1	1199	23296	0.36	NM_000038.6
79-PD5	KRAS	p.G12V	6.81	ACC/AAC	ACC	83	1135	26699	0.35	NM_033360.4
88-A	PIK3CA	p.R88Q	0.57	G/A	G	5	865	25897	0.49	NM_006218.4
88-A	PIK3CA	p.N1044K	0.07	T/G	T	3	4406	78501	0.10	NM_006218.4
88-A	APC	p.S1465WfsTer3	0.14	GAAAAG/GAAA	GAAAAG	2	1474	47445	0.29	NM_000038.6





Although usually associated with good clinical outcome, endometrial cancer incidence and mortality has been rising over the past years. To tackle the different clinical challenges required to change this negative evolution, in the current doctoral thesis we studied minimally invasive samples such as the uterine aspirate and plasma samples to better understand the molecular characteristics of this tumour and to validate accurate prognostic and follow-up tools and new therapeutic targets. Moreover, we combined these tools with the development of patient derived preclinical models for personalized pharmacological studies. Overall, the results obtained in this thesis demonstrated the value of liquid-biopsy-based pipelines to improve the management of localised and advanced endometrial cancer patients.